The role of Calprotectin (S100A8/A9) in the pathogenesis of glomerulonephritis and ANCA-associated vasculitis

Ruth Jennifer Pepper

UCL

Thesis submitted for the degree of Doctor of Philosophy

Declaration of originality

I, Ruth Pepper, confirm that the work presented in this thesis is my own. Where information has been derived from other sources, I confirm that this has been indicted in the thesis.

Abstract

Glomerulonephritis is a common cause of end-stage renal failure and a feature of ANCA-associated vasculitis (AAV). AAV is an example of a small vessel vasculitis, characterised by inflammation of the endothelium and glomeruli in which the interaction between leukocytes and endothelial cells play a crucial role. Macrophages have been demonstrated to have a critical role during the initiation and progression of glomerulonephritis, with the persistence of macrophages in the renal biopsy being associated with a poorer outlook.

Calprotectin (also termed S100A8/A9, mrp8/14), is a complex of 2 small calcium binding proteins that is abundantly expressed in neutrophils and monocytes as well as early infiltrating macrophages and is a known ligand of Toll-like receptor 4 (TLR4) and the receptor for advanced glycation end-products (RAGE). There is growing evidence in animal models and in patients with autoimmune diseases, of calprotectin being involved in the inflammatory response, as well as being a marker of activation of innate immunity.

I have initially characterised the presence of calprotectin-positive cells in the renal biopsy of patients with focal and crescentic AAV glomerulonephritis, therefore linking the presence of these cells with renal outcome. Patients with active AAV have elevated serum calprotectin levels, as well as significant expression on neutrophils and monocytes, which although decrease during remission, does not normalise.

I have demonstrated that mrp14-/- mice are protected from nephrotoxic nephritis, which is abrogated by use of LPS during disease progression. Bone-marrow derived macrophages (BMDMs) release pro-inflammatory cytokines following stimulation with calprotectin; mediated by TLR4. Mrp14-/- BMDMs do not respond to the pro-inflammatory stimulus of S100A8/A9. The co-culture of endothelial cells (EC) and wild-type BMDMs is pro-inflammatory unlike that of mrp14-/- BMDM and ECs. Mrp14-/- mesangial cells also have a decreased pro-inflammatory response.

This work demonstrates that calprotectin has a role in experimental glomerulonephritis as well as patients with AAV. This may improve our understanding of the inflammatory response and identify a new novel target for treating patients in the future.

Publications

Papers

S100A8/A9 (calprotectin) is critical for development of glomerulonephritis by mediating pro-inflammatory monocyte-renal cell interactions (in preparation).
RJ Pepper, T Vogl, N Hogg, CD Pusey, TH Cook, AD Salama

Leukocyte and serum calprotectin (S100A8/S100A9) expression reflect disease activity in ANCA associated vasculitis and glomerulonephritis
RJ Pepper, S Hamour, KM Chavele, SK Todd, N Rasmussen, S Flint, PA Lyons, KGC Smith, CD Pusey, HT Cook and AD Salama
Kidney International. 2013 Feb 20 (Epub)

Intravenous cyclophosphamide and plasmapheresis in dialysis dependent ANCA-associated vasculitis.
RJ Pepper, D Chanouzas, R Tarzi, MA Little, A Casian, M Walsh, CD Pusey. L Harper, AD Salama.
Clinical Journal of American Society of Nephrology. 2013;8 (2):219-24.

Classifying and predicting outcomes in ANCA-associated glomerulonephritis
RJ Pepper, AD Salama.
Nephrology Dialysis and Transplantation. 2012 Jun;27(6):2135-7

Elevated soluble Flt1 inhibits endothelial repair in PR3-ANCA associated vasculitis.
Le Roux S, **Pepper RJ (joint 1st),** Dufay A, Néel M, Meffray E, Lamandé N, Rimbert M, Josien R, Hamidou M, Hourmant M, Cook HT, Charreau B, Larger E, Salama AD, Fakhouri F.
Journal American Society of Nephrology 2012;23(1):155-64.

ANCA-stimulated neutrophils release BLyS and promotes B cell survival: a clinically relevant cellular process.
Holden NJ, Williams JM, Morgan MD, Challa A, Gordon J, **Pepper RJ**, Salama AD, Harper L, Savage CO. Ann Rheum Dis. 2011;70(12):2229-33.

Pathogenesis of Lupus Nephritis and novel therapies.
RJ Pepper, AV Parikh, L Lightstone, BH Rovin.
Encyclopaedia of Medical Immunology- Springer. In press.

Abstracts

Renal Association- Oral presentation 2010
Glomerular macrophage expression of calprotectin and circulating calprotectin levels are increased in patients with ANCA associated vasculitis and promote glomerulonephritis
RJ Pepper, S Hamour, KM Chavele, CD Pusey, HT Cook and AD Salama

American Society of Nephrology- Poster presentation 2010
Monocyte and glomerular calprotectin in ANCA associated vasculitis
RJ Pepper, N Mansfield, S Hamour, R Tarzi, C Pusey, T Cook and AD Salama

ANCA workshop- Oral presentation 2011
Glomerular macrophage expression of calprotectin and circulating calprotectin levels are increased in patients with ANCA associated vasculitis and promote glomerulonephritis
RJ Pepper, R Tarzi, CD Pusey, HT Cook and AD Salama

Renal Association- Oral presentation 2011
Deficiency of calprotectin protects from nephrotoxic nephritis
RJ Pepper, R Tarzi, Hsu-Han Wang, CD Pusey, HT Cook, AD Salama

American Society of Nephrology- Poster presentation 2011
Calprotectin, an endogenous TLR4 ligand, is critical for induction of glomerulonephritis
RJ Pepper, PEH Sharp, G Bhangal, Hsu-Han Wang, R Tarzi, CD Pusey, HT Cook, AD Salama.

Autoimmunity conference 2012- Oral presentation

Calprotectin is critical for disease induction in nephrotoxic nephritis and predicts disease activity in ANCA associated vasculitis

RJ Pepper, S Hamour, H Wang, CD Pusey, HT Cook and AD Salama

Renal Association- Oral presentation 2012

Leukocyte and serum calprotectin expression reflect disease activity in ANCA associated vasculitis and glomerulonephritis

RJ Pepper, S Hamour, H Wang, CD Pusey, HT Cook and AD Salama

American Society of Nephrology- Poster presentation 2012

Leukocyte and serum calprotectin expression reflect disease activity in ANCA associated vasculitis and glomerulonephritis

RJ Pepper, S Hamour, H Wang, CD Pusey, HT Cook and AD Salama

ANCA workshop- Oral presentation 2013

Calprotectin amplifies the inflammatory response

RJ Pepper, S Hamour, H Wang, CD Pusey, HT Cook and AD Salama

Table of Contents

Index of Figures

Index of Tables

Abbreviations

AAV	ANCA associated vasculitis
AFU	Arbitrary fluorescence units
ANCA	Anti-neutrophil cytoplasm antibody
ANOVA	Analysis of variance
APC	Antigen presenting cell
AZA	Azathioprine
BBS	Boric acid
BMDM	Bone marrow derived macrophages
BMT	Bone marrow transplant
BSA	Bovine serum albumin
BVAS	Birmingham vasculitis activity score
DC	Dendritic cells
cDNA	Complementary DNA
CFA	Complete Freund's adjuvant
CIA	Collagen induced arthritis
CMP	Counts per minute
CSS	Churg-Strauss syndrome
CYP	Cyclophosphamide
DAB	Diaminobenzidine
DAMP	Damage-associated molecular pattern
DAPI	4,6-diamino-2-phenylindole
DNA	Deoxyribonucleic acid
DTH	Delayed-type hypersensitivity
EAG	Experimental autoimmune glomerulonephritis
EAV	Experimental autoimmune vasculitis
EC	Endothelial cells
ECGF	Endothelial cell growth factors
EDTA	Ethylenediaminetetraacetic acid
ELISA	Enzyme-linked immunosorbant assay

EUVAS	European vasculitis study group
FACS	Fluorescence-activated call sorter
FCS	Foetal calf serum
FITC	Fluorescein isothiocynate
GBM	Glomerular basement membrane
GCS	Glomerular cross section
GN	Glomerulonephritis
GPA	Granulomatosis with polyangiitis
Gy	Gray
H+E	Haematoxylin-eosin
HLA	Human leukocyte antigen
HUVEC	Human umbilical vein endothelial cells
ICAM-1	Inter-cellular adhesion molecule 1
IF	Immunofluorescence
Ig	Immunoglobulin
INF-γ	Interferon
IL	Interleukin
IRAK	IL-1 receptor associated kinase
ITS	Insulin/transferring/Selenium Growth Supplement
IV	Intravenous
IP	Intra-peritoneal
LAMP	Lysosomal-associated membrane protein
LPS	Lipopolysaccharide
MAPK	Mitogen-associated membrane protein
MC	Mesangial cells
M-CSF	Macrophage colony stimulatory factor
MCP	Monocyte chemoattractant protein
MHC	Major histocompatibility complex
MPA	Microscopic polyangiitis
MPO	Myeloperoxidase
MMF	Mycophenolate mofetil
MR	Mannose receptor

MMP	Matrix metalloproteinases
MRP	myeloid related protein
MTX	Methotrexate
MyD88	Myeloid differentiation primary response gene (88)
NaCl	Sodium chloride
NET	Neutrophil extracellular traps
NF-κB	Nuclear factor kappa-light-chain-enhancer of activated B cells
NLR	NOD-like receptor
NK	Natural killer
NORAM	Non-renal Wegener's Granulomatosis treated alternatively with methotrexate
NTN	Nephrotoxic nephritis
NTS	Nephrotoxic serum
OD	Optical Density
P	Prednisolone
PAMP	Pathogen-associated molecular pattern
PAS	Periodic acid Schiff
PMN	Polymorphonuclear leukocytes
PR3	Proteinase 3
PRR	Pattern recognition receptor
PBMC	Peripheral blood mononuclear cell
PBS	Phosphate buffered saline
PCR	Polymerase chain reaction
PE	Phycoerythrin
PEX	Plasma exchange
RAG	Recombinase-activating gene
RLV	Renal limited vasculitis
RNA	Ribonucleic acid
RORγt	Retinoic acid-related orphan receptor-γt
ROS	Reactive oxygen species
RT-PCR	Reverse transcriptase polymerase chain reaction
RTX	Rituximab

SC	Subcutaneous
SCID	Severe combined immunodeficiency
SD	Standard deviation
SLE	systemic lupus erythematosis
SMA	smooth muscle actin
Strep-HRP	Streptavidin horseradish-peroxidase
TAE	Tris-acetate EDTA
TBS	Tris-buffered saline
TCR	T-cell receptor
TGF-β	Transforming growth factor-β
Th	T-helper
TLR	Toll like receptor
TNF-α	Tumour necrosis factor-α
TRAF	TNF receptor associated factors
Treg	Regulatory T-cell
TRIF	TIR-domain-containing adapter-inducing interferon-β
VFU	Visual fluorescence units
WKY	Wistar Kyoto
WT	Wild-type

Chapter 1 Introduction

This project explores the role of calprotectin (S100A8/A9) in the pathogenesis of ANCA associated vasculitis (AAV) and glomerulonephritis. The first chapter explores the presence of this protein in patients, in the circulation as assessed by measuring serum levels and within leukocyte subsets, and within tissues, by histological assessment of renal biopsies of patients with AAV. In addition, the effect of ANCA-IgG itself on monocyte expression of S100A8/A9 was also investigated. The second chapter explores the role of S100A8/A9 in the nephrotoxic nephritis animal model of immune complex glomerulonephritis. Lastly the third chapter explores the in-vitro effect of S100A8/A9 on several primary renal cell lines which play a role in induction of glomerulonephritis, as well as investigating the cellular responses of cells deficient in S100A8/A9.

The terminology of S100A8/A9 can be confusing due to the numerous names given to each of the 2 proteins that constitute the heterodimer.

As recommended, the genes should be referred to as Mrp8 and Mrp14, and the protein S100A8 and S100A9 as internationally recognised (Roth, Goebeler et al. 2001). The S100A8/A9 heterodimer is also termed calprotectin, and these two terms are used in the thesis. Mice deficient in calprotectin are termed mrp14-/- mice.

1.1 Anti neutrophil cytoplasm antibody (ANCA) vasculitis

1.1.1 Epidemiology

Anti neutrophil cytoplasm antibody (ANCA) associated vasculitis (AAV) is an example of a small vessel vasculitis characterised by necrotising inflammation of blood vessel walls. It is a multisystem disease often with kidney involvement characterised by the formation of ANCA auto-antibodies directed against the components of neutrophil granules and monocyte lysosomes, proteinase 3 (PR3) and myeloperoxidase (MPO). AAV consists of 3 clinical syndromes- granulomatosis with polyangiitis (GPA formerly Wegener's), microscopic

polyangiitis (MPA) and Churg-Strauss syndrome (CSS), in which measurement of these auto-antibodies has a major role in establishing the diagnosis. A 10 year study in the UK demonstrated an overall incidence of 19.8/million, with males affected slightly more than females (23.5/million v 16.4/million), and an increase in incidence with increasing age (Watts, Lane et al. 2000). Clinical phenotypes can differ between different populations, for example the overall incidence of AAV may be similar between Japan and the UK, but the subtypes vary, with MPA predominating in a Japanese cohort, but accounting for only 41% of cases in the UK AAV patients (Watts, Scott et al. 2008). Additionally, variations in the clinical subtypes occur across Europe, with an increased incidence in GPA in Northern Europe (Norway) compared to Southern Europe (Spain), and an increased incidence in MPA in Spain (Watts, Lane et al. 2001).

A link between GPA and infection has long been observed (Pinching, Rees et al. 1980), and treatment with the antibiotic co-trimoxazole was shown to result in a reduced incidence of relapses in patients with GPA (Stegeman, Tervaert et al. 1996). Further evidence for a possible role of infection is supported by the cyclical incidence of GPA, with peak incidences observed in 2005 as well as 1990 and 1996 (Watts, Mooney et al. 2012). However, the observation of a higher incidence in disease onset in winter rather than summer has been inconsistent (Ntatsaki, Watts et al. 2010). In a European cohort, auto-antibodies to lysosomal membrane protein-2 (LAMP-2) were prevalent in patients with ANCA associated pauci-immune focal necrotising glomerulonephritis and this molecule was homologous to a bacterial fimbrial protein, suggesting that molecular mimicry triggered by infection, may have a role in the pathogenesis of glomerulonephritis associated with ANCA (Kain, Exner et al. 2008). Additionally, a high incidence of preceding urinary tract infections was noted in those patients positive for LAMP2 antibodies. The relevance of autoantibodies to human LAMP-2 in systemic vasculitis has been debated following contradictory findings in two separate cohorts using different assay techniques, Kain, 2012 #4093}. Possible explanations for these different results include different patient populations and differences in the experimental techniques and reagents used.

1.1.2 Classification, Clinical course and biomarkers

The Chapel Hill Consensus Conference aimed to standardise the terms used to define the systemic vasculitides and although they were not intended for use as diagnostic criteria, they have frequently been used in this way. According to these criteria, ANCA associated small vessel vasculitides included Wegener's granulomatosis (now referred to as granulomatosis with polyangiitis), Churg-Strauss syndrome and microscopic polyangiitis (Jennette, Falk et al. 1994). These diseases are characterised by inflammation to the small blood vessel wall and commonly result in glomerulonephritis with a typical focal segmental necrotising and crescentic glomerular pattern of damage. Renal involvement is termed pauci-immune due to little or no immunoglobulin deposition. Though uncommon conditions, these diseases frequently cause end-stage renal failure (ESRF), and are a significant cause of patient morbidity, mortality and hence result in a disproportionate impact with respect to health economics. The renal registry report from 2010 states glomerulonephritis accounted for 11.3 per million cases of ESRF in the UK (Gilg, Castledine et al. 2012). These diseases follow a chronic relapsing course therefore exposing patients to repeated courses of treatment with immunosuppression and their associated adverse events.

A more useful classification system with respect to clinical course and prognosis is by distinguishing these diseases by their auto-antibody profile rather than the name as defined by the Chapel Hill Consensus conference (Lionaki, Blyth et al. 2012). It has previously been recognised that GPA and PR3-ANCA are associated with a higher risk of relapse than MPA/MPO-ANCA vasculitis (Booth, Almond et al. 2003). It is increasing recognised that these diseases based on their autoantibody profile are distinct entities, with the majority of patients with renal limited disease being positive for MPO-ANCA (81%) and those patients with lesions of the upper respiratory tract being positive for PR3-ANCA (Lionaki, Blyth et al. 2012). Therefore, there is evidence that the autoantibody profile not only help to classify patients but also to predict outcome. A genome wide association study demonstrated genetic factors contributing to disease susceptibility, which differed between GPA and MPA. These associations, including HLA, aligned with ANCA rather than the difference clinical entities (Lyons, Rayner et al. 2012). A recent classification, has further divided AAV into

categories based on the presence of renal disease, ANCA specificity and gastrointestinal/cardiovascular disease, resulting in a more homogenous groups of patients with distinct death and relapse rates (Mahr, Katsahian et al. 2012). These 2 studies provide evidence for distinct disease entities within the term ANCA associated vasculitis.

However, the actual ANCA titre, or changes in titre have been recognised as only being a modest predictor of disease relapse. An increase in ANCA as well as a persistently positive ANCA, are significantly associated with relapse (positive likelihood ratio of an increase in ANCA on future relapse of disease was 2.84). Interestingly, measuring the ANCA in MPO-ANCA patients was a more reliable indicator of possible relapse/disease activity than PR3-ANCA (Tomasson, Grayson et al. 2012). Therefore, the measurement of these auto-antibodies is of limited use in guiding individualised treatment for patients with vasculitis.

The identification of a more robust biomarker to help predict which patients will relapse is therefore highly desirable. This could enable a more tailored treatment plan for individual patients, allowing a reduction of unnecessary immunosuppression in a subset of patients in a better prognostic category, and increased vigilance and/or more prolonged treatment in those patients in a worse prognostic group with respect to relapse risk. Gene expression profiling has emerged as a potential tool in helping to predict a patient's response to treatment. One successful method used the purification of lymphocyte subsets (CD4+ and CD8+ T cells, B cells, neutrophils and monocytes) followed by the quantification of gene expression profiles using a microarray. Separating the individual leukocyte subsets allowed the identification of a novel CD8+ signature that defined a subgroup of patients with AAV who were at an increased risk of relapsing disease. This same signature also predicted an increased risk of relapse in patients with systemic lupus erythematosis (SLE). This newly identified CD8+ T cell signature was associated with the upregulation of genes involved in both T-cell receptor (TCR) and IL-7 receptor (IL-7R) pathways. These genes are both important for promoting T-cell survival and memory, therefore helping to identify those patients who may benefit from a more intensive immunosuppressive treatment regime (McKinney, Lyons et al. 2010). However, these findings need to be reproduced in a separate population, ideally in a prospective manner.

Circulating markers have also been identified in order to help differentiate between active AAV and disease remission. Matrix metalloproteinase-3 (MMP-3) has been demonstrated to be able to differentiate active from inactive AAV better than the more traditional markers of inflammation such as C-reactive protein (CRP) and erythrocyte sedimentation rate (ESR). However, this study had a few limitations, such as including a heterogeneous patient population with respect to renal involvement, as well as a mixture of different treatment regimes, and inter-assay variation in the measurement of MMP-3. This study requires further investigation (Monach, Tomasson et al. 2011).

Therefore, currently routine testing of patients' serum ANCAs titre remains the only limited tool to help us predict a patient's response to therapy and risk of relapse, and since it is a poor biomarker, we are limited in our ability to tailor patient's individual treatment.

1.1.3 Histological classification and outcome

AAV frequently affects the kidneys. A characteristic pattern of renal involvement occurs, which is discussed further in section 1.2.3. A histopathological classification of ANCA-associated glomerulonephritis was proposed in 2010 (Berden, Ferrario et al. 2010). The classification validation study included 100 patients from 2 large multi-centre European vasculitis trials (CYCAZAREM: cyclophosphamide or azathioprine as a remission therapy for vasculitis, and MEPEX: methylprednisolone versus plasma exchange as additional therapy for severe, ANCA associated glomerulonephritis). Renal histology from these patients originating in 9 European countries with at least 1 year's follow-up, and with both MPO-ANCA and PR3-ANCA were included. The classification system was based on the glomerular pathology assessed by light microscopy. Interestingly, tubulointerstitial parameters such as fibrosis and tubular atrophy did not add to the classification system and resulted in increasing the classification complexity and was thus omitted unless there was something remarkable in this compartment. The key aspect of the classification was that the renal biopsy could be defined by 4 separate categories: focal, crescentic, mixed and sclerosed, and these correlated with the clinical outcome. Briefly, focal was defined by ≥50% normal glomeruli. Crescentic included ≥50% glomeruli with cellular crescents. Importantly, the

crescents were defined as cellular not fibrous crescents, although as long as at least 10% of the crescent contained cellular material, they were labelled as a cellular crescent even if the remaining material consisted of the extra-cellular matrix. Mixed referred to <50% normal, <50% crescentic, <50% globally sclerotic glomeruli. The last category was sclerotic, which included the biopsies with ≥50% globally sclerotic glomeruli. The biopsies included in this classification were all pauci-immune and contained at least 10 glomeruli. The validation study demonstrated that different classes correlated to the severity of renal impairment during follow-up, with those patients in the focal category having the best renal outcome, followed by crescentic, mixed and lastly, sclerotic. Additionally, those patients with a sclerotic classification were at highest risk of death within the first year of diagnosis. Therefore this classification could allow biopsies from different centres to be compared within the same categories, so that patient outcome in different centres, treated in different ways, within and without clinical trials may be analysed.

The first replication of the classification system was in a Chinese cohort, and it produced some differences in patient outcome compared to the European cohort used in the Berden classification. Whilst the best renal outcome remained in the focal category and the worst in the sclerotic, surprisingly, those patients with a crescentic category had a worse outcome than those with a mixed category (Chang, Wu et al. 2012). These differences may be due to differences in treatment or differences in disease phenotype within different ethnic groups. The Berden classification has been replicated in a population of patients (n=76) from the US, with those patients with a focal class having the best outcome, and sclerotic the poorest at 1 year (Carla L. Ellis 2012). Similarly, an Australian study (n=113) has also demonstrated that sclerotic class has the poorest patients and renal survival (Sharon Lee Ford 2012). The Berden classification has also recently demonstrated in a European cohort of 109 patients, to be an important predictor of renal relapse, with risk highest in those patients with the sclerotic class (Arda Goceroglu 2012).

Although the Berden classification does provide convincing evidence for the histological pattern of renal injury predicting long-term renal outcome, not all patients undergo renal biopsies and a proportion do not have renal involvement. In addition, this does not inform clinicians as to the risk of disease relapse. There remains therefore a clinical need for better

biomarkers for predicting disease activity and risk of relapse that could be of direct clinical applicability in this group of patients with a disease that characteristically relapses.

1.2 Pathogenesis of crescentic glomerulonephritis

Crescentic glomerulonephritis (GN) describes a histopathological pattern of glomerular injury. The underlying cause for this pathological pattern can be divided into 3 groups of underlying causes: Immune-complex mediated glomerulonephritis, anti-GBM associated and pauci-immune GN. A crescent is characterised by disruption of the glomerular capillary wall resulting in a cellular infiltration into Bowman's space. This proliferation of infiltrating cells is composed of macrophages, podocytes, parietal epithelial cells, fibroblasts and T-cells(Tarzi, Cook et al. 2011; Kambham 2012). The classification of the causes of a crescentic glomerulonephritis depends on the presence/absence of immune deposits as well as their location within the glomerulus. Patients with a crescentic glomerulonephritis, which is a cause of a rapidly progressive GN, present with proteinuria, haematuria, renal impairment and if untreated may progress in end-stage renal failure in weeks to months.

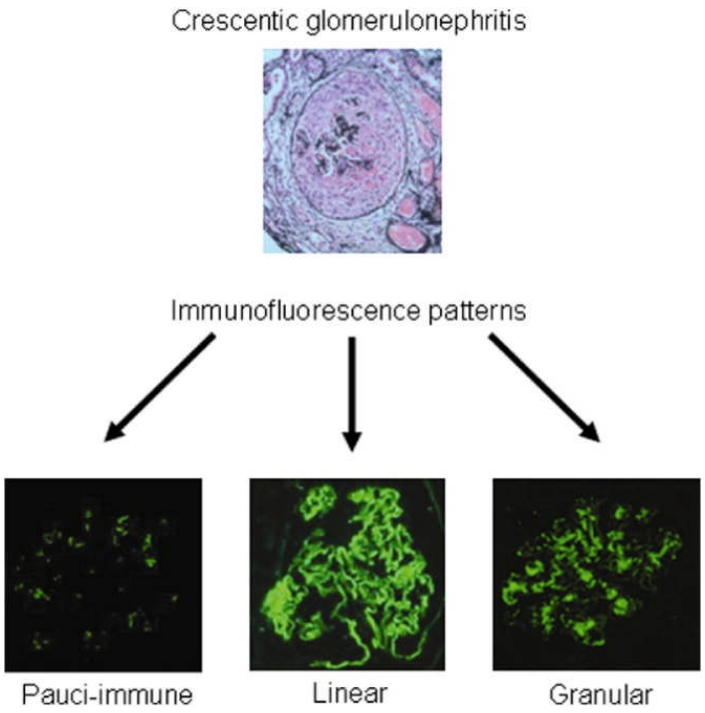

Figure 1-1 Crescentic GN has different patterns of glomerular immunoglobulin deposition.

Top figure demonstrates a crescentic glomerulus (silver stain). Bottom pictures demonstrate the 3 patterns of IgG deposition as shown by immunofluorescence in crescentic glomerulonephritis (Tarzi, Cook et al. 2011)

1.2.1 Immune complex crescentic glomerulonephritis

Immune complexes are composed of immunoglobulins, complement and a variety of other proteins. Several different renal disease are characterised by the formation of immune complexes, which can vary in size, composition and location within the glomerulus.

These complexes subsequently get trapped within the glomerulus either in the mesangium, the subendothelial surface or the subepithelium. Large insoluble immune complexes form when the amount of antigen increases resulting in cross-linking of these complexes. These

immune complexes can then bind to Fc receptors with the activation of complement and infiltration of leukocytes with the subsequent release of pro-inflammatory mediators. When the immune complexes fail to be removed by the circulation, injury and inflammation within the glomerulus can then be initiated (Nangaku and Couser 2005). In the animal model, an example of this type of injury is an acute serum sickness model in the rabbit. When crystallized bovine albumin was injected into rabbits, renal and cardiovascular lesions were identified, which were observed in the case of renal lesions to be similar to a glomerulonephritis in man (Germuth 1953). This is an example of a type III hypersensitivity reaction.

SLE is an example of an immune-complex disease. A significant feature on the renal biopsy in patients with lupus nephritis is the deposition of immunoglobulin. Patients with active disease demonstrate high serum levels of circulating anti-dsDNA antibodies. However, patients in disease remission may also demonstrate elevated levels of auto-antibodies as do individuals many years before clinical disease (Arbuckle, McClain et al. 2003), suggesting a threshold is required for development of clinical disease, with respect to the presence of certain autoantibodies with particular specificities. Autoantibodies may lead to deposition of immune complexes within the kidney, with two potential mechanisms which may explain the tropism of these autoantibodies and immune complexes for the kidney. One mechanism is the cross-reaction of anti-dsDNA antibodies to glomerular antigens such as the mesangial cell membranes, laminin and α-actinin. The second mechanism is the binding of anti-dsDNA antibodies to exposed chromatin fragments associated with the glomerular basement membranes (Mortensen and Rekvig 2009). The current theory of why autoantibodies develop initially is that apoptotic cells persist due to deficiencies in the natural clearance mechanisms such as IgM, serum amyloid P and nucleases (such as DNase 1), which aid in targeting and removal of dead and dying cells, and whose deficiencies are associated with SLE, allowing chromatin release and exposure to the immune system. Following activation of dendritic cells and chromatin-derived peptide specific T helper cells, there ensues a T cell-B cell interaction which promotes production of anti-chromatin antibodies (Mortensen and Rekvig 2009). This is supported by the evidence from both humans and mice, in which nucleosome specific T cells have been identified as well as the induction of anti-nucleosome, anti-dsDNA and anti-histone antibodies (van der Vlag and Berden 2011).

Another renal disease which is characterised by the formation of immune deposits is idiopathic membranous glomerulonephritis, which is a significant cause of nephrotic syndrome in adults. These immune complexes deposit in a subepithelial location and are mainly of the IgG4 subclass. A member of the mannose-receptor family, phospholipase A2 receptor (PLA_2R), which is located on the podocyte, was recently found to the antigenic target for the majority (70%) of patients with idiopathic membranous GN (Beck, Bonegio et al. 2009).

1.2.2 Anti-glomerular basement membrane (GBM) or Goodpasture's disease

The first suspected case of anti-GBM disease, in a patient with pulmonary- renal syndrome was reported in 1919 by Ernest Goodpasture. In retrospect this may have been a case of systemic vasculitis, but following the description of similar cases the constellation of features was named Goodpasture's syndrome, and Goodpasture's disease when associated with circulating anti-GBM antibodies. It is characterised by the formation of autoantibodies to type IV collagen, present in the glomerular and alveolar basement membranes. Most of the autoantibodies are of the IgG1 subtype, although in some patients the dominant subtype may be IgG4 (Segelmark, Butkowski et al. 1990). The typical renal lesion is a florid crescentic glomerulonephritis where most glomeruli show a similar aged lesion and have linear deposition of IgG. The auto-antigen has been identified as the non-collagenous domain (NC1) of α3 type IV collagen (Saus, Wieslander et al. 1988; Ryan, Mason et al. 1998), contained within α3, α4 and α5 triple helices, making up the collagen IV complex in the glomerular basement membrane (GBM). An early initiating process is thought to involve a conformational change in the structure of these trimers in alveolar or glomerular basement membrane, thus exposing neoepitopes which result in the formation of autoantibody production and GBM deposition (Pedchenko, Bondar et al. 2010). Cigarette smoking, as well as the organic solvents, are recognised trigger factors leading to the pathological exposure of these neoepitopes (Donaghy and Rees 1983; Stevenson, Yaqoob et al. 1995). There are important genetic associations with the development of this disease, with HLADRB1*1501 and *0401 being present in a significant number of patients with the disease compared to controls (Fisher, Pusey et al. 1997). Antigen specific T-cells demonstrate an important role in

glomerular injury. α3 (IV)NC1-specific CD4+ cells are known to be present in patients and healthy subjects, having not been adequately deleted in the thymus despite α3 (IV)NC1 thymic expression(Wong, Phelps et al. 2001). In patients with anti-GBM disease, the frequencies of these T-cells are higher than those in controls without disease, but undergo a gradual decrease in the years following diagnosis (Salama, Chaudhry et al. 2001), due to the development of antigen-specific regulatory T-cells which maintain immune tolerance and disease remission (Salama, Chaudhry et al. 2003).

1.2.3 Pauci-immune crescentic glomerulonephritis

AAV commonly results in a pauci-immune glomerulonephritis which is characterised by little or no deposition of immunoglobulin within the glomerulus. It is associated with the presence of anti-neutrophil cytoplasmic antibodies (ANCA) directed against components of neutrophil granules and monocyte lysosomes, proteinase-3 and myeloperoxidase. However, approximately 10% of patients with pauci-immune GN will be ANCA negative.

1.2.3.1 Pathogenicity of ANCA

ANCA were detected and demonstrated to be associated with vasculitic disease activity in 1985 (van der Woude, Rasmussen et al. 1985). There is now evidence that these autoantibodies are additionally involved in the disease pathogenesis. However, there is conflicting human evidence whether the presence of the autoantibodies alone can cause disease as demonstrated by 2 cases of maternal transfer of MPO-ANCA. In 1 case, the child was born with a renal-pulmonary syndrome and required immunosuppression, and in the other case the newborn was healthy with no clinical disease despite placental transfer of MPO-ANCA in both cases (Schlieben, Korbet et al. 2005; Silva, Specks et al. 2009).

After being primed by cytokines such as TNFα, both neutrophils and monocytes express PR3 and MPO on the cell surface. ANCA can then bind to the antigen with several pro-inflammatory results. Neutrophils have been shown to subsequently release reactive oxygen species (ROS) and to undergo degranulation (Falk, Terrell et al. 1990). Binding of ANCA to the cell can occur through both F(ab) and FcR engagement with crosslinking of the antigens

and activation of the cell (Kettritz, Jennette et al. 1997) leading to release of pro-inflammatory cytokines such as IL-1 and IL-8 (Harper, Cockwell et al. 2001). The interaction of ANCA-primed neutrophils with the endothelium is an important part of disease pathogenesis. MPO-ANCA has been demonstrated in a murine model to increase leukocyte adhesion and transmigration within the endothelium, with mice deficient in FcRγ chain protected from this action (Nolan, Kalia et al. 2008). Additionally, neutrophil degranulation with subsequent release of elastase and proteinase-3 has been shown to induce endothelial cell apoptosis (Yang, Kettritz et al. 1996). Further evidence of the importance of the role of ANCA in leukocyte-endothelial interactions is provided by animal models which will be discussed further.

1.2.3.2 Genetic factors

Like other complex auto-immune diseases, susceptibility depends on predisposing genetic factors and particular environmental factors. The relative risk of GPA in first degree relatives of patients with the disease is 1.56 (Knight, Sandin et al. 2008). Additionally, relatives are at a slightly increased risk of other autoimmune/inflammatory diseases (Knight, Sandin et al. 2010). Recently, a genome wide association study in a European cohort, demonstrated both MHC and non-MHC associations with AAV. There were significant differences in the genetics between PR3-ANCA and MPO-ANCA, with associations of PR3-ANCA with HLA-DP and genes coding for α1-antitypsin and proteinase 3, while MPO-ANCA was associated with HLA-DQ, confirming that the syndromes associated with these 2 different auto-antibodies are genetically distinct (Lyons, Rayner et al. 2012).

Other genetic associations of AAV which emerged from smaller cohort studies suggested polymorphisms in CTLA-4 (Lee, Choi et al. 2012), and PTPN22 gene (tyrosine phosphatase enzyme present in lymphocytes) may play a role (Carr, Niederer et al. 2009) as well as associations with the IL-2RA (IL-2 receptor) locus (Carr, Clatworthy et al. 2009). Fc-receptor genotypes have also been identified as a factor influencing the development of severe renal disease in GPA (Kelley, Monach et al. 2011), while The Z allele of the polymorphic α1 anti-trypsin, an inhibitor of PR3, has been shown to be associated with GPA (Morris, Morgan et al. 2011) in smaller cohort studies and in the GWAS.

1.2.4 Immune mediators in glomerulonephritis

Both the innate and adaptive immune responses play important roles in the pathogenesis of glomerulonephritis. There is a complex interplay between different immune cells, with evidence acquired from animal models of disease.

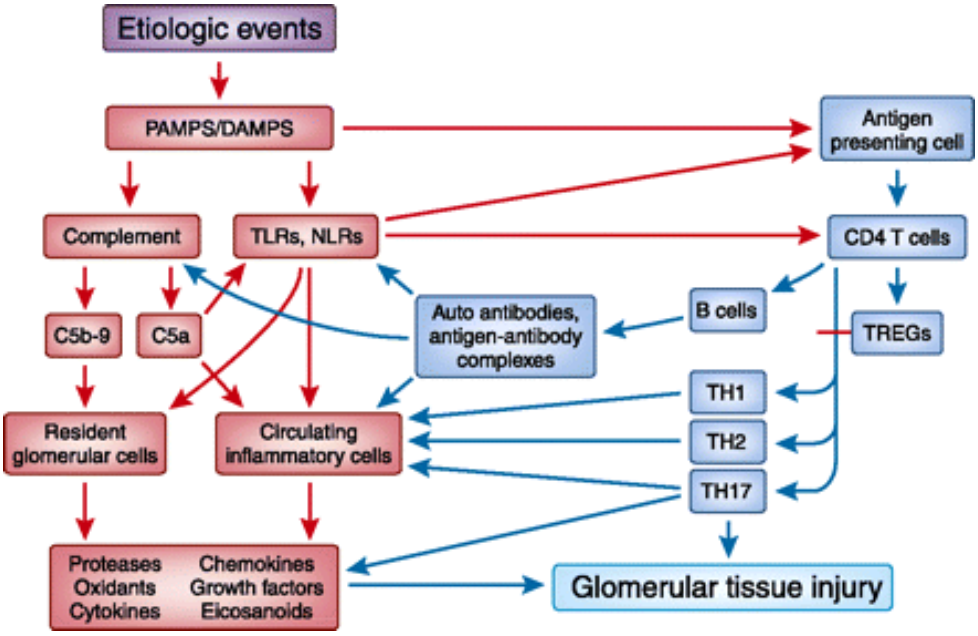

Figure 1-2 Demonstrates the interplay between both the innate and the adaptive immune mechanisms in causing glomerular injury.

Receptors, such as toll-like receptors (TLRs) additionally play an important role, with both infiltrating immune cells as well as the resident intrinsic cells playing a role (Couser 2012).

1.2.4.1 Macrophages

Macrophages have a central role in both the initiation and the progression of experimental glomerulonephritis as well as roles in healing and repair. A study of the renal biopsies of patients with lupus nephritis demonstrated the presence of glomerular monocytes and

tubular macrophages correlated the best with outcome parameters, with the persistent presence of macrophages on repeat biopsies in those treated patients correlating with poor renal survival (Hill, Delahousse et al. 2001).

1.2.4.1.1 Macrophage phenotype

There is increasing evidence that macrophages are able to alter their phenotype depending on the local environment and the cytokine milieu. Analogous to the Th1/Th2 subset, macrophages can be divided into the classically activated M1, and the alternatively activated M2 (with further subdivisions) depending on various cell surface markers as well as their functional behaviour. Macrophages originate from a progenitor myeloid cell within the bone marrow, the precursor of many different cell types. These myeloid progenitor cells eventually develop into monocytes under the influence of macrophage colony-stimulating factor, which are then subsequently released into the circulation from the bone marrow and into tissues where there is further differentiation into macrophages. Both the innate and the adaptive immune response can then influence the behaviour and the phenotype of the infiltrating macrophages.

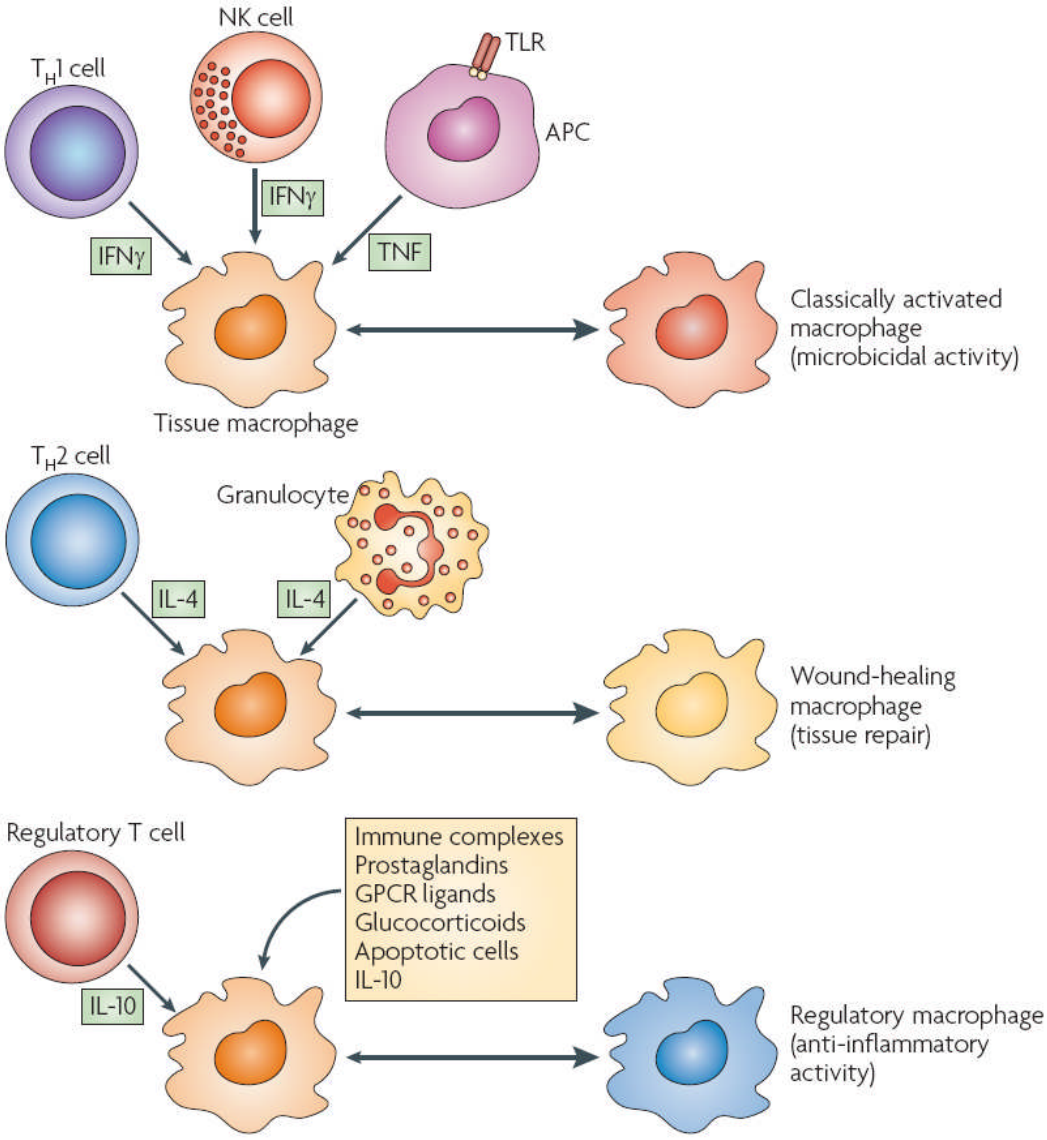

Figure 1-3 Diagram to demonstrate the generation of different macrophage phenotypes

INFγ secreted by Th1 cells, or TNF secretion by antigen presenting cells, results in the generation of classically activated macrophages. Alternatively activated macrophages result from IL4 secretion and regulatory macrophages under the influence of IL-10 (Mosser and Edwards 2008).

Classically activated macrophages (M1a) are produced under the influence of INFγ, which can be produced by both adaptive and innate cells such as antigen specific Th1 CD4+ cells, CD8+ cytotoxic T cells and NK cells. They have several particular functions such as increased phagocytosis and endocytosis and therefore increased uptake of bacteria; they mediate activation of Th1 cells through increased expression of major histocompatibility (MHC) complex class II and molecules such as CD40, CD80 and CD86 which function as critical co-stimulatory molecules. They also release several pro-inflammatory cytokines (IL-1, IL-12, TNF-α). M1b subsets, stimulated by LPS-TLR4 activation, are similar to M1a with respect to many of the pro-inflammatory properties but they are characterised by not secreting IL-12. Other endogenous stimulants of M1b include pathogen-associated molecular patterns that through interaction with pattern recognition receptors are able to activate M1b (Rees 2010). Additionally, the cytokine profile secreted by classically activated macrophages (IL-1, IL-6, IL-23) are associated with development of Th17 cells which appear to have an important role in autoimmunity (Langrish, Chen et al. 2005).

Alternatively activated macrophages (M2a) have been identified in culture following stimulation with IL-4 or IL-13. This macrophage subset is associated with very different actions to that of the classically activated macrophage, with less pro-inflammatory cytokine production, but production of IL-10. M2a cells are also characterised by decreased nitric oxide production and reactive oxygen species, recruitment of Th2 cells and expression of the cell surface mannose receptor. A further sub-type of alternatively activated macrophages is the M2b cell, macrophages formed under the influence of LPS and in the presence of IgG immune complexes. Although this subtype produces cytokines such as IL-1β, IL-6 and TNFα, the production of IL-10 results in an anti-inflammatory phenotype. The response supports a Th2 effect with IgG class switching by B cells (Rees 2010). They are associated with tissue remodelling as well as response to parasites. Apoptotic cells affect monocyte activation resulting in increased secretion of IL-10, with decreased secretion of pro-inflammatory cytokines. Therefore having an anti-inflammatory effect (Voll, Herrmann et al. 1997).

It has been suggested using rat bone marrow derived macrophages (BMDMs), following exposure to numerous cytokines, the phenotype of the macrophage is determined by the

first cytokine to which it was exposed to, following which the macrophage is then unresponsive to an alternative activating signal (Erwig, Kluth et al. 1998). In an extension of this finding, macrophages from inflamed, nephritic rat glomeruli responded differently to macrophages from normal glomeruli with respect to the amount of nitric oxide production following treatment with IL-4, therefore supporting the hypothesis that once the macrophages have a determined phenotype, they become unresponsive to alternative stimuli, as previously demonstrated with BMDMs (Erwig, Stewart et al. 2000).

However, there is experimental evidence to demonstrate that the functional phenotype of mouse macrophages can be changed, and this plasticity occurs as the microenvironment changes, and therefore polarized macrophages have an element of reversibility (Stout, Jiang et al. 2005). Whether, this in-vitro work in which macrophages are exposed to a limited number of cytokines can then be translated into the in-vivo setting is unclear. In the mouse model of ischaemia-reperfusion, pro-inflammatory M1 macrophages are the early infiltrating cells which are recruited into the kidney, followed by a predominance of M2-type macrophages a few days later. Labelled M1 macrophages were demonstrated to switch to an M2 phenotype and to change their function from a pro-inflammatory macrophage to a macrophage involved with repair of the injured kidney. Depletion studies demonstrated a protective effect on the kidney when depletion occurred early on, however, recovery was delayed when depletion occurred at a later stage (Lee, Huen et al. 2011).

1.2.4.1.2 Macrophages in animal models of disease

Macrophages have been demonstrated to play an important role in experimental glomerulonephritis. Macrophages have crucial roles in causing disease in both the initiation and the progression of inflammation. Treatment with anti-macrophage serum in an animal model of anti-GBM disease, resulted in a decrease in macrophage accumulation within the kidney and reduced renal injury (Holdsworth, Neale et al. 1981). T cell dependent macrophage recruitment has been shown to be the crucial effector response in anti-GBM disease in rats, with macrophage depletion using clodronate resulting in decreased proteinuria (Huang, Tipping et al. 1997). Additionally, macrophages have an important role in the progression of experimental glomerulonephritis. By selectively ablating tissue macrophages at days 15-20 after the initiation of a crescentic glomerulonephritis, disease

progression was terminated as demonstrated by a reduction in crescents, improved renal function and decreased proteinuria (Duffield, Tipping et al. 2005).

Supporting the importance of macrophage phenotype, several experiments have demonstrated that it's not just the mere presence of macrophages that causes disease, but it's their particular phenotype. This is clearly seen when murine macrophages were modulated ex-vivo (LPS to generate M1, IL-4/IL-13 to generate M2) then injected into a mouse with severe combined immunodeficiency (SCID- in which there is an absence of lymphocytes), in which adriamycin nephropathy was induced. Injection of M1 macrophages resulted in increased renal injury compared to M2 macrophages (Wang, Wang et al. 2007). In a similar model, treatment with M1 macrophages also resulted in more severe injury compared to treatment with resting macrophages, even when significantly more resting macrophages were injected (Wang, Cao et al. 2008). Additionally, IL-10/TGF-β modified macrophages attenuated renal injury (Cao, Wang et al. 2010). In a crescentic GN rat model, early treatment with IL-4 resulted in a decrease in glomerular inflammation and reduced macrophage activation (Cook, Singh et al. 1999). Additionally, transfer of IL-10 macrophages to ischemic rat kidneys protected against ischemic injury (Jung, Sola et al. 2012)

Further evidence to support the presence of a protective macrophage phenotype has been recently reported using the ischaemia/reperfusion model of renal injury with 2 different macrophage depleting strategies. These strategies included administration of diphtheria toxin in a mouse transgenic for the human diphtheria toxin receptor under the control of the CD11b promoter, or the administration of liposomal clodronate to deplete macrophages. These different techniques resulted in very different outcomes, with respect to renal function and renal damage, with clodronate mediated macrophage depletion resulting in less renal injury. Clodronate did not deplete all the macrophages, leaving CD206 (mannose receptor)-positive renal macrophages intact as well as some resident CD11c positive cells, suggesting that these cell populations are renoprotective. These cells may survive clodronate administration due to a decrease in phagocytic properties, or by not being accessible to the liposomal clodronate (Ferenbach, Sheldrake et al. 2012). Additionally, particular macrophage pattern recognition receptors may influence the outcome of crescentic glomerulonephritis. Mice deficient in mannose-receptor are

protected from nephrotoxic nephritis, in part due to decreased macrophage phagocytosis, and due to an interaction between macrophages and mesangial cells resulting in a less-inflammatory phenotype of macrophage and therefore disease protection (Chavele, Martinez-Pomares et al. 2010).

The Wistar Kyoto (WKY) rat is very susceptible to induction of crescentic glomerulonephritis, unlike the resistant Lewis (LEW) strain of rat. Genetic studies from congenic WKY-LEW strain combinations have demonstrated the importance of macrophage activation in determining glomerular damage in this model of immune-mediated passive nephrotoxic nephritis(Behmoaras, Smith et al. 2010). Using the same susceptible rat strain, but another model of GN, experimental autoimmune glomerulonephritis, EAG, induced by immunisation with glomerular basement membrane extract or purified alpha3 chain of type IV collagen, macrophage activation, partly through Fc receptor mediated activation, was found to be an important factor in disease susceptibility. This was demonstrated by Lewis and WKY BMDMs having significant differences in Fc receptor mediated oxidation, as well as WKY BMDMs demonstrating increased phagocytosis as well as increased MCP-1 secretion in response to LPS compared to the resistant Lewis strain. Additionally, the susceptibility to a crescentic GN in this model seemed to be independent of the levels of antibody to alpha3 chain type IV collagen (Reynolds, Cook et al. 2012).

1.2.4.2 T cells

T cells are commonly found within glomerular lesions in several different types of immune-mediated glomerulonephritis. In renal biopsies of patients with rapidly progressive glomerulonephritis, including AAV, there is prominent T cell and macrophage infiltration, which is absent in less inflammatory renal diseases (Cunningham, Huang et al. 1999), while T-cells in proliferative lupus nephritis are correlated with the number of cellular crescents and a poor outcome following induction therapy (Couzi, Merville et al. 2007). In addition, there is extensive experimental evidence to demonstrate their critical role in mediating disease, often as part of a delayed-type hypersensitivity (DTH) response, characterised by activated T cells and macrophages.

1.2.4.2.1 CD4+ T cells

CD4+ T cells appear to be the most important subtype of T cell involved in mediating renal injury in experimental glomerulonephritis, with the Th1 cytokine response dominating.

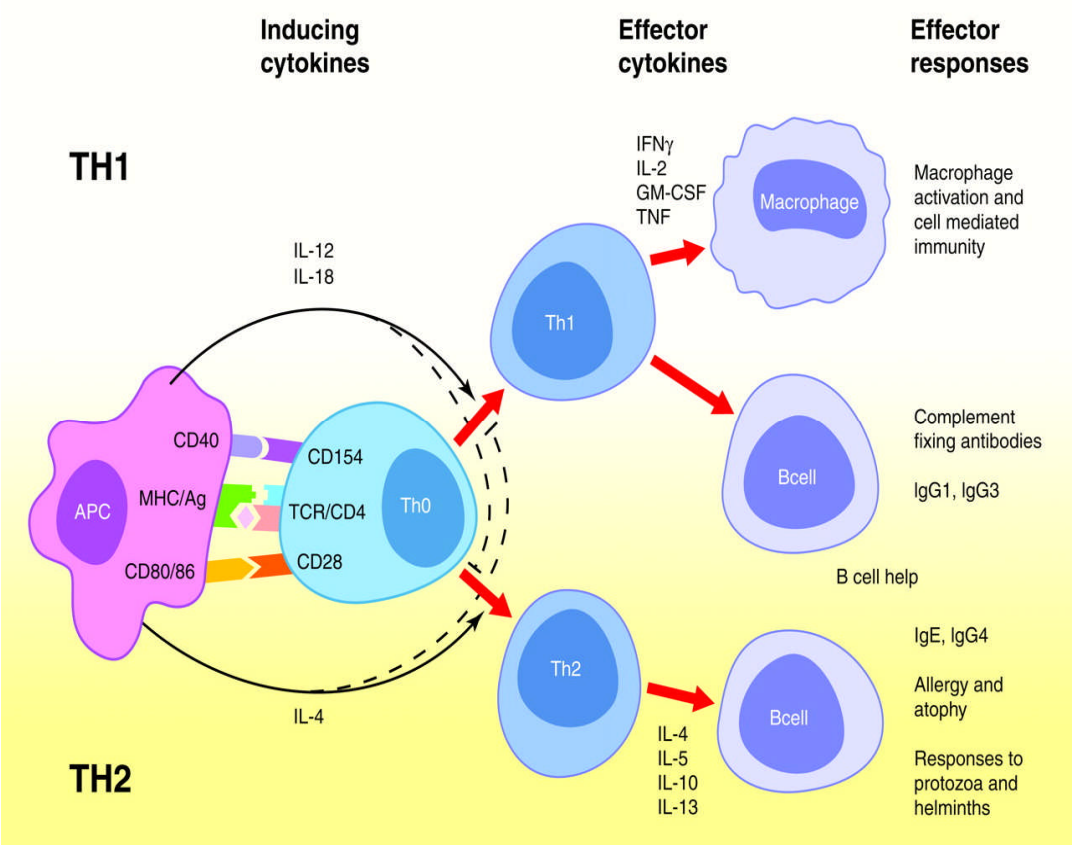

Figure 1-4 Diagram to demonstrate the differentiation of CD4+ T cells

CD4+ T cells differentiate intoTh1 and Th2 T cells under the influence of different cytokines with resulting effector responses. The Th1 response is important in a crescentic glomerulonephritis (Tipping and Holdsworth 2006).

The role of the Th1 response has been demonstrated by comparing 2 different mouse strains which demonstrate either a Th1 polarised response (C57BL/6) or a Th2 response (BALB/c) when injected with sheep anti-mouse nephrotoxic serum. Following induction of disease, C57BL/6 mice demonstrate a severe crescentic GN with both T-cell and macrophage infiltration, and cytokine profiles consistent with a Th1 response. Depletion of CD4 cells in this model using a monoclonal antibody attenuated disease, demonstrating the critical role for T cells. In the Th2 prone BALB/c mice, renal injury was significantly diminished, and was not dependent on T cells (Huang, Tipping et al. 1997). Th1 responses also predominate in murine anti-GBM disease, induced by immunisation with GBM in adjuvant, with increased production of INF-γ and diminished IL-10 production, typical of a Th1 response (Hopfer, Maron et al. 2003). Further evidence to support the importance of IFN-γ in mediating disease, and the protective effect of Th-2 cytokines is demonstrated by attenuated disease in IFN-γ deficient animals and increased disease in IL-4 or IL-10 deficient mice (Kitching, Tipping et al. 1998; Kitching, Holdsworth et al. 1999). Interestingly, to confirm the importance of cellular immunity, mice with a deletion in the mu-immunoglobulin heavy chain, which are unable to develop mature B cells, or produce any immunoglobulin, but retain an intact cell-mediated immune response, were used for induction of nephrotoxic nephritis. These mice still developed crescents and renal disease with similar severity of renal injury as wild-type mice (Li, Holdsworth et al. 1997). Regulatory T cells (CD4+CD25+ [Treg]) have an important role in the maintenance of tolerance. T regs have been transferred into mice prior to the administration of NTS during NTN, with the resultant reduction in renal injury and proteinuria. The transferred T regs were located in the secondary lymphoid organs and exerted potent immunosuppressive effects with the resultant decrease in kidney expression of pro-inflammatory cytokines as well as isolated splenocytes demonstrating a decreased production of Th-1 associated cytokines. The mice that received T regs had a similar humoral response to the control mice. This demonstrates that regulatory T cells counterbalance the actions of autoreactive T cells (Wolf, Hochegger et al. 2005).

In vasculitis the importance of T cells has also been demonstrated. GPA patients in remission, demonstrate differences in the homeostasis of CD4+ T cells compared to healthy controls. These patients demonstrate a lower proportion of naive T cells with an increase in

effector memory T cells, suggesting a persistent antigenic signal. Additionally in remission patients, the effector memory cells demonstrate a Th2 phenotype (Abdulahad, van der Geld et al. 2006). There are also abnormalities in both the number and function of regulatory T cells in patients with GPA, with patients demonstrating an increase in effector T cells, with a relative imbalance of effector and regulatory T cells. Regulatory T cells in this study were shown to play an important role in controlling the autoantigen-specific effector T cell response to PR3, with ANCA positive patients showing an increased T cell proliferation compared to ANCA negative patients and healthy controls, therefore illustrating the important role of regulatory T cells to prevent relapse during disease remission (Morgan, Day et al. 2010). The antigens in AAV, MPO and PR3, have been demonstrated to stimulate proliferation of CD4+ cells from patients, but also from healthy controls (Popa, Franssen et al. 2002). Work in our group has demonstrated that patients with MPO-AAV have diminished MPO-specific Th1 cell responses during remission compared to acute disease, but this attenuated response is not due to suppression by antigen specific regulatory T cells (Chavele, Shukla et al. 2010). A further study demonstrating the functional and phenotypic differences of T cells in AAV patients further confirms a persistently activated T cell population in patients, with impaired IL-10. (Marinaki, Neumann et al. 2005)

1.2.4.2.2 CD8 cells

There is less evidence exploring the role of CD8+ T cells in either human glomerular disease or experimental GN. Early work demonstrated that development of a crescentic glomerulonephritis in the murine nephrotoxic nephritis model was dependent on CD4 cells, with the absence of CD8 cells accelerating disease (Tipping, Huang et al. 1998). By contrast, in experimental autoimmune glomerulonephritis in the susceptible WKY rat, administration of an anti-CD8 monoclonal antibody either at the time of disease induction or during disease progression, resulted in a significant reduction in renal injury, suggesting an important role for CD8 cells in disease pathogenesis in this particular model (Reynolds, Norgan et al. 2002).

1.2.4.2.3 Th17 cells

IL-17A is a relatively newly described cytokine that has been implicated in autoimmunity. IL-17A belongs to a family of several cytokines. IL-17 is now known not just to be produced by

T cells (Th17 cells), but also by many cells on the innate immune system such as macrophages, dendritic cells and natural killer cells amongst others. CD4+ cells differentiate to Th17 subtype under the influence of the cytokines IL-1, IL-6 and TGF-β. Once differentiated, IL-23- a member of the IL-12 family, is required for the cells to proliferate and maintain their phenotype (Korn, Bettelli et al. 2009). Additionally, the steroid receptor-type nuclear receptor RORγt has a critical role in the differentiation of Th17 cells as well as IL-17 production (Ivanov, McKenzie et al. 2006). The IL-17 receptor is expressed ubiquitously (Yao, Spriggs et al. 1997).

Work done in our laboratory by Dr Sally Hamour, has demonstrated that in patients with acute AAV, serum levels of IL-17 and IL-23 are significantly increased compared to controls, and remain increased in a proportion of patients during disease remission. Additionally, increased frequencies of autoantigen-specific IL-17 producing cells were found in patients compared to healthy controls therefore demonstrating a potential role in contributing to disease (Nogueira, Hamour et al. 2010). Kidney biopsies of patients with AAV demonstrate the presence of IL-17 cells within the glomeruli and interstitium, with a suggestion that neutrophils may be the source of IL-17 in acute disease (Velden, Paust et al. 2012). IL-17 has been shown to have a role in experimental glomerulonephritis. IL-17 increases the production of proinflammatory cytokines, such as MCP-1, which plays an important role in the recruitment of both T-cells and monocytes to mesangial cells. Mice deficient in IL-23 p19 and IL-17 demonstrated less T-cell infiltration and less severe disease compared to wild-type mice (Paust, Turner et al. 2009). Γδ T cells have also been shown to produce IL-17 in experimental glomerulonephritis within the kidney and to contribute to disease by enhancing neutrophil recruitment into the kidney (Turner, Krebs et al. 2012). In a mouse model of autoimmunity to MPO, mice deficient in IL-17 were protected against renal disease, with less neutrophil infiltration and a decrease in macrophage recruitment, perhaps as a result of decreased delayed type hypersensitivity responses to the planted neutrophil autoantigens (Gan, Steinmetz et al. 2010). Interestingly, IL-17 seems to play different roles at different times during the course of experimental GN. In NTN, IL 17-/- mice developed less disease early in the model at day 6 compared to WT animals. This protection becomes less prominent by day 14, with similar infiltration of neutrophils and macrophages in both animal groups. However, by day 21, both WT and IL-17-/- mice had established crescentic

GN with the IL-17-/- mice demonstrating more severe disease, with a profound upregulation of the Th1 associated cytokine INF-γ (Odobasic, Gan et al. 2011).

1.2.4.3 B cells

B cells are known to contribute to both humoral and cellular immunity by acting as precursors to antibody producing cells, and through antigen presentation and expansion of the population of regulatory T cells mediated through expression of co-stimulatory molecules that are required for T cell activation, such as CD80, CD86 and CD40 (Sfikakis, Souliotis et al. 2007). In patients with AAV, treatment with B-cell depleting agents such as rituximab has generated very promising results (Jones, Tervaert et al. 2010; Stone, Merkel et al. 2010) suggesting that B cells have an important role in disease pathogenesis. In an experimental model of auto-immune MPO associated crescentic GN, mice deficient in B cells (μMT-/-) still develop renal injury with infiltration of CD4+ T cells, macrophages and neutrophils demonstrating that the presence of B cells is not a critical requirement in causing disease in this particular model (Ruth, Kitching et al. 2006). This is supported by another study using nephrotoxic nephritis in which mu-chain deficient mice had the same response as wild-type mice, with respect to renal injury, despite a lack of B cells and absence of immunoglobulin (Li, Holdsworth et al. 1997).

B cells have a complicated role in relation to autoimmunity, with infrequently reported cases of increased autoimmunity following B cell depletion therapies with rituximab (Dass, Vital et al. 2007; El Fassi, Nielsen et al. 2008). Additionally, a subset of B cells called regulatory B cells, are thought to play an important role in immune tolerance, mediated through their IL-10 production (Xiao, Brooks et al. 2012). In patients with vasculitis, a population of CD25+ B cells have been identified that are present in patients in remission. Although this study suggested that this population of cells may have 'immunoregulatory' properties, there was a lack of functional data to support this claim (Eriksson, Sandell et al. 2010). A population of IL-10 secreting B cells in humans does exist, which are able to influence cytokine secretion of monocytes in-vitro (Iwata, Matsushita et al. 2011). However, the role of this subset of IL-10 secreting regulatory B cells in AAV is yet to be fully determined.

1.2.4.4 Neutrophils

In the nephrotoxic nephritis animal model, the infiltration of neutrophils is an early response, occurring 2 hours after injection of nephrotoxic serum, and has a crucial role in mediating glomerular injury (Cochrane, Unanue et al. 1965). Early experiments demonstrated this by depleting neutrophils with nitrogen mustard (cyclophosphamide precursor), which resulted in attenuation of renal injury (Naish, Thomson et al. 1975).

Neutrophils have been shown to have a crucial role in mediating vasculitis and glomerular injury in humans. The interaction of ANCAs with neutrophils results in the production of reactive oxygen species (ROS) and neutrophil degranulation, a process further enhanced by priming with TNF (Falk, Terrell et al. 1990).

Additionally, recent work has demonstrated further mechanisms by which neutrophils play an important role in disease pathogenesis. Cellular microparticles are membrane vesicles released from several cell types, including neutrophils and endothelial cells, following cell activation or apoptosis and are pro-inflammatory. Primed neutrophils release microparticles in response to ANCA, which express PR3 and MPO, and are able to bind to the endothelium where they have several effects including increased release of endothelial IL-6 and IL-8 as well as upregulation of ICAM-1. The overall result is induction of an inflamed and thrombogenic endothelium (Hong, Eleftheriou et al. 2012).

Neutrophil extracellular traps (NETs) formation constitutes a newly described process of extracellular microbe killing by the release of chromatin fibres by neutrophils (Brinkmann, Reichard et al. 2004). NET formation can be triggered by incubation of neutrophils with ANCA, but not by incubation with control IgG, and there is evidence of deposition of NETs within areas of inflamed kidney including the glomeruli (Kessenbrock, Krumbholz et al. 2009). Recent work has demonstrated that myeloid dendritic cells (mDC) co-cultured with NETotic PMN and subsequently used to immunise mice, resulted in induction of murine auto-antibody production including the production of ANCA and development of glomerulonephritis (Sangaletti, Tripodo et al. 2012).

1.2.4.5 Mast cells

Mast cells are present throughout extravascular tissues where they have several roles, such as the hypersensitivity reactions found in asthma involving the IgE-mediated release of inflammatory mediators. There are additional IgE-independent mechanisms of inflammation, involving proteases such as histamine, tryptase and chymase, stored in cytoplasmic granules and released from mast cells (Caughey 1991). It is increasingly recognised that mast cells may have a role in human glomerulonephritis, with the accumulation of mast cells in the interstitium in rapidly progressive glomerulonephritis correlating with the frequency of glomerular crescents, as well as co-localising with α-SMA (smooth muscle actin) positive myofibroblasts, with mast cell products such as tryptase and chymase having fibroblast mitogenic activity and increasing collagen synthesis (Toth, Toth-Jakatics et al. 1999). Mice deficient in mast cells (KitWWv) have less crescent formation, decreased infiltration of macrophages and T cells and decreased glomerular expression of adhesion molecules, such as P-selectin, in a non-accelerated anti-GBM mouse model. Reconstitution by WT mast cells, in deficient mice, restores disease to levels found in WT mice (Timoshanko, Kitching et al. 2006). Additionally, mice that are deficient in the mouse mast cell protease-4 (mMCP-4) (a homolog of human chymase- demonstrated to have pro-inflammatory properties) have less severe kidney disease with respect to less proteinuria and improved renal function as measured by serum urea as well as less glomerular hypercellularity, tubular necrosis and a decreased mononuclear cell infiltrate in the later stages of the accelerated anti-GBM model. mMCP-4 was demonstrated to play a role in type 1 collagen deposition within the kidney, a process associated with fibrosis (Scandiuzzi, Beghdadi et al. 2010).

However, the evidence that mast cells promote disease in experimental glomerulonephritis is conflicted with reports of mast cells having a protective role in disease pathogenesis. In accelerated nephrotoxic nephritis, Kit WWv mice deficient in mast cells, had greater glomerular injury and mortality that their WT counterparts, with increased macrophage and T cell infiltration. (Hochegger, Siebenhaar et al. 2005). In a model of NTN in which Tregs were adoptively transferred, Treg derived IL-9 was implicated to have a role in mast cell recruitment to the local inflammatory lymph node which results in a immunosuppressant

effect. However, the exact mechanisms by which mast cells have this immunosuppressive effect in the local lymph node were not elucidated to (Eller, Wolf et al. 2011). A recent study explores the relationship between mast cells and Treg in autoimmunity. Mast cell deficient mice (Kit(W-sh/W-sh)) immunized with myeloperoxidase resulted in a greater production of myeloperoxidase specific CD4+ T cells and more severe glomerular injury compared to WT mice. Mast cell deficient mice also had a decrease in Tregs and reduced IL-10 production. This was reversed by reconstitution of WT bone marrow. The role of mast cell enhancement of IL-10 production was confirmed by in-vitro experiments (Gan, Summers et al. 2012).

1.2.4.6 Dendritic cells

Dendritic cells are important antigen presenting cells (APC). First identified as skin Langerhans cells in 1868, they are now increasingly recognised as having a role in both innate and adaptive immunity, with different phenotypes of cell now being identified according to various cell surface markers, and different DC subsets having the ability to skew cytokine production towards Th1 or Th2. Additionally, DC may originate from either monocyte-derived myeloid DCs or plasmacytoid-derived DCs. Dendritic cells are present in most tissues promoting the immune response to foreign antigens as well as tolerance to self-antigens. They have the ability to take up and process antigens, then migrate to lymphoid organs and present to antigen specific T-cells through extensive MHC complexes at the cell surface with up-regulation of co-stimulatory molecules. Dendritic cells are also able to stimulate the production of antibodies and B cell proliferation (Banchereau and Steinman 1998). In the kidney, there is an extensive network of resident dendritic cells.

In patients with AAV, there is a decrease in circulating plasmacytoid Dc (pDC) and myeloid DC during both active and inactive disease, with increased CD62L expression, which has a role in DC migration to lymph nodes. This decrease in DCs may subsequently impact on Tregs, resulting in a DC-mediated decrease in Treg suppressive function (Rimbert, Hamidou et al. 2011). In the kidney biopsies of patients with ANCA associated glomerulonephritis, aggregates of DCs are seen around the glomeruli and the peri-tubular interstitial compartment, with immature DCs co-localising with T cells, although it is unknown whether DCs here are having a pro-inflammatory effect or dampening down the immune response (Wilde, van Paassen et al. 2009). In addition, PR3 itself has been demonstrated to induce

dendritic cell maturation, similar to that seen with TNFα. PR3-treated dendritic cells were also able to stimulate auto-antigen specific CD4+ T cells, which were subsequently able to produce IFNγ, therefore influencing Th1 polarisation of CD4+ T cells (Csernok, Ai et al. 2006).

In experimental glomerulonephritis, the role of DCs is unclear with DCs having both protective and detrimental effects during disease. DC depletion during NTN using the diphtheria toxin mouse model, resulted in worse disease possibly due to a reduction in regulatory T cells (Scholz, Lukacs-Kornek et al. 2008). However, when DC are depleted in the later stages of NTN (day 7), macrophage and T cell infiltration is decreased and there is a reduction in crescent number. Co-culture of kidney DC, isolated from normal control kidneys and also from nephritic mice during NTN (day 10), with CD4+T cells, DCs stimulate the production of proinflammatory cytokines (TNF-α, IFN-γ, IL-17, IL-6) as well as IL-10 (Hochheiser, Engel et al. 2011).

1.2.4.7 Complement

The complement system is a crucial constituent of the innate immune system. It is activated by 3 different pathways: classical, lectin and alternative, leading to cleavage of C3 and the generation of C3a and C3b. Their deposition on the surface of a pathogen results in its removal by the phagocytic system or damage by the membrane attach complex. It is a system tightly regulated by both circulating factors as well as membrane bound inhibitors. Activation of the classical pathway is due to C1q binding to antibody- antigen complexes while the lectin pathway is stimulated in response to carbohydrate ligands on the surface of organisms, recognised by soluble mannose-binding lectin. Alternative pathway activation in the plasma occurs continuously; with the hydrolysis of C3 resulting in an amplification of a loop with the generation of more C3b. It is regulated by inhibitory molecules such as factor H and factor I, which allow for controlled turnover of the pathway. Activation of the complement system has long been recognised to play an important role in diseases such as SLE. Additionally, mutations in the regulatory components are now recognised causes of atypical haemolytic uraemic syndrome which commonly affects the kidney.

In AAV, complement was initially thought not to play a role, due to the pauci-immune nature of the pathologic lesions. However, there is now evidence from both human and

animal work which challenges this idea. In patients, complement activation during active AAV may be found, with elevated levels of numerous complement components including C3a, C5a and membrane attack complex. In addition, alternative pathway activation was shown to be important by elevated plasma Bb levels which correlated with disease activity, as assessed by Birmingham vasculitis activity score- (BVAS) and the number of glomerular crescents (Gou, Yuan et al. 2012).

The role of complement was demonstrated in animal models, using the MPO-model of vasculitis. Depletion of complement using cobra venom factor protects WT mice from disease, despite the formation of circulating antibodies against MPO. Additionally, mice deficient in complement C5 are also protected from disease, as are factor B deficient mice, confirming the role of the alternative pathway in disease induction. Human TNF-α primed neutrophils, when stimulated with MPO-ANCA or PR3-ANCA, generated C3a, which did not occur following stimulation with control IgG (Xiao, Schreiber et al. 2007). In support of C5a being a potential therapeutic target, inhibition of C5a, both prior to disease induction and, more relevantly, following induction of disease, resulted in attenuation of the renal lesions (Huugen, van Esch et al. 2007). C5a generation has been demonstrated following neutrophil incubation with MPO-ANCA or PR3-ANCA, and animals deficient in C5a-receptor are protected from disease in the same MPO-ANCA animal model, with C5a-receptor on neutrophils playing an important role (Schreiber, Xiao et al. 2009).

1.2.4.8 Fc receptors

Fc-receptors (Fc-R) are present on many cells of the immune system and appear critical to the generation of glomerulonephritis. In mice, there are several different Fc-receptors with varying affinities for IgG; the high affinity activatory FcγRI (interacting with IgG2a) and the lower affinity receptors FcγRII (inhibitory) and FcγRIII (activatory and interacting with IgG1, IgG2a, IgG2b). Although mice deficient in FcRγ have antibody bound to the glomerular basement membrane in the nephrotoxic nephritis model, they are protected from nephritis (Park, Ueda et al. 1998). To assess whether circulating or resident renal cell Fcγ expression contributed to the pathogenesis of nephrotoxic nephritis, bone marrow chimeras were created which demonstrated the importance of Fcγ expression on bone marrow derived cells in mediating disease, with no role for Fcγ expression on resident cells (Tarzi, Davies et

al. 2002). To further elucidate the roles of the different activatory receptors, mice deficient in FcγRIII or FcγRI/III were subjected to NTN, and it appeared that both FcγRI and FcγRIII play a role, with absence of both of these receptors necessary for significant protection from disease (Tarzi, Davies et al. 2003).

FcγRII is a low affinity inhibitory IgG receptor. Mice that are deficient in this receptor demonstrate an increased incidence of glomerulonephritis compared to wild-type mice in an anti-GBM model of renal disease. This receptor needs to be absent on a combination of cells for an increased incidence of disease, with deletion in B cells or myeloid cells alone not being sufficient (Sharp, Martin-Ramirez et al. 2012).

The Wistar Kyoto (WKY) rat is highly susceptible to a crescentic glomerulonephritis following passive nephrotoxic serum transfer, unlike the Lewis strain. Genomic screening identified 2 loci which were associated with crescentic glomerulonephritis, with the activatory Fc receptor, Fcgr3*,* identified as a likely candidate within one of the loci. WKY macrophages additionally showed enhanced antibody-dependent cellular cytotoxicity, explained by the absence of an inhibitory Fcgr3-related sequence, found in the less susceptible Lewis strain, which allows FcR-mediated macrophage over activity. In keeping with this finding, human studies demonstrated that reduced copy number of FCGR3B, the human orthologue of rat Fcgr3 is a risk factor for development of lupus nephritis (Aitman, Dong et al. 2006). Another study in humans confirmed an association between low FcgRIIIB copy number and a risk of developing both SLE and AAV, with the impaired clearance of immune complexes implicated in SLE and enhanced neutrophil activation in AAV suggested as proposed mechanisms (Fanciulli, Norsworthy et al. 2007). Additionally, FcR genotypes that affect disease phenotype have been identified, with the NA1 allele of FCGR3B having an effect on the severity of renal disease in patients with GPA (Kelley, Monach et al. 2011).

1.2.4.9 Toll-like receptors

Toll like receptors (TLRs) are expressed on a variety of leucocytes as well as parenchymal cells. They recognise pathogen-associated molecular patterns (PAMPs) as well as danger-associated molecular patterns (DAMPs). TLRs can be divided into receptors on the cell surface (TLR4, TLR2, TLR1, TLR6, TLR5), and intracellular receptors (TLR3, TLR7, TLR8, TLR9).

Once stimulated, a signal transduction pathway is initiated with myeloid differentiation factor 88 (MyD88) playing an important role in the subsequent transcription of several key cytokines which have a role in the inflammatory response. TLRs have been demonstrated to be expressed within renal tissue (Robson 2009). Mouse renal tubular cells in vitro have been demonstrated to express TLR1,-2,-3,-4 and -6, with the upregulation of TLR2,-3 and -4 in response to LPS. Human and murine mesangial cells have been demonstrated to express TLR1 and TLR4, with TLR3 expression in intracellular endosomes, TLR2, TLR4 and TLR6 have been demonstrated to be induced in mesangial cells following stimulation with TNF-α and IFN-γ (Anders and Schlondorff 2007)

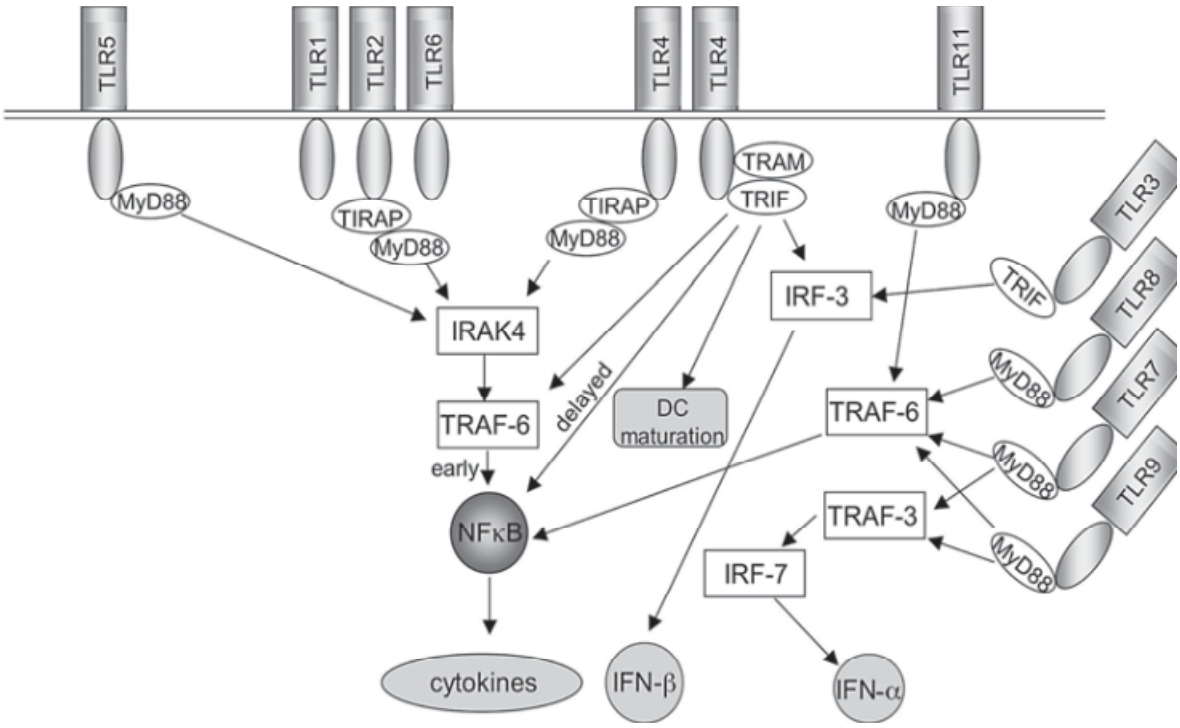

Figure 1-5 Diagram to demonstrate the site and signalling pathways of the TLRs.

The cell surface receptors signal through MyD88 resulting in the activation of nuclear factor κB (NKκB) as well as a MyD88 independent pathway (TRAF- TNF receptor- associated factor; IRAK- IL-1R-associated kinase; IRF- IRN regulatory factor, DC- dendritic cell) (Robson 2009).

The link between infection and glomerulonephritis is well known. Components of pathogens are able to bind to TLRs and therefore may contribute to disease by stimulating the production of pro-inflammatory cytokines. TLR2 recognises molecular patterns associated with both gram positive and gram negative bacteria and a synthetic TLR2 agonist administered at the time of nephrotoxic nephritis induction , results in more severe disease compared to mice not immunised with the TLR2 agonist (Brown, Sacks et al. 2006). In a murine MPO model, mice were injected with MPO plus a TLR2 or TLR9 ligand, followed by a sub-nephritic dose of sheep anti-mouse GBM 14 days later. The addition of the TLR ligands resulted in enhanced autoimmunity and greater renal injury. A TLR9 ligand resulted in an enhanced Th1 response with increased glomerular macrophage infiltration, and the addition of a TLR2 ligand resulted in greater neutrophil recruitment and increased IL-17 production (Summers, Steinmetz et al. 2011).

TLR4, the LPS receptor, is of particular interest as it has been demonstrated that calprotectin (S100A8/A9) is one of its endogenous ligands (Vogl, Tenbrock et al. 2007) (discussed further in section 1.4). TLR4 plays an important role in experimental glomerulonephritis demonstrated using both the heterologous and accelerated nephrotoxic nephritis models, the former which is characterised by early neutrophil influx following administration of the sheep anti-mouse GBM antibody. TLR4 has been shown using in-situ hybridization to be expressed in normal kidney on mesangial cells parietal and visceral glomerular epithelial cells. Lipid A is a pure TLR4 agonist and was administered at the same time as nephrotoxic serum to both WT and TLR4 deficient mice. TLR4-/- mice were protected from neutrophil influx, despite similar glomerular sheep IgG deposition. Since TLRs are present on both bone marrow and non-bone marrow derived cells, bone marrow chimeras were generated and demonstrated that both these cell types contributed to disease. Mesangial cells stimulated with LPS produce chemokines which have an important role in neutrophil chemotaxis through TLR4 (Brown, Lock et al. 2007). Further studies have shown that TLR4 stimulation in the autologous accelerated NTN model (pre-immunised with sheep IgG and Complete Freund's Adjuvant) resulted in disease exacerbation. Bone marrow chimeras demonstrated that it is renal cell TLR4 stimulation which promotes glomerular crescent formation and thrombosis following LPS and NTS administration (Giorgini, Brown et al. 2010).

In the experimental anti-MPO glomerulonephritis animal model, administration of a highly purified LPS with MPO resulted in a synergistic effect on glomerular neutrophil influx, an effect mediated through TLR4 (Summers, van der Veen et al. 2010). Confocal microscopy demonstrated that TLR4 co-localised with glomerular endothelial cells, while other renal cells types such as podocytes and possibly mesangial cells, also expressed this receptor. Bone marrow chimeras demonstrated bone marrow derived TLR4 had a more prominent role with respect to glomerular neutrophil recruitment, but TLR4 expression was required on both bone marrow and tissue derived cells for maximal neutrophil recruitment. Mice administered LPS and anti-MPO antibodies demonstrated that the increased expression of chemokines important for neutrophil recruitment (CXCL1 and CXCL2) was partly dependent on TLR4. (Summers, van der Veen et al. 2010).

In patients with AAV, there is increased expression of TLR2 in monocytes, and an increase in monocyte TLR4 expression in a subset of patients. Additionally, NK cells express several TLRs (TLR2, 4 and 9), with an increased proportion of TLR-expressing NK cells in patients compared to healthy controls (Tadema, Abdulahad et al. 2011).

1.2.4.10 Mesangial cells

Mesangial cells, along with endothelial cells and podocytes, form a network of closely interacting cells within the glomerulus. Mesangial cells are considered to be a modified smooth muscle cell. The cells are present within their matrix therefore providing structural support to the glomerular tuft. Components of the matrix are able to influence mesangial cell proliferation and activation (Schlondorff and Banas 2009). Mesangial cells have several important roles. They have been demonstrated to play a role in the regulation of glomerular ultrafiltration as well as efferent arteriolar resistance (Blantz, Gabbai et al. 1993). Mesangial cells are able to sense and subsequently respond to capillary stretch and therefore to glomerular pressure, and respond by the release of vasoactive substances, for example TGF-β1 (Riser, Cortes et al. 1996). Finally, mesangial cells play an important role during glomerular inflammation. They secrete MCP-1 and IL-8, as well as the monocyte attractant, RANTES (regulated upon activation, normal T cell expressed and secreted), and express the chemokine receptor CCR1 (Banas, Luckow et al. 1999). Mesangial cells demonstrate increased levels of RANTES and ICAM-1 mRNA after stimulation with TNF-α or aggregated

IgG, both of which have a role in leukocyte recruitment (Satriano, Banas et al. 1997). In-vitro studies have demonstrated that mesangial cells are able to secrete and respond to several cytokines, such as IL-1β, TNF-α, PDGF (Cove-Smith and Hendry 2008). Further studies have demonstrated the importance of leukocyte derived IL-1β in crescentic glomerulonephritis in the mouse NTN model, with the intrinsic renal cells (which are composed of mesangial cells amongst others), being the primary target, as a lack of IL-1RI on intrinsic renal cells offers a degree of protection against renal disease (Timoshanko, Kitching et al. 2004). Another cytokine produced by intrinsic renal cells which plays an important role in nephrotoxic nephritis is IL-12. IL-12 has several important effects on T cells including priming CD4 cells to produce high quantities of IFN-γ as well as polarising T cells to a Th1 phenotype. Again, bone marrow chimeric mice have demonstrated the importance of intrinsic renal cell production of IL-12 in the development of a crescentic glomerulonephritis (Timoshanko, Kitching et al. 2001), with in-vitro work demonstrating that mesangial cells are able to produce this cytokine (Bussolati, Mariano et al. 1999).

Mesangial cells also express Fc receptors and can bind immune complexes with the resultant production of reactive oxygen species (ROS) (Santiago, Satriano et al. 1989). MCP-1, a mediator of monocyte/macrophage recruitment and accumulation, is also synthesised and released in response to FcR engagement on mesangial cells (Hora, Satriano et al. 1992). Mesangial cell lines derived from the susceptible WKY rat produce increased amounts of MCP-1 basally and following IgG or TNF-α stimulation, when compared to the Lewis rat, which is resistant to renal injury (Smith, Lai et al. 2007).

There is an interesting interaction between macrophages and mesangial cells during inflammation, which is clearly of importance due to significant macrophage infiltration during glomerulonephritis. In the rat, autocrine and macrophage-derived production of nitric oxide has a detrimental cytotoxic effect on mesangial cells (Hruby and Beck 1997). Additionally, activated rat macrophages isolated from either bone marrow or from inflamed glomeruli, express inducible nitric oxide synthase, and following co-culture with mesangial cells, result in mesangial cell apoptosis and inhibition of mitosis (Duffield, Erwig et al. 2000).

Mesangial cells also play an important role in antigen presentation to CD4 T cells. IFN-γ induces expression of MHC class II in rat mesangial cells, and synergises with IL-1β and

TNFα, to induce a higher frequency of mesangial cells expressing MHC class II in a time and concentration dependent manner (Martin, Schwinzer et al. 1989). The importance of expression of MHC class II on intrinsic renal cells has been further demonstrated in the mouse using MHC II deficient mice. These experiments demonstrated that crescentic nephritis (in murine NTN) was an MHC II dependent process, with bone marrow chimeras, showing that the absence of MHC II on intrinsic radioresistant cells, with normal levels of MHC II on bone marrow derived cells, prevented renal injury (Li, Kurts et al. 1998). Additionally, glomerular CD40 expression during NTN has been shown to be important in disease, with mice deficient in non-bone marrow derived CD40 showing less T cell glomerular infiltration, less renal injury and decreased production of cytokines such as MCP-1 (Ruth, Kitching et al. 2003).

1.3 Animal Models

The experimental work in this thesis utilises the murine nephrotoxic nephritis (NTN) animal model. This has the advantage of being reproducible in genetically modified mice. This has greatly advanced the knowledge and understanding of the pathogenesis of immune-mediated glomerulonephritis. NTN is not an animal model of vasculitis, but it is a model of crescentic glomerulonephritis, characterised by T cell and macrophage infiltration, glomerular thrombosis and crescent formation, similar to many forms of immune mediated glomerulonephritis seen in humans. There is a reproducible MPO- ANCA and, more recently, a single report of a PR3-ANCA model of vasculitis and glomerulonephritis described, however these were not yet established in our laboratory.

1.3.1 Nephrotoxic nephritis

In 1900 W. Lindemann at the Pasteur Institute, developed a model of immune mediated glomerulonephritis by the injection of rabbits with anti-serum which had been developed in guinea pigs immunised with rabbit kidneys. NTN can be divided into 2 phases, the heterologous and autologous phases. The first heterologous phase is the early phase

occurring after injection of the nephrotoxic serum when the sheep or rabbit antibody is 'planted' on the glomerular basement membrane. This early response causes neutrophil infiltration, and proteinuria, and occurs within the first few hours (Cochrane, Unanue et al. 1965). The second autologous phase is characterised by an antibody response by the host to the heterologous globulin and occurs 5 to 6 days after the injection of nephrotoxic serum. It was noted that if animals were immunised with serum from the species in which the nephrotoxic serum was generated, prior to the injection with the NTS (pre-immunisation), then the appearance of nephritis was more rapid (Kay 1940).

1.3.2 Experimental autoimmune glomerulonephritis

The injection of human or animal GBM mixed with Complete Freud's adjuvant (CFA) into sheep consistently results in uraemia and death of the sheep with the characteristic finding of a severe progressive crescentic glomerulonephritis (Steblay 1962). This model has subsequently been refined in order to model the human disease more closely by the administration of homologous or isologous GBM antigens using the Brown-Norway strain of rat known to be susceptible to renal disease (Pusey, Holland et al. 1991). Experimental autoimmune glomerulonephritis (EAG) has also been replicated in several other stains of rat demonstrating that genetic differences are an important factor in inter-strain variability of disease, with the WKY rat demonstrating greatest susceptibility to this model with a severe GN, pulmonary haemorrhage and renal failure 4 weeks after disease induction (Sado, Naito et al. 1986). As with NTN, Lewis rats are resistant to disease induction. Following the identification of the target antigen in human Goodpasture syndrome (anti-GBM disease) as the non-collagenase domain of α3 chain of type IV collagen [α3(IV)NC1], the EAG model has been refined further using recombinant rat [α3(IV)NC1] or synthetic peptides derived from it. Immunisation of WKY rats with α3(IV)NC1 peptides induces glomerulonephritis and pulmonary haemorrhage, resembling human disease (Abbate, Kalluri et al. 1998). T cells have been demonstrated to play an important role in this model, as treatment with an anti-CD8 antibody either during initiation of disease, or more importantly, once disease was established, resulted in a significant reduction in disease severity demonstrated by an improvement in renal histology (Reynolds, Norgan et al. 2002). Similarly, treatment with an

anti-CD4 monoclonal antibody has been shown to inhibit the development of EAG in the rat (Reynolds and Pusey 1994).

1.3.3 Vasculitis animal models

In the past 10 years there have been numerous advances in the study of ANCA associated vasculitis due to the development of animal models which mimic the pauci-immune nature of human disease more closely and are dependent on ANCA, in contrast with models of crescentic GN which are mediated by immune-complex deposition. There are differences between human and murine PR3, which in part explains the difficulties in generating a model of PR3 vasculitis. However, there are now several models of MPO-ANCA vasculitis, which have provided evidence for the pathogenicity of ANCA.

Xiao et al described a MPO-ANCA model in 2002. Mouse MPO was purified and subsequently injected into mpo-/- mice at several time points, and was shown to induce anti-MPO antibodies. Transfer of isolated splenocytes into rag2-/- (recombinase-activating gene-2-deficient) mice lacking T and B cells, or of anti-MPO IgG isolated from the serum, into WT or rag2-/- recipients, induced vasculitis, necrotising crescentic GN and pulmonary haemorrhage (Xiao, Heeringa et al. 2002). To demonstrate the significance of neutrophils in this model, a monoclonal antibody to mouse neutrophils was administered which resulted in profound neutrophil depletion for up to 5 days. Neutrophil depletion prevented anti-MPO induced GN. These experiments demonstrated that glomerular neutrophil influx occurred at the areas of necrotising glomerular injury (Xiao, Heeringa et al. 2005). Another important factor in the pathogenesis in this model is complement activation with the generation of C5a and the subsequent priming of neutrophils (Schreiber, Xiao et al. 2009).

This model was subsequently refined by the same group. Similar to the previously described model in which mpo-/- mice were immunised with MPO, the mice with high titres of anti-MPO antibodies subsequently underwent lethal irradiation, but were rescued by bone marrow transplantation with WT bone marrow, creating a chimera that produced anti-MPO IgG and expressed MPO on its leukocytes. Mice with MPO positive bone marrow cells

(unlike the mice transplanted with MPO-/- bone marrow) went on to develop disease, (Schreiber, Xiao et al. 2006)

A further murine model has been described which explores the roles of both the humoral and effector arms of the autoimmune response in the pathogenesis of AAV. WT mice were immunised with human MPO in CFA, which resulted in the formation of anti-human MPO antibodies, and were subsequently injected with a sub-nephritogenic dose of NTS. Using mpo-/- mice, there was a reduction in CD4+ T cell, macrophages and neutrophil infiltration as well as significantly less crescent formation in the glomeruli despite these mice still generating an anti-MPO antibody response. CD4+ T cell depletion in WT mice also resulted in less glomerular injury despite an equivalent antibody response to MPO. In this model, B-cell deficient mice (µMT-/-) do not produce MPO-ANCA yet still develop a crescentic GN with a similar infiltration of CD4+ T cells, macrophages and neutrophils within the glomerulus. In this model, glomerular MPO is thought to act as a planted antigen which is then able to recruit effector cells (Ruth, Kitching et al. 2006). This model has not yet been replicated by other groups.

Rat models have also been described. The experimental autoimmune vasculitis model described a reliable, reproducible model of MPO-ANCA vasculitis in the susceptible WKY rat. Rats were immunised with human MPO in CFA, with development of anti-MPO antibodies. With increasing concentrations of human MPO, there was greater amount of pauci-immune renal injury as well as lung haemorrhage. The addition of further adjuvants, such as LPS or pertussis, resulted in a more consistent disease phenotype, although other rat strains still remained resistant to disease induction despite the generation of an antibody response to human MPO (Little, Smyth et al. 2009). These models do have their limitations. The murine model replies on the immunisation of mpo-/- mice with MPO, an alloantigen for mice which are naive to MPO. Additionally, the rat model relies on the use of adjuvants to reproduce a consistent crescentic glomerulonephritis. Therefore these models do not replicate the spontaneous breaking of tolerance, and induction of autoimmunity, which occurs in the human disease.

Until recently, there was no model of PR3-ANCA vasculitis due to numerous differences between both PR3 and anti-PR3 IgG in the mouse and human, and therefore there was a

lack of experimental evidence confirming the pathogenicity of PR3-ANCA. A PR3-ANCA model has now been developed which is based on generating mice with a humanised immune system. This used NOD-scid-IL2Rγ-/- mice which lack native T, B and NK cells and the IL2 receptor. Following irradiation the mice were transplanted with human stem cells. The mice were then injected with LPS to mobilise mature neutrophils and monocytes from the bone marrow and injected with human PR3-ANCA, while a subset of mice were injected with control human IgG. Mice that had been injected with human PR3-ANCA subsequently showed evidence of a pauci-immune GN, as well as evidence of pulmonary haemorrhage with patchy areas of haemorrhage and leucocyte recruitment. Although the extent of renal involvement in this model was mild, this model was the first to describe the pathogenicity of human PR3-ANCA in an animal model (Little, Al-Ani et al. 2012). However, an animal model replicating the human granulomatous disease seen in AAV has yet to be developed.

1.4 Calprotectin, mrp8/14, S100A8/A9

My thesis concentrates on a protein complex called calprotectin. This is a heterodimer composed of S100A8, also known as myeloid-related protein (mrp)-8 or calgranulin A, and S100A9, also known as mrp-14 or calgranulin B. The heterodimer is known as calprotectin as well as S100A8/A9 and mrp8/14. S100A8 and S100A9 preferentially form a heterodimer.

1.4.1 Introduction

The S100 proteins represent a family of proteins which obtained its name following isolation from bovine brain upon fractionation with 100% ammonium sulphate (Moore 1965). In humans, 25 members of the S100 family have been identified of which most form homodimers or heterodimers (Manolakis, Kapsoritakis et al. 2011). This family of S100 proteins are only found in vertebrates. S100A8 and S100A9, like the majority of S100 family of proteins, are EF-hand calcium binding proteins. The EF-hand motif is a helix-loop-helix structure, which typically undergoes a conformational change upon the central loop binding to Ca^{2+} (Yap, Ames et al. 1999). S100A8 and S100A9, form non-covalently associated complexes and, in the human, calcium induced tetramer formation (Vogl, Roth et al. 1999).

As well as the ability to bind calcium, this heterodimeric complex can also bind zinc, with anti-microbial activity (Sohnle, Hunter et al. 2000).

These proteins are expressed in cells of myeloid origin, such as neutrophils, monocytes and early differentiated macrophages (Lagasse and Clerc 1988). They are absent from normal tissue macrophages (Odink, Cerletti et al. 1987). They have been termed damage (or danger) associated molecular patterns (DAMPs) and are released from phagocytes at the site of inflammation and in response to cell damage. Recognition of damage associated molecular patterns (DAMPs) by pattern recognition receptors (PRR) is a crucial part of innate immunity providing host defence against invading microorganisms. The heterodimer constitutes 45% of neutrophil cytosolic proteins and about 1% in monocytes. Both S100A8 and S100A9 are similar to many of the other S100 proteins with respect to their coding pattern. The genes consist of 3 exons with 1 intron on chromosome 1q12-q21. Within the human bone marrow, the neutrophil precursor, the metamyelocyte, as well as early monocytes express the heterodimer. Since resident tissue macrophages do not express this complex, the complex is lost as monocytes differentiate into more mature macrophages except under inflammatory conditions (Hessian, Edgeworth et al. 1993). In human cells, S100A9 gets upregulated during monocyte maturation, expression of which correlated with expression of CD11b and CD14. In the development of neutrophils, S100A9 is detected in CD15+ cells (Goebeler, Roth et al. 1993). Both S100A8 and S100A9 mRNA in human monocytes is upregulated by TNF-α and IL-1β (Kido, Hayashi et al. 2005). Additionally, cell surface expression on monocytes has been shown to be increased by LPS and IFN-γ (Zwadlo, Schlegel et al. 1986). Monocytes which are positive for S100A8/A9 release substantial amounts of IL-1 and TNF-α (Bhardwaj, Zotz et al. 1992). In a study of human monocytes and the Th2 cytokines, the addition of IL-4 and IL-10 to stimulated monocytes resulted in decreased secretion of S100A8/A9, as detected by ELISA (Lugering, Kucharzik et al. 1997).

A study investigated the expression of these 2 proteins during murine haematopoiesis using a cloning technique. Cloning demonstrated a protein homology of 59% with the human counterpart, with the greatest homology between mouse and human located in the calcium binding regions, which is known to be conserved across species. In the murine spleen, the expression of mrp-positive cells correlates with markers of myeloid cells and are

predominantly located in the red pulp and marginal areas of the spleen, with the mrp-positive cells in the spleen and peripheral blood being myelomonocytic, monocytes and neutrophils. This study also demonstrated that the majority of non-activated tissue macrophages do not express this complex. During an animal model of peritoneal inflammation, high levels of S100A8 and S100A9 proteins in peritoneal neutrophils and monocytes were observed, which disappeared 4 days later despite the presence of macrophages (Lagasse and Weissman 1992). There are no differences between murine S100A9 and human S100A9 with respect to cellular localisation, quantity expression or its interaction with S100A8 (Nacken, Sopalla et al. 2000). Targeted disruption of the mrp8 (S100A8) gene results in embryo resorption by day 9.5 of development with infiltration of maternal leucocytes and resorption, and is therefore an embryologically lethal mutation (Passey, Williams et al. 1999). However, mrp-14-/- mice live a normal life span with no obvious abnormalities. The neutrophils in mrp-14 null mice express mrp-8 mRNA but lack the mrp-8 protein, agreeing with the human data that mrp-8 is unstable in the absence of mrp-14. The loss of these mrp proteins results in a decrease in neutrophil density but not in adhesion molecules, cell size or granularity. Additionally, there were no differences in apoptosis or cell death in neutrophils and monocytes of WT and mrp-14 null mice in response to calcium mobilisers, or to cytokines known to induce apoptosis and cell death. Lastly, there was no difference between WT and mrp-14 null mice in response to thioglycolate-induced peritonitis (Hobbs, May et al. 2003).

This complex of S100A8/A9 has additionally been demonstrated to be induced in wound keratinocytes and to be expressed during the hyperproliferative phase of cutaneous wound repair (Thorey, Roth et al. 2001). Human and murine S100A8 and S100A9 have also been detected in osteoclasts by immunohistochemistry (Zreiqat, Howlett et al. 2007). Additionally, S100A8 has been demonstrated to be induced in response to pro-inflammatory cytokines in murine microvascular cells, but there is no evidence of its binding partner S100A9 (mrp14) being induced (Yen, Harrison et al. 1997). Similarly, S100A8 mRNA is induced in murine fibroblasts following stimulation with fibroblast growth factor-2 (FGF-2), without detection of S100A9 mRNA. IL-1β also had the capacity to induce S100A8 in a primary fibroblast cell line (3T3) either alone or in conjunction with FGF-2 (Rahimi, Hsu et al. 2005). Additionally, an epithelial cell line has been demonstrated to be able to express this

complex of S100A8/A9, which was able to bind to keratin intermediate filaments in a calcium dependent manner (Goebeler, Roth et al. 1995). Dendritic cells are discussed in section 1.4.4 Isolated murine endothelial cells following treatment with TNF-α, upregulated S100A8 mRNA. However, secreted S100A8/A9 was not detectable, suggesting that the secretion must be significantly less than that of myeloid cells (Averill, Barnhart et al. 2011). Recent data demonstrated that a transcription factor, Kruppel-like factor-5 (KLF5) mainly expressed in renal collecting duct epithelial cells, upregulated S100A8 and S100A9 and induced monocyte recruitment in the unilateral ureteral obstruction (UUO) model. Direct injection of these proteins into the kidney, resulted in recruitment of inflammatory monocytes which subsequently developed into an M1 type of macrophage with the promotion of renal injury and inflammation (Fujiu, Manabe et al. 2011).

1.4.1.1 Intracellular roles of S100A8/A9

S100A8/A9 has a significant role in the transendothelial migration of phagocytes. In human monocytes, S100A8/A9 translocates from the cytoplasm to the cytoskeleton and the membrane in the presence of calcium, and co-localises with vimentin and microtubules and resulting in tubulin polymerisation and stabilisation (Roth, Burwinkel et al. 1993). Activation of p38 MAPK causes phosphorylation of S100A9 at site threonine 113 and in the presence of an elevation in intracellular calcium a conformational change in S100A9 occurs. As a result of this phosphorylation of S100A9, the complex no longer stabilises the microtubules and results in an inhibition of tubulin polymerisation. Small GTPases are activated and transmigration is facilitated. Mrp14-/- granulocytes demonstrate a decreased activation of small GTPases (Rac1 and Cdc42) which have an important role in cellular migration processes and actin metabolism. In a chamber assay, activation of p38 MAPK results in an increase in granulocyte transmigration whereas mrp14-/- granulocytes do not demonstrate an acceleration of migration compared to WT granulocytes (Vogl, Ludwig et al. 2004).

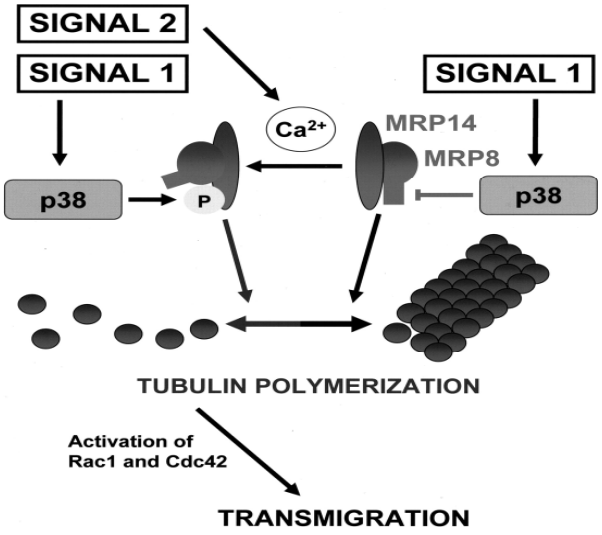

Figure 1-6 Effect of mrp14 on transmigration

The complex of mrp8/14 binds to and promotes the stabilisation of microtubules in phagocytes at rest. In the presence of 2 independent signals (activation of p38 MAKP and increase in intracellular calcium) there is a conformational change in the complex which allows phosphorylation of mrp14 (S100A9) and the resultant dissociation of the microtubules (Vogl, Ludwig et al. 2004)

S100A8/A9 may also have a role in phagocyte NADPH oxidase activity, an enzyme complex which results in the production of the superoxide anion. S100A8/A9 binds neutrophil arachidonoic (AA) acid in a calcium dependent manner and facilitates NADPH oxidase activation, potentially by transferring AA to the NADPH complex (Kerkhoff, Nacken et al. 2005).

1.4.1.2 Extracellular roles of S100A8/A9

The identification of elevated plasma levels of S00A8/A9 (mrp8/14) lead to the conclusion that this complex may have a role in the inflammatory process (Roth, Teigelkamp et al. 1992). The mechanism by which this complex is secreted and released by phagocytes has been investigated. Human monocytes release this complex in an energy dependent manner

involving protein kinase C activation. The secretory pathway is independent of the endoplasmic reticulum and Golgi apparatus and is dependent upon an intact microtubule network as secretion was inhibited by microtubule-depolymerisation agents (Rammes, Roth et al. 1997).

1.4.1.2.1 Phagocyte chemoattraction and activation

Murine S100A8 is a potent chemoattractant for neutrophils (Lackmann, Cornish et al. 1992). Human in-vitro work has demonstrated that S100A9 can induce neutrophil adhesion to fibrinogen by increasing the affinity of the integrin, Mac-1 (CD11b), on neutrophils. However, the human heterodimer of S100A8/A9 was unable to induce a similar effect to that of S100A9 (Newton and Hogg 1998), suggesting that differences in effector function exist between the individual proteins of the heterodimer as well as differences between species. However, these differences may be attributed to improper folding of the proteins or inactivation during the purification process. In a separate study, recombinant human S100A8, S100A9 and S100A8/A9, were all chemotactic for neutrophils and induced upregulation of Mac-1 (CD11b) and stimulated neutrophil adhesion to fibrinogen. Injection of these proteins into the murine air pouch, resulted in leukocyte accumulation and a rapid collection of neutrophils confirming that all these proteins are potent inducers of neutrophil chemotaxis, adhesion and migration (Ryckman, Vandal et al. 2003). Corroborating these findings, murine mrp14-/- neutrophils exhibit a reduction in IL-8 mediated upregulation of CD11b, and demonstrate a decreased ability to migrate through an endothelial cell monolayer in response to the chemotactic stimuli of IL-8. However, this did not translate to the in vivo setting as mrp14-/- and wild-type leukocytes showed similar responses following induction of thioglycolate peritonitis (Manitz, Horst et al. 2003). With regards to leukocyte activation, recombinant human S100A9 is able to induce neutrophil degranulation and induce the release of granule proteins such as MMP-9, contributing to tissue damage following neutrophil degranulation (Simard, Girard et al. 2010). Additionally, S100A8/A9 secretion, following neutrophil programmed cell death (PCD), partially protects surrounding neutrophils from PCD by having an anti-apoptotic effect. Blocking TLR4 partially abrogated the S100A8/A9 survival effect, as well as blocking CD11b/CD18 (Atallah, Krispin et al. 2012).

1.4.1.2.2 Effect on the endothelium

S100A8/A9 has an important role mediating the interaction between the myeloid cells and the endothelium in addition to its role described previously in which it facilitates migration of the myeloid cells. The heterodimer has the capacity to be rapidly released from monocytes as they move from the circulation into tissues without being re-synthesised. Indeed, maximal secretion of S100A8/A9 follows an interaction between monocytes and endothelial cells and facilitates monocyte transmigration through both microvascular and macrovascular endothelial cells, mediated by CD11b (Mac-1) expression and activation, as well as an increase in monocyte surface ICAM-1 (Eue, Pietz et al. 2000). Endothelium may stain positive for the S100A8/A9 complex, in association with the presence of a myeloid cell or following myeloid cell traffic, despite lacking the capacity to induce expression of the complex (Hogg, Allen et al. 1989). Despite a murine endothelial cell line expressing S100A8 (mrp-8) under certain conditions (Yen, Harrison et al. 1997), the human endothelial cell line (HMEC-1) has been shown not to produce this complex, but is able to bind S100A8/A9 via a heparin sulphate moiety (Robinson, Tessier et al. 2002), and via carboxylated glycans expressed on endothelial cells (Srikrishna, Panneerselvam et al. 2001). The secretion of the heterodimer, once myeloid cells comes into contact with endothelial cells, is tightly controlled, requiring TNF priming of the endothelium allowing the release of S100A8/A9 to occur when myeloid cells adhere to inflamed endothelium (Frosch, Strey et al. 2000). Peripheral blood monocytes are known to consist of a heterogeneous population of cells. Those monocytes positive for intracellular S100A8/A9 demonstrated increased spontaneous migration rates through a monolayer of both micro- and macrovascular human endothelial cells compared to monocytes that were negative for S100A8/A9. The migration of monocytes positive for the heterodimer was dependent on ICAM-1 expression on the endothelial cells (Eue, Pietz et al. 2000).

Experiments incubating S100A8/A9, isolated from human granulocytes, with HMEC-1 further delineated the response of the endothelium to binding of the heterodimer. Genes involved with platelet aggregation (Thombospondin-1), pro-inflammatory cytokines and cell adhesion molecules were upregulated while genes involved with growth, differentiation and endothelial cell monolayer integrity were down-regulated. Specifically, S100A8/A9

treatment of HMEC monolayers resulted in secretion of IL-8, as well as up-regulation of ICAM-1 and disrupted intracellular endothelial cell boundaries (Viemann, Strey et al. 2005). Additionally, S100A8/A9 was able to induce apoptosis and necrosis of endothelial cells, with induction of caspase-3 and caspase -9 as well as inducing caspase-independent cell death (Viemann, Barczyk et al. 2007).

In an experimental mechanical arterial injury model, mice deficient in mrp14-/- demonstrated decreased macrophage and neutrophil infiltration, as well as reduced vessel proliferation and neointimal formation. There were additionally fewer vasculitic lesions following the local Scwartzman-like reaction induced by injection of LPS and cytokines. In-vitro experiments demonstrated important differences between WT and mrp14-/- macrophages in response to LPS, with mrp14-/- macrophages producing less TNF-α, MCP-1, IL-1β and IL-12 by ELISA. Lastly, human evidence was provided by demonstrating abundant expression of mrp8/14 associated with CD68 positive macrophages within human carotid atheroma, unlike normal arteries without detectable expression of mrp8/14 (Croce, Gao et al. 2009).

Therefore, S100A8/A9 results in several pro-inflammatory and thrombogenic effects on the endothelium, and induces endothelial cell apoptosis and necrosis; Features which are characteristic of small vessel vasculitis and which may implicate a role for S100A8/A9 in the pathogenesis of vasculitis.

1.4.1.2.3 Other paracrine effects

In-vitro experiments have shown that S100A8/A9 (isolated from rat) is able to inhibit growth of both mouse embryonic as well as human dermal fibroblasts and had the ability to induce their apoptosis. The apoptosis effect was observed to occur very slowly. This data therefore suggests that S100A8/A9 may suppress the proliferation of fibroblasts (Yui, Mikami et al. 1997).

1.4.2 Endogenous TLR4 ligand and RAGE

Bone marrow cells isolated from mrp14-/- mice, demonstrate a reduced response to LPS stimulation despite similar expression levels of the LPS receptor, TLR4, with reduced

activation of the transcription factor NF-κB and decreased induction of TNF-α, an effect reversed by the extracellular administration of S100A8/A9. Phagocytes from a mouse expressing a non-functional TLR4 demonstrate a similar lack of response to both LPS and S100A8, demonstrating that S100A8 is an endogenous ligand of TLR4, and its binding results in activation of NF-κB and subsequent gene expression. S100A8/A9 acts as an amplification signal during the inflammatory response through its actions on TLR4, as demonstrated by the LPS induced septic shock model in which mrp14-/- mice, were found to have a significantly longer survival than WT mice (Vogl, Tenbrock et al. 2007).

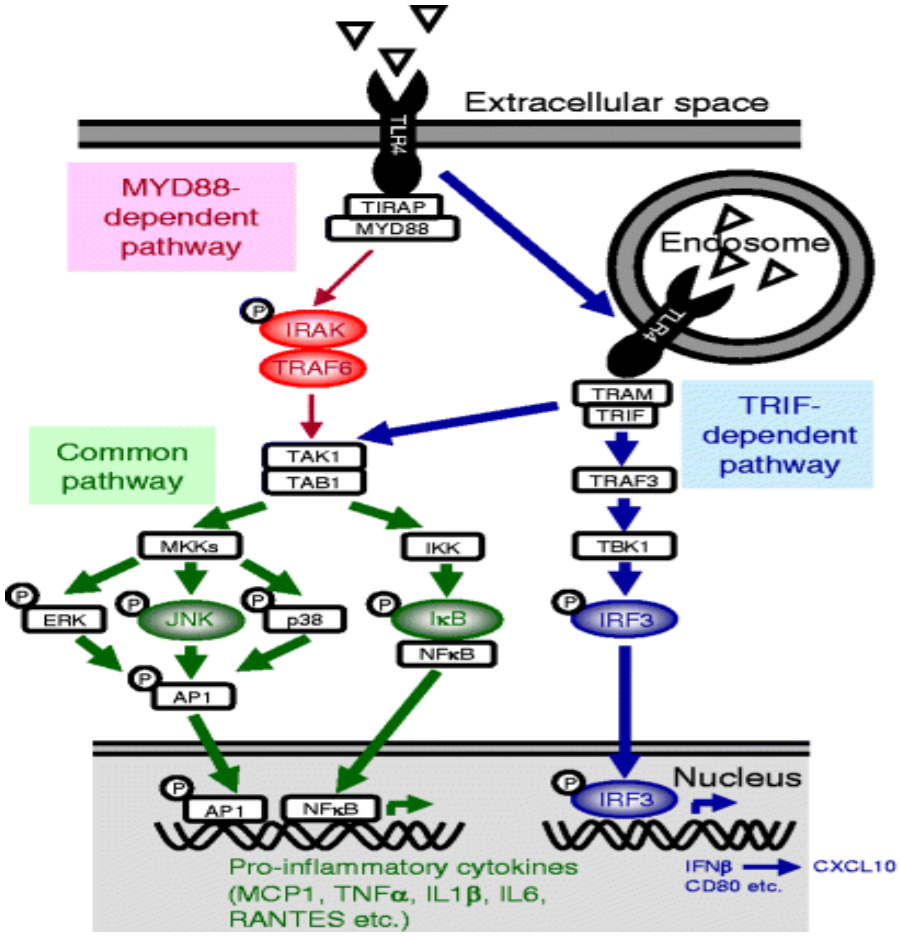

Figure 1-7 Diagram demonstrates the intracellular TLR4 signalling pathway using both MyD88-dependent and MyD88 independent pathways.

Stimulation of the receptor results in the propagation of a signalling cascade with the eventual activation of the transcription factor NF-κB- which results in the transcription of several pro-inflammatory cytokines (Kuwabara, Mori et al. 2012)

In-vitro work using human CD14 cells has demonstrated that S100A9 (mrp-14) is able to stimulate the transcription factor NF-κB in a dose dependent manner with the resultant production of pro-inflammatory cytokines such as IL-1β, TNF-α, IL-6, IL-8 and IL-10, though the effect was less potent than that of LPS. This pro-inflammatory effect was then demonstrated in murine TLR4-/- bone marrow derived dendritic cells to be dependent on TLR4 (Riva, Kallberg et al. 2012). In addition, S100A8/A9, acting through TLR4, can upregulate transcription factors associated with IL-17 production, as demonstrated in a CD40L-overexpressing murine model of autoimmunity which is characterised by CD8 T cell-activation and IL-17 production (Loser, Vogl et al. 2010).

RAGE (receptor for advanced glycation end-products) is a multi-ligand cell surface receptor that belongs to the immunoglobulin superfamily. Known ligands include advanced glycation end-products as well as some members of the S100 family such as S100A12 and S100B (Yan, Ramasamy et al. 2003), while recent evidence confirmed that the heterodimer, S100A8/A9 is another RAGE ligand. In an animal model of post-ischaemic heart failure, hypoxia results in the stimulation of fibroblasts and macrophages with S100A8/A9 induction and the stimulation of pro-inflammatory cytokines. This effect was abrogated after knock-down of either the heterodimer or RAGE. Administration of recombinant S100A8/A9 resulted in reduced cardiac function, and this effect was mediated through RAGE (Volz, Laohachewin et al. 2012). This is supported by work using a prostate cancer cell line, in which recombinant S100A8/A9 co-localised with RAGE (Hermani, De Servi et al. 2006), and over-expression of S100A8/A9 in cardiac tissue resulted in RAGE dependent effects (Boyd, Kan et al. 2008). Finally, human umbilical vein endothelial cells (HUVEC) incubated with advanced glycation end-products (AGE) followed by stimulation with S100A8/A9; increased production of IL-6, ICAM-1 and s-VCAM-1. This increase was not seen in cells that were not pre-incubated with AGE prior to stimulation with S100A8/A9 (Ehlermann, Eggers et al. 2006).

Human S100A9 has been identified as the target of quinoline-3-carboxamides (referred to as Q compounds), which have been used in the treatment of autoimmune diseases, such as multiple sclerosis. S100A9 binding to RAGE, is dependent on both calcium ions and zinc, and was competed for by the Q compounds. Similarly, a dose-dependent inhibition of S100A9

interaction with TLR4 occurred in the presence of the Q compound, however, Q compound binding to the heterodimer was poor compared to that of S100A9 (Bjork, Bjork et al. 2009).

1.4.3 Anti-inflammatory action of S100A8 and S100A9

There are data demonstrating the anti-inflammatory and protective effects of these S100 proteins with their role in leukocyte recruitment and chemotaxis being vital in the host defence to infection (Lim, Raftery et al. 2011). Murine S100A8 in macrophages, and human S100A8 and S100A9 in monocytes and macrophages have been shown to be dependent on IL-10- an important anti-inflammatory cytokine, although murine S100A8 has also shown to be upregulated by LPS, IFN-γ and TNF-α (Hu, Harrison et al. 1996; Xu and Geczy 2000; Xu, Yen et al. 2001). Additionally, murine S100A8 was upregulated by a combination of LPS and glucocorticoids, while glucocorticoids alone had no effect with the authors noting that S100A8 may demonstrate additional anti-inflammatory roles independent of the roles of the heterodimer, S100A8/A9. (Hsu, Passey et al. 2005).

Dendritic cells have been demonstrated to express S100A8/A9 under inflammatory conditions in-vitro when stimulated with LPS and IFN-γ, to an even greater degree than that seen in macrophages. However, S100A9-/- DC when stimulated with LPS and IFNγ demonstrate increased secretion of the pro-inflammatory cytokine IL12p40 and upregulation of iNOS mRNA, in contrast to LPS stimulated S100A9-/- macrophages. DCs from S100A9-/- demonstrate this increased pro-inflammatory response as well as an increased ability to induce T-cell proliferation. S100A9 deficiency in DC resulted in an increase in inflammation, therefore demonstrating that in diseases in which DCs play an important role, a deficiency of S100A9 may actually increase inflammation (Averill, Barnhart et al. 2011). Interestingly, it has been demonstrated that the anti-inflammatory cytokine, IL-10, up-regulates S100A8 and S100A9 in human dendritic cells, as demonstrated using real-time PCR (Kumar, Steinkasserer et al. 2003). Additionally, S100A9 has a role in the inhibition of the important co-stimulatory molecules, CD80 and CD86, and its deficiency results in augmented CD80/86 expression on dendritic cells, with a resultant increase in IFN-γ production and T-cell proliferation (Shimizu, Libby et al. 2011). This effect resulted in

diminished cardiac allograft survival in mrp14-/- mice with augmented infiltration and accumulation of an inflammatory cell infiltrate consisting of CD8, CD4 T cells and macrophages, compared to wild-type counterparts. Finally, both S100A8 and S100A9 are known to undergo oxidative modifications, which may then inhibit certain (pro-inflammatory) activities of these proteins. S-glutathionylation of S100A8 suppresses neutrophil adhesion to fibronectin, and thus modulation of their transmigration. S-glutathionylation did not have a similar effect on S100A9 and the effect on the more physiologically relevant heterodimer was not tested (Lim, Raftery et al. 2011). S100A8 can additionally undergo S-nitrosylation, which results in inhibition of mast cell activation (Lim, Raftery et al. 2008).

1.4.4 Calprotectin and infection

Targeting S100A9 may result in decreased protection to infection. Calprotectin has been identified to be a major component of NETS (neutrophil extracellular traps). NETs are composed of chromatin and granule proteins, and are released from the neutrophil during a novel cell death mechanism (NETosis). In response to fungal infection (C.albicans, C.neoformans), S100A8/A9 has been demonstrated to be a major component of NETs. Loss of calprotectin in NETs resulted in a loss of the anti-fungal activity of NETs (Urban, Ermert et al. 2009). During murine Klebsiella pneumonia infection, levels of mrp8/14 increase in the bronchoalveolar lavage fluid, and mice deficient in mrp14-/- demonstrated a greater degree of bacterial dissemination than WT animals. However, mrp14 deficient mice did not demonstrate a difference in neutrophil lung recruitment during Klebsiella infection. Neutrophils and macrophages isolated from mrp14-/- mice had a reduction in the ability to phagocytose Klebsiella. The addition of the heterodimer to a bacterial Klebsiella culture resulted in growth inhibition, and confirmed the function of NETS in controlling infection was partly dependent on the heterodimer (Achouiti, Vogl et al. 2012). Similarly, a further in-vitro study demonstrated S100A9 stimulated neutrophil phagocytosis (Simard, Simon et al. 2011).

1.4.5 Calprotectin in disease

There is now evidence from both clinical studies and animal models that the heterodimer has a role both as a marker of disease and also disease pathogenesis.

1.4.5.1 Juvenile Idiopathic arthritis

S100A8/A9 serum levels in juvenile idiopathic arthritis (JIA) were measured during a trial of methotrexate (MTX) therapy and investigated as a potential predictor of disease relapse. In this trial patients were treated with MTX for either 6 or 12 months and S100A8/A9 levels were obtained during disease remission. Those patients who subsequently had a disease flare, (defined by active arthritis/ active systemic symptoms), demonstrated a significantly higher level of S100A8/A9 without other more traditional markers of disease activity (Foell, Wulffraat et al. 2010). S100A8/A9 levels have been shown to correlate with response to treatment and disease activity in JIA, with significant increases during disease flares, and a level of >740ng/ml during remission having a high sensitivity and specificity at predicting future disease flares (Holzinger, Frosch et al. 2012), suggesting that the heterodimer may have some value in indicating subclinical inflammation.

In a small subset of patients, treatment with anakinra (IL-1Ra) resulted in a significant decrease in S100A8/A9 serum levels; with in-vitro work demonstrating S100A9 had the ability to induce IL-1β secretion in human monocytes in a dose dependent manner. Patients' serum had the ability to induce monocyte IL-1β secretion, an effect which was blocked by the addition of anti-S100A9 antibodies. This suggests that S100A8/A9 and IL-1β are in a positive amplifying feedback loop (Frosch, Ahlmann et al. 2009).

Patients with cryopyrin-associated periodic syndromes (CAPS) have significantly elevated levels of S100A8/A9. Treatment with anti-IL-1 therapies resulted in a decrease in levels although they did not all normalise, suggesting subclinical phagocyte activation in some, with the exception being those patients treated with canakinumab (Wittkowski, Kuemmerle-Deschner et al. 2011).

1.4.5.2 Renal Inflammation

The presence of glomerular macrophages containing S100A8/A9 has previously been described, in a range of renal pathologies, including a small number of patients with proliferative glomerulonephritis. Overall, those patients with more severe renal injury, such as with SLE or endocapillary glomerulonephritis (including 4 patients with GPA) demonstrated a greater population of S100A8/A9 positive glomerular macrophages compared with patients with a diagnosis of focal segmental glomerulosclerosis or minimal change disease suggesting that CD68+ S100A8/A9+ glomerular macrophages represent a pro-inflammatory macrophage, which the authors presume had been recruited from blood monocytes (Frosch, Vogl et al. 2004).

S100A8/A9+ macrophages have also been noted in ANCA associated GN, with almost all glomerular macrophages expressing this complex as well as markers of proliferation, whereas far fewer macrophages expressed this complex in cryoglobulinemic vasculitis despite macrophage infiltration in the kidney (Rastaldi, Ferrario et al. 2000). Urinary calprotectin (S100A8/A9) has been used to differentiate between pre-renal and intrinsic renal failure with significantly higher levels found in the urine of cases with intrinsic acute kidney injury (Heller, Frischmann et al. 2011).

Similar to GN, acute renal allograft rejection was associated with the presence of S100A8/A9 positive macrophages. However, chronic allograft rejection was characterised by macrophages generally being negative for the heterodimer (Goebeler, Roth et al. 1994). In a study of patients with biopsy proven allograft rejection, the presence of S100A8 and S100A9 (mRNA, as well as protein expression) was increased in patients who went on to have stable graft function compared to those patient whose graft dysfunction progressed and a diagnosis of chronic allograft nephropathy was made (Eikmans, Roos-van Groningen et al. 2005).

As well as being a histological marker, serum levels of S100A8/A9 have also been investigated during episodes of acute renal transplant rejection. S100A8/A9 levels were significantly elevated in a group of patients with rejection, in a pilot and a validation study, while treatment with pulsed intravenous methylprednisolone resulted in a decrease in

serum levels. In patients who experienced graft rejection within the first 4 weeks, a cut-off level of 4.2µg/mL was sensitive and specific with a high predictive value for graft rejection. Factors such as delayed graft function and ischemic time did not affect serum levels, however, there was a correlation between HLA mismatches and S100A8/A9 levels (Burkhardt, Radespiel-Troger et al. 2001).

1.4.5.3 Arthritis

Several studies, both clinical and experimental, have elucidated a role for the heterodimer in disease pathogenesis, in which macrophages have been shown to play an important role in joint inflammation. Patients with rheumatoid arthritis (RA) have higher serum and synovial fluid levels of S100A8/A9 than healthy controls and patients with osteoarthritis (OA)(mean values in the serum RA 38900µg/ml, synovial fluid 54.8µg/ml), with high expression of the heterodimer in CD68 positive macrophages infiltrating the synovial tissue (Sunahori, Yamamura et al. 2006). In addition, serum levels of S100A8/A9 strongly correlated with musculoskeletal ultrasound appearances in patients with RA, with sensitive decreases in the serum levels after the initiation of treatment (Hammer, Fagerhol et al. 2011).

In the antigen induced arthritis murine model, there is abundant expression of the complex. Mice deficient in mrp14-/- demonstrated the same cellular and humoral response as WT mice in this model; however, there was decreased joint inflammation in the mrp14-/- mice. Injection of S100A8 resulted in upregulation of pro-inflammatory cytokines, such as IL-1, IL-6 and TNF-α. S100A8/A9 had a role in cartilage destruction by mediating induction of different matrix metalloproteinases (MMPs)(particularly MMP 3,9 and 13), enzymes known to mediate cartilage destruction (van Lent, Grevers et al. 2008). Furthermore, following intra-articular injection of S100A8 into the normal knee joint of mice, there is upregulation of activating FcγR (FcγRI, FcγRIV). Similar, although less potent effects were observed following injection of S100A8/A9. This effect was abrogated in TLR4-/- macrophages (van Lent, Grevers et al. 2010), again demonstrating the importance of the interaction between S100 proteins and TLR4.

In addition, S100A8 has been shown to mediate osteoclast formation and increase bone resorption. Osteoclasts derived from TLR4-/- bone marrow show a significantly reduced bone resorption capacity after stimulation with S100A8 compared to wild-type osteoclasts (Grevers, de Vries et al. 2011).

S100A8/A9 is also released by neutrophils following incubation with monosodium urate monohydrate (MSUM) crystals. This effect was blocked by antibodies directed against CD11b and CD16, as well as by a src-kinase inhibitor, and a combination of syk and PI-3-kinase-inhibitors, demonstrating that src, syk as well as PI-3K are involved in the release of S100A8/A9 following neutrophil stimulation with MSUM crystals (Ryckman, Gilbert et al. 2004).

The murine LPS-collagen-induced arthritis model (LPS-CIA) has also been utilised to investigate a role of S100A9 and S100A8/A9 in the pathogenesis of joint destruction. Mice treated with an antibody to S100A9 demonstrated lower serum levels of S100A8/A9 as well as decreased severity of arthritis, decreased bone destruction and a reduction in monocyte/granulocyte infiltration. The histological results were similar to those seen in mice treated with anti-TNF-α antibody therapy at the time of disease induction. Treatment with an antibody to S100A9 also resulted in decreased IL-6 and TNF-α detected by western blotting at the site of inflammation (Cesaro, Anceriz et al. 2012).

Similar results have been obtained in human and animal studies into osteoarthritis. In the murine collagenase-induced OA model, synovial S100A8 and S100A9 mRNA is strongly upregulated with similar results in synovial biopsy samples from patients with early OA. Patients who subsequently progressed with respect to joint destruction, had higher serum levels of S100A8/A9 that those patients who did not progress (487ng/ml v 581ng/ml), again suggesting that the complex may be of use in predicting which patients may progress (van Lent, Blom et al. 2012). A possible mechanism for the increased chondrocyte damage in patients was further explored and, agreeing with previous studies, S100A8 and S100A9 upregulated pro-inflammatory mediators (MMP1, MMP3, MMP9, MMP13, IL-6, IL-8 and MCP-1 mRNA measured by quantitative PCR). These effects were abrogated by TLR4 blockade (Schelbergen, Blom et al. 2012).

1.4.5.4 Cardiovascular disease

There is now some evidence from both human and animal data that S100A8/A9 may also have a role in cardiovascular disease and cardiac dysfunction. LPS has been demonstrated to induce expression of S100A8/A9 in a cardiomyocyte cell line (HL-1). Following transfection with plasmids encoding S100A8, S100A9 and S100A8/A9, the cardiomyocyte cell line demonstrated a decrease in calcium flux. In mice, there is a decrease in cardiac contractility following delivery of the S100 proteins, an effect abrogated by the addition of blocking antibodies to RAGE (Boyd, Kan et al. 2008). However, there are conflicting reports, with a rat model of ischaemia showing no induction of S100A8 or S100A9 in cardiac myocytes, and data suggesting that infiltrating neutrophils are the source of the heterodimer (Du, Yang et al. 2012).

A patient study demonstrated that S100A8/A9 plasma concentration was independently associated with the risk of recurrent cardiovascular events in a population of patients presenting with an acute coronary syndrome (Morrow, Wang et al. 2008). However, a study confirmed that in patients presenting with chest pain, measuring this heterodimer did not aid diagnosing a cardiac event due to its low sensitivity and poor positive predictive value (Vora, Bonaca et al. 2012). However, a higher level of S100A8/A9 was observed in non-survivors compared to survivors of acute myocardial infarction (Schaub, Reichlin et al. 2012). Elevated S100A8/A9 levels are also observed in diabetic patients with confirmed coronary artery disease, and were higher than those non-diabetic patients with coronary heart disease (Peng, Jian et al. 2011).

1.4.5.5 Systemic lupus erythematosus

Patients with SLE have significantly higher serum levels of S100A8/A9 than healthy controls (mean value 1412ng/ml versus 339ng/ml), with higher levels in those patients with disease flares compared to those patients in disease remission (Soyfoo, Roth et al. 2009). S100A8/A9 has also been detected on the cell surface of several different populations of cell subsets in patients with SLE. In patients with active disease, there was increased cell surface expression detected on CD+16 monocytes, myeloid dendritic cells (mDC), plasmacytoid dendritic cells (pDC) and neutrophils compared to patients with inactive disease. There was

no difference between those patients with inactive disease and healthy controls, unlike serum levels in which a significant difference was detected. Not all of these cell types actually produced S100A8/A9, as confirmed by intracellular detection in PMNs, monocytes and pDCs, suggesting that detection may have been due to external deposition of this complex. Of interest to this thesis is that SLE patients with renal involvement and arthritis demonstrated the highest serum levels of S100A8/A9. This study was also able to demonstrate the upregulation of S100A8/A9 on pDCs, which may be significant, due to the central role pDCs are believed to play in the pathogenesis of SLE (Lood, Stenstrom et al. 2011). S100A9 expression has been demonstrated to be increased in the PBMCs of patients with SLE compared to healthy controls at both protein and mRNA level (Pavon, Garcia-Rodriguez et al. 2012)

1.4.5.6 Diabetic nephropathy

A murine model of diabetes can be generated by intra-peritoneal injection of streptozotocin (STZ) followed by a high fat diet which results in hyperglycaemia, increased triglycerides and albuminuria with evidence of damage to podocytes, macrophage infiltration, mesangial expansion and upregulation of S100A9 gene expression in the kidney. Immunohistochemistry demonstrates S100A8 staining in both human and murine glomerular lesions, while mice deficient in TLR4 develop less severe renal injury than WT counterparts following administration of STZ and a high fat diet. Similar mild renal changes were observed in both mouse groups after STZ and a normal diet suggesting that TLR4 may have a role in the propagation of diabetic nephropathy rather than influencing the initial onset (Kuwabara, Mori et al. 2012).

In patients with type II diabetes, serum levels of S100A8/A9 were associated with microvascular complications of diabetic retinopathy and nephropathy as assessed by digital measurements of retinal vessels and proteinuria (Burkhardt, Schwarz et al. 2009).

1.4.5.7 Kawasaki disease

Kawasaki disease is a medium vessel vasculitis particularly affecting the coronary arteries in children. The initial levels of S100A8/A9 in the serum are elevated in this cohort of

paediatric patients as are the RNA expression levels of mrp8 and mrp14 in granulocytes compared with healthy controls. Following treatment with intravenous immunoglobulin (IVIG), those children who fail to respond to treatment demonstrate higher serum levels than the responders. Similarly, those patients who develop complications of coronary artery lesions have higher levels than those patients without coronary artery lesions. Patients also demonstrate increased numbers of circulating endothelial cells, with the majority of circulating cells positive for S100A8/A9. These data suggest that S100A8/A9 could be used to aid diagnosis and predict response to treatment (Hirono, Foell et al. 2006).

1.4.5.8 Inflammatory bowel disease

There is evidence that measuring faecal calprotectin in both ulcerative colitis and Crohn's disease is a reliable reflection of bowel inflammation (Ricanek, Brackmann et al. 2011). Measurement of faecal calprotectin is now used by the physician in the investigation and diagnosis of patients, with increasing evidence that this test may correlate with mucosal disease activity therefore helping diagnose active disease/relapse as well as monitoring the response to treatment (Smith and Gaya 2012)

	MRP-8/MRP-14, ng/ml	No. of subjects
Healthy controls	340 ± 70	50
Arthritis		
Systemic-onset JIA	14,920 ± 4,030	60
JIA	2,380 ± 530	89
RA	640 ± 110	40
SpA	1,010 ± 150	40
PsA	910 ± 250	28
Vasculitis and autoimmune diseases		
Kawasaki disease	3,630 ± 480	21
Giant cell arteritis	810 ± 90	42
SLE	570 ± 245	6
DM	450 ± 80	6
Autoinflammatory diseases		
NOMID	2,830 ± 580	18
Infections		
Proven bacterial infections	3,720 ± 870	66
Pneumonia	1,960 ± 620	19
Leprosy (type 2 reaction)	2,530 ± 670	16
Malignancies		
Acute lymphoblastic leukemia	650 ± 280	40
Acute myeloblastic leukemia	840 ± 940	5

Table 1 Demonstrates the serum levels of S100A8/A9 (calprotectin) in various diseases.

Values above demonstrate the mean +/- 95% confidence interval for the serum levels of S100A8/A9 (calprotectin, mrp18/14) in a selection of diseases.

1.5 Project hypothesis

As described above, S100A8/A9 has been implicated in the pathogenesis of several autoimmune and inflammatory conditions. There is evidence from both human and animal studies that this heterodimer is a biomarker of disease severity and experimental evidence suggesting that it also plays a part in disease pathogenesis. However, other evidence suggests that the S100 proteins may additionally have anti-inflammatory effects which could possibly be independent of the heterodimer and be a property of the individual proteins.

Currently our treatment options in AAV are limited with significant adverse effects contributing to the early disease mortality (Little, Nightingale et al. 2010). As our understanding of the pathogenesis of AAV improves, newer therapies develop which aim to have more of a targeted immunomodulatory action as opposed to a generalised immunosuppressive effect, such as rituximab (Jones, Tervaert et al. 2010).

This project aims to explore S100A8/A9 in the pathogenesis of AAV. I hypothesis that patients with AAV demonstrate increased calprotectin expression both in the serum and in acute glomerular lesions associated with monocyte/macrophage infiltration. Additionally, I hypothesise that mice deficient in mrp14-/-, and therefore deficient in the heterodimer, may demonstrate disease protection in nephrotoxic nephritis, which may mostly be due to S100A8/A9 deficient phagocytes but with non-bone marrow derived cells additionally contributing.

The aims of the work in this thesis are:-

- Investigation of serum levels of S100A8/A9 in patients with AAV with both active disease and in disease remission compared to healthy controls- Chapter 3

- The measurement of cell surface S100A8/A9 expression on monocytes and neutrophils, with the investigation of patients' renal biopsies and correlation with the presence of S100A8/A9 glomerular lesions with the new Berden classification of ANCA associated glomerulonephritis- Chapter 3.

- Investigation of disease protection of mice deficient in S100A8/A9 in the nephrotoxic nephritis animal model- Chapter 4

- Investigation of the in-vitro the effect of S100A8/A9 on bone marrow derived macrophages extracted from WT, TLR4 and mrp14-/- deficient animals. The effect of S100A8/A9 on mesangial cells will be explored- Chapter 5.

- Investigation of the interaction between microvascular endothelial cells and either WT or mrp14-/- bone-marrow derived macrophages. The comparison of the phagocytic ability of WT and mrp14-/- macrophages. This chapter aims to delineate the mechanisms by which mice deficient in mrp14-/- may be protected from renal disease- Chapter 5.

Chapter 2 Materials and methods

2.1 Materials

2.1.1 Animals

Mrp14-/- mice were kindly provided by Professor F Ivars, University of Lund, Sweden. Mrp14-/- mice were generated by the replacement of 760bp of genomic DNA containing exon 2 resulting in the deletion of the initial start codon. The resulting construct was subsequently inserted into an embryonic stem cell line and microinjected into blastocysts of C57BL/6 mice (Manitz, Horst et al. 2003). Homozygous mice aged 8-12 weeks were used for experiments and were bred at the Central Biological Services Unit, Hammersmith Hospital Campus, Imperial College London. TLR4-/- mice (The Jackson Laboratory) were kindly provided by Dr. Nathan Davis, Royal Free Hospital Campus, UCL. Control mice were aged and sex matched. C57BL/6 control mice used at the Hammersmith Hospital were obtained from Charles River laboratories. Control mice at UCL were bred within the animal house. The mice were located in a pathogen-free environment with access to food and water. Experiments were performed in accordance with Home Office guidelines.

2.2 Methods

2.2.1 Human Studies

Written consent was obtained from patients and controls included in the following experiments. Clinical sample collection and use and received ethical approval from the hospitals involved (Hammersmith Hospital and the Royal Free hospital, London and Addenbrooke's Hospital, Cambridge).

2.2.1.1 Immunohistochemistry on renal biopsies

Immunohistochemistry (IHC) was performed on formalin fixed paraffin embedded sections using standard techniques staining for macrophages (anti-CD68) and S100A8/A9

(calprotectin) using the Dako Envision system-HRP (DAB). Antigen retrieval was performed using a 0.1% calcium chloride solution in 0.5 mM TBS with 1% trypsin to pH 7.8 for 10 minutes at 37°C. Primary antibodies used were mouse anti-human CD68 (Dako)(dilution 1:25) or mouse anti-human S100A8/A9 (calprotectin)(Bachem)(dilution 1:50). Isotype control antibody was used as a negative control at the same dilution as the primary antibody. The primary antibodies were incubated at room temperature in a humidified chamber for 1 hour. Peroxidase activity was detected with 3,3-diaminobenzidine (DAB). The slides were then rinsed in water and counterstained with filtered Harris' haematoxylin (Cell Path plc, Powys, UK), then dehydrated and mounted with DePeX Gurr mounting medium and coverslips where then placed. The slides were categorized according to the recently described Berden classification for AAV (Berden, Ferrario et al. 2010) and the quantification of S100A8/A9 staining in both the glomerulus and the interstitium was graded 0 (no staining) to 3 (extensive staining) by blinded observers. The Trio (Caliper life sciences) multispectral imaging system was used to assess the sections.

2.2.1.2 Patients included for measurement of serum and cell surface levels.

AAV patients were identified through the vasculitis clinics at hospitals in London (Royal Free and Hammersmith Hospitals) and Cambridge (Addenbrooke's hospital). All fulfilled the Chapel Hill Consensus criteria for diagnosis of either Granulomatosis with polyangiitis (GPA, formerly Wegener's granulomatosis) or microscopic polyangiitis (MPA). Disease activity was assessed clinically, biochemically and histologically. Active disease at presentation was defined by symptoms consistent with vasculitis, an elevated Birmingham vasculitis activity (BVAS) score and biochemical findings demonstrating an acute inflammatory response, without evidence of infection. Acute patients were either newly diagnosed, with positive autoantibody serology, or in the case of ANCA negative patients, histological evidence of a pauci-immune glomerulonephritis, or were known patients undergoing disease relapse which was defined clinically as requiring an escalation in immunosuppression in order to control disease activity. Acute blood samples were obtained where possible before induction therapy initiation or shortly thereafter. Remission patients were assessed by experienced clinicians and had no symptoms related to active vasculitis, and had a BVAS score of 0. Healthy controls were volunteers from the individual units. Additionally, serum

stored from a cohort of patients with limited systemic AAV, from the NORAM trial conducted by the European Vasculitis Society (EUVAS) were also investigated, in collaboration with the EUVAS serum biobank.

2.2.1.3 Measurement of serum calprotectin levels

Serum was isolated from blood samples obtained from patients with active disease, as well as patients in disease remission and healthy controls. The serum from the patients in the NORAM trial was obtained from the EUVAS serum bank and consisted of samples from patients at between 0-2 months from entry into the study and commencement of immunosuppressive treatment with initial active disease, at 5-7 months from entry when in remission on immunosuppressive treatment, and at 12-14 months from entry when a number of patients had relapsed. Serum was stored at -20°C until analysis. Calprotectin levels were assessed by sandwich ELISA (BMA Biomedicals) according to manufacturers' instructions. Sample dilution was optimized and incubated overnight at 4°C before analysis the following day.

2.2.1.4 Leukocyte cell surface expression

Whole blood was collected from patients in ethylenediaminetetraacetic acid (EDTA) and processed shortly following collection. The sample was centrifuged at 2400 rpm for 5 minutes to remove plasma. Red cell lysis was carried out for 10 minutes at room temperature followed by 2 washing steps. Extracellular staining was performed with CD14 PE (BD biosciences), CD3 PE (eBioscience) and calprotectin FITC (Santa-Cruz biotechnology), as well as isotype control antibodies. The cells were incubated with the antibodies on ice for 30 mins followed by 2 washing steps. Cells were fixed in 2% paraformaldehyde prior to flow cytometry.

2.2.1.5 Purification of human IgG

Total human ANCA containing-IgG was purified using a protein G column (GE Healthcare Life Sciences) from the plasma exchange fluid from patients with AAV receiving plasma exchange as a treatment during active disease. The 5ml protein G column was connected to a 20ml syringe via a suitable adapter and was washed with 50mls binding buffer (20mM

sodium phosphate pH 7.0). 7.5mls of filtered plasma exchange fluid was applied to the column with the same volume of binding buffer. The column was then washed with a further 50mls of binding buffer. 10mls elution buffer (0.1M glycine-HCl, pH 2.7) was then added to the column and the eluted IgG was collected in 1.5ml reaction tubes containing 120µl 1M Tris-HCl. The amount of IgG eluted was determined using a spectrophotometer, measuring absorbance at 280nm. The sample was dialysed over night using a dialysis membrane in sterile PBS. After dialysis, the samples were quantified again using a spectrophotometer at 280nm and then stored at -20°C until used. The same method was used to isolate IgG from the serum of healthy controls.

2.2.1.6 Endotoxin removal and detection assay

In order to ensure there was no LPS contamination of the isolated IgG, the preparations were applied to a polymyxin B column (Detoxi-Gel Endotoxin Removing Gel, Thermo Scientific). The column was regenerated by adding 5mls of 1% sodium deoxycholate (Sigma) and then washed with pyrogen-free water. Each individual sample was added to the column and incubated in the column for 1 hour before being collected and frozen at -20°C. To test for the presence of LPS, the limulus amebocyte lysate assay (Lonza) was used. Standard LPS concentrations were obtained by following manufactures' instructions and diluting E.coli endotoxin into the following concentrations: 1.0, 0.5, 0.25 and 0.1EU/mL. The assay was performed in a water bath at 37°C. The Limulus amebocyte lysate was added to 50µl of sample or standard and following 10 minutes incubation, a chromogenic substrate supplied in the kit was added. The absorbance was then read at 405nm. The final concentration of the LPS-free IgG was determined using a spectrophotometer at 280nm.

2.2.1.7 Isolation of human polymorphonuclear cells (PBMCs) and stimulation with IgG-ANCA.

Buffy coat was obtained from NHS blood and transplant from healthy donors. PBMCs were isolated by Lymphoprep density centrifugation. CD14 positive cells were subsequently selected by incubation of the PBMCs with CD14 microbeads (Miltenyl biotec Ltd). One million CD14 cells were plated in 12-well plates (Costar) in 1ml of RPMI/10% FCS solution. Each well was subjected to various conditions: unstimulated, IgG from healthy control,

MPO-ANCA IgG, PR3-ANCA IgG, (IgG concentrations 250µl/ml) TNFα (10ng/ml) and LPS (1µg/ml). The samples were incubated at 37°C overnight. Cells were then assessed for intracellular S100A8/A9 expression by flow cytometry (section 2.3.1.9)

2.2.1.8 Human umbilical vein endothelial cells

Human umbilical vein endothelial cells were a kind gift from Professor Justin Mason, Imperial College London. They were obtained at passage 3, and used between passage 3-4. The cells were supplemented with M199 culture media (Sigma-Aldrich), with 20% foetal calf serum (FCS) and 30µg/ml endothelial cell growth supplement (ECGS)(Sigma-Aldrich). 10 units/ml of heparin (CP Pharmaceuticals Ltd) was added and 100U/ml penicillin and 100µg/ml streptomycin. Tissue culture flasks were coated with 2% sterile gelatine (Sigma-Aldrich) for 10 minutes at 37°C. Excess liquid was aspirated prior to use of the tissue culture flasks. For experiments once the HUVECs have been plated out: 2.5 units/ml of heparin with 7.5µg/ml of ECGF was added to M199 culture media. 1ml of 300,000/ml HUVECs were added to each well. TNF 10ng/ml and LPS 1µg/ml were added to the cells in triplicate overnight, before trypsinising the following day

2.2.1.9 Flow cytometry

Following incubation, adherent PBMCs and HUVECs were obtained by trypsinisation. For extracellular staining, cells were washed in 1% FCS/PBS and re-suspended in 200µl 1% FCS/PBS in a 96 well V-shaped plate (Nunc, Denmark). Cells were stained with 20µl mouse anti-human S100A8/A9 FITC antibody (Santa-Cruz) or mouse isotype control IgG antibody (Santa-Cruz) on ice in the dark for 30 minutes. Cells were then washed in 1% FCS/PBS twice and subsequently fixed in 2% paraformaldehyde and stored in the dark at 4°C before analysis by flow cytometry. For the PBMC experiments, surface staining for CD14 was performed on the same day as CD14 isolation. 20µl mouse anti-human CD14 PE antibody (BD Pharmingen) was added to cells in a 96 well V-shaped plate, followed by cell fixation in 2% paraformaldehyde.

For intracellular staining, following trypsinisation of adherent cells, cells were fixed in 4% paraformaldehyde for 10 minutes at room temperature, followed by 2 washing steps with

PBS/1% FCS/ 0.1% saponin (Sigma-Aldrich). Cells were stained with either 20µl mouse anti-human S100A8/A9 FITC antibody, or 20µl mouse isotype control IgG FITC antibody. Cells were incubated for 30 mins on ice in the dark and then washed with PBS/1% FCS/ 0.1% saponin. 200µl of paraformaldehyde was added to all the wells and the plates were covered in the dark at 4°C until analysis by flow cytometry using a FACS Calibur machine running Cell Quest software (BD Biosciences) within 1 week.

2.2.1.10 Measurement of ANCA titres

ANCA positivity was analysed by indirect immunofluorescence. To measure ANCA antigenic specificity and titre, Luminex-based technology, using the FIDIS vasculitis kit (Technoclone, Vienna, Austria), in the Hammersmith Hospital Immunology Laboratory was performed.

2.2.2 Animal studies- in vivo

2.2.2.1 Genotyping of mrp14-/- mice by polymerase chain reaction

Genomic DNA was isolated from an ear clipping. The samples were lysed overnight in 100µl of DNA lysis buffer (100mM Tris-HCl pH 8.5, 5mM EDTA, 0.2% sodium dodecyl sulphate (SDS), 200mM NaCl) at 55°C with 100µg/ml proteinase K (Sigma-Aldrich). The DNA was then diluted with 3 volumes distilled water and heat inactivated for 15 minutes at 75°C. A 25µl PCR was then performed using the following primer sequences kindly provided by Professor Ivars.

1. S100A9 AS: 5'-CACCTTCATAAAGGTTGCCAACTG-3'

2. S100A9-S 5'-TACCAACATCTGTGACTCTTTAGC-3'

3. S100A9AS-Neo 5'-TGCACATTGGGTGGAAACATTCCA-3'

The first 2 primers are used to detect a 565bp product of the wildtype allele and primers 2 and 3 are used to detect a shorter product from the knock-out allele (230 bp). A total volume of 25µl PCR reaction was carried out (GeneAmp 9700, Applied Biosystems). Each

reaction tube consisted of Illustra puReTaq PCR beads (GE Healthcare). Each bead contained the following:- 2.5 units PuReTaq DNA polymerase, 10mM Tris-HCl, 50mM KCl, 1.5mM $MgCl_2$, 200µM each dNTP. To each reaction tube, the following was added: 1µl DNA, 1µl WT/mutant primers, 22µl water. A final volume of 25µl was obtained. PCR cycling conditions were kindly provided by Prof. Ivars.

PCR conditions

Denaturation	94°C 2 mins
Amplification	94°C 30 sec
	60°C 30 sec
	72°C 30 sec
	x30 cycles
Extension	72°C 10 mins

Following PCR, the products were then analysed by gel electrophoresis. 2g agarose (Sigma-Aldrich) was diluted in 100ml Tris acetate EDTA (TAE), microwaved for 2 mins. 2µl of ethidium bromide (Sigma) was then added. The gel was left for 40 mins at room temperature to set. 10µl of each sample was mixed with 2µl of loading dye (New England BioLabs inc) and loaded onto the gel. 10µl of 100bp DNA ladder (New England BioLabs inc) was used. The samples underwent electrophoresis in TAE buffer for 60 mins at 80V. DNA was then visualized using a transilluminator under ultra-violet light.

2.2.2.2 Induction of nephrotoxic nephritis

To induce accelerated nephrotoxic nephritis, mice were initially pre-immunised subcutaneously or intra-peritoneally, with 0.2mg of sheep IgG (Sigma-Aldrich) made up in 0.9% sterile saline, mixed in a ratio of 1:1 with Complete Freunds Adjuvant (CFA) (Sigma Aldrich). This combination was prepared by the continuous mixing of this solution between two glass syringes joined by a double-luer lock (Sigma Aldrich). To assess if the mixing was

adequate, a drop of the solution was placed on water and observed to ensure it retained its form. Five days following the immunisation, the mice were injected with 200µl sheep nephrotoxic globulin (NTS) diluted 1:1 in 0.9% NaCl, via the tail vein. Mice were placed in metabolic cages for 24 hours one day before they were humanely killed 7-9 days after NTS injection. The kidneys were harvested, and urine and blood collected. Blood was allowed to clot at room temperature followed by the separation of serum by centrifugation, which was then stored at -80°C.

For the non-accelerated model of nephrotoxic nephritis, mice were not pre-immunized with sheep IgG. Instead, mice were injected with 200µl of nephrotoxic serum diluted 1:1 with sterile saline (0.9%) into the tail vein and killed 2 hours later.

2.2.2.3 Bone marrow transplantation

To obtain donor bone marrow, the femur and tibia were dissected followed by flushing through the bone using a 21G needle with sterile PBS and bone marrow cells collected. The cells were subsequently spun down at 2000 rpm for 10 minutes at 4°C. The cells were re-suspended and washed again. The re-suspended cells were counted, followed by another centrifugation step. Finally, the cells were re-suspended in RPMI media at a concentration of $5x10^7$cells/ml and kept on ice. Ten million cells (0.2ml) were injected per mouse intravenously into the tail vein.

The female recipients of the bone marrow were irradiated in an IBL 637 irradiator at CBS Hammersmith Hospital. A radiation dose of 8Gy was used- established from previous bone marrow transplantation experiments. Within an hour of receiving this dose of radiation, the mice were injected with donor bone marrow cells. Following transplantation the mice were housed in cages in the CBS, Hammersmith Hospital with access to food and water for 8 weeks prior to undergoing nephrotoxic nephritis.

2.2.2.4 PCR of circulating DNA

Genetic reconstitution of leucocytes following bone marrow transplantation was analysed at the end of the experiments once mice had been sacrificed. Blood was collected after sacrifice and the clotted portion of blood was used for DNA extraction and analysis to

confirm reconstitution of the donor bone marrow. 100µl of clotted blood was placed into an autoclaved Eppendorf tube. 0.5ml of DNA lysis buffer containing proteinase K (100µg/ml) was added to each blood sample, followed by incubation while rotating at 56°C overnight.

300µl of saturated NaCl was added to each lysed sample, followed by vortexing of the sample. 200µl of chloroform was added, and the sample briefly vortexed again. The samples were spun at 13000rpm for 10 minutes at room temperature. The supernatant (0.5mls) subsequently contained the DNA for analysis and was carefully removed and transferred into another tube. 50µl of 3M sodium acetate was added to the tube containing the supernatant, followed by 550µl of isopropanol to precipitate the DNA. After careful inversion of the tube, the samples were centrifuged at 13000rpm for 10 minutes. 70% ethanol was used to wash the DNA pellet a total of 2 times, and allowed to air dry. 20µl Tris-EDTA was used to dissolve the washed DNA pellet. DNA concentration was measured using a NanoDrop spectrophotometer and diluted to 100ng/ml.

1µl of the DNA was added to the 24µl of the PCR reaction mixture, containing primers for WT and mrp14-/- DNA. To compare the reconstitution, DNA from WT and mrp14-/- mice was also included at varying mixtures. Although this was not a quantitative PCR, by comparing the intensities of the bands obtained with DNA from WT and mrp14-/- mice, it was possible to estimate the relative reconstitution.

2.2.2.5 Measurement of proteinuria and serum urea.

Serum urea and creatinine were measured in the department of clinical chemistry, Hammersmith Hospital, by Mr. John Meek and Dr. John Morris.

Twenty-four hours prior to sacrifice, the mice were placed in individual metabolic cages and urine collected. Mice had access to food and water. Proteinuria was quantified using the sulphosalicylic acid assay. Standards were obtained using several concentrations of bovine serum albumin (BSA)(Sigma-Aldrich). The following dilutions prepared: 1, 0.8, 0.6, 0.4, 0.2, 0.1, 0.05, 0.02 and 0mg/ml. Urine from individual animals was plated into a 96 well plate in triplicate at either a dilution of 1:10 (or 1:100 if significant proteinuria on urine dipstick analysis (Multistix 8 SG, Siemens)). 10µl per well of 25% sulphosalicylic acid was added to 2

wells, with water added to the third well. The optical density was then analysed using an ELISA plate reader (Lab Tech International, UK) at 450nm and proteinuria concentration calculated from the standard curve generated by BSA.

2.2.2.6 Measurement of murine serum S100A8/A9

Serum levels of calprotectin in WT mice following NTN were measured by Prof. Thomas Vogl, Germany. Measurement was by ELISA developed by Prof. Vogl.

2.2.2.7 Processing of histological specimens

Half of a kidney was used for light microscopy. These specimens were initially fixed in neutral buffered formalin overnight before then being transferred to 70% ethanol and subsequently processed into paraffin blocks. Sections were stained with periodic acid Schiff (PAS) and haemotoxylin-eosin (H+E) (Leucocyte biology, biological sciences, Imperial College London, South Kensington). Sections to be used for immunofluorescence and immunoperoxidase were initially fixed in paraformaldehyde-lysine-periodate (PLP) fixative at 4°C for 4 hours before being transferred to a 10% sucrose solution overnight and then snap frozen and embedded in OCT (Cellpath, Powys, UK) with isopentane cooled with liquid nitrogen. Sections of 5µm were then cut using a cryostat and were left to air dry for 24 hours before being transferred to -80°C until used.

2.2.2.8 Immunofluorescence staining

Direct immunofluorescence was performed on PLP fixed- frozen kidney sections to detect mouse and sheep IgG. 20% goat serum (Sigma) was applied to block non-specific binding, followed by either goat anti-mouse IgG FITC (Sigma) 1:200 or monoclonal anti goat/sheep IgG FITC (Sigma) 1:200 for 1 hour in a humidified chamber. Antibodies were diluted in PBS. After washing the sections, they were mounted in AF1 solution (Citiflor).

2.2.2.9 Immunoperoxidase staining

Immunoperoxidase staining was performed to detect macrophages, T cells and calprotectin (S100A8/A9) positive cells using the Polink-2 HRP Plus kit (Newmarket scientific). 5µm sections of PLP fixed tissue were used. Endogenous peroxidase activity was blocked with 3%

hydrogen peroxide for 10 minutes. Subsequently, after rinsing the sections in distilled water, sections were blocked with skimmed milk (Marvel) for 30 minutes. The sections were then incubated with the primary antibody: rat anti-mouse CD68 (Serotec), rat anti-mouse CD4 (BD Pharmingen) both at a dilution of 1:100, and rat anti-mouse S100A8/A9 antibody (kind gift from Dr. N. Hogg)(1:120 dilution). The antibodies were diluted in PBS. Negative controls were also included in which the primary antibody was replaced with PBS. The sections were incubated with the primary antibody for 1 hour in a humified chamber at room temperature. Following incubation, sections were washed in PBS followed by 2 drops of Antibody Enhancer was then added to each section for 10 minutes. Slides were washed 3 times again and 2 drops of the Polymer-HRP incubated with the sections for a further 10 minutes. Slides were washed 3 times in PBS, followed by adding the detection antibody made up by adding 2 drops of the DAB chromagen (3,3'diaminobenzidine chromagen solution) to 1ml of DAB substrate. Once a brown colour development was obtained, slides were rinsed in distilled water and counterstained in filtered Harris' haematoxylin (Cell Path PLC) for 30 seconds. Followed by a rinsing step in distilled water, the slides were briefly placed in acid alcohol, followed by a washing step for 5 minutes until the sections turned blue. Sections were dehydrated by serial immersions for 3 minutes each in 100% ethanol twice and xylene twice, before mounting with DePeX Gurr mounting medium (BDH) and coverslip placement.

Antibody specificity

	Source	Host/Clone	Concentration (mg/ml)	Dilution
Immunofluorescence				
Sheep IgG FITC-Fc specific	Sigma	Mouse IgG1 Clone GT34	1.7	1:200
Mouse IgG FITC-Fc specific	Sigma	Goat polyclonal	5.2	1:200
Primary antibodies				
CD68	Serotec	Rat FA11	0.1	1:100
CD4	BD Pharmingen	Rat GK1.5 (L3T4)	0.5	1:100
S100A8/A9	Gift Dr. N Hogg	Rat 2B10	1.2	1:120

Table 2 Antibodies used for immunofluorescence and immunohistochemistry on mouse sections.

2.2.2.10 Histological analysis

Sections were blinded so the animal identity was unknown.

2.2.2.10.1 Thrombosis

To calculate a score for glomerular thrombosis, PAS kidney sections were used to grade the amount of PAS positive material occupying the glomeruli. A score of 0 indicated no PAS material, 1= 0-25%, 2= 25-50%, 3=50-75% and 4=75-100%.

2.2.2.10.2 Macrophages and CD4+ T cells

Macrophages and T cells inside the glomeruli on immunoperoxidase were also counted. 25 glomeruli were counted and the mean score then calculated for each mouse.

2.2.2.10.3 Immunofluorescence

Immunofluorescent sections were scored using Image Pro Plus software (Media Cybernetics). To quantitate using Image Pro Plus, images of glomeruli were captured using a QImaging Retiga 2000R Fast 1396 camera (QImaging). Glomeruli were outlined manually on the computer screen and the mean fluorescence intensity over each glomerulus was measured electronically. For each section 10 glomeruli were examined and the mean fluorescence intensity recorded. Where Image Pro Plus software was used results are expressed in arbitrary fluorescence units (AFU).

2.2.2.11 Systemic immune response to sheep IgG analysis

Serum mouse anti-sheep IgG and IgG sub-classes levels were measured by ELISA. For total IgG, ELISA plates (Nunc Maxisorb, Life Technologies, Paisley, UK) were coated overnight at 4°C with 100µg/ml of sheep IgG (Sigma-Aldrich) diluted in 100mM boric acid (BBS). Plates were washed and blocked with 3% BSA (Sigma-Aldrich). Serum was diluted 1:1000 in 1% BSA. Alkaline phosphatase conjugated goat anti-mouse IgG (Southern Biotechnology, Birmingham, Alabama) at 1:1000 in 1% BSA was used as the secondary antibody. All incubations were for 1 hour at 37°C. Plates were developed using *p*-nitrophenyl phosphate (Sigma-Aldrich) and measured on an ELISA plate reader at 405nm. For IgG subclasses, the same protocol was performed. For IgG1 serum was added at a dilution of 1:1000, for IgG2a, IgG2b, IgG3 1:500. The secondary antibodies were used at a dilution of 1:1000 for IgG1 and IgG2b and 1:500 for IgG2a and IgG3 (all Southern Biotechnology).

2.2.3 Animal Studies- in-vitro

2.2.3.1 T cell proliferation assay

Mice were pre-immunised as previously described, followed by injection of nephrotoxic serum 5 days later. After sacrifice of the mice at day 7, the spleens were harvested for the T-cell proliferation assay. Each mouse spleen was passed through a 100µM cell strainer followed by re-suspension in HL-1 serum free media (Lonza Group Ltd., Basel, Switzerland)

including 100U/ml penicillin, 100µg/ml streptomycin and L-glutamine (Gibco Life Technologies). The isolated splenocytes were spun down for 10 minutes at 2000rpm followed by re-suspension in 1ml RBC lysis buffer (4.17g NH_4Cl, 0.00185g EDTA, 0.5g $NaHCO_3$, 500ml sterile water). Red blood cells were lysed on ice for 5 minutes, followed by the addition of media to a final volume of 15mls. Splenocytes were then spun down at 1800rpm for 10 minutes and re-suspended in 20mls of media. After counting the cells, a final suspension of $5x10^6$ cells per ml/media.

500,000 splenocytes in 100µl were plated out per well in a 96-well plate. Splenocytes were plated alone in triplicate, or with CD28/CD3 beads (Invitrogen)(5µl of beads- 1µl beads/40,000 T cells), or 10µg/ml of aggregated (heated to 60°C for 5 minutes to aggregate) sheep IgG, or 50µg/ml of aggregated sheep IgG. The cells were stimulated at 37°C, 5% CO_2 for 72 hours. Following the stimulation, 1µCu of ^3H thymidine was added to each well, followed by incubation for a further 24 hours at 37°C, 5% CO_2. The radioactivity uptake was then counted after 24 hours using a 1450 MicroBeta TriLux liquid scintillation and luminescence counter (PerkinElmer, Waltham, Massachusetts).

2.2.3.2 Bone marrow derived macrophages

Following sacrifice of the animals, the femurs and tibias with the attached tissues were cleaned in the tissue culture hood in an aseptic manner. The tissues attached to the bones were excised using a sterile scalpel. The bones were washed in sterile PBS and Hanks media (Sigma-Aldrich). In a clean Petri dish, the ends of the femurs and tibias were cut off and the bone marrow was flushed through using a 25G needle and Hanks medium. The collected bone marrow was washed with Hanks media and spun at 1,500 rpm for 5 minutes. The cells were re-suspended in sterile culture medium of DMEM (Invitrogen) supplemented with 20% FCS (Biosera), 100U/ml penicillin (Gibco Life technologies), 100µg/ml streptomycin and 25% L929 cells (European collection of cell cultures) conditioned media containing M-CSF. The cells were cultured at 37°C, 5% CO_2. After 3 days, the media was replaced with the removal of the non-adherent cells. Fresh media was added. The macrophages were harvested day 7 by washing with Hanks solution (Sigma-Aldrich), followed by 2mls of trypsin. The cells were subsequently spun at 1500 rpm for 5 mins and re-suspended with DMEM media. For stimulation experiments, $1x10^6$ cells were used per condition.

2.2.3.3 Mesangial cell purification and culture

Kidneys were removed from WT, TLR4-/- and mrp14-/- mice and placed in RPMI media (Invitrogen) with penicillin/streptomycin. The kidneys were blended using a 5ml syringe plunger followed by being forced through sieves of initially size 70µm then size 40µm. Glomeruli were collected on the smaller sieve and collected into a falcon tube with sterile PBS. The glomeruli were spun down at 1000 rpm for 5 minutes followed by a digestion step. Collagenase (Sigma-Aldrich) was added (380U/ml) for 30 minutes at 37°C, followed by a centrifuge step and re-suspension in RPMI media, supplemented with glutamine, 20% FCS, 100U/ml penicillin, 100µg/ml streptomycin, 1% ITS (Sigma-Aldrich) and 20mM Hepes (Invitrogen). The cells were cultured in tissue culture flasks and incubated at 37°C with 5% CO_2 .Media was replaced every 2-3 days.

When the cells became confluent, the media was aspirated and cells washed with sterile PBS. Trypsin-EDTA (Invitrogen) was added to each flask and incubated for 5 minutes at 37°C. The effect of trypsin was neutralised by the addition of media with 20% FCS and the cells were split into 2 culture flasks. Mesangial cells were used between passage 6-12.

2.2.3.4 Isolation of WT kidney endothelial cells

Kidneys from WT mice were harvested and placed in DMEM media on ice. The kidneys were blended using a syringe plunger and passed through a 70µm sieve. The kidney was then digested using collagenase (Sigma-Aldrich) 3mg/ml in an agitated water bath at 37°C for 30 minutes. The digested cells were collected and washed twice in DMEM/0.5% FCS and re-suspended in media. 10µg rat-anti-mouse CD31 (BD Pharmingen) and 5µg rat anti-mouse CD105 (BD Pharmingen) was added to the cells and incubated at 4°C for 30minutes. The cells were then washed twice in 0.5% FCS/DMEM and re-suspended in 80µl 0.5% FCS/DMEM and 20µl of goat anti-rat microbeads (Miltenyi Biotec) and incubated for 15 minutes at 4°C. A column (Miltenyi Biotec) was washed with 0.5% FCS/DMEM, and after the cells were washed, they were added to the column which was attached to a magnet. The cells were pushed out the column and placed into a 25 cm flask which had been pre-coated with 2% gelatine (Sigma-Aldrich). The cells were cultured in glutamax DMEM (Gibco), 20% FCS, endothelial growth supplement (Sigma-Aldrich), 100U/ml penicillin and 100µg/ml

streptomycin. Media was changed every 3 days. When confluence was achieved, cells were split into different culture flasks. The cells were used for experiments at passage 8-12.

2.2.3.5 Stimulation of BMDM and mesangial cells

The primary cell lines were used for stimulation experiments. Between 0.5-1x10^6 cells were used per well depending on cell availability. The number of cells used for each condition in a given experiment was constant, as were the number of cells when more than 1 cell line was being compared. When the cell number differed between 2 cell lines, this is stated in the results. The BMDMs or the mesangial cells were left overnight in serum free media prior to the addition of fresh media the following day. S100A8 and S100A8/A9 (kind gift from T.Vogl) was used at a concentration of 1µg/ml for stimulation experiments, as this dose has been consistently used in the published literature. TNF-α was used at a concentration of 10ng/ml and LPS 1µg/ml. Cells were stimulated overnight and supernatants collected for ELISAs the following day.

2.2.3.6 Phenotyping of cells

Mesangial cells and endothelial cells were characterised by immunohistochemistry.

2.2.3.6.1 Mesangial cells

Mesangial cells were plated onto an 8-well culture slide. They were fixed the following day by immersion in cold acetone for 10 mins. Mesangial cells were phenotyped using 2 different antibodies: anti-pancytokeratin FITC (Sigma-Aldrich)(1:50) and rabbit anti-mouse myosin antibody (Sigma-Aldrich)(1:10) followed by a secondary goat anti-rabbit (Dylight 488,Vector labs)(1:100). Cell nuclei were counterstained using DAPI (4',6' diamino-2-phenylindole). The cells were mounted and viewed with a fluorescent microscope.

2.2.3.6.2 Endothelial cells

100,000 cells per well were plated out into an 8-well chamber slide before being fixed in cold acetone the following day. The cells were stained with pancytokeratin FITC antibody (Sigma-Aldrich)(1:50), rabbit anti-mouse mysoin antibody (Sigma-Aldrich)(1:10) and anti-mouse CD31 antibody (Abcam)(1:100). Secondary antibodies were used following the anti-

myosin antibody: goat anti-rabbit Dylight 488 (Vector labs)(1:100), and following the anti-CD31 antibody: horse anti-mouse FITC (Vector labs)(1:75). After 1 hour's incubation, cells were washed in PBS and mounted prior to being viewed by a fluorescent microscope.

2.2.3.7 Co-culture of endothelial cells and macrophages

Cultured endothelial cells were plated into a 6 well plate (Corning). 320,000 cells per well were plated out and left to grow in DMEM/10% FCS for 48 hours. The media was the aspirated. BMDM from WT and from mrp14-/- mice were grown and were isolated day 7. $1x10^6$ BMDMs were added to the endothelial cells in DMEM. The following groups of cells were co-cultured together:

- Endothelial cells alone
- Endothelial cells + WT BMDMs
- Endothelial cells + mrp14-/- BMDMs
- WT BMDMs
- Mrp14-/- BMDMs

Each group of cells were co-cultured in triplicate. The cells were incubated at 37°C with 5% CO_2 for 24 hours. The supernatants were then collected and kept at -20°C prior to cytokine analysis.

2.2.3.8 Phagocytosis assay

WT and mrp14-/- BMDMs were cultured for 7 days as previously described. 100,000 BMDMs were plated out into an 8-well chamber slide in media before being used the following day in the assay.

2µm microspheres latex polystyrene microspheres (Polysciences Inc) were incubated with BSA (Sigma-Aldrich) in PBS (10 mg/ml) at 4°C overnight while rotating. The beads were subsequently washed in PBS before being re-suspended in 100µl of PBS. The IgG fraction of a rabbit anti-bovine albumin antibody (Sigma-Aldrich) was added to the suspension of microsphere beads, to obtain a final dilution of 1:2. After incubation for 1 hour at 4°C, the beads/antibody were then washed and re-suspended in PBS. 20µl of opsonized beads and

20µl of unopsonised beads were added to the wells in triplicate and incubated for 30 minutes at 37°C in 5% CO_2. The media was aspirated and the cells washed with PBS before being stained with Diff-Quick fix (Dade Behring). The beads ingested by 50 macrophages per well were counted.

2.2.3.9 Measurement of Fcγ-receptors at baseline

The expression of Fcγ-receptors of WT and mrp14-/- BMDMs at baseline was compared. BMDMs were cultured as described above. At day 7, BMDMs were plated into a 96 well V-shaped plate and stained with 10µl rat anti-mouse CD16/32 PE conjugated antibody (BD Pharmingen) in triplicate or with an isotype control IgG2bκ antibody (BD Pharmingen). The cells were incubated with antibodies on ice for 30 mins in the dark before 2 washing steps and cell fixation in 2% paraformaldehyde. The cells were analysed by flow cytometry using a FACS Calibur machine running Cell Quest software (BD Biosciences).

2.2.3.10 RNA extraction

RNA was extracted from mouse kidney endothelial cells. Endothelial cells were plated into 6 well plates and stimulated for 4 hours with LPS 1µg/ml. Media was then aspirated and 1ml Trizol (Invitrogen) was added, and the cells homogenised before being placed into sterile eppendorfs. The sample was left at room temperature for 5 minutes. 0.2ml of chloroform (Sigma-Aldrich) was then added followed by shaking the tube for 15 seconds and then incubating at room temperature for 2-3 minutes. The eppendorf tube was then centrifuged at 12,000g for 15 minutes at 4°C which separated the mixture into a lower phenol-chloroform DNA phase, and an upper clear aqueous phase containing RNA. The upper clear aqueous phase was subsequently transferred into a new eppendorf tube and 0.5ml of isopropanol (VWR International) was added at room temperature for 10 minutes. The tube was centrifuged at 12000g for 10 minutes at 4°C which resulted in the RNA forming a gel-like pellet at the tube bottom. The supernatant was removed and the pellet washed with 1ml of 75% ethanol. The sample was briefly vortexed, followed by centrifugation at 7500g for 5 minutes at 4°C. The supernatant was removed and the pellet allowed to air-dry, with care taken to avoid the pellet drying out. 20µl of RNAse-free water (Sigma-Aldrich) was the added to dissolve the pellet. RNA concentration was measured by UV absorption using a

NanoDrop spectrophotometer and quality assessed using the absorption ratio at 260/280 nm.

2.2.3.11 Reverse-transcription polymerase chain reaction

Reverse transcription was used to synthesis complementary DNA (cDNA) from RNA. 1µl Oligo(dT)$_{12\text{-}18}$, 1µl 10mM dNTP mix (Invitrogen), 1µg RNA and up to 10µl RNAse-free water (to make a total volume of 11µl) was heated in a thermal cycler for 5 minutes in a sterile PCR tube at 65°C, followed by spinning down briefly and a 1 minute incubation on ice. 4µl 5x1st strand buffer, 1µl 0.1M Dithiothreitol and 1µl RNAse out (all Invitrogen) were added, the contents spun down and incubated on ice. To assess for genomic DNA contamination, 3µl was removed from the tube and placed into a separate PCR tube not to undergo reverse transcription but instead to be used as a control to exclude DNA contamination. 1µl of SuperScript III Reverse Transcriptase (Invitrogen) was then added to the 1st reaction tube, followed by careful pipetting. After 5 minutes incubating at room temperature, the reaction tube underwent a heating step of 50°C for 50 minutes to allow reverse transcription to take place. The sample was subsequently heated at 70°C for 15 minutes to complete reverse transcription.

2.2.3.12 Detection of TLR4 mRNA

PCR was performed to detect TLR4 cDNA following the reverse transcription step. RT-PCR was performed to analyse the presence or absence of TLR4 as opposed to the relative gene expression under different conditions. The following TLR4 primers were used, as used in the following reference (Peng, Sigua et al. 2008)

Forward: 5'ACCTGGCTGGTTTACACGTC'3

Reverse: 5'CAGGCTGTTTGTTCCCAAAT'3

Similar to the genotyping experiments, PCR was performed using a reaction tube consisting of Illustra puReTaq PCR beads (GE Healthcare). To each reaction tube, the following was added: 1µl DNA, 1µl of forward and reverse primers, 22µl water. A final volume of 25µl was obtained. A negative control was also included.

PCR conditions

Denaturation	94°C 2 mins
Amplification	94°C 30 sec
	60°C 30 sec
	72°C 30 sec
	x30 cycles
Extension	72°C 4 mins

The product was analysed by gel electrophoresis as previously described.

2.2.3.13 Supernatant ELISAs

Several cytokine ELISAs were used to analyse cytokine production stimulated by S100A8, S100A8/A9 and TNF-α. Following overnight stimulation, supernatants were collected and kept at -20°C until use. The dilutions for each individual cytokines were optimised and varied accordingly.

2.2.3.13.1 MCP-1 and IL-6

MCP-1 and IL-6 were measured using mouse CCL2 (MCP-1) ELISA Ready-SET-Go and IL-6 ELISA Ready-SET-Go kit (eBiosciences, Insight Biotechnology Ltd, UK) according to the manufacturer's instructions. ELISA plates were coated overnight with the capture antibody in the Coating Buffer included in the ELISA kit, at 4°C. Plates were washed 5 times with 0.05% Tween 20/PBS, followed by blocking with assay diluent (included in the ELSIA kit) for 1 hour at room temperature. After a further 5 washes, the samples and standards were incubated for 2 hours at room temperature. After 5 washing steps, the detection antibody was diluted according to instructions in the provided assay diluent, and was incubated at room temperature for 1 hour. Plates were washed 5 times, followed by adding avidin-HRP diluted in assay diluent for 30 minutes. After 7 further washes, substrate solution (TMB) was

added until a colour change was observed, and the reaction terminated with stop solution. Plates were read at 450nm, with correction set to 570nm.

2.2.3.13.2 TNF-α and IL-8

TNF-α and IL-8 were analysed using Duoset ELISA Development System (R&D systems, Abingdon, UK). MaxiSorp-Immuno plates (Nunc, Denmark) were coated with goat anti-mouse TNF-α (concentration 0.8μg/ml) and rat anti-mouse IL-8 (2μg/ml) and left overnight at room temperature. The ELISA plates were washed 3 times, followed by a blocking step of at least 1 hour at room temperature. The samples and the standards were incubated (TNF-α: 2000- 31.2pg/ml)(IL-8: 1000-15.6pg/ml). Each sample/standard was added in duplicate. The samples were not diluted to measure TNF-α. For IL-8, the dilutions were optimised. The samples incubated for 2 hours before 3 further washes and the addition of the detection antibody (biotinylated goat anti-mouse for TNF-α (400ng/ml) and IL-8 (200ng/ml)) for 2 hours). Streptavidin-HRP was added for 20 minutes followed by TMB substrate (colour reagent A (H_2O_2) and colour reagent B (tetramethylbenzidine) until colour development. Optical density readings were taken at 450 nm, with correction at 570nm.

2.2.4 Statistical analysis

The animal studies results are expressed as median (range); patient studies are expressed as median (range). All statistics were performed using GraphPad prism 4.0 (GraphPad Software, San Diego California, USA). Non-parametric tests of significance were applied. For comparing 2 groups, Mann-Whitney U test was used. In chapter 5, unpaired-t-test was used to compare 2 groups. One way analysis of variance (ANOVA) was carried out using non-parametric Kruskal-Wallis test and Dunn's multiple comparison post test for groups of three or more. Two-way ANOVA was used to analyse differences between groups from more than one experiment to analyse if experimental data could be combined. Correlations were assessed using the non-parametric Spearman rank correlation analysis. A significant value was defined $p<0.05$ with 95% confidence.

2.3 Buffers and solutions

2.3.1 Polymerase chain reaction

Lysis buffer for tail lysis

100mM Tris-HCL (pH 8.5), 5mM EDTA, 0.2% SDS, 200mM NaCl and 100µg/ml-added immediately before use.

Tris/EDTA (TE) buffer

1M Tris-HCL (pH 7.5), 1 mM EDTA (pH 8.0)

TAE buffer 50x

40mM Tris-acetate, 1mM EDTA (pH 8.0). For DNA electrophoresis; diluted to 1x with distilled water.

2.3.2 Tissue fixation

Neutral buffered formalin (pH 7.0)

100ml full-strength formalin (37-40% formaldehyde), 6.5g Na_2HPO_4, 4g NaH_2PO4 and 900ml dH_20.

Paraformaldehyde lysine periodate (PLP) fixative

Lysine stock solution: 0.2M lysine monohydrochloride (3.65g/100ml) and added to an equal volume of 0.1M disodium hydrogen orthophosphate (1.41g/100ml for anhydrous). The solution adjusted to pH 7.4 and stored at 4°C till use.

4% Paraformaldehyde: Paraformaldehyde was dissolved in dH_20 at 4g/100ml with stirring at 60°C in a fume hood. The solution was cleared by adding a few drops of 1M NaOH and then stored at 4°C.

Immediately prior to use, 1 volume of 4% paraformaldehyde was added to 3 volumes of lysine stock solution and sodium metaperiodate 0.214g/100ml (10mM) was added.

2.3.3 Immunohistochemistry

Phosphate buffered saline

137mM NaCl, 0.27mM KCL, 8.1mM Na_2PO_4, 1.5mM KH_2PO_4, adjust to pH 7.2

Tris buffered saline (TBS)

20mM tris(hydroxymethyl)aminomethane (TRIS), 150mM NaCl, adjust to pH 7.5

Acid alcohol

1% HCl, 70% ethanol

2.3.4 ELISA

Borate buffered saline (BBS) coating buffer

100mM boric acid, 25mM anhydrous sodium tetraborate, 75mM NaCl, pH8.3

Wash buffer

0.05% Tween 20 in PBS

Blocking buffer

1% BSA in PBS

Reagent diluent

0.1-1% BSA

Substrate solution

1:1 mixture of Colour Reagent A (H_2O_2) and Colour Reagent B (Tetramethylbenzidine) (R&D systems).

Stop solution

2N H_2SO_4

2.3.5 Tissue Culture

Mesangial cell medium

RPMI 1640 medium, 10% FCS, 100U/ml penicillin, 100µg/ml streptomycin, 2mM L-glutamine, 1% insulin/ selenium/transferrin growth supplement (ITS liquid), 20mM HEPES.

Endothelial cell medium

DMEM-glutamax 10% FCS, 100U/ml penicillin, 100µg/ml streptomycin, 75µg/ml endothelial cell growth supplement.

Macrophage cell medium

DMEM-glutamax, 10% FCS, 100U/ml penicillin, 100µg/ml streptomycin, 25% L929 conditioned media

Human umbilical vein endothelial cell medium

Culture: M199 media, 20% FCS, 30µg/ml endothelial cell growth factor, 10U/ml heparin. 100U/ml penicillin, 100µg/ml streptomycin, 2mM L-glutamine

Experiments: M199 media, 10% FCS, 7.5µg/ml endothelial cell growth factor, 2.5U/ml heparin, 100U/ml penicillin, 100µg/ml streptomycin, 2mM L-glutamine

2.3.6 FACS solutions

Wash buffer and antibody diluents

Extracellular staining: 1% FCS diluted in PBS

Intracellular staining: 0.05% saponin diluted in PBS

Fixation solutions

4% and 2% paraformaldehyde

Chapter 3 Investigation of S100A8/A9 in human ANCA associated vasculitis

3.1 Introduction

Anti-neutrophil cytoplasm antibody (ANCA) associated vasculitis (AAV) is characterized by small vessel inflammation and immune reactivity against the neutrophil and monocyte components proteinase 3 (PR3) and myeloperoxidase (MPO). ANCA have been demonstrated to have a role in the pathogenesis of AAV by activation of neutrophils and monocytes in vitro (Falk, Terrell et al. 1990), as well as by inducing disease in certain animal models (Xiao, Heeringa et al. 2002),(Little, Smyth et al. 2005).

Patients have frequent monitoring of ANCA titres, although it is known that these titres are not always a useful biomarker of disease activity or risk of relapse for many patients. A recent meta-analysis has demonstrated that serial measurements are of limited use during disease remission in guiding individualized patient treatment and do not strongly predict future disease relapse (Tomasson, Grayson et al. 2011). Increasing ANCA titres are only poorly predictive of disease relapse, therefore emphasising the need for a reliable clinical biomarker of disease activity and of remission. AAV can often feature renal involvement characterized by a focal necrotising and crescentic glomerulonephritis, which is pauci-immune and characterized by infiltration of glomerular monocytes/macrophages and T cells (Ruth, Kitching et al. 2006). A recent study which used cohorts of European Vasculitis study group (EUVAS) trial-enrolled patients investigated the types of glomerular lesions and correlated them with renal outcome, demonstrated that the extent of glomerular inflammation on renal biopsy predicted renal outcome (Berden, Ferrario et al. 2010). The more inflamed the glomeruli, with predominance (more than 50%) of crescents or focal necrosis, the better the renal outcome compared to mixed or sclerotic lesions, suggesting that crescentic and focal lesions respond the best to immunosuppressive therapy.

Phagocytes have been demonstrated to release S100A8/A9 after their interaction with activated, inflamed endothelium (Frosch, Strey et al. 2000). Once secreted, the complex has several pro-inflammatory effects following its binding to the endothelium, via heparan

sulphate proteogylcans (Srikrishna, Panneerselvam et al. 2001; Robinson, Tessier et al. 2002). This includes increased secretion of IL-8, upregulation of ICAM-1, and further recruitment of leucocytes. Additionally, this interaction results in impairment of the endothelial monolayer integrity and induction of both caspase-dependant and caspase-independent cell death mechanisms resulting in both endothelial cell (EC) apoptosis and necrosis (Viemann, Strey et al. 2005; Viemann, Barczyk et al. 2007). These characteristics make S100A8/A9 a potential candidate in the pathogenesis of AAV, in which endothelial activation and vascular damage are prominent, and suggest a possible role for it as a biomarker of disease activity. A previous study demonstrated formation of S100A8/A9 complexes on glomerular infiltrating macrophages in different forms of glomerulonephritis, with expression correlating with the severity of disease, and most prominent staining being found in proliferative forms of GN such as focal necrotizing or immune complex GN, as opposed to conditions such as minimal change disease (Frosch, Vogl et al. 2004). In addition, in renal vasculitis most activated glomerular macrophages express this complex and produce TNFα and IL-1 (Rastaldi, Ferrario et al. 2000). Other systemic inflammatory conditions have, in addition, been associated with elevated serum S100A8/S100A9 levels including systemic lupus erythematosus (SLE), rheumatoid arthritis (RA), renal allograft rejection, juvenile idiopathic arthritis and Kawasaki disease (Haga, Brun et al. 1993; Burkhardt, Radespiel-Troger et al. 2001; De Rycke, Baeten et al. 2005; Hirono, Foell et al. 2006; Frosch, Ahlmann et al. 2009; Soyfoo, Roth et al. 2009), while increasing levels have been associated with disease relapse in juvenile onset arthritis (Foell, Wulffraat et al. 2010) and decreasing levels with improvements in joint swelling in RA (Andres Cerezo, Mann et al. 2011). The most elevated levels found in SLE have been seen in patients with both arthritis and renal involvement, with a correlation between the serum concentration and disease activity assessed by SLE disease activity index (SLEDAI) score, however no correlations were found between S100A8/S100A9 cell surface and serum levels (Lood, Stenstrom et al. 2011). Additionally, S100A8/S100A9 was used as a biomarker of disease progression in a recent study measuring S100A8/S100A9 levels in patients with early osteoarthritis which demonstrated significantly higher levels of S100A8/S100A9 in patients whose disease progressed compared to those non-progressors (van Lent, Blom et al. 2011). A previous study in patients with juvenile idiopathic arthritis treated with methotrexate, demonstrated

that higher levels of serum S100A8/S100A9 were predictive of disease flares and reflected underlying subclinical inflammation (Foell, Wulffraat et al. 2010).

3.2 Aims

The aims of this chapter were to investigate S100A8/A9 expression in tissues, cells and serum from patients with AAV. Renal biopsies of patients with different classes of ANCA associated glomerulonephritis (focal, crescentic, sclerotic and mixed) were assessed for both macrophage and neutrophil infiltration (using CD68 and CD15 as cell markers respectively) as well as S100A8/A9 expression by immunohistochemistry. Serum S100A8/S100A9 levels were measured from AAV patients with both renal and non-renal involvement by ELISA and then correlated with parameters of disease activity and outcome. Both monocyte and neutrophil surface expression of S100A8/A9 was measured by flow cytometry (FACS) in acute patients and those in disease remission and compared to healthy controls. The intracellular expression of S100A8/A9 in CD14+ monocytes in response to purified MPO-ANCA or PR3-ANCA IgG, and control IgG stimulation was investigated by incubating purified CD14+ cells with IgG overnight before fixing the cells and staining them with a FITC-conjugated antibody the following day then analysing them by flow cytometry.

3.3 Experimental design

Biopsies of patients with ANCA associated glomerulonephritis were collected from the Hammersmith Hospital pathology department. Patients were classified into the following classes of GN according to the recent Berden classification: focal (>50% normal glomeruli), crescentic (>50% crescentic glomeruli), sclerotic (>50% sclerotic glomeruli) and mixed (not fitting any of the above categories). The patients were classified by reading the formal histopathology report. Patients whose biopsies contained less than 10 glomeruli were excluded. Glomerular staining was assessed by quantification of positive glomerular staining by observation, and grades from 0 (no staining) to 3 (extensive staining). The extent of

S100A8/A9 staining was then compared across the GN classes to assess a correlation between the staining pattern, class of GN and hence renal outcome.

Serum measurements were obtained by analysis of sera obtained from patients during active and inactive disease at both Hammersmith and Royal Free Hospitals. Additionally, we measured serum S100A8/S100A9 levels in a cohort of patients from the vasculitis clinic at Addenbrooke's hospital, Cambridge. All samples were obtained following informed consent under local ethics committee approval from all 3 centres. Patient's medication at the time of venesection was recorded, as were details of organ involvement and other parameters of disease activity and demographic data. An additional cohort of serum samples was obtained from the NORAM (Nonrenal Wegener's Granulomatosis Treated Alternatively with Methotrexate [MTX]) trial (De Groot, Rasmussen et al. 2005) conducted by EUVAS. Serum samples were obtained from 3 different time points, following one and six months of treatment, and at 14 months, following withdrawal of medication. Unfortunately no pre-treatment samples were available. This trial was characterised by high relapse rates following medication withdrawal at 12 months, therefore correlation between the serum levels of S100A8/A9 and relapse rate was assessed. Following optimisation of the ELISA, S100A8/A9 levels were measured using a commercially available ELISA, and analysed with a plate reader at 450nm. Results were expressed in ng/mL.

In addition, patients from the Royal Free Hospital with active and quiescent disease had leukocyte cell surface levels of S100A8/A9 measured. Following venesection of anti-coagulated blood, red cell lysis was performed. Surface expression of S100A8/A9 was assessed by staining with a FITC-conjugated antibody, while additional CD14 and CD3 staining was performed to identify the monocyte and lymphocyte populations. Flow cytometry analysis was performed within 24 hours following staining. Neutrophils were identified by forward and side scatter characteristics, while monocytes and lymphocytes were identified by forward and side scatter characteristics as well as by double immunofluorescent staining. The percentage of positive cells gated as well as the mean fluorescence index (MFI) was recorded and compared to the isotype antibody stained samples.

As well as quantifying the S100A8/9 expression on patients' cells at different disease time points, the effect of healthy control IgG, MPO-ANCA IgG and PR3-ANCA IgG on isolated CD14+ monocyte S100A8/9 expression was also investigated. ANCA IgG was purified from the samples of first or second plasma exchange fluid, obtained from AAV patients at either the Royal Free or Hammersmith Hospitals during their acute presentation. Currently, patients undergo plasma exchange as adjunctive therapy for severe acute AAV when there is advanced renal involvement, with serum creatinine>500μmol/l or dialysis dependency or features such as pulmonary haemorrhage or cerebral involvement. Plasma exchange fluid, containing high levels of ANCA-IgG, or plasma isolated from healthy controls, were first passed over a Protein A column to isolate IgG, and subsequently over a polymyxin column to remove any lipopolysaccharide (LPS), since LPS is known to up-regulate S100A8/A9. PBMCs were isolated from donor buffy coat using Lymphoprep density centrifugation, followed by positive selection for CD14 cells using magnetic beads (Mylteni). These CD14+ cells were then incubated with MPO-ANCA IgG, PR3-ANCA IgG or control IgG overnight then stained for intracellular S100A8/A9 expression the following day and analysed by flow cytometry.

Lastly, to test whether endothelial cells could also be a source of S100A8/A9 found in the serum, human umbilical vein endothelial cells (kind gift from Prof. Justin Mason, Imperial College London) were stimulated with LPS, and S100A8/A9 cell surface- and intracellular-expression (% positive cells gated and mean fluorescence intensity) were quantified by FACS. CD14 positive cells were used in these experiments as positive controls.

GraphPad prism 4.0 (GraphPad Software, San Diego, California, USA) was used for statistical analysis. To compare more than 2 groups, one way analysis of variance was used (ANOVA) using non-parametric Kruskal-Wallis test and Dunn's multiple comparison post test. To compare 2 groups, the Mann-Whitney-U test was used. The non-parametric Spearman rank correlation analysis was used to assess correlation. ROC (receiver operator curves) were calculated for serum S100A8/A9 levels in relapsing and non relapsing patients from the NORAM study. Results were significant when $p<0.05$.

3.4 Results

3.4.1 Renal biopsy immunohistochemistry

Immunohistochemistry was performed on renal biopsies from patients either presenting with newly diagnosed AAV, or patients known to have a diagnosis of AAV and presenting with suspected disease relapse. Following review of the formal histopathological renal biopsy report, it was possible to classify the patients according to the Berden classification as follows: focal (n=4), crescentic (n=12), mixed (n=8) and sclerotic (n=4). In addition, there were 4 patients with no active vasculitic lesions.

The staining of the renal biopsies is illustrated in figure 3.1. S100A8/A9 positivity was localised to active glomerular lesions, found within crescents or in areas of endocapillary proliferation (figure 3.1 (v) and (vi)). Sclerotic lesions were generally negative for S100A8/A9 expression, despite the presence of CD68+ macrophages on the renal biopsy in 75% (3 out of 4) of the patients (Figure 3.1 (i) and (iv)). There was varying amounts of S100A8/A9 staining in the interstitium depending on the extent of active tubulointerstitial nephritis and there was particularly prominent S100A8/A9 staining around active, necrotizing small vessels (Figure 3.2). However, the staining pattern of S100A8/A9 was predominantly glomerular and in a similar glomerular distribution to that of CD68 positive macrophages [Figure 3.3 (i and iii)]. Neutrophils also abundantly express S100A8/A9, so to assess the relative contribution of neutrophils to glomerular S100A8/A9 positivity; biopsies were also stained for CD15, a neutrophil marker. Although some of the glomerular S100A8/A9 positive cells were CD15 positive (ii), most of the cells were positive for macrophage CD68 (i). There was a statistically significant difference between levels of expression in the crescentic lesions compared with the sclerotic or inactive lesions (Figure 3.4) ($p<0.01$ one way ANOVA), while there was a trend to lower levels of expression with decreasing degrees of inflammation. The Berden histological classification of ANCA associated glomerulonephritis has been shown to correlate with renal outcome. The best renal survival was found in patients with a focal class of GN followed by the crescentic class, and the worst renal outcome was found in the sclerotic class of biopsy. The immunohistochemistry data suggest that glomerular S100A8/A9 expression within the renal biopsy effectively mirrors the severity of the histological findings and impacts on the long term renal outcome, with the

greatest staining in the crescentic lesions followed by focal lesions. By contrast, scarred glomeruli lack calprotectin expression, but may still contain CD68 positive macrophages, suggesting that those macrophages are of a different phenotype to those found in active inflammatory lesions, and are associated with scarring and poorer long term renal survival.

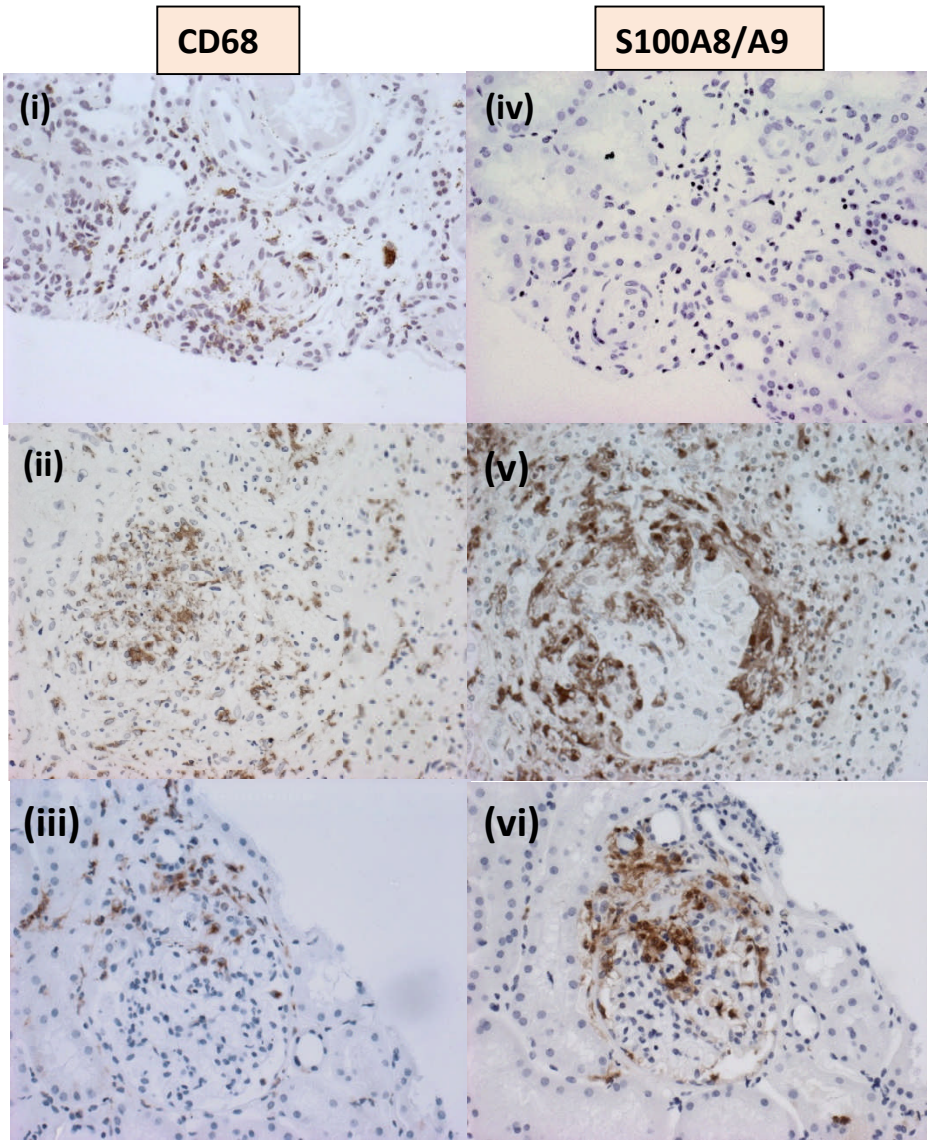

Figure 3-1 S100A8/A9 positivity in acute glomerular lesions

Immunohistochemistry demonstrating both macrophage CD68 staining and S100A8/A9 staining in different classes of ANCA associated glomerulonephritis. (i) Shows a sclerotic biopsy with CD68 staining in the sclerosed glomerulus. (iv) No S100A8/A9 staining in a sequential section of the same patient's sclerotic biopsy. (ii) Infiltration of CD68 positive macrophages in and around a glomerular crescent. (v) Prominent infiltration of S100A8/A9 cells around a sequential section of the same crescent seen in (ii). (iii) Focal GN with macrophage infiltration. (vi) Infiltration of S100A8/A9 cells around an acutely inflamed glomerulus in the same focal GN as (iii).

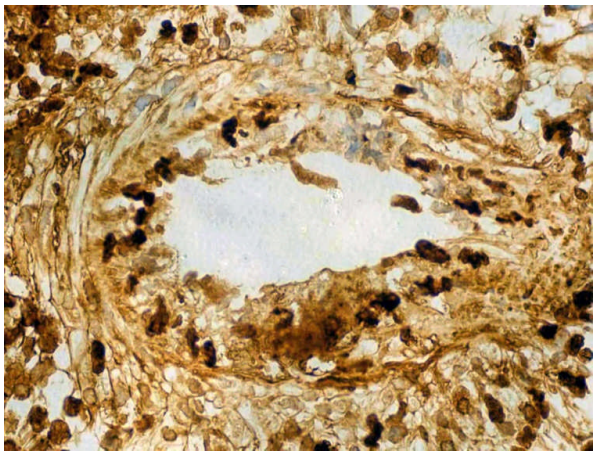

Figure 3-2 Prominent staining around an inflamed small vessel

Immunohistochemistry of a small vessel in the renal biopsy of a patient with active AAV glomerulonephritis. There is very prominent S100A8/A9 positivity around the inflamed vessel.

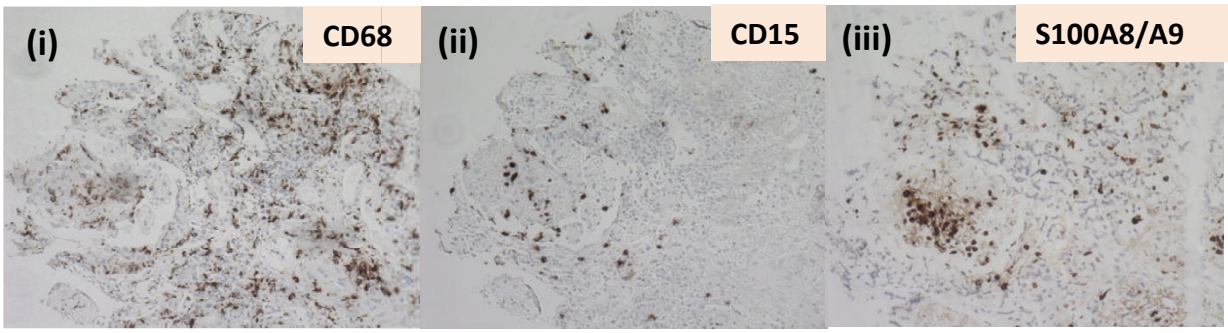

Figure 3-3 S100A8/A9 mirrors macrophage CD68 staining more than neutrophil CD15 staining.

The staining pattern and distribution of S100A8/A9 as well as the macrophage marker CD68 and the neutrophil marker CD15 on sequential sections of the same renal biopsy are shown. (i) Prominent infiltration of macrophages into the inflamed glomerulus as well as a prominent interstitial infiltrate. (ii) A few neutrophils are present with the renal biopsy as demonstrated using the granulocyte marker CD15. (iii) A prominent glomerular infiltrate of S100A8/A9 positive cells. The glomerular distribution of S100A8/A9 positive cells reflects CD68 staining.

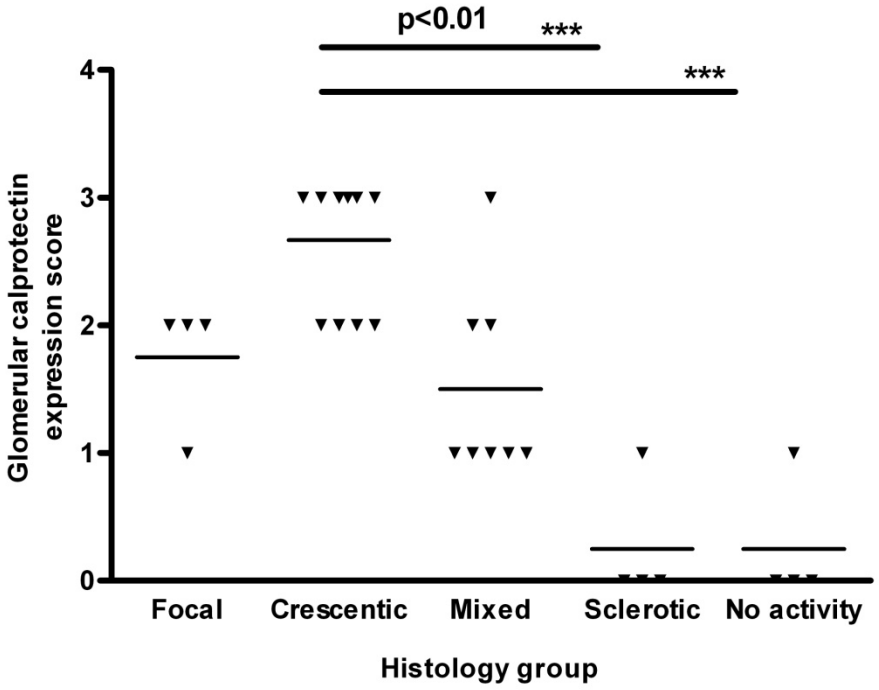

Figure 3-4 Acute lesions demonstrate the most S100A8/A9 positivity

Graph to demonstrate the glomerular S100A8/A9 score of the renal biopsies according to the Berden classification of ANCA associated GN classes: focal, crescentic, mixed and sclerotic. Each biopsy is represented by the quantification of the amount of glomerular staining (3= large amount, 2= moderate, 1= little, 0= none). Biopsies from patients with no active disease were also included. There was a significant difference between crescentic and sclerotic expression ($p<0.01$, one way ANOVA).

3.4.2 Patients with AAV demonstrate high levels of S100A8/A9 during acute disease, which decreases during remission but still remains abnormal.

Serum was obtained from patients during acute disease as well as disease remission. A total of 57 patients were included- 32 patients from London (Hammersmith and Royal Free Hospitals), 25 patients from Cambridge. 57 patients in disease remission were included as well as 16 healthy controls. Out of these patients, 26 patients had samples taken and S100A8/A9 levels measured during both acute disease and disease remission. Table 1 summarises the patient characteristics. The 16 healthy controls consisted of 7 females and 9 males with a mean age of 35 years.

	Acute n=57	**Remission n=57 (70 samples)**
Age	61 (range 16-84)	61 (16-85)
Gender	F 30, M 27	F 23, M 34
MPO-ANCA	21	33
PR3-ANCA	30	20
Both	2	0
ANCA negative	4	4
Median Creatinine	185	124
Organ involvement	Renal and extra-renal 42 Extra-renal 15	Renal and extra-renal 48 Extra-renal 9
Treatment at the time of sample taken	Nil 35 RTX, CYP, P 3 CYP, P 2 MMF 1 P/MP 10 P, MTX 3 P, AZA 1 P, CYP 2	Nil 5 P and Aza 31 P and CYP 10 MMF 2 Aza 4 P, RTX, CYP 1 P and MMF 5 P and MTX 3 P alone 2 RTX and P 4 RTX, P and Aza 2 RTX, P and MMF 1

Table 3 Clinical and demographic characteristics of the patients.

RTX=Rituximab, CYP=Cyclophosphamide, MMF=Mycophenolate Mofetil, P=Prednisolone, MP=Methylprednisolone, AZA=Azathioprine, MTX=Methotrexate.

The median serum levels and ranges of S100A8/A9 were for healthy controls 2,836 ng/ml (range 1,058-6,175 ng/ml), acute AAV patients 13,453 ng/ml (4,769-40,000ng/ml) and remission AAV patients 8,957 ng/ml (3860-25,083 ng/ml). There were significant differences between healthy controls, and both acute and remission AAV sera as well as between acute and remission samples (one way ANOVA $p<0.001$) (Figure 3-5 (i)). This is consistent with the hypothesis that serum levels of S100A8/A9 reflect clinical inflammation, with patients with active disease demonstrating very high circulating levels of the heterodimer. In addition, there was a significant but weak correlation between serum calprotectin levels and total neutrophil count ($r=0.29$)($p<0.05$). There was no correlation with blood monocyte count or serum creatinine. However, to confirm that abnormal renal function was not the cause of the elevated serum calprotectin levels a cohort of 59 dialysis patients also had serum S100A8/A9 levels measured. These patients, undergoing chronic haemodialysis, demonstrated significantly lower levels of S100A8/A9 than those patients with either active and inactive AAV (both $p<0.001$)(mean 5398ng/ml HD patients). Seventeen patients had serum S100A8/A9 measured at more than 1 time point within the first year following diagnosis (Figure 3-5 (iii)). One patient 19 weeks into treatment, demonstrated a large increase in S100A8/A9 at the time of a clinical relapse and required an escalation in immunosuppression. In the patients who entered remission, there was a decrease in serum S100A8/A9 levels from presentation to 4-6 months during remission ($p<0.05$), but this didn't reach normal levels, while the ANCA titre decreased in all the patients (Figure 2 (iv)). There was no difference in S100A8/A9 levels in those acute patients in whom prednisolone had already been initiated in the previous week compared to those who were yet to commence immunosuppression.

C-reactive protein (CRP) demonstrated a similar pattern to S100A8/A9 (figure 3-5 (ii)), with a median level of 30mg/L (range 2-248) during active disease, decreasing to a median of 3mg/ml (0.6-138) during remission. The decrease between active disease and remission was statistically significant ($p<0.0001$)(Mann-Whitney).

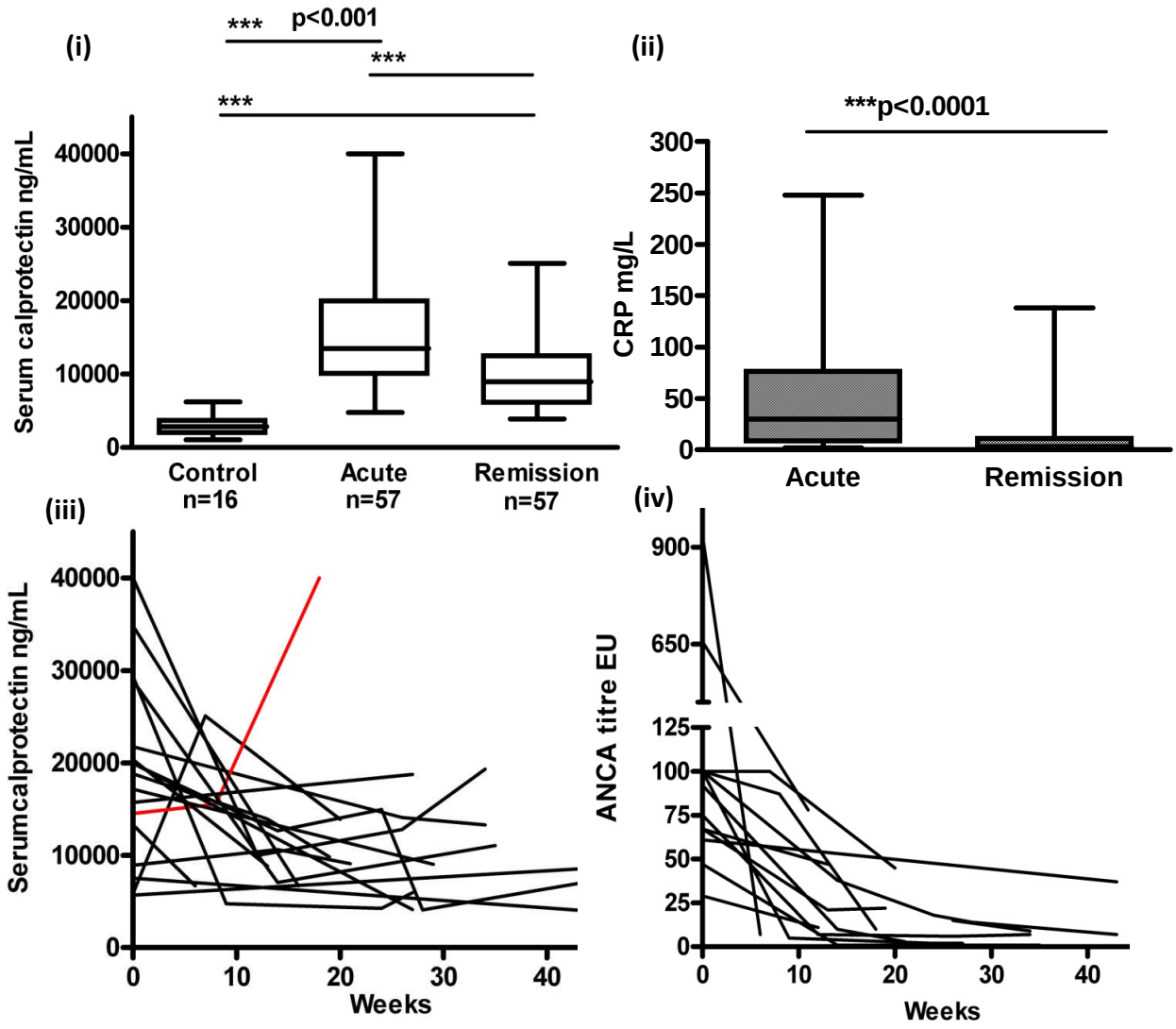

Figure 3-5 Graph to demonstrate the serum S100A8/A9 levels in patients with AAV.

(i) Acute (n=57), remission (n=57) and healthy controls (n=16). Significantly higher levels of calprotectin in acute and remission patients compared to controls ($p<0.001$)(One-way ANOVA). The serum level decreases from acute to remission but not back to the same level as healthy controls. The graph shows a box-and-whisker plot demonstrating median value, upper and lower quartiles and the maximum and minimum values for each group. (ii) Graph to demonstrate the corresponding CRP, with significant decreases in CRP between acute and remission (Mann-Whitney)($p<0.0001$). (iii) 17 patients had more than 1 level measured during the first year of treatment. Line in red demonstrates a patient with a significant increase in the level of S100A8/A9 compared to the level at time 0, corresponding with a suspected disease relapse and was treated with an escalation in immunosuppression. (iii) Corresponding ANCA titres from the patients with the sequential levels in (iii). (iii)-(iv) Each individual line represents an individual patient.

3.4.3 Relapsing patients with limited systemic disease demonstrate higher S100A8/A9 levels than the non-relapsers

The cohort of patients described above had predominantly renal involvement with a low relapse rate. Therefore it was not possible to compare the serum level of S100A8/A9 between relapsers and non-relapsers. The European vasculitis study group (EUVAS) kindly provided serum from patients who participated in the NORAM trial. This trial included patients with early systemic involvement treated with either steroids and methotrexate or steroids and cyclophosphamide. Patients were excluded from the trial if they had serum creatinine >150µmol/l or evidence of glomerulonephritis. The trial was characterised by a high relapse rate following termination of immunosuppression at 12 months. If any patients relapsed before the 12 month time point when immunosuppression was being reduced, then treatment was continued beyond 12 months. Additionally, if patients relapsed after the 12 month time-point off treatment, then it was re-started.

Serum was not available at time 0, before patients started any treatment. However, from a total of 100 patients recruited to the trial, serial samples from 27 patients were available for analysis. The samples were taken at taken at 3 time points within 14 months of diagnosis: the first sample was between time 0-2 months, then subsequently between 5-7 months of therapy when treatment was with tapering doses of prednisolone from 60 to 25 mg/day, and finally samples taken between 12-14 months, when immunosuppression had either been withdrawn or was continued/re-started in those patients who had already relapsed. Out of this group of 27 patients, 14 were relapsers, and 13 non-relapsers. The patients who did not relapse had treatment stopped at 12 months. Five of the relapsing patients relapsed before 12 months while still on immunosuppression, and 9 patients relapsed after 12 months and restarted immunosuppression. Six of the late relapsers had S100A8/A9 measured prior to the relapse and before re-introduction of immunosuppression.

In all the treated NORAM patients' samples serum S100A8/A9 levels were significantly lower than in those with generalized (renal) disease even during remission (median levels NORAM samples at one month 418 ng/ml (range 71-2167) compared to generalized disease remission 8,957 ng/ml (3860-25,083) ($p<0.0001$). However, there was a significant increase in S100A8/A9 levels in NORAM subjects after 12 months (median level at 14 months 1689

ng/ml (384-6245) vs 1 month 418 ng/ml (range 71-2167)($p<0.0001$, Mann Whitney U test). The 14 patients who went on to relapse during the study (at a median 13 months from entry, range 6-18 months) had significantly higher levels of calprotectin at the first two time points, compared with the 13 non-relapsing patients whilst on treatment at these time points (both $p<0.01$)(Figure 3-6). At the final time point there was a trend to higher values in the relapsers, but this did not reach statistical significance ($p=0.055$). Table 4 demonstrates the serum levels in the relapsing and non-relapsing groups. These data suggest that failure to sufficiently suppress S100A8/A9 levels, whilst on treatment, can predict subsequent disease relapse. Receiver operating curves comparing relapsers to non-relapsers demonstrated that at both one and six months there was a threshold which was associated with a significant risk of relapse, at one month a S100A8/A9 level greater than 626 ng/ml was associated with a sensitivity of 78.6% and specificity of 92.3% and a likelihood ratio of 10.3 (table 5), while at six months a level greater than 454 ng/ml was associated with a sensitivity of 78.6% and specificity of 92.3% (table 6). The area under curve at one month was 0.87, $p=0.0009$, while at six months it was 0.841, $p=0.002$ (Figure 3-6). This cohort of patients, unlike those with renal involvement, consisted predominantly of PR3-ANCA positive patients (25 PR3-ANCA positive, 1 MPO-ANCA and 1 ANCA negative) and the early samples were taken at a time when patients were established on significant immunotherapy.

	Time 1-2 months		**Time 5-7 months**		**Time 12 months**	
	Relapsers	**Non-relapsers**	**Relapsers**	**Non-relapsers**	**Relapsers**	**Non-relapsers**
Median ng/ml	1084	287	630	252	2066	957
Range ng/ml	128-2167	71-980	180-2515	88-953	634-6245	384-5400

Table 4 Serum S100A8/A9 levels from 27 patients in the NORAM trial at different time points.

The table demonstrates the median S100A8/A9 levels (and range) at the 3 time points when patients in the NORAM study were sampled. The patients are divided into relapsers and the non-relapsers.

Cutoff ng/ml	Sensitivity	95% CI	Specificity	95% CI
> 80.00	1.000	0.7684 to 1.000	0.07692	0.001946 to 0.3603
> 108.0	1.000	0.7684 to 1.000	0.1538	0.01921 to 0.4545
> 127.5	1.000	0.7684 to 1.000	0.2308	0.05038 to 0.5381
> 129.0	0.9286	0.6613 to 0.9982	0.2308	0.05038 to 0.5381
> 142.0	0.9286	0.6613 to 0.9982	0.3077	0.09092 to 0.6143
> 157.0	0.9286	0.6613 to 0.9982	0.3846	0.1386 to 0.6842
> 185.5	0.9286	0.6613 to 0.9982	0.4615	0.1922 to 0.7487
> 249.0	0.8571	0.5719 to 0.9822	0.4615	0.1922 to 0.7487
> 299.5	0.8571	0.5719 to 0.9822	0.5385	0.2513 to 0.8078
> 318.0	0.8571	0.5719 to 0.9822	0.6154	0.3158 to 0.8614
> 355.0	0.8571	0.5719 to 0.9822	0.6923	0.3857 to 0.9091
> 390.5	0.8571	0.5719 to 0.9822	0.7692	0.4619 to 0.9496
> 406.5	0.7857	0.4920 to 0.9534	0.7692	0.4619 to 0.9496
> 494.0	0.7857	0.4920 to 0.9534	0.8462	0.5455 to 0.9808
> 626.5	**0.7857**	**0.4920 to 0.9534**	**0.9231**	**0.6397 to 0.9981**
> 712.5	0.7143	0.4190 to 0.9161	0.9231	0.6397 to 0.9981
> 790.0	0.6429	0.3514 to 0.8724	0.9231	0.6397 to 0.9981
> 909.0	0.5714	0.2886 to 0.8234	0.9231	0.6397 to 0.9981
> 985.0	0.5714	0.2886 to 0.8234	1.000	0.7529 to 1.000
> 1084	0.5000	0.2304 to 0.7696	1.000	0.7529 to 1.000
> 1314	0.4286	0.1766 to 0.7114	1.000	0.7529 to 1.000
> 1484	0.3571	0.1276 to 0.6486	1.000	0.7529 to 1.000
> 1563	0.2857	0.08389 to 0.5810	1.000	0.7529 to 1.000
> 1627	0.2143	0.04658 to 0.5080	1.000	0.7529 to 1.000

Table 5 Table to demonstrate sensitivities and specificities of serum S100A8/A9 at 1 month

The table above shows the sensitivities and specificities for predicting future disease relapse in the patients from the NORAM trial. The S100A8/A9 level at 1 month following commencement of treatment in bold illustrates the cut-off level which retained the greatest sensitivity and specificity.

Cutoff	Sensitivity	95% CI	Specificity	95% CI
> 156.0	1.000	0.7684 to 1.000	0.2308	0.05038 to 0.5381
> 189.0	0.9286	0.6613 to 0.9982	0.2308	0.05038 to 0.5381
> 205.0	0.9286	0.6613 to 0.9982	0.3077	0.09092 to 0.6143
> 215.0	0.9286	0.6613 to 0.9982	0.3846	0.1386 to 0.6842
> 221.0	0.9286	0.6613 to 0.9982	0.4615	0.1922 to 0.7487
> 238.0	0.8571	0.5719 to 0.9822	0.4615	0.1922 to 0.7487
> 256.0	0.8571	0.5719 to 0.9822	0.5385	0.2513 to 0.8078
> 286.0	0.8571	0.5719 to 0.9822	0.6154	0.3158 to 0.8614
> 317.0	0.8571	0.5719 to 0.9822	0.6923	0.3857 to 0.9091
> 357.5	0.7857	0.4920 to 0.9534	0.6923	0.3857 to 0.9091
> 406.0	0.7857	0.4920 to 0.9534	0.7692	0.4619 to 0.9496
> 422.0	0.7857	0.4920 to 0.9534	0.8462	0.5455 to 0.9808
> 454.0	**0.7857**	**0.4920 to 0.9534**	**0.9231**	**0.6397 to 0.9981**
> 487.5	0.7143	0.4190 to 0.9161	0.9231	0.6397 to 0.9981
> 524.5	0.6429	0.3514 to 0.8724	0.9231	0.6397 to 0.9981
> 590.0	0.5714	0.2886 to 0.8234	0.9231	0.6397 to 0.9981
> 630.0	0.5000	0.2304 to 0.7696	0.9231	0.6397 to 0.9981
> 711.3	0.4286	0.1766 to 0.7114	0.9231	0.6397 to 0.9981
> 825.8	0.3571	0.1276 to 0.6486	0.9231	0.6397 to 0.9981
> 880.0	0.2857	0.08389 to 0.5810	0.9231	0.6397 to 0.9981
> 923.5	0.2143	0.04658 to 0.5080	0.9231	0.6397 to 0.9981
> 965.5	0.2143	0.04658 to 0.5080	1.000	0.7529 to 1.000
> 1199	0.1429	0.01779 to 0.4281	1.000	0.7529 to 1.000

Table 6 Table to demonstrate sensitivities and specificities of serum S100A8/A9 at 6 months

The table above shows the sensitivities and specificities for predicting future disease relapse in the patients from the NORAM trial. The S100A8/A9 level at 6 months following commencement of treatment in bold illustrates the cutoff level which retained the greatest sensitivity and specificity.

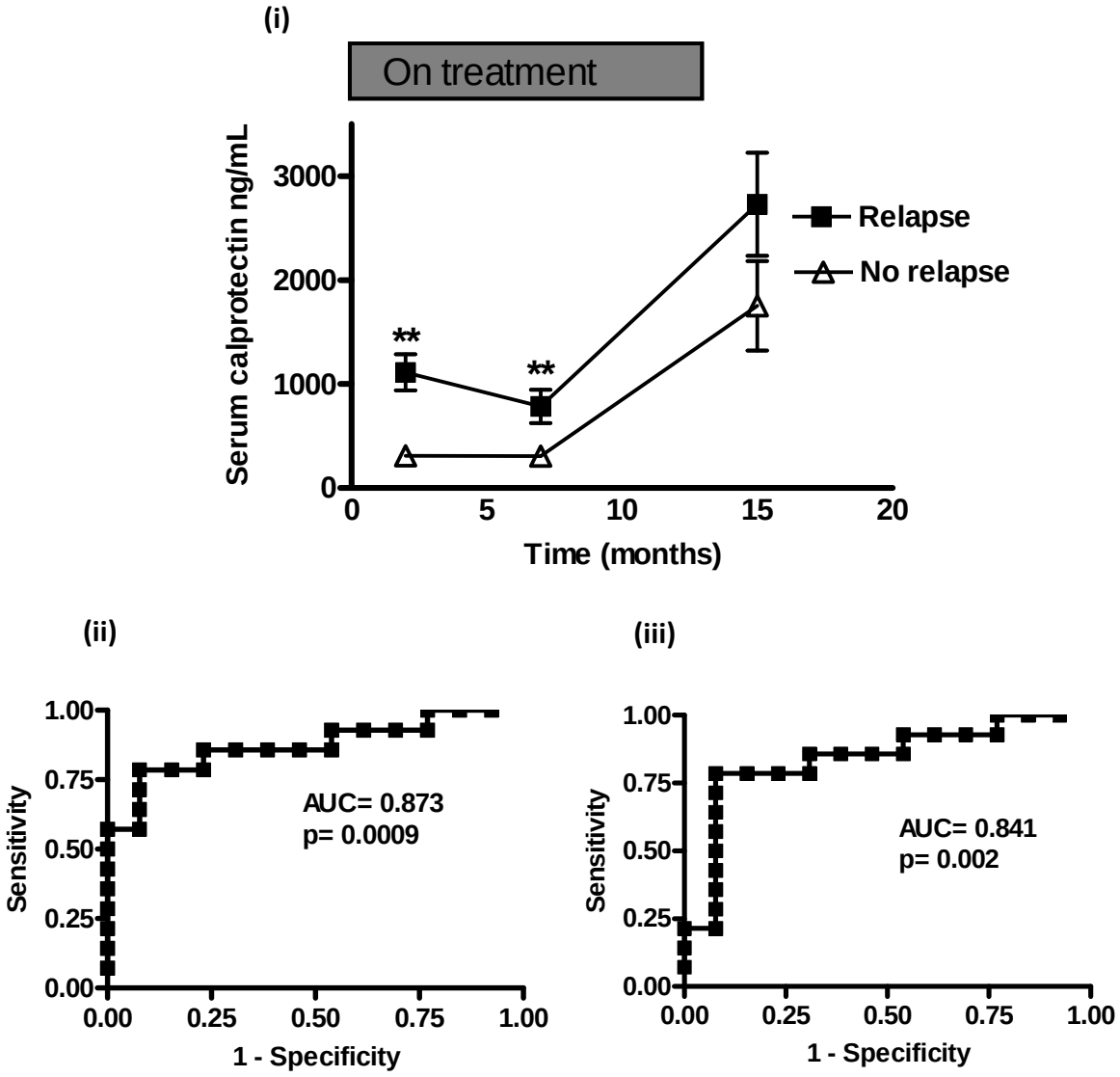

Figure 3-6 Non-relapsing patients demonstrate lower levels of S100A8/A9 than relapsing patients.

(i) Graph demonstrating the serum levels of S100A8/A9 at the 3 different time-points in the relapsing and non-relapsing groups. The relapsing group had significantly higher levels of S100A8/A9 at the first 2 time points and a trend to a higher level at the 3rd time-point. The final time point for relapsing patients included a mixture of patients on and off immunosuppression depending on the timing of disease relapse. The graph demonstrates the mean and standard error of the mean (SEM) for each time-point. (ii) ROC using serum levels of S100A8/A9 to predict relapse at 1 month following diagnosis. (iii) ROC using serum levels of S100A8/A9 taken at 6 months to predict relapse.

3.4.4 Neutrophil and monocyte surface expression of S100A8/A9

Surface S100A8/A9 expression was investigated in a subset of healthy controls (n=7), active AAV (n=10), and remission AAV (n=18) patients. Twenty three patients had renal disease, while five had only extra-renal disease. Fifteen patients were MPO-ANCA positive and eight PR3-ANCA positive, while five were ANCA negative. Monocyte gates were determined on the flow cytometer by counterstaining with CD14, T lymphocyte gates were determined by a CD3 counterstain, while neutrophil gates were identified by forward and side scatter characteristics alone (Figure 3-7 (i)). Table 7 summarises the staining results. There was a greater proportion (% of S100A8/A9 expressing gated cells compared to % of cells gated with isotype control conjugated antibody) of both neutrophils and monocytes in AAV patients during active disease and convalescence compared with healthy controls (percentage neutrophils expressing S100A8/A9- median (range): healthy controls 0% (0-3.6%), acute AAV 78.9% (14.7-98.1%), convalescent AAV 6.8% (0-98.8%), active AAV compared to controls $p<0.001$ and active AAV compared to convalescent AAV $p<0.05$ (one way ANOVA)(figure 3-8 (i)); percentage monocytes expressing S100A8/A9- median (range): healthy controls 5.4% (0-16.9%), acute AAV 50.5% (0-91.6%), convalescent AAV 5.6% (1-94.6%)(p=NS)(Figure 3-8 (ii)). We were unable to detect any surface S100A8/A9 expression on CD3 positive cells. Among patients, the decrease in the proportion of monocytes expressing cell surface S100A8/A9 between the acute and convalescent samples was large but did not reach statistical significance (Figure 3-8 (ii)). There was a statistically significant difference in S100A8/A9 mean fluorescent intensity (MFI) between acute patients and healthy controls for both neutrophil ($p<0.001$)(Figure 3-8 (iii)) and monocyte ($p<0.01$)(Figure 3-8 (iv)) cell surface expression.

Characteristic	Controls	Acute	Remission
Number (n)	7	10	18
% calprotectin positive neutrophils	0 (0-3.6%)	78.9% (14.7-98.1%)	6.8% (0-98.8%)
% calprotectin positive monocytes	5.4% (0-16.9%)	50.5% (0-91.6%)	5.6% (1-94.6%)
MFI calprotectin positive neutrophils	0.52 (0.19-0.93)	2.95 (1-14.18)	1.39 (0.48-5.08)
MFI calprotectin positive monocytes	1.22 (0.21-1.72)	3.66 (1.09-8.75)	1.78 (0.83-5.2)

Table 7 Cell surface S100A8/A9 expression in controls and patients with active and inactive disease

The table contains a summary of the results comparing controls, acute AAV and remission AAV patients' cells stained for surface calprotectin expression, according to cell subtype. The % of cells gated for S100A8/A9 surface expression and the mean fluorescent intensity (MFI). The samples were subtracted from the % of cells gated and divided by the MFI of the Isotype control antibody.

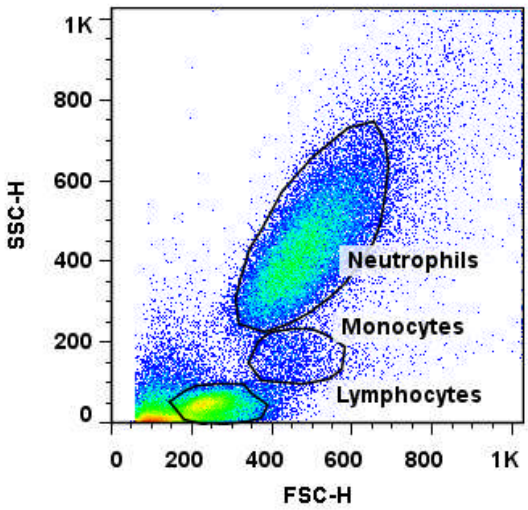

Figure 3-7 Shows the flow cytometry plot demonstrating the different cell populations and their identification. Neutrophils identified by forward and side scatter. T-cells identified by anti-CD3-PE antibody, and monocytes by anti-CD14 FITC-antibody.

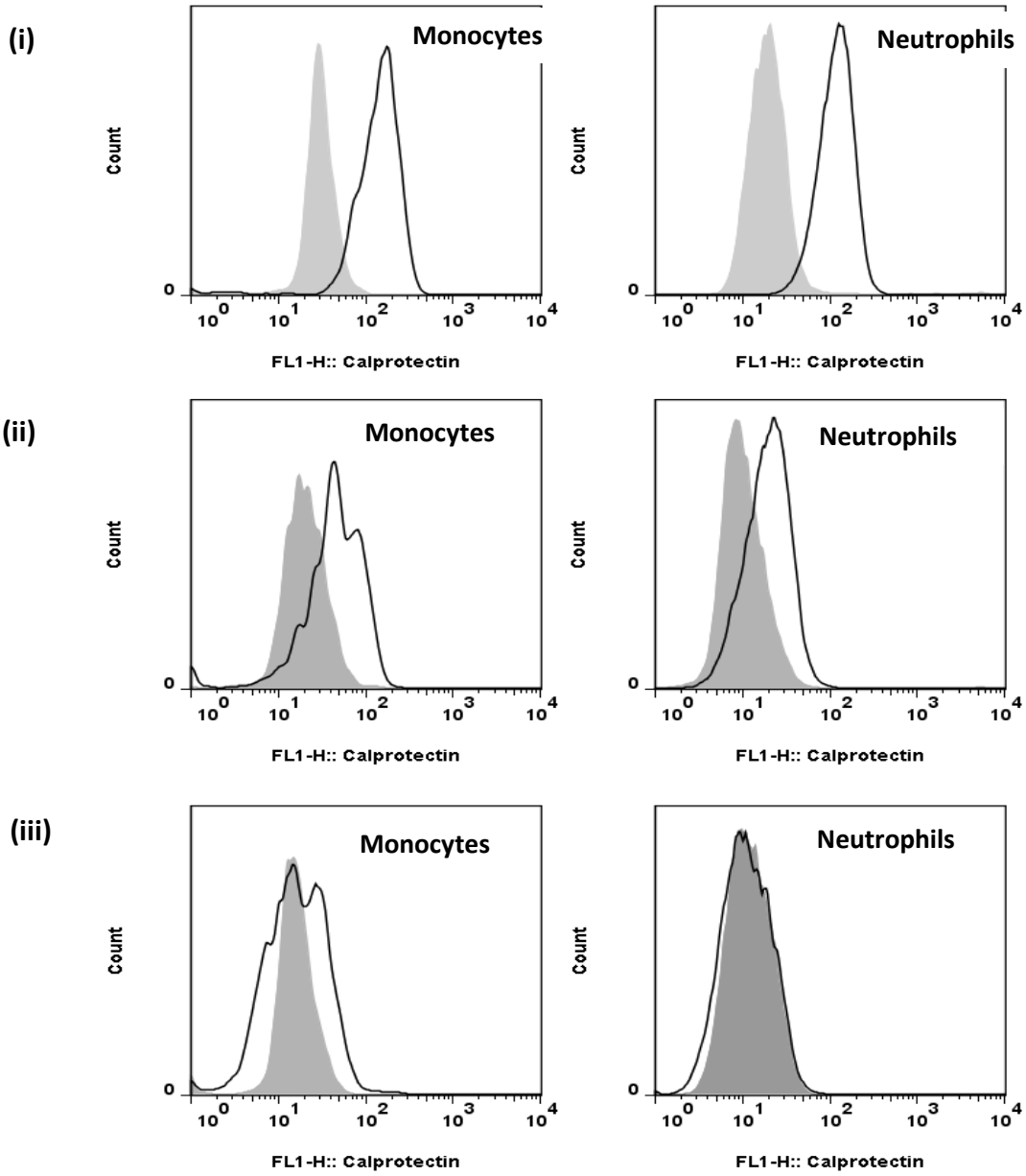

Figure 3-8 Acute patients demonstrate high surface expression of S100A8/A9 on monocytes and neutrophils.

(i) FACS plots of an acute patient (isotype control shaded grey, S100A8/A9 FITC black) illustrating the increase in monocytes and neutrophils gated for S100A8/A9. (ii) Patient in disease remission demonstrates lower % cells gated for S100A8/A9. (iii) Demonstrates the FACS plots to show the level of S100A8/A9 surface expression of neutrophils and monocytes of a healthy control.

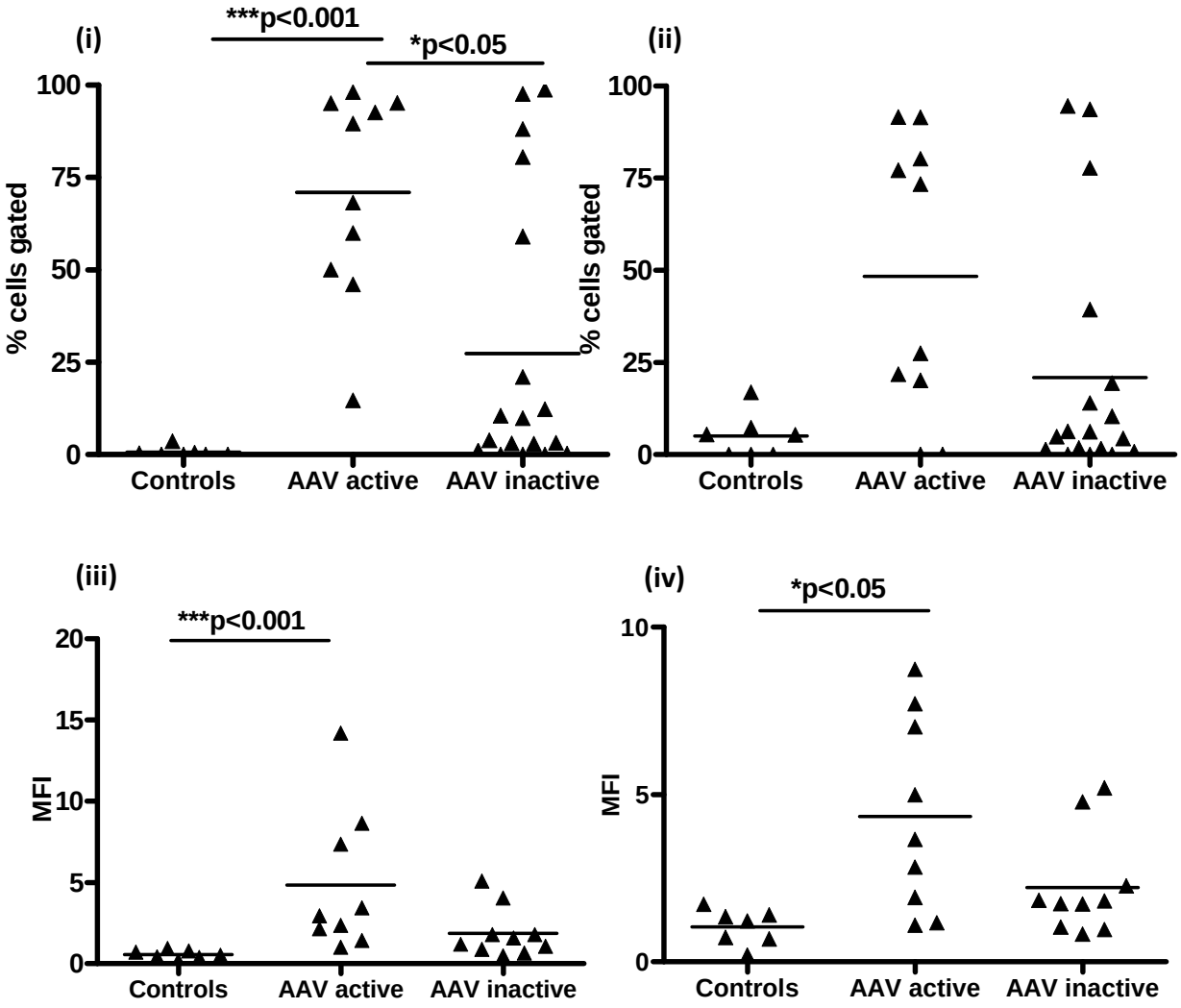

Figure 3-9 Cell surface expression of S100A8/A9 in inactive and active AAV

Each graph demonstrates a scatter plot with the mean represented by the horizontal line. (i) Demonstrates % gated neutrophils expressing extracellular S100A8/A9 (% of positive cells based upon gating of the isotype control) (controls v AAV active $p<0.001$, AAV active v AAV inactive $p<0.05$, one-way ANOVA). (ii) Graph to show % gated monocytes expressing extracellular S100A8/A9 which follows a similar but non-significant trend to the neutrophils (p=ns). (iii) Mean fluorescent intensity (MFI) (S100A8/A9 FITC antibody/isotype control antibody) of cells stained for S100A8/A9, comparing controls, active and inactive AAV. There was a significant increase in the MFI on neutrophils from acute patients compared with healthy controls ($p<0.001$). (iv) MFI of S100A8/A9 on monocytes demonstrating a significant increase in MFI between patients with active disease and healthy controls ($p<0.01$).

3.4.5 Human IgG up-regulates intracellular S100A8/A9 in monocytes

The effect of MPO-ANCA IgG, PR3-ANCA IgG (isolated from plasma exchange fluid) and healthy control IgG on human monocytes was investigated. To avoid the variability of donor monocytes and the quantity of blood required from venesection, monocytes were purified from leukocytes isolated from a buffy coat sample from NHS blood and transplant service. All IgG samples were depleted of LPS using a polymyxin column with resultant undetectable LPS as assessed by a limulus assay. Following PBMC isolation, CD14+ cells were purified using CD14-magnetic beads and the resultant CD14 cell population was found to be 98% pure. The CD14+ cells were stimulated with 250µg/mL of the different IgG preparations. Five ANCA-IgG samples were used (2 PR3-ANCA, 3 MPO-ANCA) and healthy control IgG isolated from 3 controls.

IgG from healthy controls and from patients with AAV was able to increase the proportion of S100A8/A9 expressing cells. This corresponded to an increase in both percentage of S100A8/A9 expressing cells and the mean fluorescent intensity (MFI) of the positive population. Figure 3-9 demonstrates the increase in the percentage of calprotectin positive cells, and the increase in MFI compared to unstimulated cells, suggesting an increase in the number of cells expressing S100A8/A9 as well as the amount each cell expressed. The results show that MPO-ANCA and PR3-ANCA IgG isolated from 5 different patients had a similar effect on the calprotectin expression, without a significant increment when TNF (10ng/mL) was added. IgG isolated from healthy controls had a more variable effect and although there was a trend to lower level of S100A8/A9 expression compared to ANCA containing IgG, the result was not significant (figure 3-9). Similarly, the mean fluorescent intensity of CD14+ cells increased following stimulation with control IgG and was similar to those obtained with MPO-ANCA and PR3-ANCA. Overall, these data demonstrate that IgG is able to upregulate intracellular S100A8/A9 expression in CD14 expressing monocytes but the effect is not specific to ANCA.

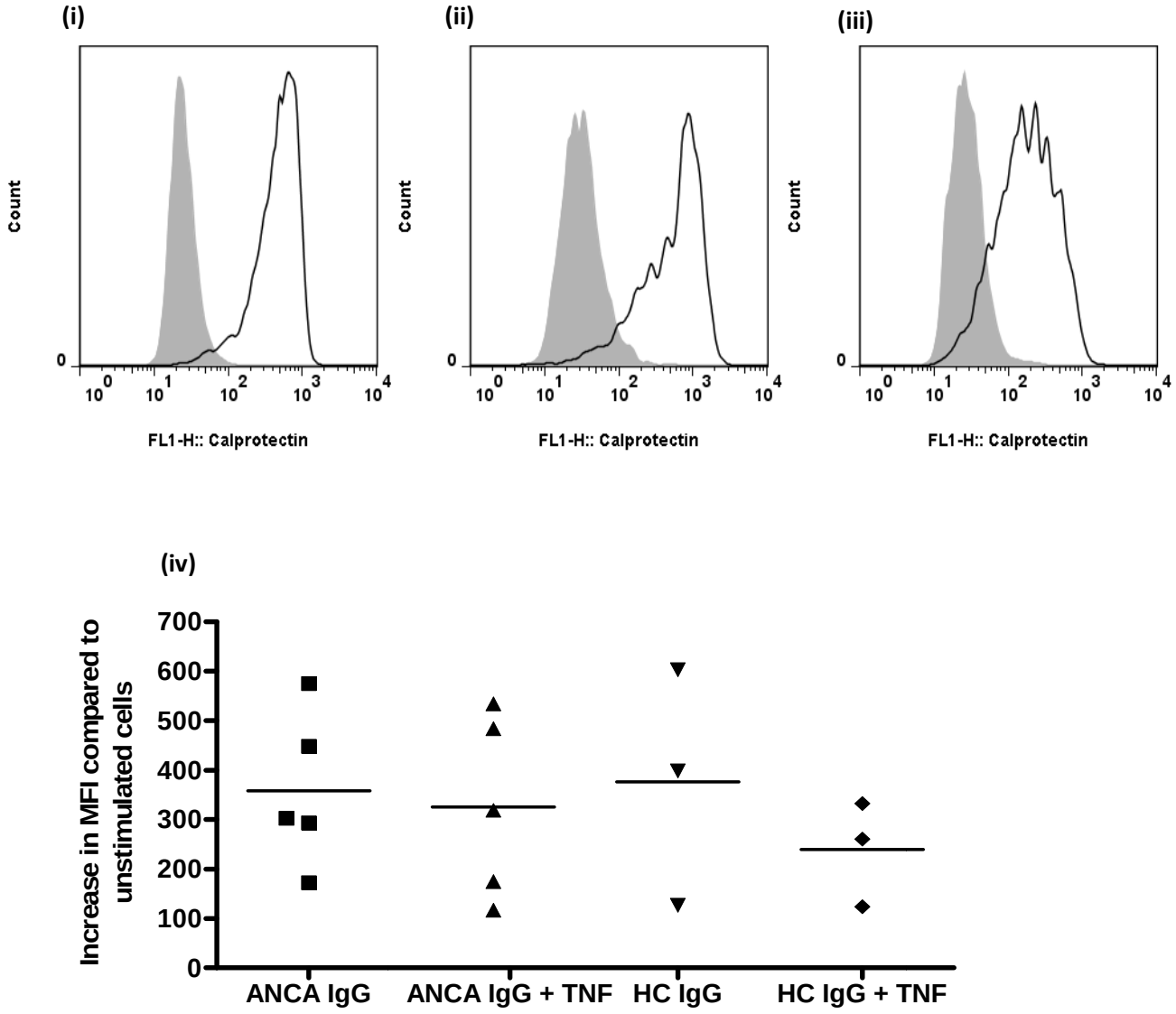

Figure 3-10 IgG upregulates S100A8/A9 expression in CD14+ cells

(i) FACS plot demonstrating the increase in MFI (S100A8/A9 FITC compared to isotype control [shaded grey]) following CD14 cell stimulation by ANCA-IgG. (ii) Similar increase in MFI following stimulation of CD14 cells with healthy control (HC) IgG. (iii) MFI of unstimulated cells. (iv) Graph to demonstrate the increase in MFI of CD14 cells under different conditions, compared to unstimulated cells. The increases between all the groups are not significant.

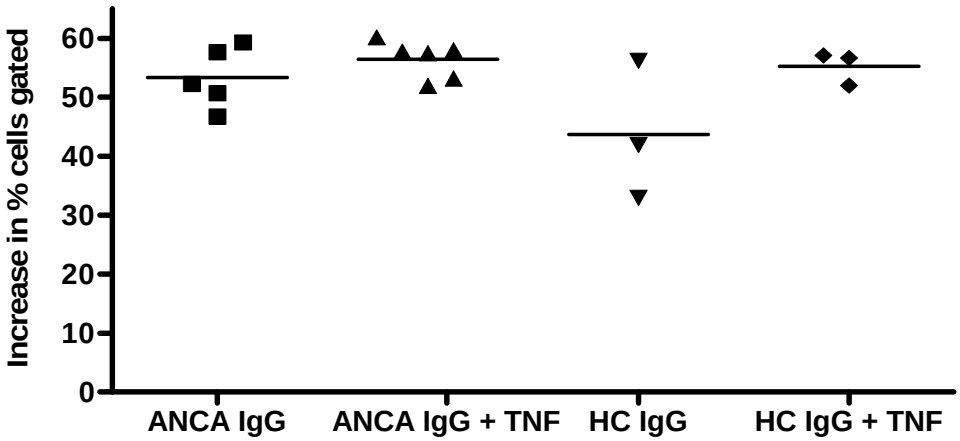

Figure 3-11 IgG increases the proportion of CD14 cells expressing intracellular S100A8/A9

Graph above demonstrates the % increase in cells gated for S100A8/A9 compared to unstimulated CD14 cells. IgG stimulation resulted in an increased proportion of cells with detectable intracellular expression. There was no difference in expression compared to ANCA-IgG and IgG isolated from healthy controls.

3.4.6 Human umbilical vein endothelial cells do not express S100A8/A9

Human umbilical endothelial cells (HUVEC) were a kind gift from Professor Justin Mason, Imperial College London, and were used at 300,000 cells per condition and stimulated to investigate HUVEC S100A8/A9 expression. Healthy control PBMC were isolated, followed by positive selection of CD14+ cells and used as a positive control ($1x10^6$ CD14+ cells per condition). The cells were left unstimulated or stimulated with LPS (1-10µg/ml) in triplicate. Following stimulation with LPS, cells were stained for intracellular and extracellular calprotectin expression and assessed by flow cytometry.

CD14+ cells, as expected, had detectable surface expression of S100A8/A9 (mean % S100A8/A9 expressing cells 34.3%%, increasing to 50% with 1 µg/ml LPS stimulation, unpaired t-test $p<0.05$). The mean fluorescent intensity (MFI) also increased following 1µg/ml LPS (508.1 to 675, unpaired t-test $p<0.005$). The majority of CD14+ cells demonstrated intracellular S100A8/A9 expressed and showed a non-significant increase in expression following 1 µg/ml LPS (mean unstimulated 86.7% increasing to 94.6% with LPS), with similar results with respect to change in MFI (unstimulated MFI 862.9 increasing to 986.8 following LPS). However, there was no HUVEC calprotectin expression detected either on the cell surface or intracellularly in unstimulated cells or following LPS stimulation.

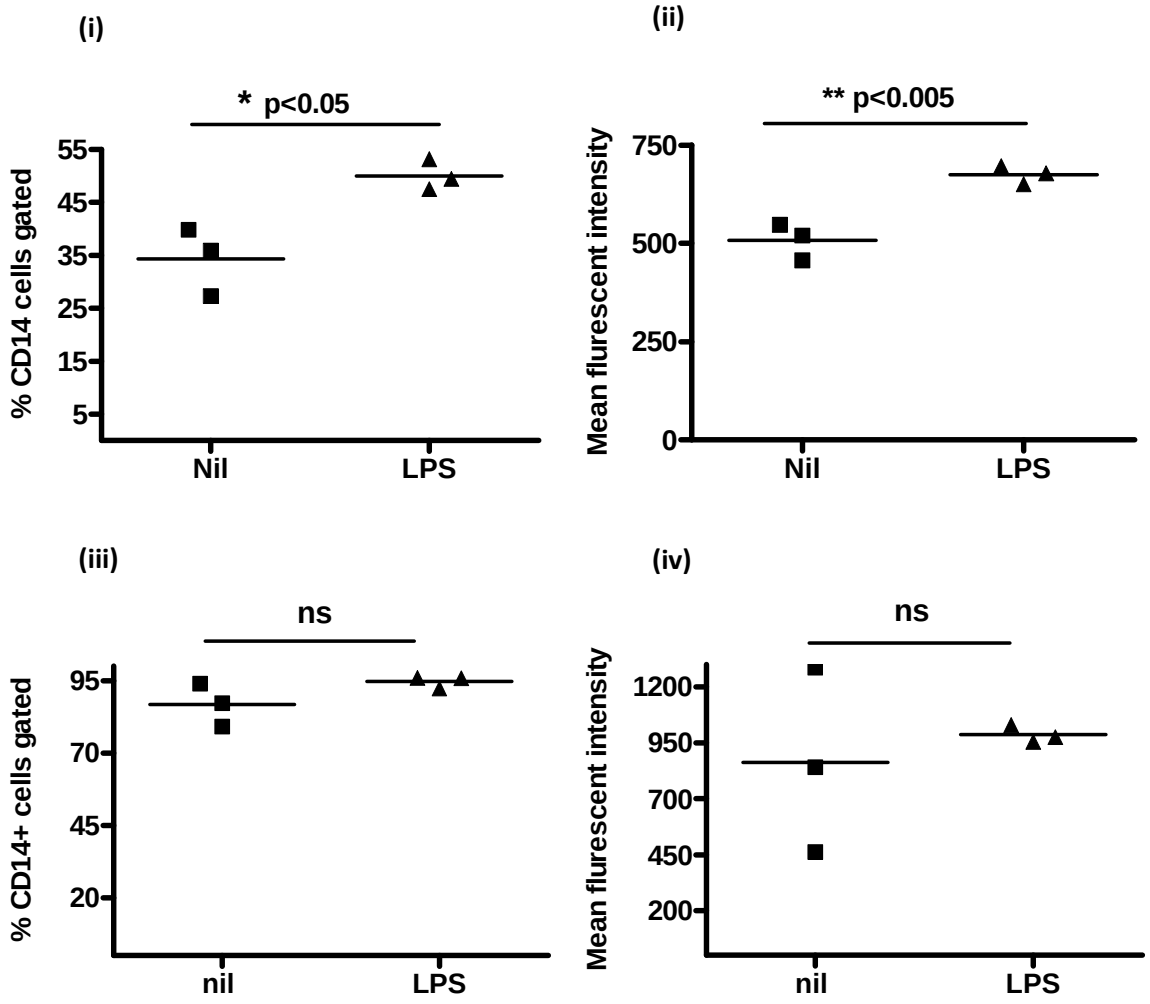

Figure 3-12 CD14 express S100A8/A9 while HUVECs do not.

Graphs to demonstrate the increase in both surface and intracellular expression of S100A8/A9 in CD14 cells. (i) and (ii) demonstrate % of cells with surface expression and MFI respectively. There is a significant increase in extracellular expression following stimulation with LPS. (iii) % of cells with intracellular expression with a non-significant increase following LPS where almost 100% of cells express calprotectin. (iv) Similarly, MFI of intracellular staining showed minimal increase following LPS stimulation. No surface or intracellular expression of S100A8/A9 in HUVECs, nor was there an increase following varying doses of LPS.

3.5 Discussion

Glomerular lesions consisting of monocytes/macrophages, as well as neutrophil degranulation are key features of pauci-immune glomerulonephritis secondary to AAV, while circulating monocyte and neutrophil activation is found during active disease. This chapter expands data from a previous study which reported glomerular macrophage expression of S100A8/A9 in several different glomerular pathologies (Rastaldi, Ferrario et al. 2000), including a small subset of patients with AAV, who demonstrated prominent expression in areas of necrotizing extracapillary damage. Those patients with more severe glomerular pathologies demonstrated prominent S100A8/A9 expression unlike those patients with less inflammatory glomerular lesions, such as minimal change nephropathy. This work demonstrates glomerular infiltration of cells expressing S100A8/A9 in the renal biopsies of patients with glomerulonephritis secondary to AAV. Prominent S100A8/A9 expression was seen within active crescents and in areas of focal necrosis, but was absent in sclerotic or normal glomeruli. S100A8/A9 expression was greatest in the active histological lesions that predict better long term renal outcome according to the recent Berden classification. By contrast sclerotic glomeruli, did not contain S100A8/9 expressing macrophages, demonstrating that inflammatory and sclerotic glomeruli contain monocyte/macrophages of a different phenotype. Therefore, S100A8/A9 expressing monocytes are associated with the most severely inflammed glomerular lesions and those associated with better renal outcome following treatment, making it a potentially important biomarker and potential therapeutic target.

In acute AAV, circulating monocytes and neutrophils are activated. Patients with AAV have elevated levels of cell surface S100A8/A9 on both neutrophils and monocytes compared with healthy controls, with levels greatest during active disease, to the extent that some patients had almost 100% of their neutrophils and monocytes with detectable cell surface S100A8/A9. Moreover, AAV patients expressed more S100A8/A9 on each cell, demonstrated by increased mean fluorescent intensity, compared to healthy controls. Additionally, serum levels of S100A8/A9 reflected these cellular findings, with significantly higher levels in active disease compared to remission and those found in healthy controls. Interestingly, those patients in clinical remission still had persistently elevated serum S100A8/A9 levels and

leukocyte expression, suggesting that there is a degree of subclinical innate immune activation. However, it is not possible from these experiments to conclude whether the significant cellular surface expression of myeloid cells is due to intracellular production of the heterodimer or whether circulating S100A8/A9 has become deposited on the cell surface.

There are similar data illustrating persistent inflammation and cell activation in convalescent AAV patients, such as persistent monocyte IL-12 and interferon gamma production (Hruskova, Rihova et al. 2009), augmented indoleamine dioxygenase expression (an IFN-γ regulated enzyme) (Chavele, Shukla et al. 2010) as well as elevated monocyte TLR expression (Tadema, Abdulahad et al. 2011). Importantly, levels of S100A8/A9 diminished following immunomodulatory therapy, but achieved lower degrees of suppression in those patients who went on to relapse. Additionally, analyzing the patients with severe systemic disease and sequential levels of S100A8/A9 revealed one patient with a steep increase in the serum S100A8/A9 level which corresponded to an increase in clinical disease activity in the context of a decreasing MPO-ANCA IgG titre.

Analysis of ROC of the patients in the NORAM study, suggests that failure to suppress S100A8/A9 at one or six months may be a useful predictor of future relapses, with a likelihood ratio at one month of 10.3. This is significantly better than the predictive value of a rising ANCA titre, which has recently been estimated in meta-analysis to provide a likelihood ratio of 2.8 for disease relapse (Tomasson, Grayson et al. 2011). However, since we did not have pre-treatment S100A8/A9 levels, there remains a possibility that relapsers simply maintain higher levels of S100A8/A9. The levels at 1 month and 6 months were measured when patients were receiving immunosuppression which may partially account for the much lower levels compared to those patients with renal involvement. These results are similar to those found in SLE (Haga, Brun et al. 1993; Soyfoo, Roth et al. 2009). The most elevated S100A8/A9 levels in SLE have been seen in patients with arthritis and renal involvement, and a correlation between the serum concentration and SLEDAI scores (Lood, Stenstrom et al. 2011). Additionally, a recent study measuring S100A8/S100A9 levels in patients with early osteoarthritis demonstrated significantly higher levels of S100A8/S100A9 in patients whose disease progressed compared to the group of non-progressors (van Lent,

Blom et al. 2011). Patients with severe sepsis also demonstrate elevated levels of calprotectin, although the levels are generally lower than those seen in vasculitis patients, with no apparent correlation between serum levels and severity on the infection (van Zoelen, Vogl et al. 2009).

With regards the source of serum S100A8/A9, I was not able to demonstrate intracellular or surface expression of the heterodimer in human umbilical vein endothelial cells at rest or following stimulation with LPS. By using CD14 cells as a positive control, both surface expression and intracellular expression of S100A8/A9 could be demonstrated as could the predicted increase following LPS stimulation. However, using the same techniques no similar expression was detectable in HUVEC, suggesting that most serum S100A8/A9 in patients with AAV is likely derived from circulating neutrophils and monocytes.

Both serum levels and cell surface S100A8/A9 expression are augmented during disease activity, and in early systemic disease higher levels are associated with disease relapse. These findings suggest that serum S100A8/A9 levels may help guide immunosuppression treatment and may be of more clinical utility than CRP, an acute phase reactant, which is generally within the normal range in patients during remission and does not provide prognostic information. A previous study in patients with juvenile idiopathic arthritis treated with methotrexate, demonstrated that higher levels of S100A8/A9 were predictive of flares, and reflected underlying subclinical inflammation (Foell, Wulffraat et al. 2010).

S100A8/9 an example of a damage associated molecular pattern (DAMP) and a marker of activation of innate immunity, has recently been demonstrated to play a role in autoimmunity and induction of autoimmune T cells, exerting its action through TLR4 (Loser, Vogl et al. 2010). TLR4 expression has been demonstrated in the kidney and has been shown to contribute to renal injury in animal models (Brown, Lock et al. 2007). Furthermore, TLR4 expression on both bone marrow derived cells as well as glomerular endothelial cells has been shown to have a role in neutrophil recruitment and renal injury in the experimental myeloperoxidase glomerulonephritis model (Summers, van der Veen et al. 2010). In another animal model, S100A8 was able to upregulate activatory FcγR in macrophages through binding TLR4 (van Lent, Grevers et al. 2010). Recently, it has been demonstrated that

neutrophil extracellular traps (NETs) contain calprotectin (Urban, Ermert et al. 2009) and that NETS are released by ANCA stimulated neutrophils. The formation of NETS may have a role in triggering vasculitis and promoting the autoimmune response in patients with small vessel vasculitis (Kessenbrock, Krumbholz et al. 2009).

This chapter demonstrates that S100A8/A9 is upregulated in patients with AAV and represents a marker of cellular immune activation and disease activity. Alongside the traditional markers of disease activity such as CRP and ANCA titre, measuring S100A8/A9 may have a role is aiding diagnosis but also in helping to predict those at risk of future disease relapse. This may then help guide immunosuppression therapy. Clearly, replicating these data in other cohorts, with renal involvement, is critical to understand the utility of measuring calprotectin as a prognostic marker, and efforts are underway to measure calprotectin in samples from other EUVAS studies.

Summary of results:

- Patients with focal and crescentic glomerulonephritis have a prominent infiltration of S100A8/A9 positive cells linking the expression of S100A8/A9 with response to therapy and disease outcome.
- Patients with AAV and renal involvement have elevated serum level of S100A8/A9, which decreases but does not normalize during remission
- Patients with non-renal involvement who subsequently relapse have higher early levels of S100A8/A9 than non-relapsers therefore S100A8/A9 may potentially be a biomarker in this cohort of patients
- Patients have greatly elevated monocyte and neutrophil cell surface levels of S100A8/A9.

Chapter 4 The role of S100A8/A9 in nephrotoxic nephritis

4.1 Introduction

Nephrotoxic nephritis is a commonly used animal model of immune complex glomerulonephritis. Sheep antibodies directed against the mouse glomerular basement membrane act as a planted antigen, and focus the resulting immune response towards the GBM. NTN is characterised by an early neutrophil influx at 2 hours after injection of nephrotoxic serum, followed by glomerular injury induced by T cell and macrophage infiltration. The pathology of this model is characterised by Th1 cell and macrophage infiltration, and glomerular thrombosis with subsequent renal dysfunction. Although the results can be variable, this model has been widely used to delineate crucial aspects of both innate and adaptive immune systems to improve our understanding of immune-mediate glomerulonephritis.

Macrophages have been shown to play an important role in both the initiation and propagation of glomerulonephritis as discussed in the introduction. It has been increasingly recognised that macrophages respond to the local cytokine milieu, and have an element of plasticity in response to that local environment. S100A8/A9, which is present in neutrophils, monocytes and some inflammatory macrophages, but absent is chronic lesions, has been investigated in other animal models of inflammation and autoimmunity. Mrp14-/- mice, in an antigen-induced arthritis model, are protected from joint erosions and destruction, with S100A8/A9 having a role in the induction of matrix metalloproteinases (MMPs), which are known to mediate joint destruction. S100A8 additionally has a role in the upregulation of activatory FcγR (FcγRI, FcγRIV) receptors, as well as the upregulation of pro-inflammatory cytokines (van Lent, Grevers et al. 2008; van Lent, Grevers et al. 2010). This work is relevant in the nephrotoxic nephritis animal model, in which the importance of Fc receptors on infiltrating leucocytes has previously been investigated, with these receptors playing an important role in the pathogenesis of disease (Tarzi, Davies et al. 2002). Additionally, S100A8/A9 plays a role in the generation of autoreactive T cells (CD8+), linking the innate immune system with the development of antigen-specific autoimmunity (Loser, Vogl et al.

2010). The role of pattern-recognition receptors in the pathogenesis of autoimmunity and inflammation is increasingly being recognised along with damage-associated molecular patterns (DAMPs), which bind to these receptors. This mechanism may provide a link between the innate and the adaptive immune system as well as providing a link between infection and autoimmunity. This chapter explores S100A8/A9 in NTN, in both the accelerated and non-accelerated models.

4.2 Aim

This chapter investigates the role of S100A8/A9 in nephrotoxic nephritis animal model by comparing disease between WT and mrp14-/- mice. The experiments were repeated with both low-dose and high-dose LPS to assess if disease protection, could be overcome. The non-accelerated NTN model was also used to assess the early neutrophil infiltration in both animal groups.

4.3 Experimental design

Macrophage phenotype in NTN was initially investigated using animals which had been demonstrated in our lab to be protected from disease in NTN. These animal sections were kindly provided by Dr. K. Chavele (mice deficient in mannose-receptor) and Dr. S. Hamour (mice deficient in IL17). Sections were assessed for the presence of cells positive for S100A8/A9 (antibody kindly provided by Dr. N. Hogg, Cancer Research UK). To investigate the early cell influx of cells positive for S100A8/A9, WT mouse sections during the early time-points in the nephrotoxic nephritis model were assessed for the presence of cells positive for S100A8/A9.

Mrp14-/- mice were kindly provided by Prof. Fredrik Ivars, University of Lund, Sweden. Animals were bred and housed according to guidelines at the Central Biological Services department, Hammersmith Hospital Campus, Imperial College London. WT (C57BL/6) and mrp14-/- were aged and sex matched. Females were used for all the experiments. Initial

pilot experiments were performed to assess disease using varying concentrations of nephrotoxic serum. Disease severity was assessed by the quantification of proteinuria, measurement of serum urea to assess renal function, and histological assessment on PAS and H+E sections to assess glomerular thrombosis. The humoral response was investigated using an ELISA to measure mouse anti-sheep IgG, as well as immunofluorescence of kidney sections to measure mouse and sheep IgG deposition on the glomerular basement membrane. Cellular responses were investigated by CD68 and CD4 staining on kidney sections to assess T cell and macrophage infiltration. A subset of animals had serum S100A8/A9 measured by Professor T. Vogl, University of Muenster, Germany.

Statistical analysis was performed by GraphPad Prism. The Mann-Whitney test was used to compare 2 groups of non-parametric data. To analyse more than 2 groups, 1-way analysis of variance was used (ANOVA). Correlation data was assessed by using Spearman's non-parametric analysis.

4.4 Results

4.4.1 Mice protected from NTN demonstrate few calprotectin (S100A8/A9) expressing macrophages

Previous work done by Dr. K. Chavele had demonstrated that mice deficient in mannose receptor (MR-/-) were protected from accelerated nephrotoxic nephritis. This protection was explained by an alteration in the phenotype of MR-/- macrophages to a less inflammatory phenotype, as well as impaired Fc mediated activity. Other work in our lab by Dr. S. Hamour demonstrated that mice deficient in IL17-/- were also protected from renal disease in NTN. In both these animal groups, the mice protected from disease had similar CD68 macrophage infiltration as WT animals with disease. Using paraffin fixed formalin embedded kidney sections from these previous experiments, the presence of macrophages positive for S100A8/A9 was investigated.

WT (n=9), IL17-/- and MR-/- mice (n=4 of each) were tested. These animals had previously been assessed for CD68 macrophage infiltration by immunohistochemistry on frozen sections. In the IL17-experiments, WT mice demonstrated a median of 1.94 CD68 macrophages per glomerular cross section (range 1.68-2.72), while IL17-/- mice demonstrated a median of 2.5 macrophages per glomerular cross section (range 1.72-3.28). However, IL17-/- mice demonstrated significantly less S100A8/A9 positive cells (median 0.32 [range 0.08-0.36]) than WT mice (median 2.54 [range 0.68-3.28])(Mann-Whitney t-test $p<0.05$).

Similarly, in the MR experiments; 5 WT mice and 4 MR-/- mice demonstrated a non-significant difference in CD68 macrophage infiltration (median CD68 infiltration in WT mice 1.32 [range 0.24-1.6], MR-/- mice median 0.82 [range 0.64-1.28]). The MR-/- mice demonstrated very few S100A8/A9 positive cells; median 0.14 [range 0.04-0.32]. When comparing the ratios of S100A8/A9 positive cells/CD68 cells, IL17-/- and MR-/- cells demonstrated similar ratios of 0.11 and 0.18 respectively, with WT mice demonstrating a higher ratio of 1.1.

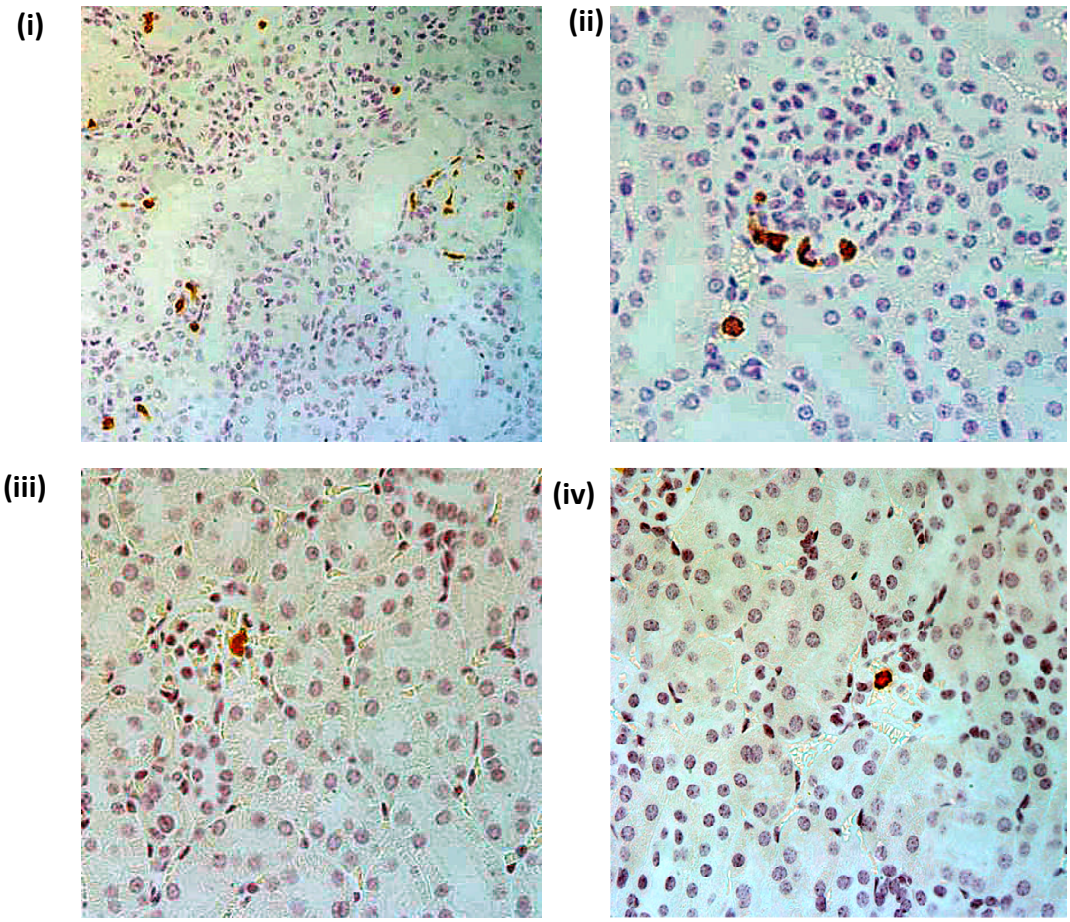

Figure 4-1 Photomicrographs of immunohistochemistry on formalin fixed paraffin embedded sections staining for S100A8A9

Kidney sections from WT mice demonstrating the presence of S100A8/A9 positive cells at low power (i)(x200) and high power (ii)(x400). Kidney sections from IL17-/- mouse (iii)(x400) and from a MR-/- mouse (iv)(x400) during NTN demonstrating very little S100A8/A9 positivity.

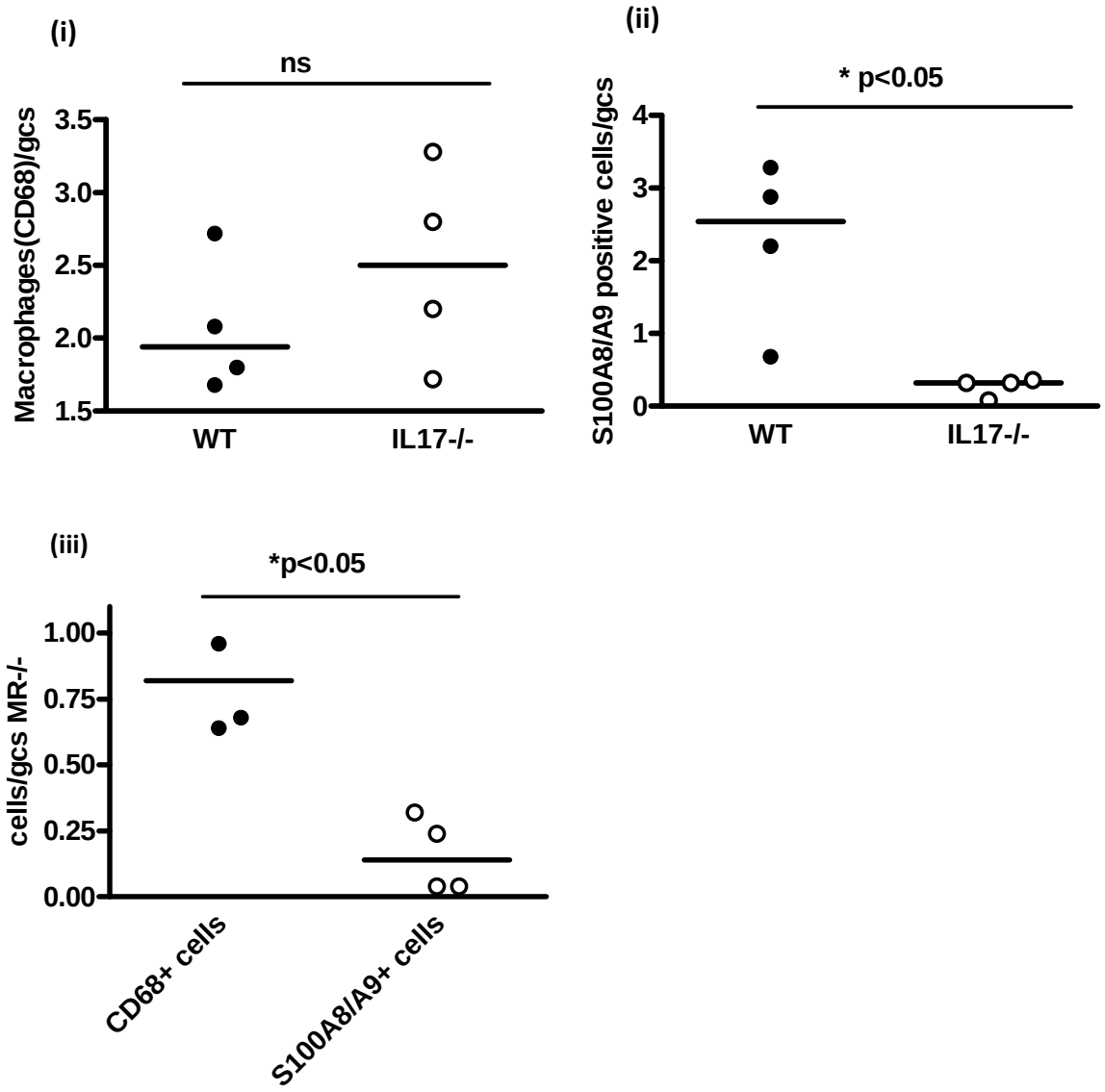

Figure 4-2 IL17-/- and MR-/- mice protected from nephrotoxic nephritis have less pro-inflammatory macrophages than WT mice with disease

(i) Graph shows similar intra-glomerular CD68 macrophage infiltration in WT and IL17-/- mice despite IL17-/- mice being protected from nephrotoxic nephritis. (ii) WT mice demonstrate similar numbers of S100A8/A9 and CD68 positive cells infiltrating the glomerulus, while IL17-/- mice demonstrate significantly fewer S100A8/A9 cells infiltrating the glomerulus. (iii) Similar results with MR-/- mice. Few of the CD68 positive macrophages in the glomerulus of MR-/- mice are also S100A8/A9 positive.

4.4.2 WT mice demonstrate early infiltration of S100A8/A9 positive cells

Immunohistochemistry was performed to assess the early infiltration of cells positive for S100A8/A9. During 2 separate nephrotoxic nephritis time course experiments in WT mice, animals were sacrificed at 4 time points following the induction of disease; at 0 hours, 4 hours, 24 hours and 48 hours. Formalin fixed paraffin embedded sections were used to stain for the presence of S100A8/A9 positive cells. 25 glomeruli were counted per section, and then the average number of glomeruli calculated per animal.

At 0 hours, there was a mean of 0.06 S100A8/A9 positive cells. This increased to a mean of 2.48 cells/glomerular cross-section (gcs), but by 24 hours, this has decreased to a mean of 1.06 cells/gcs and decreased further by 48 hours to 0.66. This demonstrates that in NTN, there is an early influx of S100A8/A9 positive cells, consistent with the known early neutrophil infiltration in this model.

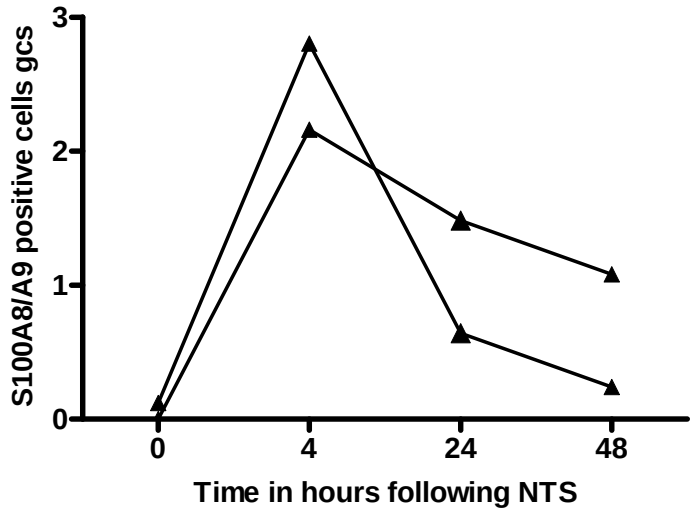

Figure 4-3 During NTN there is early infiltration of S100A8/A9 positive cells.

Graph demonstrates the number of S100A8/A9 positive cells analysed by immunohistochemistry on WT kidney sections during 2 separate NTN time-course experiments. There is an early infiltration of S100A8/A9 positive cells which has peaked by 4 hours.

4.4.3 Genotyping of mrp14-/- mice

PCR analysis was used to confirm the genotype of mrp14-/- mice. Ear clippings were used as a source of genomic DNA which was isolated and amplified as described in the methods. The primer sequence for the WT and the mutant DNA was kindly provided by Prof. Ivars. WT mice demonstrate a band of 540 base pairs while mutant mice demonstrate a smaller band at 235 base pairs.

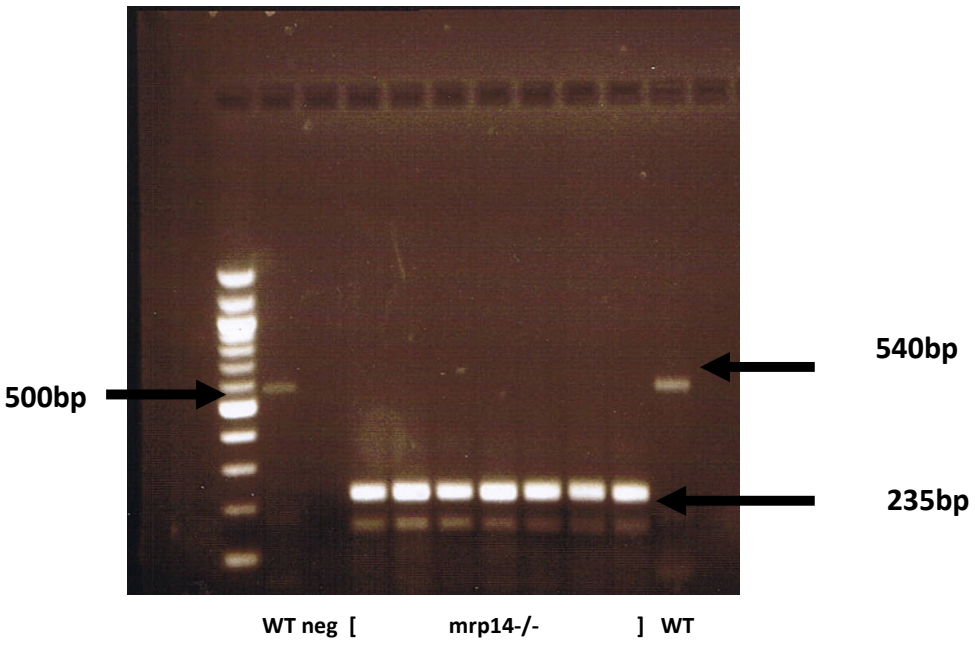

Figure 4-4 PCR genotyping in WT and mrp14-/- mice

Using a 100 base pair ladder, 2 bands were amplified from WT and mutant DNA. 2 WT animals and 7 mrp14-/- animals were genotyped.

4.4.4 Mrp14-/- mice are protected from nephrotoxic nephritis

The accelerated nephrotoxic nephritis animal model was used. Animals were pre-immunised at day -5 with 200µl of a 1:1 dilution of complete Freund's adjuvant (CFA) and 0.2mg sheep IgG diluted in 0.9% sterile saline. At day 0, nephrotoxic serum (NTS) was injected by the tail vein at a dilution of 1:1 with 0.9% sterile saline. Mice were placed in metabolic cages the day prior to sacrifice and urine was collected. Mice were sacrificed between days 7-9.

A pilot study was initially performed as a new batch of NTS was used and there is known to be batch to batch variation in NTS. 5 WT mice using a dilution of NTS 1:1, 5 WT mice using NTS 1:4 and 3 mrp14-/- mice using a dilution 1:1 were included in the pilot study. The pilot study demonstrated a non-significant trend to an improved renal function in the mrp14-/- mice (WT 1:1 urea median 10.3mmol/l [range 7.8-17.5], WT 1:4 median 10.6mmol/l [range 6.6-79.1mmol/l], mrp14-/- median 8.2mmol/l [range 7.6-8.4]). There was a trend to less thrombosis in the mrp14-/- group (median thrombosis score WT 1:1 0.36, WT 1:4 0.16 and mrp14-/- 0.04). There was also a trend to less CD68 macrophage infiltration median WT 1:1 1.54 [range 1.25-1.72], WT 1:4 0.8 [range 0.2-2] and mrp14-/- 0.31 [range 0-0.68])(WT 1:1 v mrp14-/- 1:1 p=0.057 Mann-Whitney t-test). The results lacking significance reflect the small numbers of mrp14-/- animals used in this pilot study. Subsequent NTN experiments were therefore performed using an NTS dilution of 1:1.

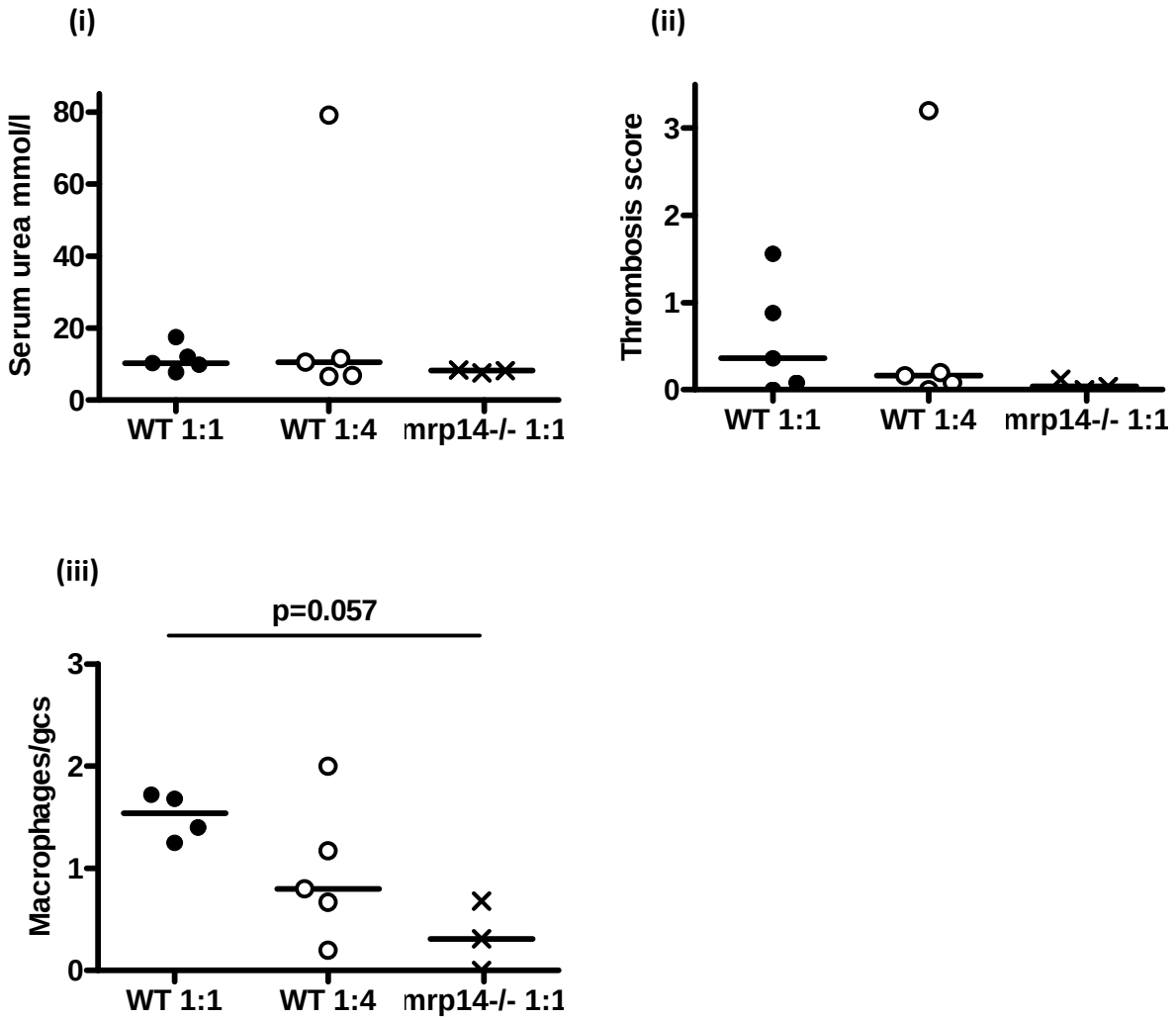

Figure 4-5 mrp14-/- demonstrate a trend of less severe renal injury in NTN compared to WT using NTS at 1:4 and 1:1 dilutions.

(i) Graph to demonstrate renal function (serum urea) in the 2 groups of WT mice and in mrp14-/- mice. The differences between the groups were not significant. (ii) mrp14-/- mice demonstrate no glomerular thrombosis, while WT mice using both 1:1 and 1:4 dilution of NTS have more thrombosis but the differences are not significant. (iii) WT mice demonstrate more glomerular CD68 macrophage infiltration using NTS at both 1:1 and 1:4 dilution than mrp14-/- mice. Comparing WT and mrp14-/- mice (both using NTS dilution 1:1), the difference is not significant (p value 0.057)(Mann-Whitney t-test).

NTN experiments were performed using NTS diluted 1:1 in 0.9% sterile saline. The mice were monitored closely for 7-8 days before being place in metabolic cages and scarified the following day.

Two nephrotoxic nephritis experiments were carried out using 9 WT and 9 mrp14-/- mice in the first experiment and 9 WT and 8 mrp14-/- mice in the second experiment. The experiments differed in that in experiment 1 the animals had milder disease, the nephrotoxic serum was administered intra-peritoneally, and the mice were sacrificed on day 7. In the second experiment, the mice were administered with intravenous nephrotoxic serum and sacrificed on day 9.

4.4.4.1 Renal histology

WT mice developed significant glomerular abnormalities with thrombosis and marked tubular dilatation. Few crescents were seen. In experiment 1, WT mice demonstrated a median thrombosis score of 0.2 (range 0-3.84). None of the mrp14-/- demonstrated any thrombosis. The difference between these 2 groups was not significant. In experiment 2 the median thrombosis score in WT mice was 0.52 (range 0-3.48), and in mrp14-/- mice the median score was 0 (range 0-3.28). The difference between theses 2 groups was not significant. A 2-way ANOVA determined there was no significant differences between these 2 experiments ($p=0.14$) allowing me to combine data from experiments 1 and 2. When combined, the median thrombosis score in WT mice was 0.32 (0-3.84) and in mrp14-/- 0 (0-3.28), with the 2-way ANOVA demonstrating a significant difference between WT and mrp14-/- mice, ($p<0.05$).

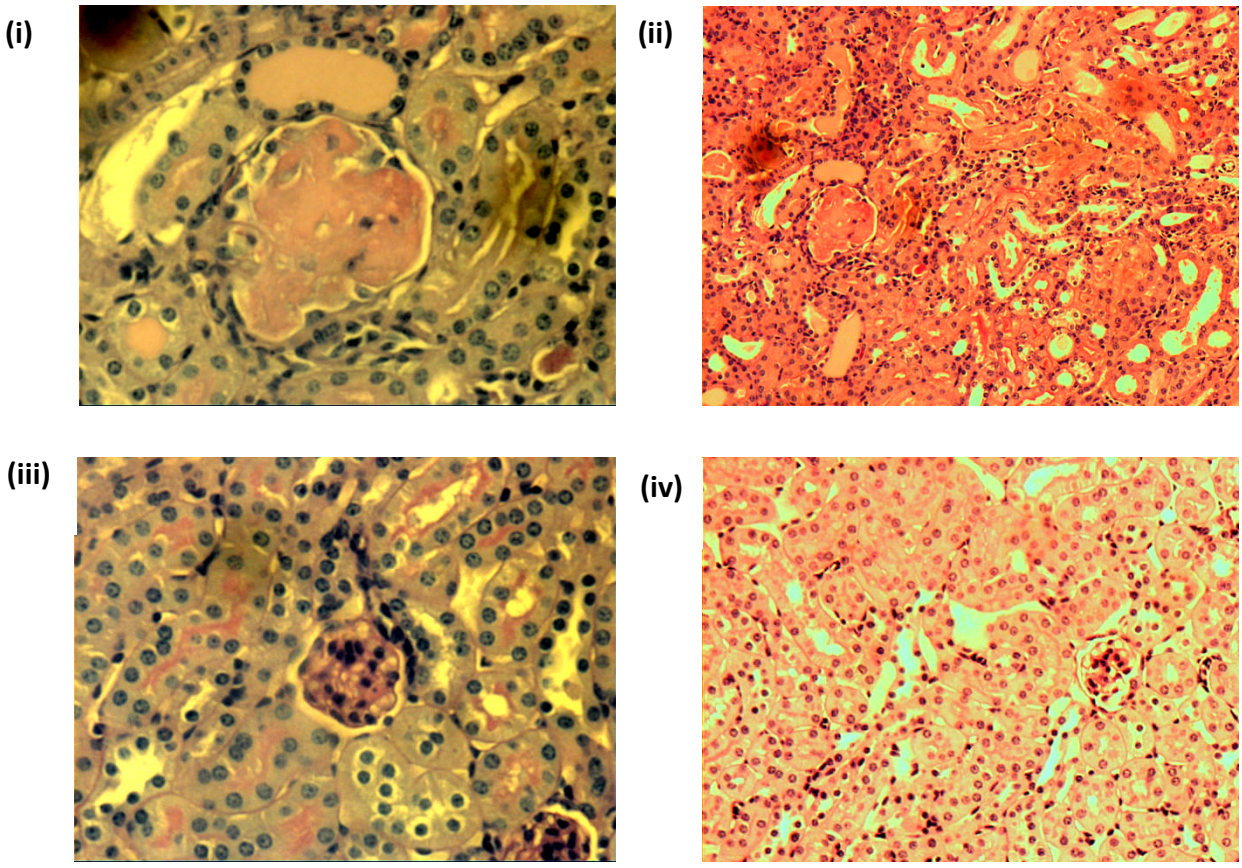

Figure 4-6 Mrp14-/- mice are protected from renal injury in NTN.

(i) WT mice have glomerular thrombosis as shown by PAS staining x400. (ii) WT mice have tubular dilatation with casts, H+E staining x200. (iii) Preserved renal architecture of mrp14-/- mice with some mild hypercellularity seen PAS x400. (iv) Preserved tubules of mrp14-/- mice seen in H+E staining x200.

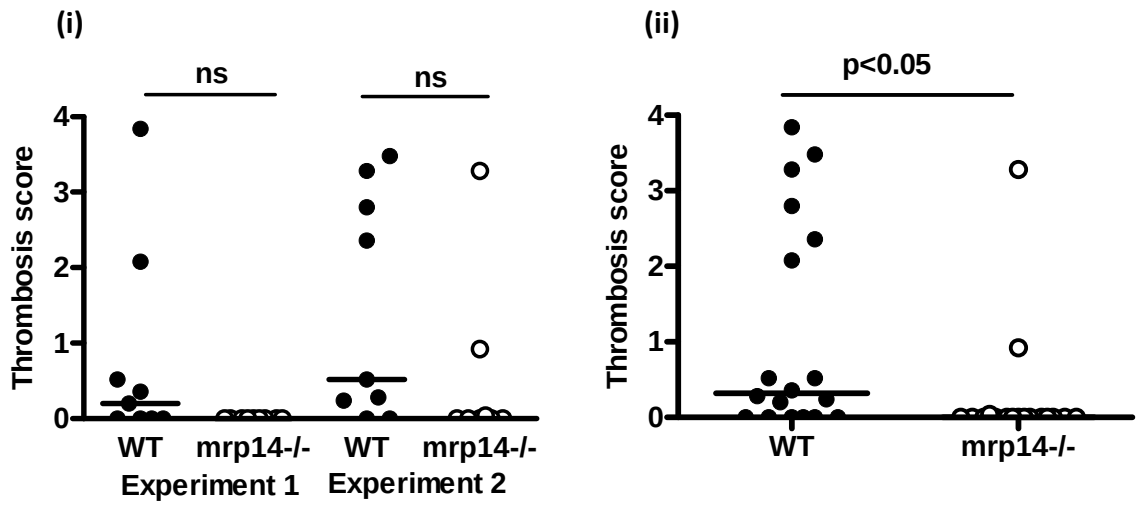

Figure 4-7 Glomerular thrombosis scores in WT and mrp14-/- mice during NTN.

(i) Demonstrates the thrombosis scores from the 2 separate experiments. There is no significant difference between the WT and mrp14-/- animals in either experiment. 2 way ANOVA demonstrates no significant difference between the experiments, therefore the WT (n=18) and mrp14-/- (n=17) animals groups were combined. (ii) Data from experiment 1 and 2 combined, demonstrating significant differences between WT and mrp14-/-, with mrp14-/- having less glomerular thrombosis than WT mice ($p<0.05$). Both graphs demonstrate the individual mice with a line representing the median.

4.4.4.2 Proteinuria and renal function

Urine was collected in metabolic cages overnight. Proteinuria was measured using the sulphosalicylic acid method. In experiment 1, there was very little proteinuria in the mrp14-/- mice (median 0.33mg/24 hours [range 0-0.84] The WT mice demonstrated varying amounts of proteinuria (median 0.37mg/24hours [range 0-22.75] and although the trend was less proteinuria in the mrp14-/- mice, this difference was not significant. Similarly, in experiment 2, mrp14-/- had less proteinuria (median 0.83mg/24hours [range 0.37-9.4] than WT mice (median 6.54mg/24 hours [range 0.35-20.13] but was this trend was not significant. 2-way ANOVA analysis showed there was no difference between the 2 experiments, therefore the animals from experiment 1 and 2 were combined. There was a significant difference in the proteinuria between WT mice and mrp14-/- mice ($p<0.05$).

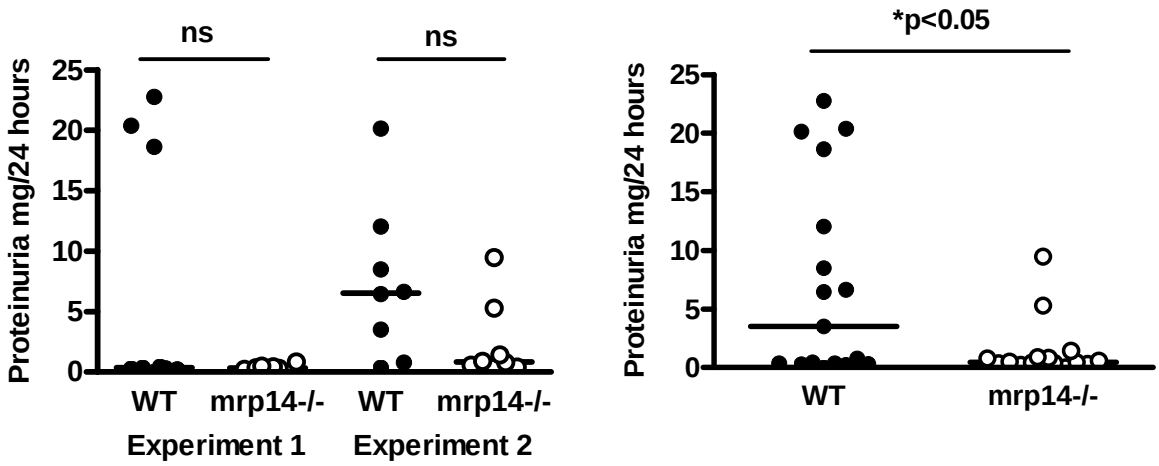

Figure 4-8 Mrp14-/- mice show a trend to less proteinuria than WT mice when induced with NTN

(i) Graph demonstrates the amount of proteinuria (mg/24 hours) in experiment 1 and 2. The difference between the 2 animal groups was not significant; however the trend is similar in experiment 1 and experiment 2. (ii) The results were analysed with a 2-way ANOVA. There was not a significant difference between the experiments ($p=0.61$), but there was a significant difference between the animal groups ($p=0.015$). Graphs (i)-(ii) show the data from each individual animal with a line representing the median.

In experiment 1, disease in the WT mice was less severe than that in experiment 2. There was no difference in the urea results in experiment 1 with WT mice having a median urea of 8.6mmol/l (range 6.6-42.5) and mrp14-/- mice a median urea of 7.6mmol/l (range 5-11.3). In experiment 2, there was a significant difference between the 2 groups. WT mice had a median urea of 14.1mmol/l (range 10.8-139). Mrp14-/- mice had a median urea of 7.45mmol/l (range 3.2-69.3)(Mann-Whitney $p<0.05$).

Serum creatinine is a poor marker of renal injury in mice, so was not used in the analysis.

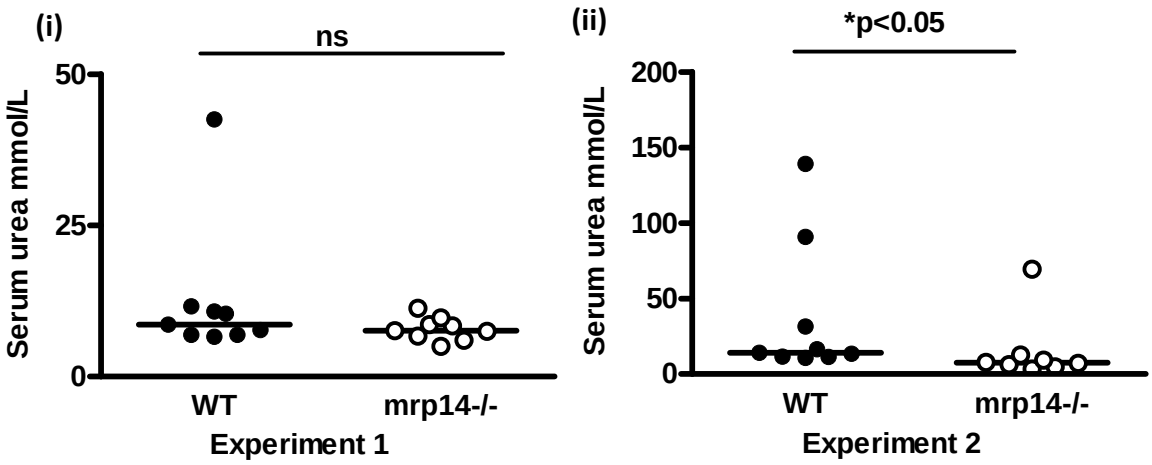

Figure 4-9 Mrp14-/- mice have greater preserved renal function than WT mice

(i) There was no significant difference in renal function in the first experiment. (ii) In experiment 2, there was a significant difference between WT and mrp14-/- mice ($p<0.05$). The graphs show the individual mice with a line at the median.

4.4.4.3 Leucocyte infiltration

Frozen sections of kidney were cut and stained for CD68 positive macrophages to investigate macrophage infiltration into the glomerulus. 25 glomeruli per section were included and the macrophages counted in each glomerulus before a mean was calculated. In both experiment 1 and experiment 2 there were significantly more macrophages infiltrating the glomeruli of WT animals compared to mrp14-/-.

In experiment 1; WT median number of macrophages per glomerulus was 1.2 (range 0-1.72), compared to mrp14-/- median 0.08 (range 0-1)($p<0.05$ Mann Whitney U test).

In experiment 2; WT median macrophages/gcs 3.64 (range 1.48-4.96) compared to mrp14-/- median 1.32 (range 0.6-2.64)($p<0.001$). A 2-way ANOVA demonstrated significant differences between the experiments as well as the animal groups so the data was therefore not combined.

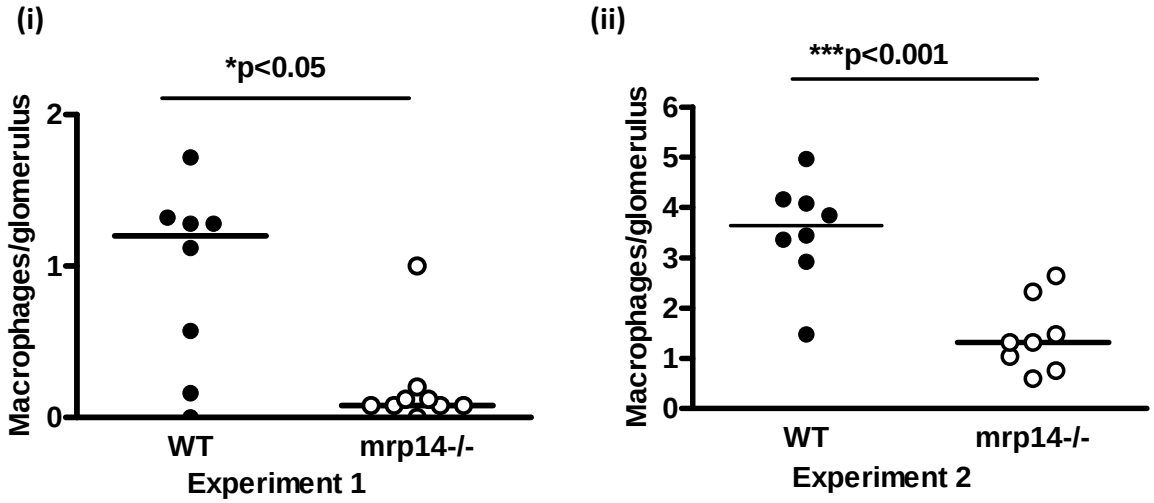

Figure 4-10 Mrp14-/- mice have less macrophage infiltration than WT mice when induced with NTN.

(i) Shows the results from experiment 1; there are significantly more glomerular macrophages in WT than in mrp14-/- mice. (ii) Experiment 2 results also demonstrate significantly more infiltrating glomerular macrophages in WT compared to mrp14-/- mice. Lines represent the median values.

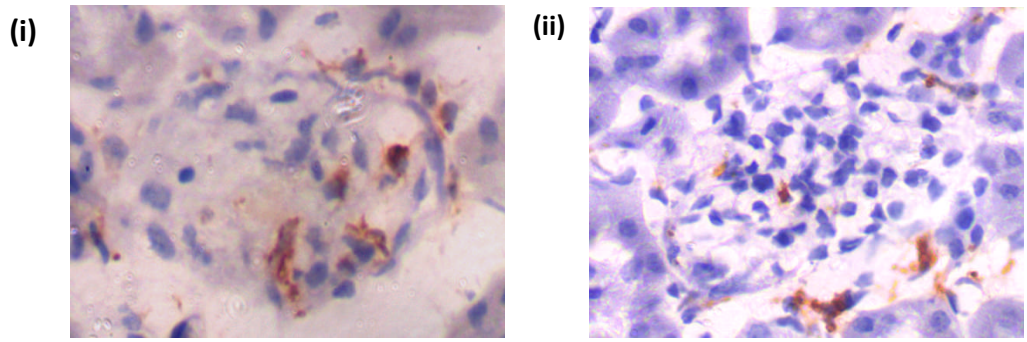

Figure 4-11 Photomicrographs to demonstrate macrophage infiltration in WT and mrp14-/- mice induced with NTN.

Immunohistochemistry using the macrophage marker, CD68 to demonstrate intra-glomerular macrophage infiltration during NTN. (i) WT mouse showing glomerular macrophage infiltration, (ii) mrp14-/- glomerulus (Both x630)

In experiment 2, CD4+ T cell immunohistochemistry was performed to investigate T-cell infiltration into the glomerulus. WT mice had significantly more T-cell infiltration than mrp14-/- mice with a median number of 0.88 cells per glomerular (range 0.72-1.89) compared to a median of 0.28 (range 0.08-0.92)($p<0.005$).

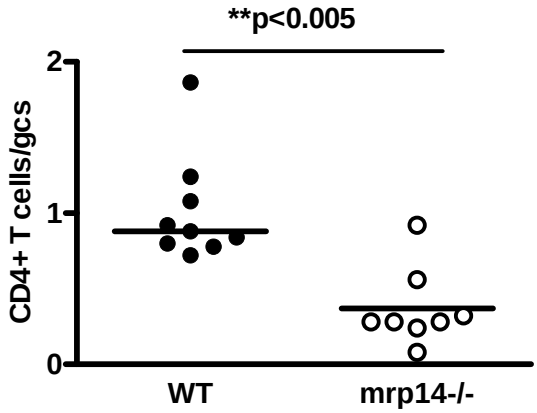

Figure 4-12 Mrp14-/- mice with NTN have less T-cell infiltration

Graph demonstrates CD4+ T-cell glomerular infiltration in WT and mrp14-/- mice induced with NTN. Mrp14-/- mice have significantly less infiltration than WT mice ($p<0.005$)(Mann-Whitney-U test). Line represents the median.

4.4.4.4 Systemic immune response

4.4.4.4.1 Experiment 1

Mouse serum was isolated from blood, collected after the animals were sacrificed, to assess the murine response to sheep IgG, by ELISA. Experiments 1 and 2 will be discussed separately. Serum from a control mouse without NTN induction demonstrated very low levels of total mouse anti-sheep IgG, which was not significantly above control ELISA level. All the mice analysed had generated an appropriate immune response.

In experiment 1, there was no difference in the total IgG between WT and mrp14-/- mice, WT median OD 0.88 (0.28-1.88) compared to 0.44 (0.01-1.34). Although the difference may suggest that mrp14-/- mice generate lower antibody titres against total sheep IgG, this was not statistically significant. Mouse antibodies against sheep IgG subclasses were also investigated (IgG1, IgG2b, IgG2c, IgG3) by ELISA. Both animal groups had a similar IgG1, IgG3 and IgG2b responses to sheep IgG with a median OD for IgG1 WT 0.43 (range 0.002-0.66) and a mrp14-/- median of 0.39 (range 0.05-0.57), IgG3 WT median OD of 0.042 (0-0.15) and an mrp14-/- median OD 0.004 (range 0-2.4) and for IgG2b WT median 0.3 (0.06-0.78) compared to mrp14-/- median OD 0.15 (0.02-0.5). However, WT mice generated a greater IgG2c responses than mrp14-/- mice with a median IgG2c OD 0.095 (0-0.22) compared to a mrp14 -/-median of 0 (0-0.02)($p<0.05$, Mann Whitney U)

Overall, despite similarities in total the IgG response, WT mice demonstrated a significantly higher IgG2c response than mrp14-/- mice.

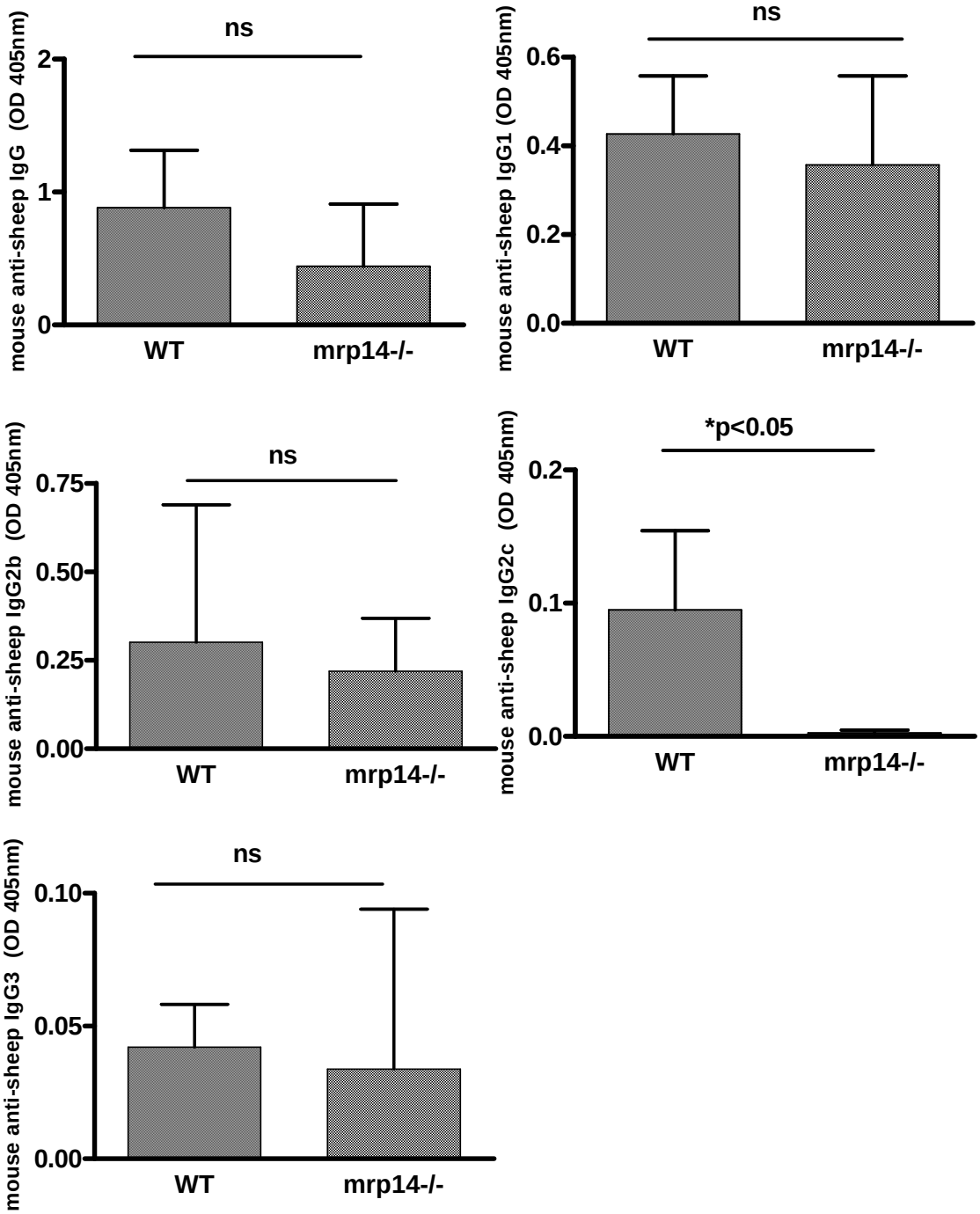

Figure 4-13 WT and mrp14-/- mice have a similar total IgG response but mrp14-/- mice have a decreased IgG2c response to sheep IgG during NTN [experiment 1].

Graphs show the median (interquartile range) of total IgG(i), IgG1(ii), IgG2b(iii), IgG2c(iv) and IgG3 (v) of the mice in experiment 1. The difference is not significant in the IgG subclasses except IgG2c ($p<0.05$)(Mann-Whitney-U test)

4.4.4.4.2 Experiment 2

Serum from experiment 2 was also analysed for the circulating mouse IgG response to sheep IgG. Similar to experiment 1, ODs were measured by ELISA at 405nm. In this experiment, there was no difference between WT and mrp14-/- mice with respect to total IgG analysed, IgG3, IgG1, IgG2b, or IgG2c subclasses; WT vs mrp14-/- median OD total IgG 0.38 (range 0.04-0.89), vs 0.47 (range 0.29-1.67), IgG3 0.015 (range 0.007-0.09) vs 0.03 (range 0.005-0.07); IgG1 0.75 (range 0.40-1.28) vs 0.54 (range 0.31-1.09); IgG2b 0.05 (range 0.02-0.2) vs 0.13 (range 0.03-0.31); IgG2c 0.03 (range 0.02-0.12) vs 0.046 (range 0.007-0.09).

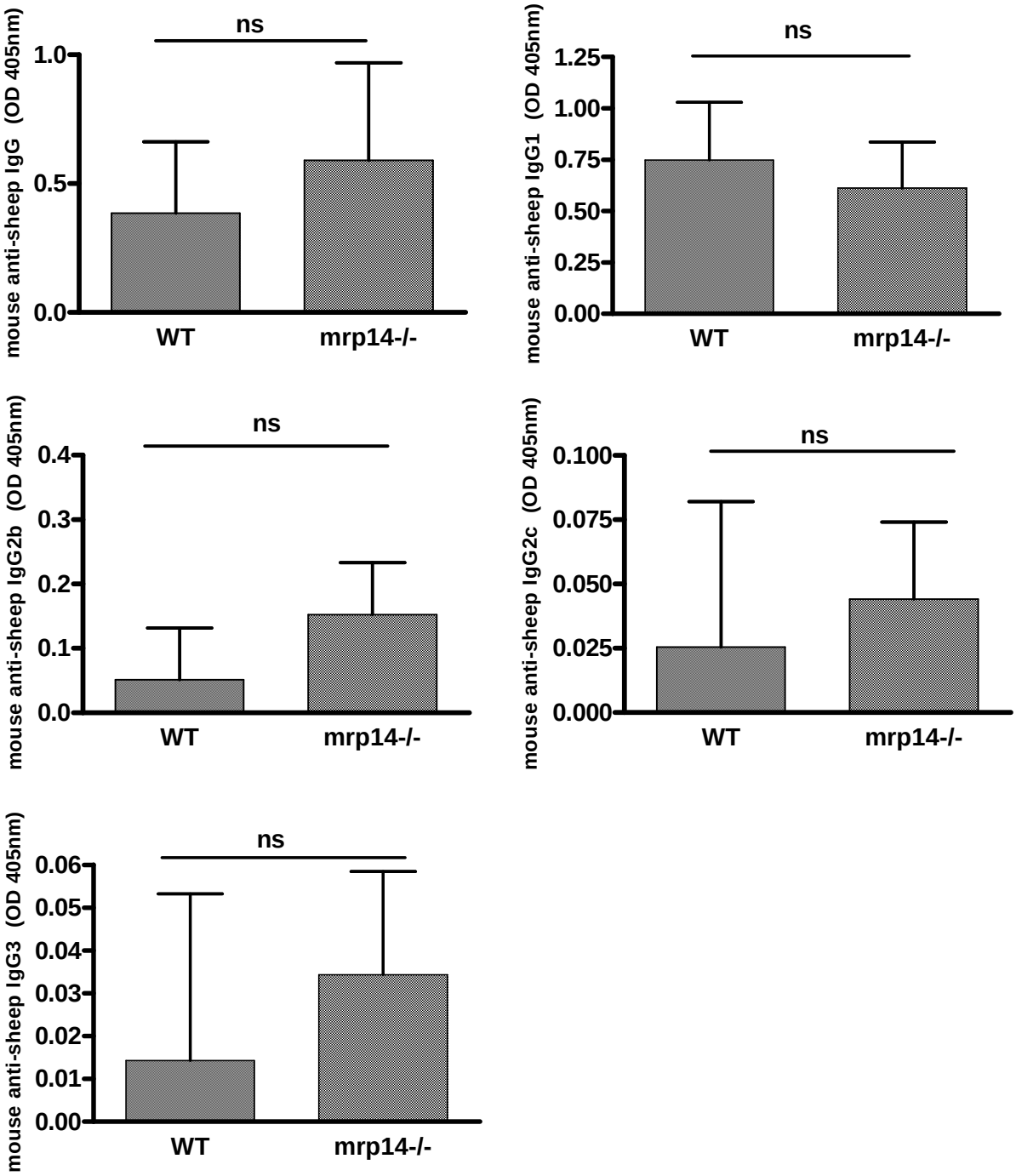

Figure 4-14 WT and mrp14-/- have a similar IgG response to sheep IgG during NTN (experiment 2).

Graphs show the median (interquartile range) of total IgG(i), IgG1(ii), IgG2b(iii), IgG2c(iv) and IgG3 (v) of the mice in experiment 2. The difference in OD of the IgG subclasses between WT and mrp14-/- mice was not significant.

4.4.4.5 T cell responses

Splenocyte T cell proliferation was compared between WT and mrp14-/- mice during nephrotoxic nephritis. Following experiment 2, spleens were harvested at termination. The isolated splenocytes were subsequently stimulated with anti-CD28/CD3 or aggregated sheep IgG (10µg/ml and 50µg/ml) and compared with unstimulated splenocytes. After 72 hours of incubation, ^{3}H thymidine was added followed by assessment of T-cell proliferation using a micro-beta counter (counts per minute c.p.m)

WT splenocytes demonstrated a lower proliferation rate than mrp14-/- splenocytes. Median 6976 c.p.m (4568-8758) for WT splenocytes; and 13422 c.p.m (range 10139-22949) for mrp14-/- splenocytes. To calculate the proliferation in response to anti-CD3/CD28 and sheep IgG, the proliferation rate unstimulated was subtracted from the conditions above. There was no significant difference between the 2 animal groups in response to anti-CD3/CD28, low dose sheep IgG (10µg/ml) and high dose sheep IgG (50µg/ml). Although proliferation in the mrp14-/- splenocytes was less than WT splenocytes following higher-dose aggregated sheep IgG (50µg/ml), it did not reach statistical significance.

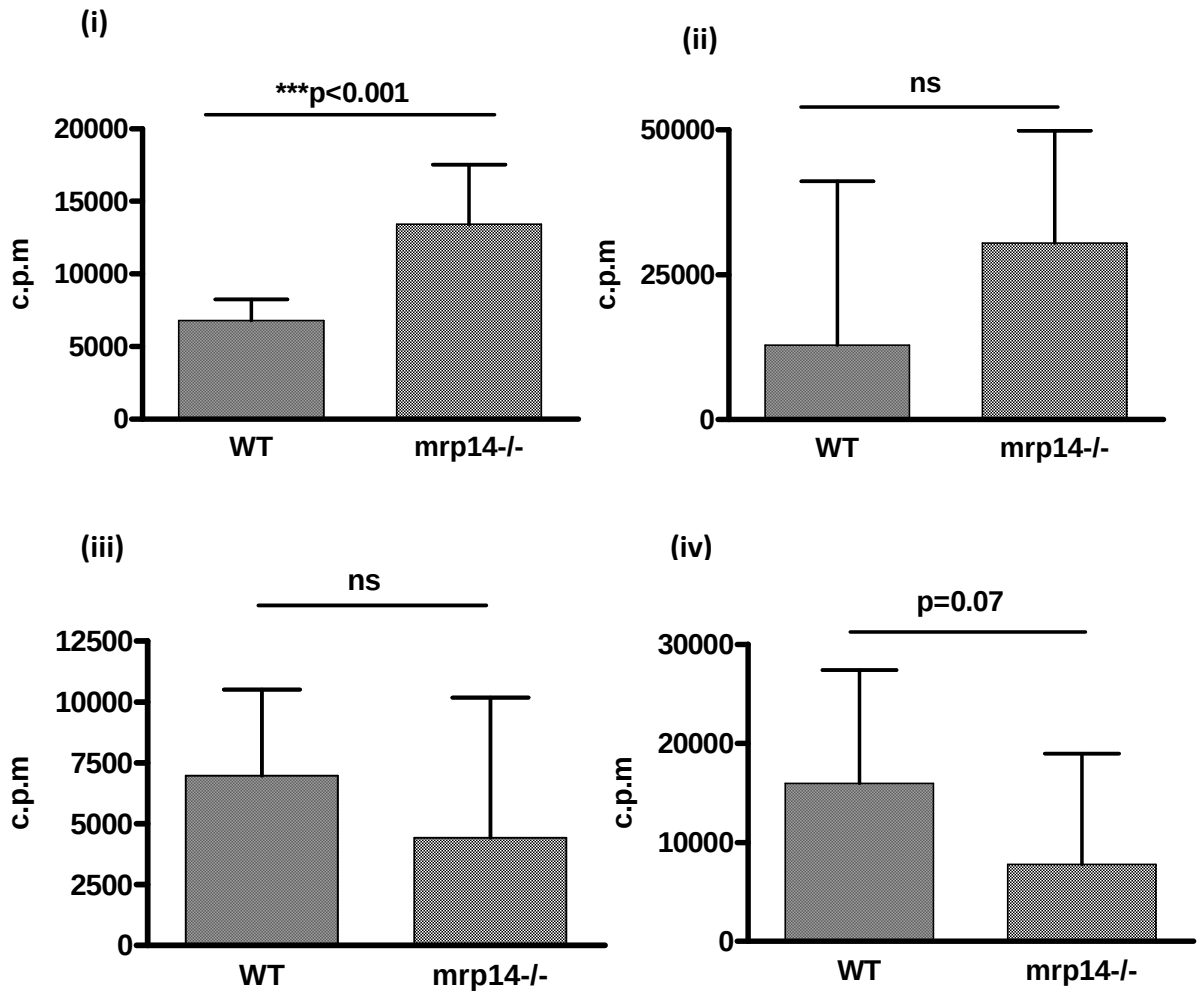

Figure 4-15 Mrp14-/- mice during NTN have increased splenocyte proliferation at rest, but not following stimulation with anti-CD3/CD28 or sheep IgG (measured in counts per minute c.p.m).

(i) Demonstrates the c.p.m of WT and mrp14-/- splenocytes at rest which shows a significant difference in proliferation ($p<0.001$)(Mann-Whitney t-test). (ii) In response to anti-CD3/CD28 stimulation, the increase in c.p.m between the 2 groups is not significantly different, although mrp14-/- show a trend to increased proliferation. (iii)-(iv) Graphs show the increase in proliferation in response to (iii) 10µg/ml of sheep IgG and (iv) 50µg/ml of sheep IgG. The trend is similar with mrp14-/- splenocytes not proliferating as much as WT splenocytes but fails to reach statistical significance. Graphs show the median (and interquartile range).

4.4.4.6 Not all WT macrophages are positive for S100A8/A9

Formalin fixed paraffin embedded sections from WT mice used in experiment 2 were stained for S100A8/A9 following NTN and the mean number of cells positive for S100A8/A9 for each animal was calculated and compared to the number of CD68 macrophages in the same sections. Only a subset of CD68 positive macrophages was positive for S100A8/A9. This demonstrates that different macrophage subsets are present within the inflamed glomerulus with only a proportion of infiltrating macrophages expressing S100A8/A9. There was no correlation between glomerular thrombosis and the number of either S100A8/A9 positive or CD68 positive cells.

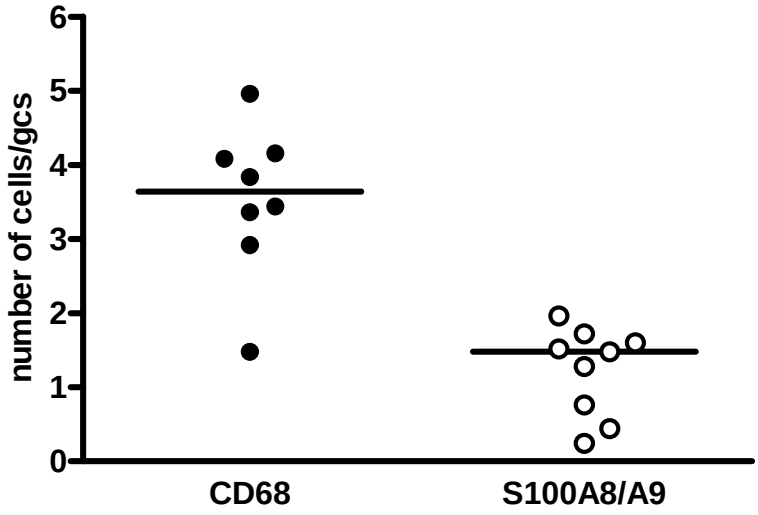

Figure 4-16 A subset of infiltrating glomerular macrophages express S100A8/A9

The graph demonstrates that in WT animals with nephrotoxic nephritis only a proportion of infiltrating glomerular macrophages express S100A8/A9. The median number of CD68 macrophages per glomerulus was 3.64 (range 1.48-4.69). This decreased to a median of 1.48 (range 0.24-1.96) for S100A8/A9 positive cells. The ratio of S100A8/A9 positive cells/CD68 cells was 0.34. This is higher than the ratio of 0.11 and 0.18 for IL17-/- and MR-/- mice respectively.

(i)

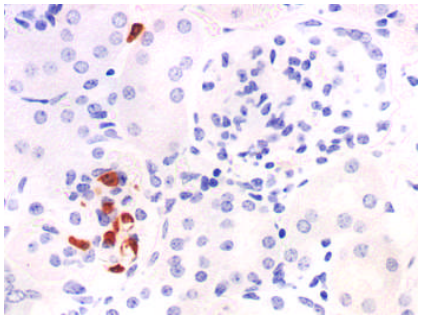

(ii)

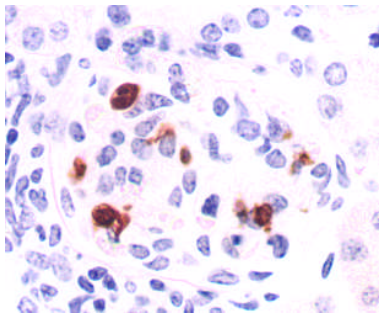

Figure 4-17 Photomicrographs [(i) x400 and (ii) x630] of glomerular infiltrating cells expressing S100A8/A9 in NTN mouse glomeruli

A proportion of mouse glomeruli have infiltrating macrophages expressing S100A8/A9 during NTN.

4.4.5 Mrp14-/- mice are protected from nephrotoxic nephritis using low dose LPS- experiment 3.

Since experiments 1 and 2 demonstrated disease in WT mice that was attenuated in mrp14-/- mice, it was interesting to test if disease protection could be overcome in mrp14-/- by direct TLR4 stimulation. To stimulate TLR4 alone highly purified LPS was used at a low dose. Highly purified LPS (from E.coli) has been demonstrated to stimulate TLR4 and not other TLR receptors, such as TLR2, unlike other less purified LPS preparations. After several pilot studies investigating varying doses of LPS, a dose was chosen which, when administered to WT mice intravenously, in the absence of nephrotoxic serum, did not cause significant histopathological changes (figure 4-18). However, the chosen dose, when used in combination with NTS, results in a severe thrombotic glomerulonephritis.

WT (n=8) and mrp14-/- (n= 7) mice were pre-immunised with CFA and sheep IgG on day -5, then on day 0, a dose of LPS (0.009 mcg) was given to each mouse at the same time as nephrotoxic serum (diluted 1:1 with the above concentration of LPS). Mice were placed in metabolic cages on day 7 to collect urine and were culled on day 8.

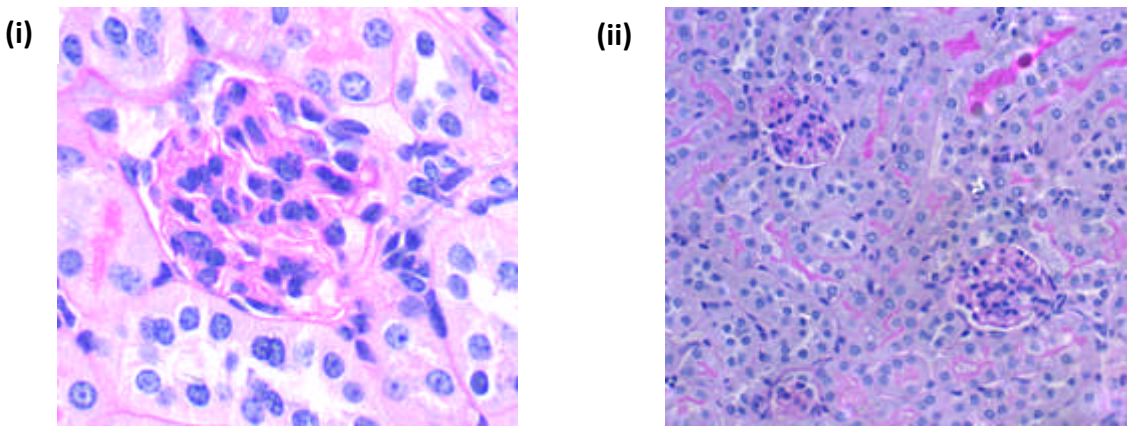

Figure 4-18 LPS alone doesn't cause a glomerulonephritis.

Photomicrographs of mouse kidney following intravenous LPS injection without NTS. There is no apparent glomerular abnormality seen by day 8 (PAS staining; x630 (i) and x400 (ii)

4.4.5.1 Renal histology

Kidney sections stained with H+E and PAS where assessed and scored for glomerular thrombosis. The median glomerular thrombosis score in WT mice was 1.98 (range 0-4) and in mrp14-/- mice the median score was 0 (range 0-2.88). The difference between these 2 groups was not significant at p=0.07. Combining this experiment with the thrombosis scores in experiments 1 and 2 and analysing by a 2-way ANOVA demonstrates no difference between the experiments (p=0.178). However, there is a significant difference between the WT and mrp14-/- mice (p<0.005).

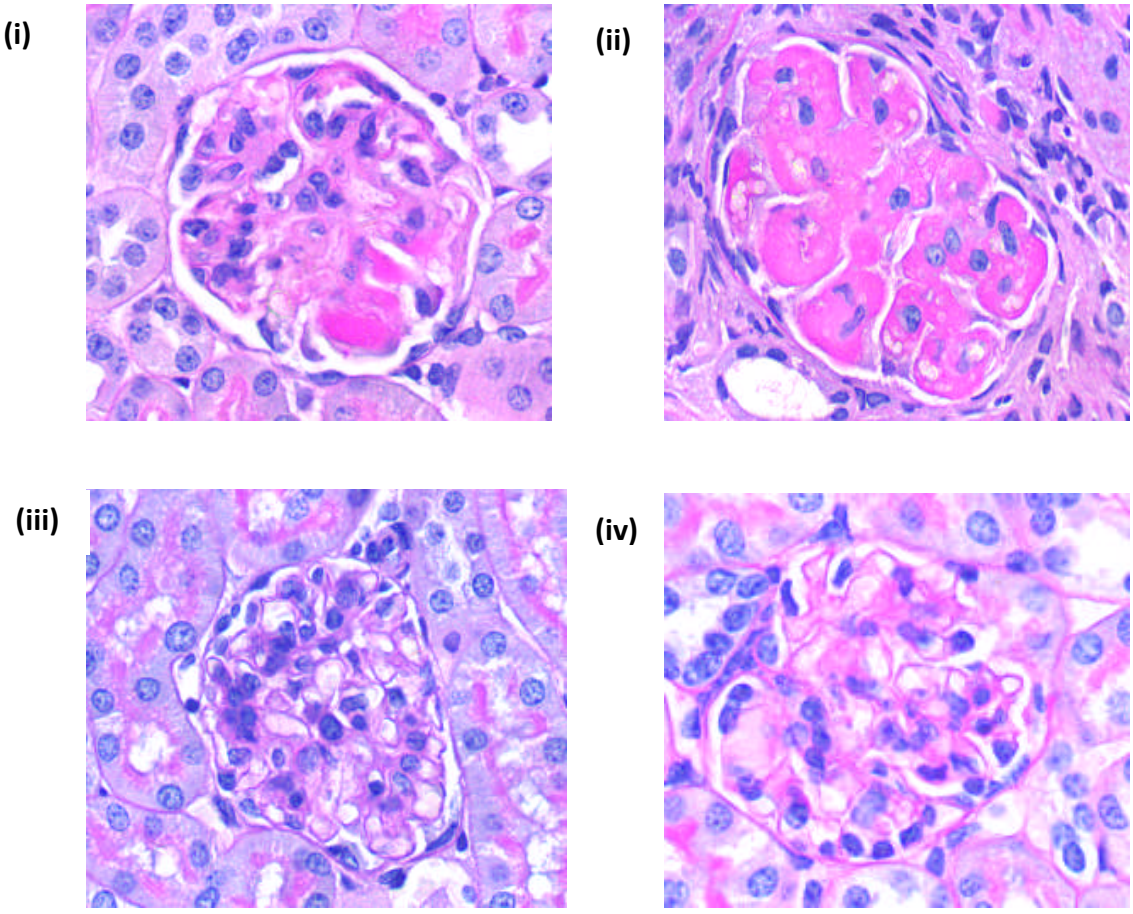

Figure 4-19 WT mice have a severe thrombotic glomerulonephritis (PAS staining).

(i)-(ii) WT mice display varying degrees of glomerular thrombosis, from 25% in (i) to 100% in (ii), while Mrp14-/- mice generally display mild glomerular hypercellularity(iii)-(iv). (H and E, x630.)

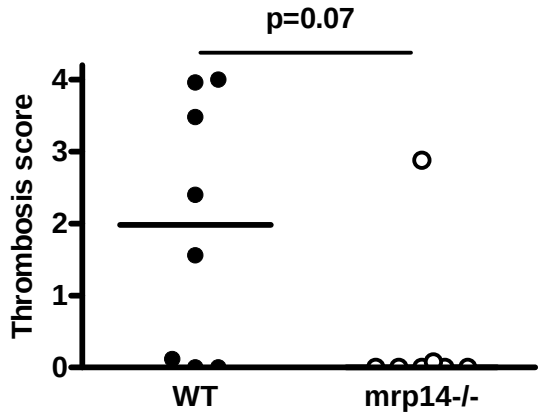

Figure 4-20 Mrp14-/- mice demonstrate a trend to less glomerular thrombosis

Graph demonstrating the individual thrombosis score of the WT and mrp14-/- mice. There is a trend to less thrombosis in the mrp14-/- mice, but this was not significant (p=0.07). Line represents the median.

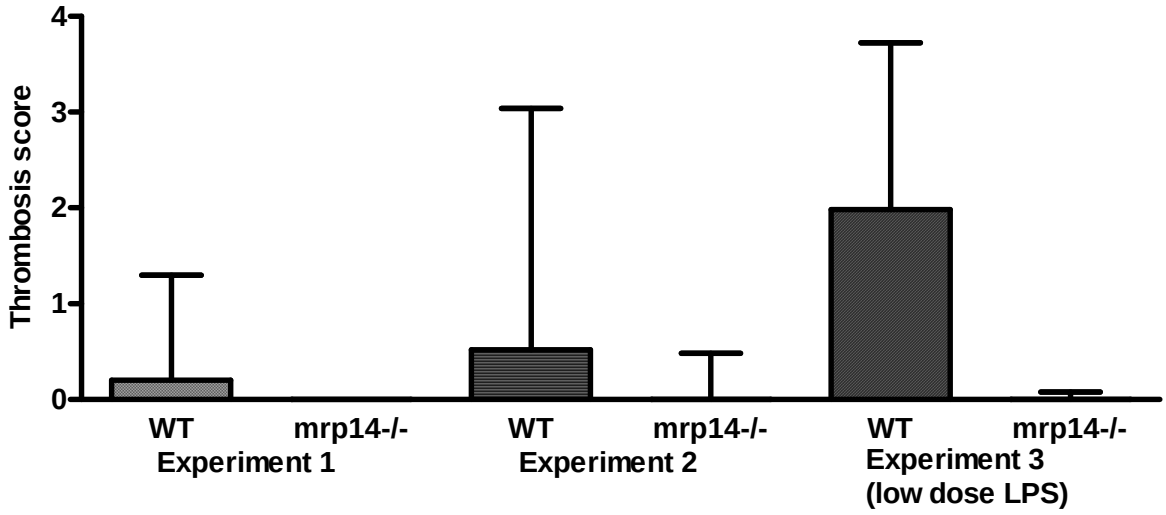

Figure 4-21 Mrp14-/- mice with NTN consistently develop less glomerular thrombosis than WT counterparts.

Graph demonstrating the glomerular thrombosis score in WT and mrp14-/- mice in each of the 3 experiments described. Each experiment when analysed separately shows a consistent trend to less thrombosis in the mrp14-/- mice. A 2-way ANOVA demonstrated no significant differences between the 3 experiments but did demonstrate a highly significant difference between the 2 animal groups (**p<0.005). Graph demonstrating the median (interquartile range) for each experiment.

4.4.5.2 Proteinuria and renal function in experiment 3

There was proteinuria in both animal groups. WT animals had a median of 1.329 mg/24 hours (range 0-29.5), and mrp14-/- a median of 0.32mg/24 hours (range 0-2.9). The difference between the 2 groups did not reach statistical significance. Using 2 way ANOVA analysis, there was no difference between the 3 sets of experiments (p=0.87), but there was a significant difference between the 2 animal groups (p<0.05).

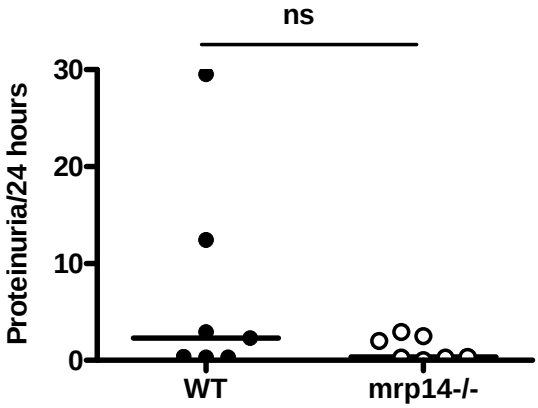

Figure 4-22 Mrp14-/- mice with NTN demonstrate a trend to less proteinuria than WT

Graph demonstrating proteinuria (mg/24 hours) in WT and mrp14-/- animals. Line represents the median

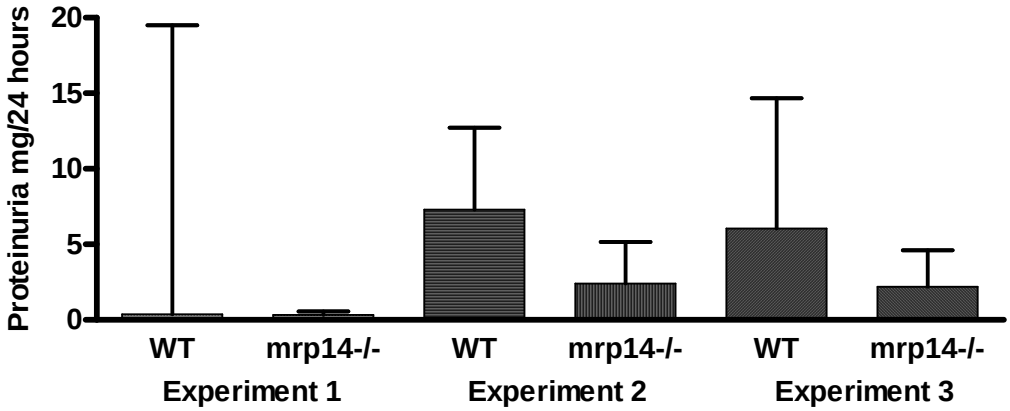

Figure 4-23 Mrp14-/- mice have consistently less proteinuria in the 3 sets of NTN experiments described

Although the separate experiments did not reveal a statistical difference in proteinuria between WT and mrp14-/- mice, combined they did show a difference (p<0.05). Graph shows the median and interquartile range for proteinuria from the 3 NTN experiments described.

Mrp14-/- mice had a significantly lower serum urea than WT animals (median urea 6.6mmol/l (range 5.2-42.2) compared with 15.2mmol/l (range 6.9-128.8) respectively, ($p<0.05$).

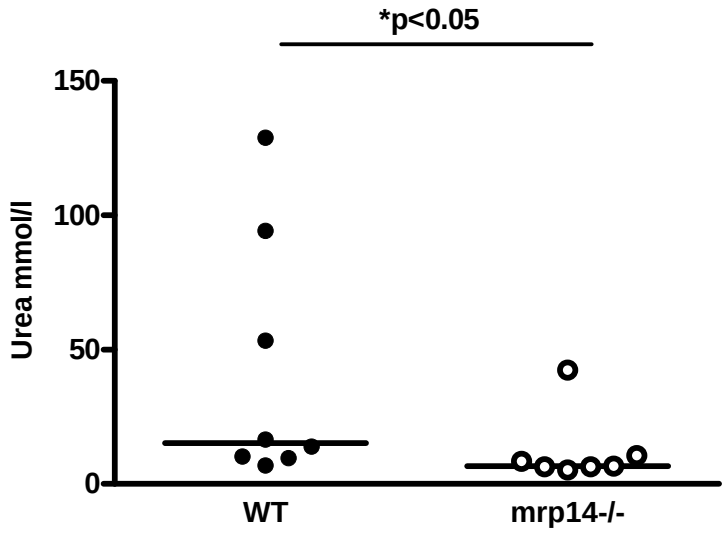

Figure 4-24 Mrp14-/- mice have better preserved renal function compared to WT mice.

Graph demonstrating the renal function (assessed by serum urea) in the 2 animal groups. Mrp14-/- mice demonstrate preserved urea compared with WT animals ($p<0.05$). Each dot represents a single animal with a line representing the median.

4.4.5.3 Systemic immune response during NTN with low dose LPS

Mouse serum was isolated from blood collected at the time of sacrifice after nephrotoxic nephritis. Serum was analysed by ELISA to assess the murine response to sheep IgG. Overall the results demonstrate no difference in the humoral murine anti-sheep response between WT and mrp14-/- mice, including no differences in total IgG response WT median OD 0.14 (range 0.03-1.3) vs mrp14-/- median 0.41 (0.01-1.1)(p=0.57); IgG1 WT median 0.15 (range 0.02-0.71) vs mrp14-/- median 0.23 (range 0.06-0.57)(p=0.35); IgG2b median WT 0.21 (0.008-0.55) and mrp14-/- median 0.26 (range 0.028-0.48)(p=0.46); IgG2c WT median 0.056 (range 0.006-0.717) vs mrp14-/- median 0.02 (0.015-0.048)(p=0.46); IgG3 WT median 0.14 (range 0.03-1.31) vs mrp14-/- median 0.42 (range 0.01-1.07)(p=0.57).

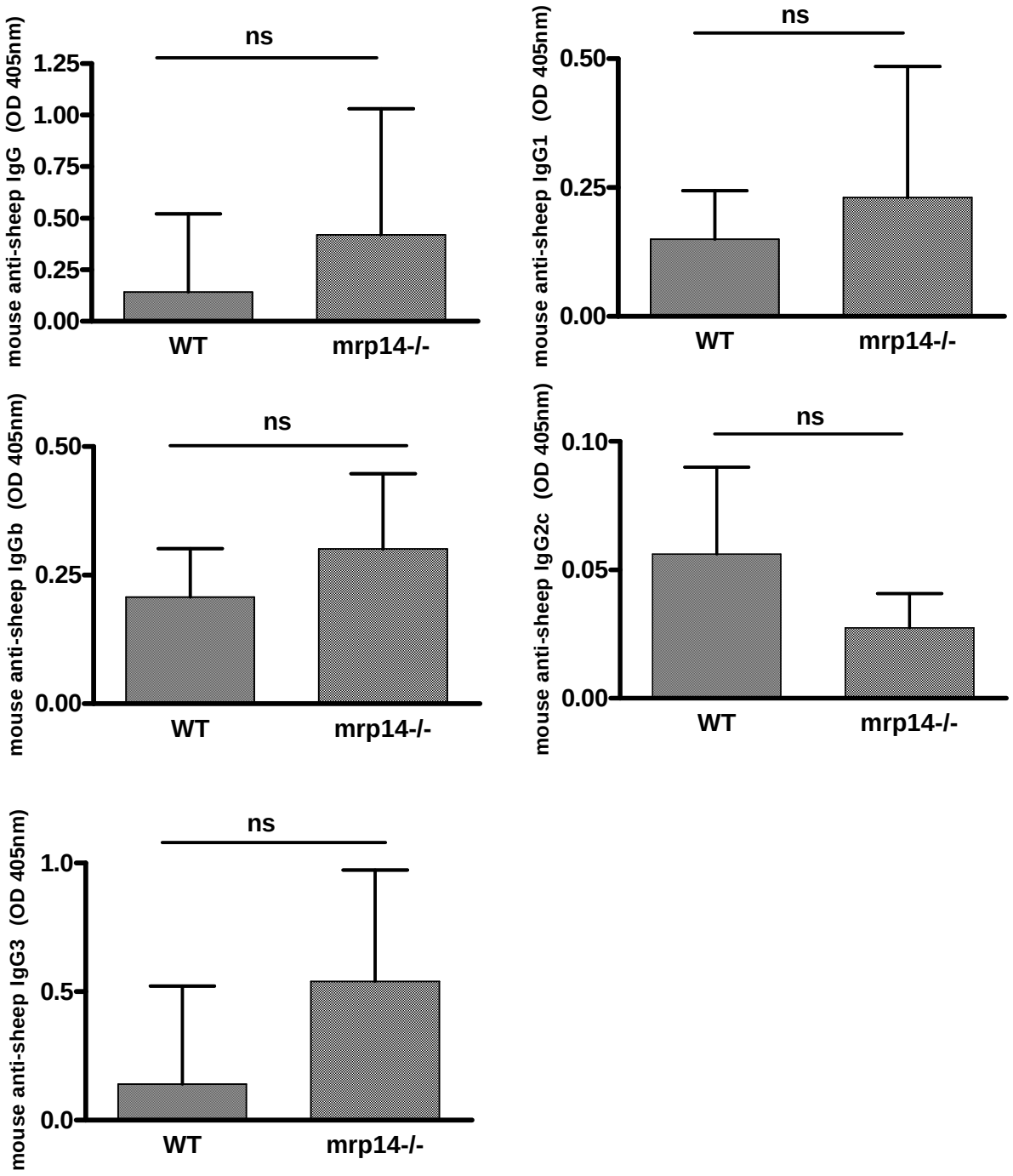

Figure 4-25 Mrp14-/- mice have the same humoral response as WT animals following NTN.

Graphs show the median (interquartile range) of total IgG(i), IgG1(ii), IgG2b(iii), IgG2c(iv) and IgG3 (v) in the sera of mice in experiment 3.

Frozen kidney sections were stained for deposited sheep and mouse IgG by direct immunofluorescence. For each mouse, 10 glomeruli were identified and photographed and fluorescence measured by image analysis software.

With respect to mouse IgG deposition, there was similar fluorescence between WT and mrp14-/- mice. The median WT score was 96.18 (range 65.35-140.2) and mrp14-/- median 123.1 (range 66.26-165)(p=ns)

With respect to glomerular sheep IgG, there was no difference between the 2 groups. The median WT fluorescence was 25.96 (range 21.69-46.53) and Mrp14-/- median 38.76 (range 22.14-66.44).

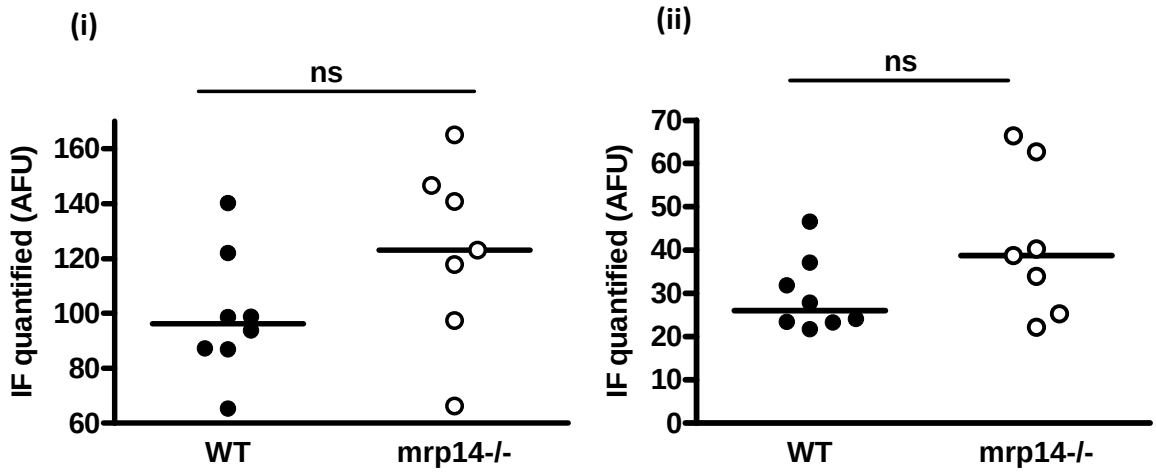

Figure 4-26 Mrp14-/- and WT mice with NTN have a similar humoral responses

(i) Demonstrates the quantitative glomerular immunofluorescence due to the deposition and the analysis of mouse IgG. (ii) Quantitative immunofluorescence of sheep IgG deposited in the glomerulus of WT and mrp14-/- mice. Line represents the median.

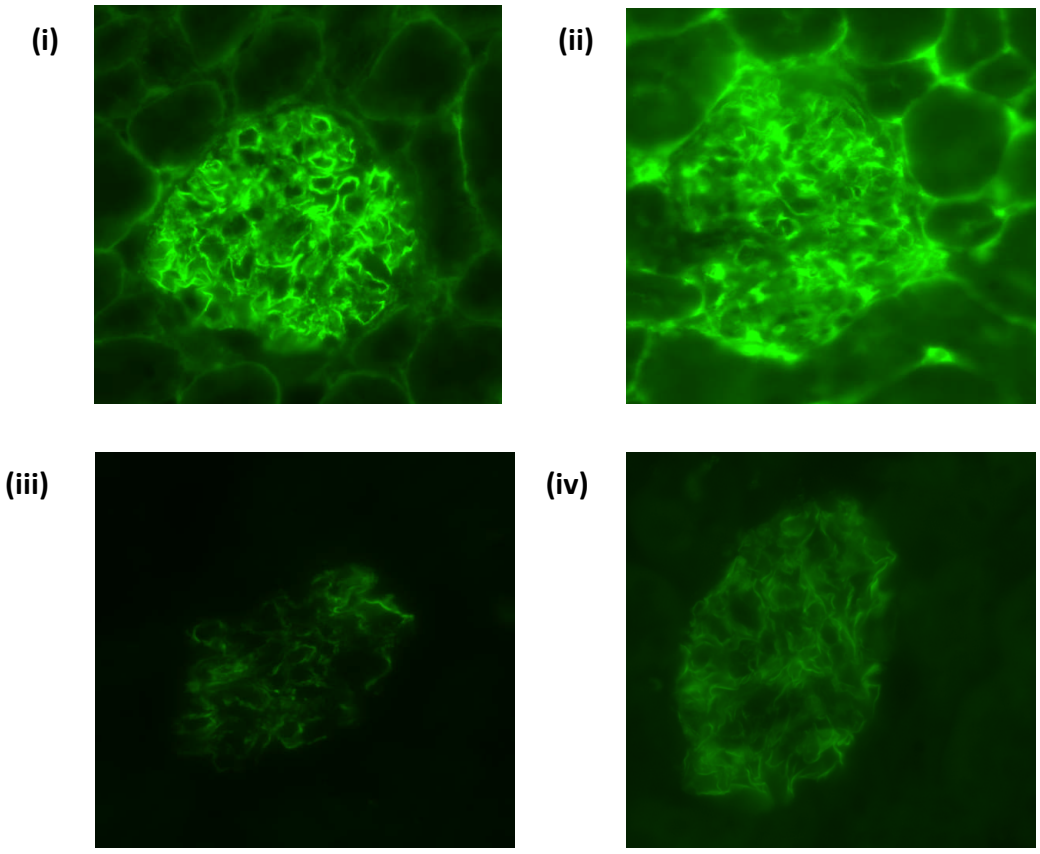

Figure 4-27 Mrp14-/- and WT mice have similar humoral responses. Photomicrographs of a single glomerulus demonstrating IgG immunofluorescence. (x400)

(i) WT and (ii) mrp14-/- mice have similar deposition of mouse IgG in the glomerulus. (iii) WT and (iv) mrp14-/- mice have similar deposition of sheep IgG in the glomerulus.

4.4.5.4 Leucocyte infiltration during NTN with low dose LPS

Frozen sections of mouse kidney were stained for CD68 and CD4 T cell infiltration. For each animal, 25 glomeruli were counted and the mean number of cells per glomeruli calculated.

WT mice demonstrate significantly more glomerular CD68 infiltration than mrp14-/- mice. Median WT number of CD68 cells per glomeruli was 1.7 (0.8-2.2) compared to mrp14-/- mice with a median of 0.6 (range 0.44-2.1)($p<0.05$).

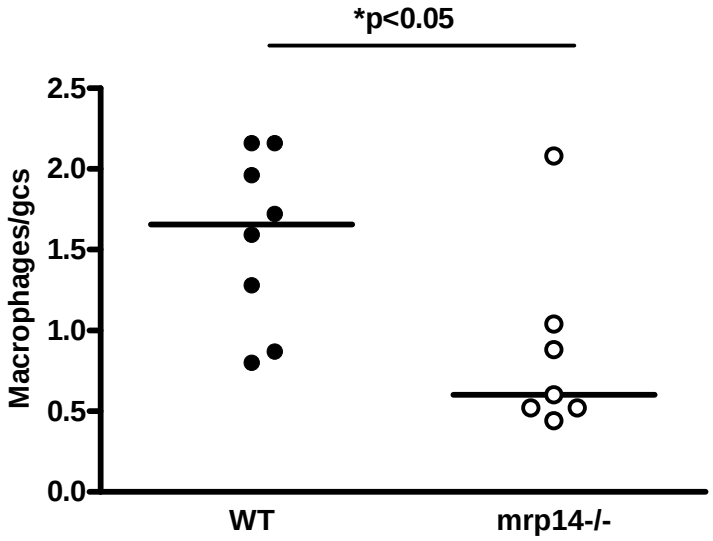

Figure 4-28 Mrp14-/- mice have less glomerular CD68 infiltration than WT mice

Graph demonstrating the individual mouse values for CD68 infiltration in WT and mrp14-/- animals. Line represents the median. There is a significant difference between the 2 groups ($p<0.05$).

(i)

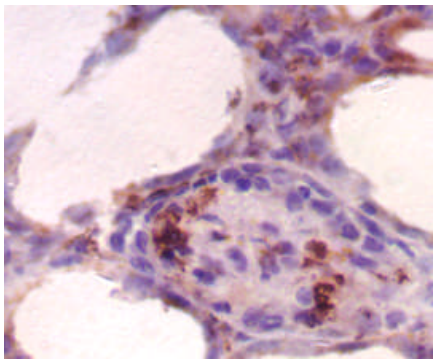

(ii)

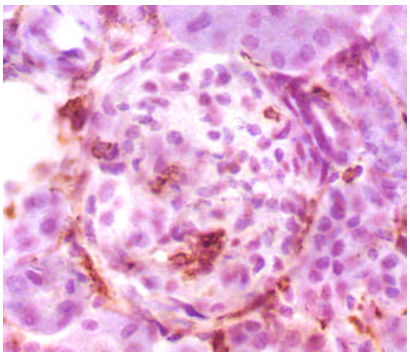

Figure 4-29 Mrp14-/- mice have significantly less CD68 macrophage infiltration than WT mice.

Photomicrographs demonstrating immunohistochemistry using the macrophage marker, CD68 to illustrate intra-glomerular macrophage infiltration (x630). (i) WT mouse with severe injury and gross tubular dilatation and CD68 macrophage infiltration into the glomerulus. (ii) Mrp14-/- mouse with conserved renal histology. Few CD68 macrophages infiltrate the glomerulus.

There was no difference in the number of infiltrating glomerular CD4+ T cells demonstrated by immunohistochemistry. The overall numbers were small with few T cells present. The median number of T cells present in WT glomeruli was 0.12 (range 0-0.21), while in mrp14-/- mice, the median was 0.12 (0-0.33). Although a difference was found in the previous NTN experiment without low dose LPS, no difference was demonstrated in this experiment.

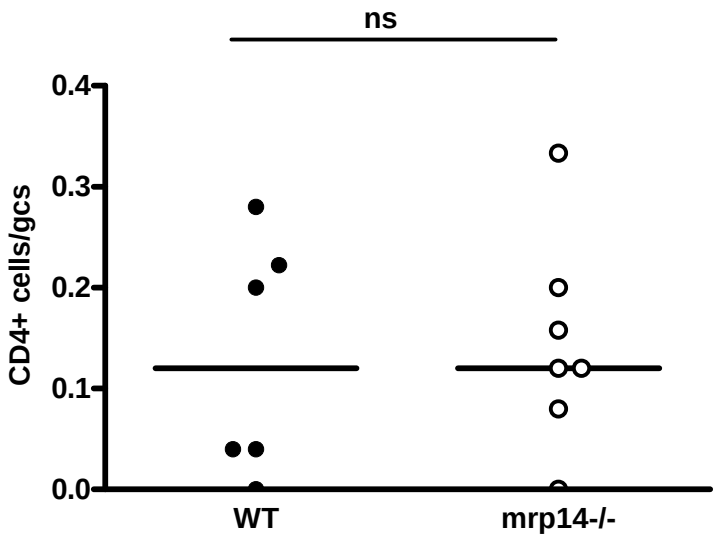

Figure 4-30 WT and mrp14-/- mice with NTN have a similar number of infiltrating CD4+ T-cells.

Graph demonstrating similar glomerular T cell numbers. Line represents the median.

(i) **(ii)**

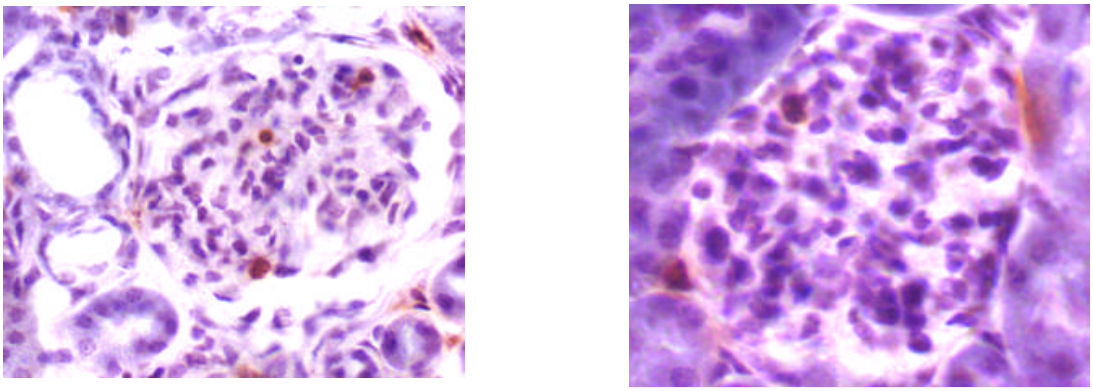

Figure 4-31 WT and mrp14-/- mice have similar T cell infiltration as demonstrated by immunohistochemistry for CD4+ T cells.

Photomicrograph of WT (i) and mrp14-/- (ii) kidney sections stained for CD4+ T-cell infiltration (x630)

4.4.5.5 Serum S100A8/A9 levels during NTN with low dose LPS

Serum S100A8/A9 levels were kindly measured by Dr T. Vogl, a collaborator at University of Munster, Germany. WT mice (n=8) induced with NTN and low dose LPS had serum levels measured following sacrifice on day 8 following administration of nephrotoxic serum. The levels of S100A8/A9 were then analysed to detect any correlation with other parameters of disease. The table below demonstrates the individual animal results.

Animal	**S100A8/A9** **ng/ml**
1	309
2	902
3	30363
4	3877
5	31428
6	776
7	11152
8	2020

Table 8 Table to demonstrate the serum S100A8/A9 levels (ng/ml) as measured by ELISA in WT mice during NTN

Using Spearman's correlation co-efficient for the 8 WT animals, there were significant positive correlations between S100A8/A9 levels and serum urea ($r=0.74$)($p<0.05$) as well as glomerular thrombosis ($r=0.9$)($p<0.005$). The mice with the most severe disease had the highest levels of serum S100A8/A9, whereas those animals without much disease had much lower levels, linking the serum levels of S100A8/A9 to disease severity.

4.4.6 Mrp14-/- mice have a similar response to WT mice following administration of high dose LPS after disease induction

The nephrotoxic nephritis model was altered slightly compared to the previous experiment by increasing the dose and delaying the timing of additional LPS administration. Each mouse received 1µg LPS intra-peritoneally at day 3 following the administration of nephrotoxic serum. Day 7 the mice were placed in metabolic cages and were terminated on day 8.

4.4.6.1 Renal histology

The disease induced in the WT and the mrp14-/- animals was variable; however both the animal groups had a similar response. Despite previous disease protection, mrp14-/- mice now demonstrated similar disease severity as the WT mice, with no difference in the thrombosis score; WT median thrombosis score was 1.36 (range 0.04-3.52) vs. mrp14-/- mice median score of 0.92 (range 0-3.52)(p=ns).

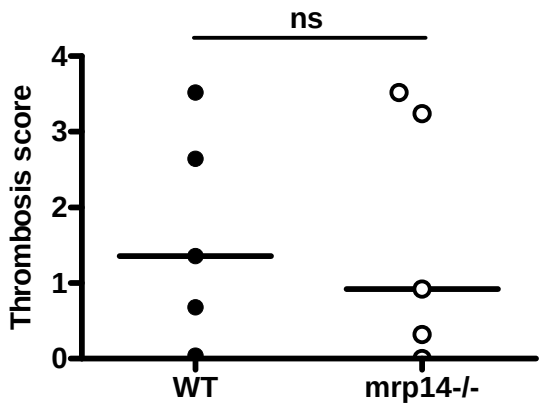

4-32 Mrp14-/- and WT mice have similar thrombosis scores in NTN with high dose LPS.

Graph demonstrating the individual animals and their thrombosis scores. Line represents the median. There is no difference between the 2 groups with both animal groups demonstrating a variable degree of glomerular thrombosis.

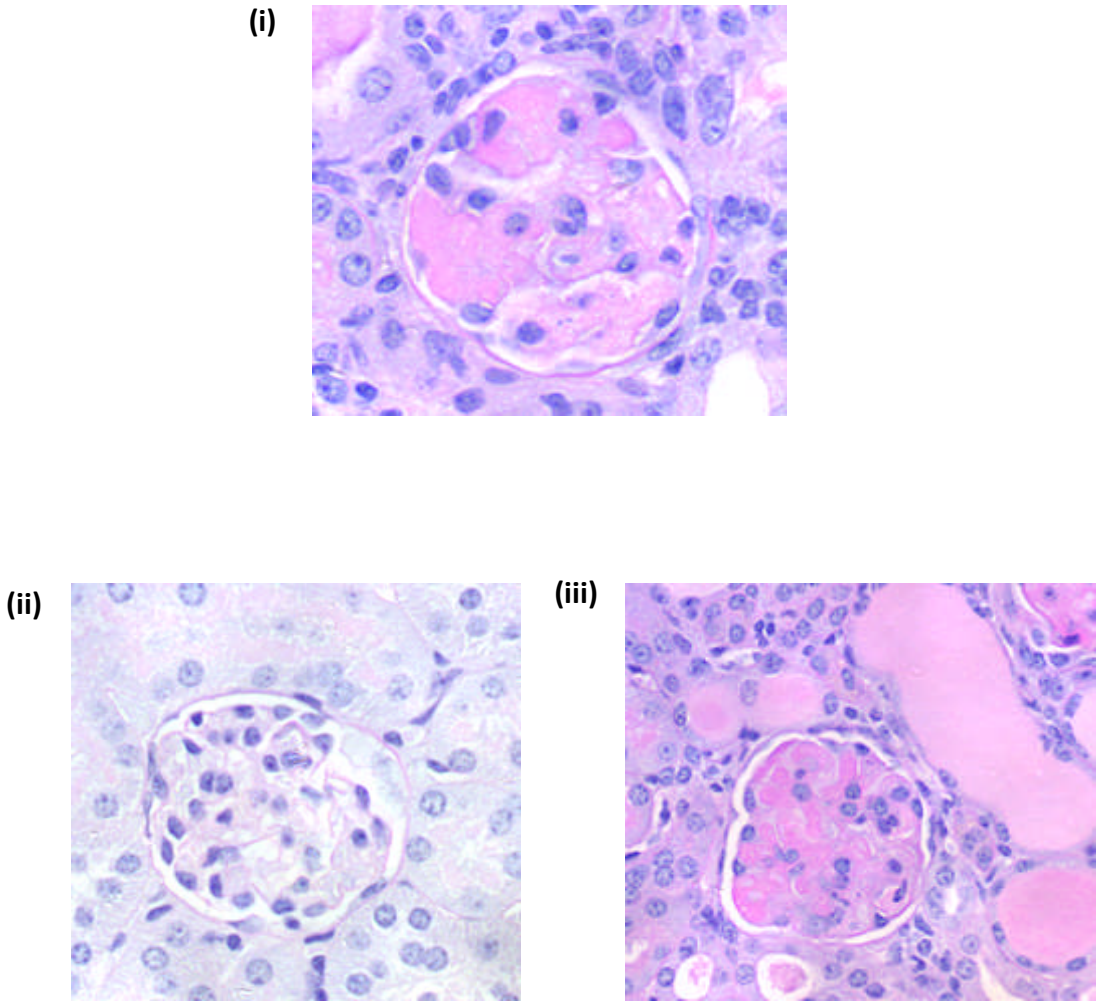

Figure 4-33 Photomicrographs of WT and mrp14-/- glomeruli during NTN. (H and E x630)

(i) WT mouse with 2/4 glomerular thrombosis score. (ii)-(iii) Mrp14-/- mice demonstrating variable glomerular pathology with some animals demonstrating glomerular hypercellularity (ii), while others have more severe disease with thrombotic glomeruli and severely dilated glomerular tubules and severe renal injury.

4.4.6.2 Proteinuria and renal function in NTN with high dose LPS after disease induction

In line with the thrombosis score, there was a similar amount of proteinuria in the WT and mrp14-/- groups. The median amount of proteinuria in the WT mice was 3.73mg/24 hours (range 0.36-7.99). Mrp14-/- median was 4.19 (range 2.36-11.36). The difference was not significant.

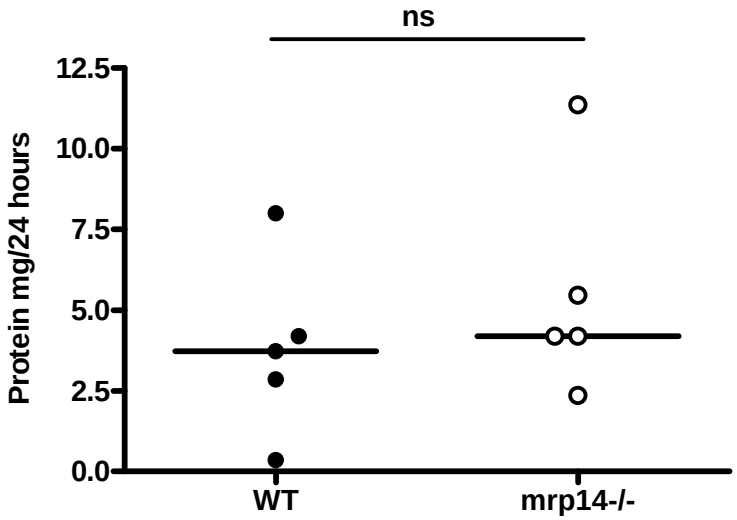

Figure 4-34 WT and mrp14-/- mice with NTN and additional LPS have similar proteinuria.

Graph above demonstrating each individual animal with the line representing the median. There is no difference between the 2 animal groups.

The renal function was also similar in both groups. Out of the 5 WT animals, all had an abnormal urea median 13.3mmol/l [range 9.1-55.4]). In the mrp14-/- group, 3 of the animals had preserved renal function, with the remaining 2 animals having severe renal disease with a greatly deranged urea. The median urea in mrp14-/- mice was 7.4 (range 6.3-81.6).

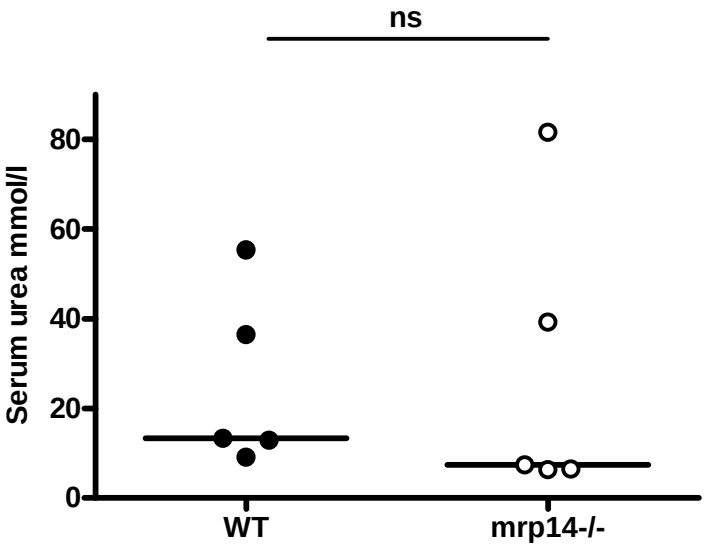

Figure 4-35 WT and mrp14-/- mice have similar renal dysfunction during NTN with LPS.

The graph above demonstrates the serum urea of each individual animal with the line representing the median. There is no difference between the 2 animal groups.

4.4.6.3 Leukocyte infiltration in NTN with high dose LPS after disease induction

Frozen sections of murine kidney were stained for macrophage (CD68) and CD4+ T cell infiltration. 25 glomeruli were included and the mean number of macrophages per animal calculated. Mrp14-/- mice demonstrated a trend to less CD68 macrophage infiltration compared to WT mice, but this did not reach statistical significance. The median number of macrophages infiltrating WT animals was 2.77 (range 1.57-6.8) and the mrp14-/- animals median 1.84 (range 0.76-1.88)(p=0.056)

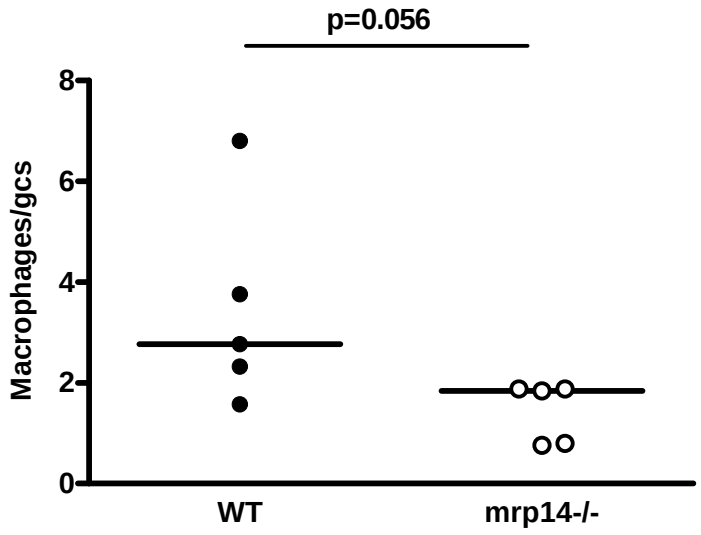

Figure 4-36 Mrp14/- mice demonstrate a trend to less CD68 infiltration during NTN with LPS than WT mice.

Graph demonstrating macrophage infiltration. Mrp14-/- mice demonstrate a trend to less CD68 glomerular infiltration following NTN compared with WT mice, but this is not significant (p=0.056). Line represents the median.

(i) 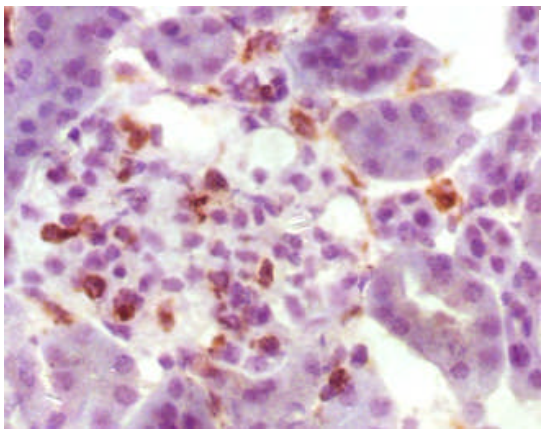 (ii) 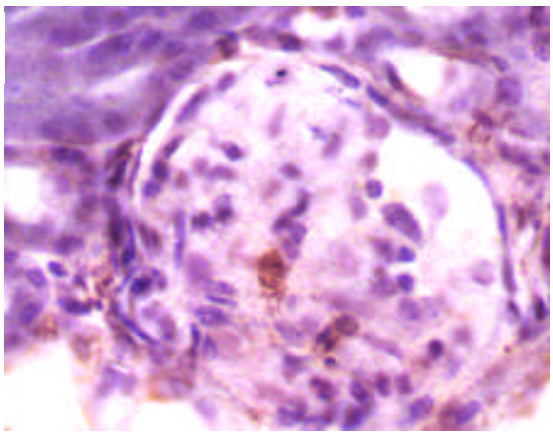

Figure 4-37 Mrp14-/- mice demonstrate a trend to less macrophage infiltration during NTN with high dose LPS.

Photomicrograph of WT (i) and mrp14-/- (ii) mouse kidney demonstrating immunohistochemistry for the macrophage marker CD68, demonstrating glomerular macrophage infiltration. The difference in infiltration between WT and mrp114-/- mice does not reach statistical significance although mrp14-/- mice demonstrate a trend to less glomerular macrophage infiltration ($p<0.056$); (All x630)

Both animal groups demonstrated a similar amount of glomerular CD4+ T-cell infiltration in NTN; the results were not significantly different between the 2 groups. WT median 0.12 (range 0.04-0.44), mrp14-/- median 0.20 (range 0.16-0.24).

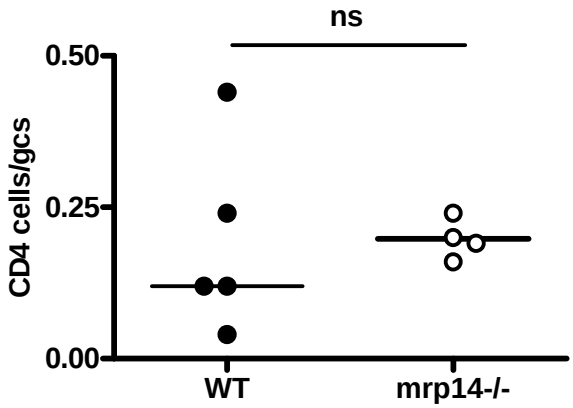

Figure 4-38 Mrp14-/- and WT mice display similar T cell infiltration during NTN with high dose LPS

There was no difference between the number of infiltrating glomerular CD4+ T cells in WT and Mrp14-/- mice with NTN and high dose LPS. Line represents the median.

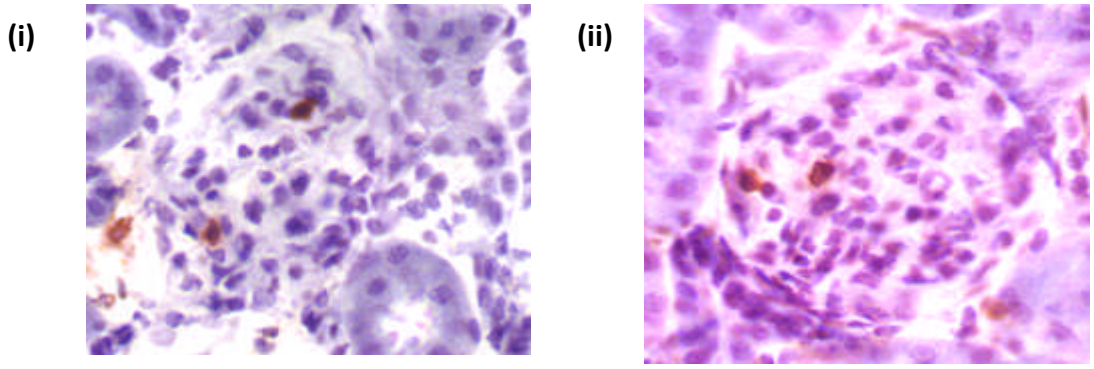

Figure 4-39 WT and Mrp14-/- mice demonstrate similar degrees of CD4+ T-cell infiltration during NTN with high dose LPS

Photomicrographs of (i) WT and (ii) mrp14-/- mouse kidneys demonstrating immunohistochemistry for CD4 T-cells during NTN with high dose LPS.

4.4.6.4 Systemic immune response in NTN with high dose LPS after disease induction

Following sacrifice, mouse serum was collected and used to analyse the murine response to sheep IgG. There were several differences in the response of the WT and mrp14-/- mice.

The total IgG response was similar between the 2 groups. WT mice had a median OD of 0.56 (range 0.1-1.9) and mrp14-/- mice a median of 0.27 (range 0.09-0.77). The difference was not significant. The IgG3 response was also similar between groups WT median 0.56 (0.1-1.9), mrp14-/- median OD 0.27 (0.09-0.77). However, mrp14-/- mice demonstrated decreased IgG1, IgG2b and IgG2c responses; WT vs mrp14-/- : IgG1 median 0.25 (0.196-0.75) vs 0.046 (0.03-0.156)($p<0.01$); IgG2b median 0.25 (0.09-0.5) vs 0.067 (0.05-0.08)($p<0.01$); IgG2c 0.03 (0.014-0.25)vs 0.01 (0.009-0.015)($p<0.05$).

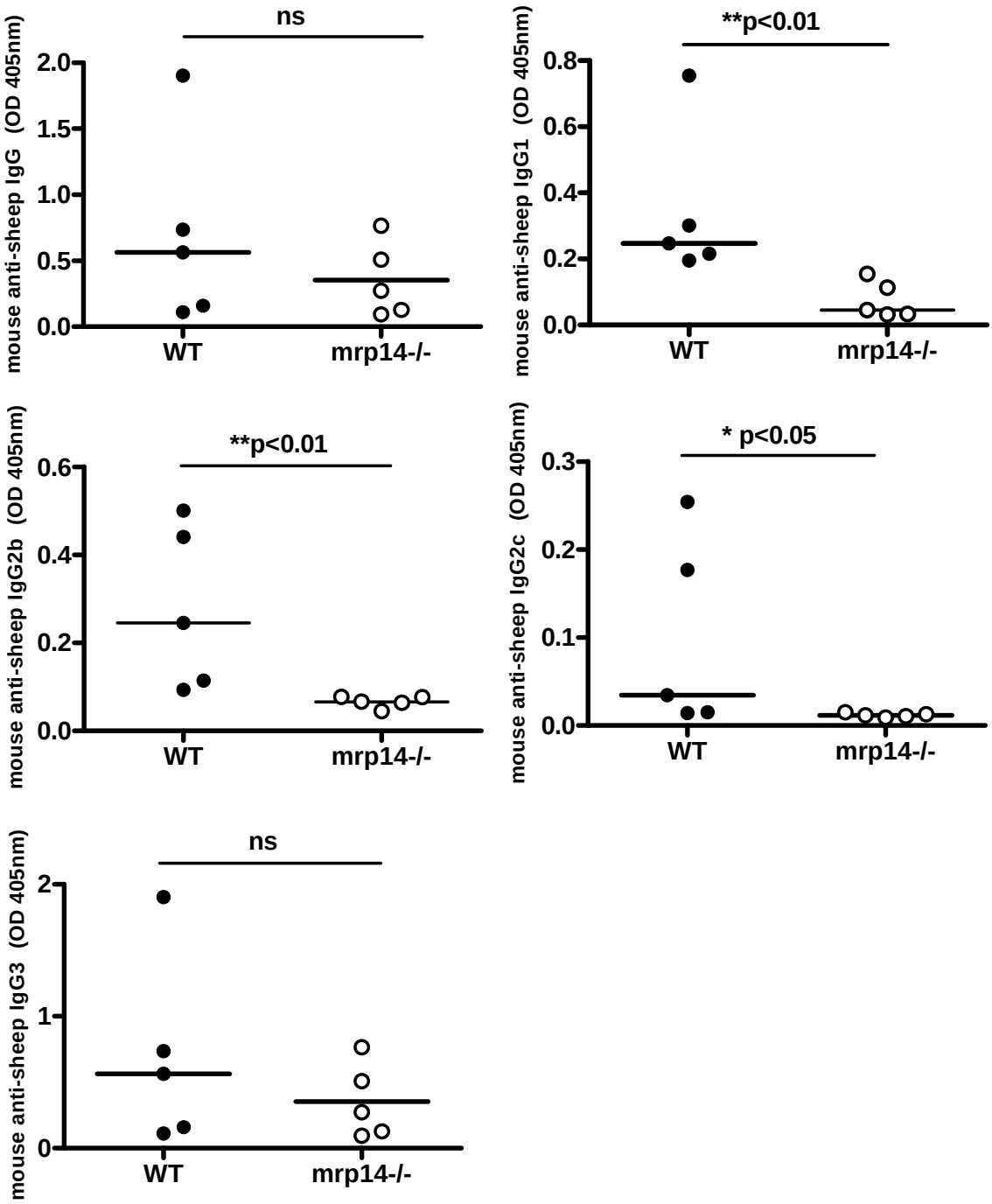

Figure 4-40 WT and mrp14-/- mice demonstrate different IgG responses during NTN with high dose LPS

Graphs demonstrating the IgG and IgG subset responses of the mice to sheep IgG. Mrp14-/- mice have a decreased IgG1 ($p<0.01$), IgG2b ($p<0.01$) and IgG2c ($p<0.05$) compared to WT mice.

Direct immunofluorescence was used to analyse the deposition of sheep and mouse IgG on the glomerular basement membrane. Although there was a difference in the systemic response to sheep IgG; there was no difference between the animal groups with regard to sheep or mouse antibody deposition on the glomerular basement membrane.

Immunofluorescence was quantified using arbitrary fluorescent units (AFU) and both groups compared. There was no difference in the amount of mouse antibody deposition, median WT AFU 113 (range 74-140) and mrp14-/- median 122 AFU (range 73-149).

Although there was a trend to greater amounts of sheep IgG deposition in the mrp14-/- glomerulus, this was not significant. WT median 22 AFU (range 18-45) and mrp14-/- median 44 AFU (range 31-105)($p>0.05$).

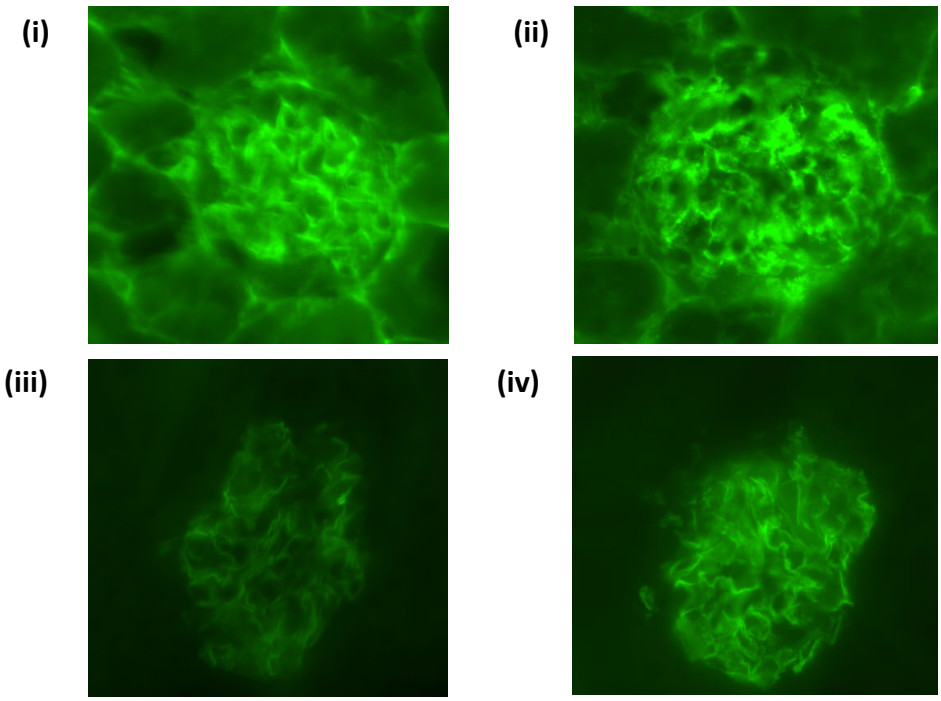

Figure 4-41 WT and mrp14-/- mice have similar glomerular deposition of sheep and mouse IgG during NTN with high dose LPS.

Photomicrographs demonstrating IgG deposition by immunofluorescence in (i) WT and (ii) mrp14-/- mice stained for mouse IgG and (iii) WT and (iv) Mrp14-/- stained for sheep IgG deposition. All x400.

4.4.7 The role of S100A8/A9 on circulating and intrinsic cells

To investigate the role of S100A8/A9 from haematopoietic cells and intrinsic cells, a bone marrow transplant was performed. 8 WT to WT animals was used as a control. The other 2 groups consisted of 9 animals in each group; mrp14-/- to WT mice and WT to mrp14-/- mice. Following bone marrow transplantation, the animals were left for 8 weeks to allow haematopoietic reconstitution. NTN was then performed.

4.4.7.1 Reconstitution of bone marrow chimeras

At the end of the experiment, all mice were bled and the clotted blood used to assess for bone marrow reconstitution. The intensity of the bands obtained was used to demonstrate if reconstitution had occurred.

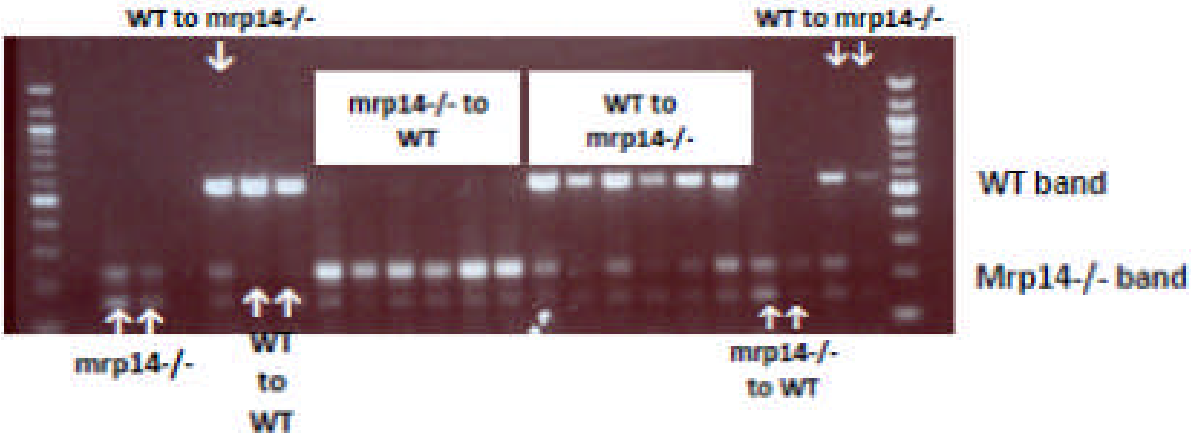

Figure 4-42 Genotyping of blood cells from bone marrow transplanted animals demonstrating genetic reconstitution compared to WT or mrp14-/- mice

4.4.7.2 All animals were susceptible to renal disease

NTN was induced in the mice 8 weeks following bone marrow transplantation. The protocol for inducing disease was similar to previous NTN experiments; mice were pre-immunised, followed by intravenous injection of NTS (with low dose LPS) 5 days later. The mice were sacrificed 8 days later. Disease was assessed by measurement of serum urea, proteinuria and analysis of glomerular thrombosis. All groups were susceptible to disease.

4.4.7.2.1 Renal function

All groups had severe renal disease. The median serum urea was 23mmol/l (range 4.6-53.2) in the WT to WT group; in the mrp14-/- to WT the median was 37.5mmol/l (range 6.1-210) and in the WT to mrp14-/- group the median was 38.9mmol/l (range 7.1-234). There was no significant difference between the 3 groups (1-way ANOVA).

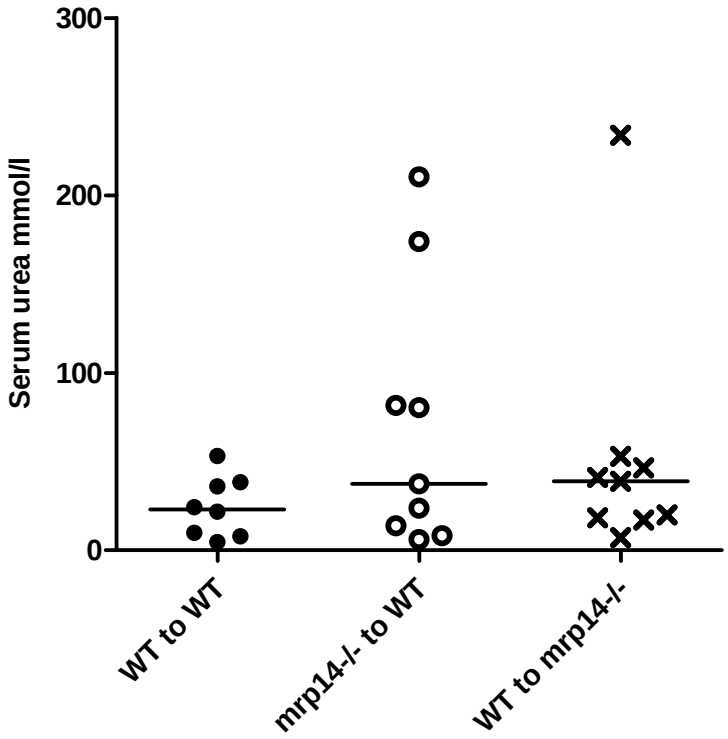

Figure 4-43 Renal function in bone marrow transplant recipients following NTN.

The graph above demonstrates the renal function (serum urea) in the 3 bone marrow transplant groups- there was no significant difference between the groups. Line represents the median.

4.4.7.2.2 Proteinuria

Due to the limited capacity of the metabolic cages, 19 animals were placed in the cages overnight and urine was collected for proteinuria. There was no significant difference between the 3 transplanted groups. The median proteinuria (mg/24 hours) in the WT to WT group was 9.83mg (2.7-16.86). In the mrp14-/- to WT group the median proteinuria was 8.95mg (0.45-32.8). WT to mrp14-/- group had median proteinuria of 2.73 (0.58-31.68).

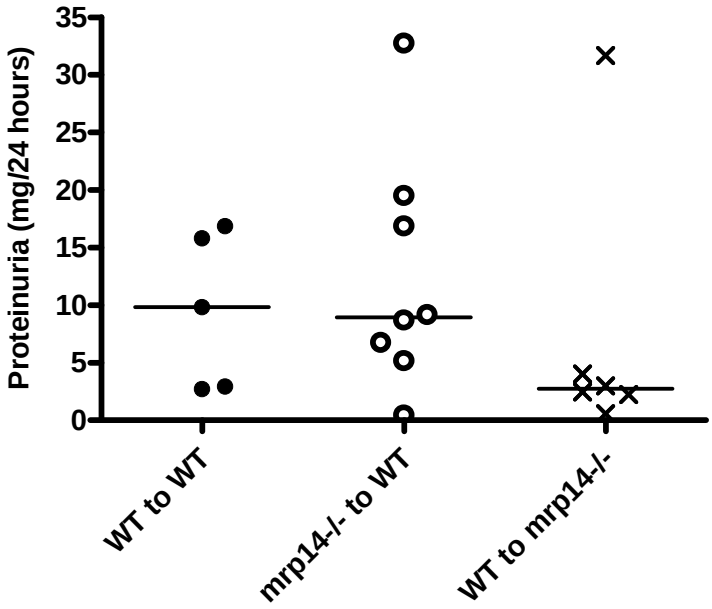

Figure 4-44 Proteinuria in the bone marrow transplant recipients following NTN

There was no difference in the amount of proteinuria between the 3 groups. Line represents the median.

4.4.7.2.3 Glomerular thrombosis

Renal histology was assessed using the PAS stained paraffin sections. Consistent with the other parameters of renal disease, there was no difference in the glomerular thrombosis score between the 3 groups (1-way ANOVA). The median glomerular thrombosis score in the WT to WT group was 1.72 (0-3.26); in the mrp14-/- to WT group was 1.58 (0-3.52) and in the WT to mrp14-/- group the median was 2.08 (0.3.64).

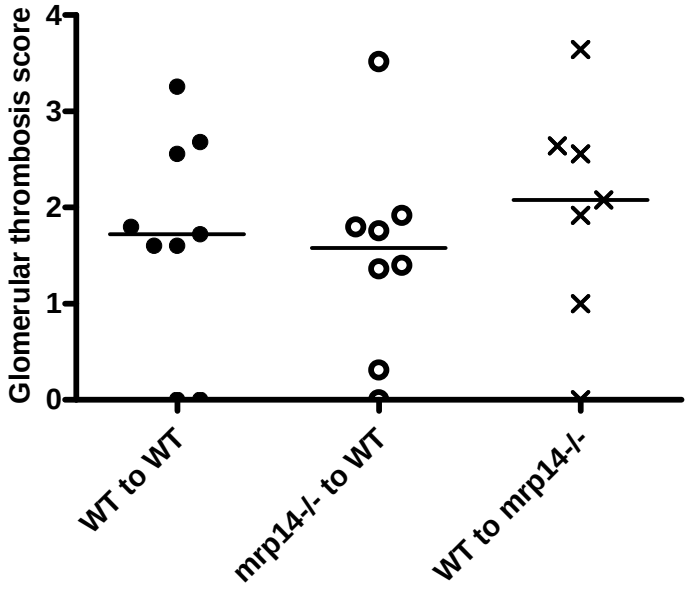

Figure 4-45 Glomerular thrombosis score in bone marrow transplant recipients following NTN

The graph demonstrates the thrombosis score in the 3 transplanted animal groups- there was no statistical difference between the 3 groups (One-way ANOVA).

4.4.8 Mrp14-/- and WT mice have similar neutrophil infiltration using the non-accelerated nephrotoxic nephritis model

The non-accelerated model of NTN was performed. This assesses the early neutrophil influx at 2 hours. 9 animals in each group were included. Unlike the previous models of NTN, mice were not pre-immunised. Instead, mice were administered with nephrotoxic serum via the tail vein and then killed 2 hours later.

NTS given 200µl via tail vein

↓

Killed 2 hours later

Following sacrifice, frozen sections were cut and neutrophil influx was investigated by immunohistochemistry using a granulocyte marker, GR-1.

There was no difference in the early neutrophil influx between WT and mrp14-/- mice. The median number of neutrophils at 2 hours in the WT mice was 0.6 (0.44-2) and in the mrp14-/- mice, the median number of neutrophils was 0.71 (0.56-1.2)(p=ns).

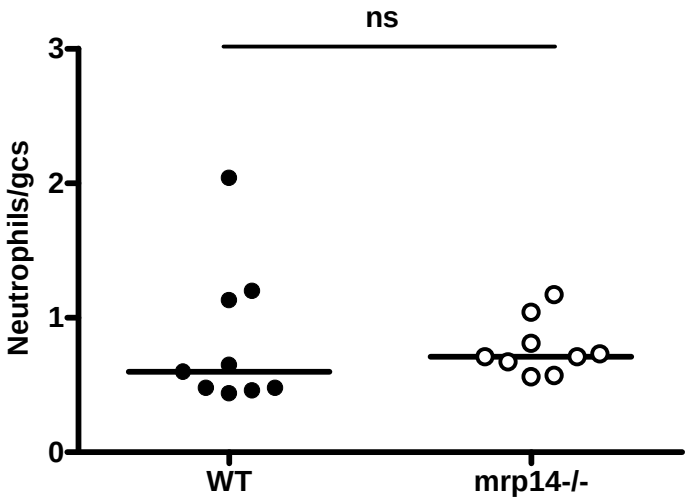

Figure 4-46 WT and mrp14-/- have similar early neutrophil influx in non-accelerated NTN

Graph demonstrating the individual animals and the calculated mean number of neutrophils per animal. The line represents the median. The differences between the 2 animal groups are not significant.

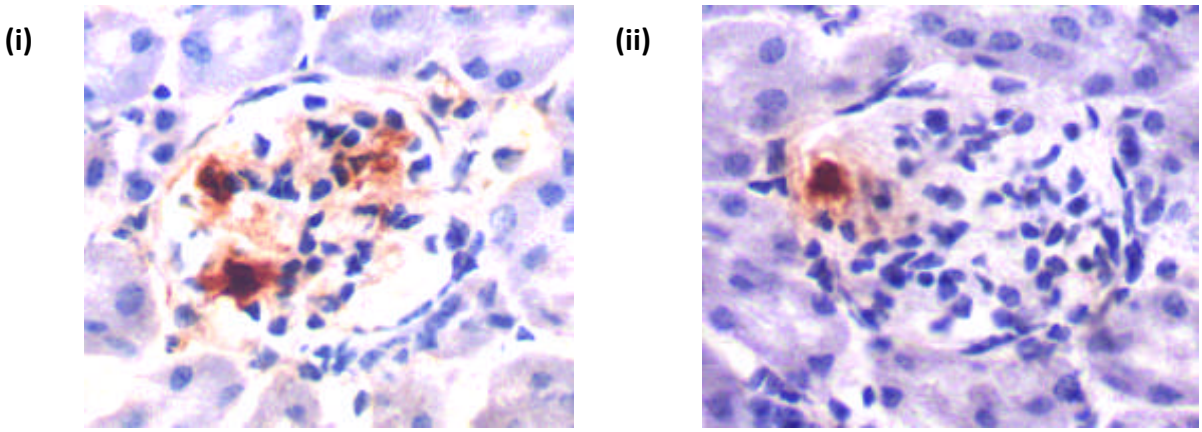

Figure 4-47 WT and mrp14-/- mice have similar early neutrophil glomerular influx in response to NTS.

Photomicrograph demonstrating immunohistochemistry of the neutrophil marker GR-1 to illustrate neutrophil influx in (i) WT and (ii) mrp14-/- mice during non-accelerated NTN (All x630).

4.5 Discussion

The experiments included in this chapter demonstrate that S100A8/A9 has a significant role in nephrotoxic nephritis. Macrophage glomerular infiltration is a feature of the NTN model and I found the presence of different macrophage phenotypes in mice during NTN with respect to S100A8/A9. Two strains of knock-out mice (MR-/- and IL17-/-) protected from NTN, demonstrate reductions in S100A8/A9 expression in their infiltrating macrophages- linking disease associated macrophages with S100A8/A9.

Surprisingly, S100A8/A9 did not seem to play a role in mediating neutrophil influx in NTN. Neutrophil influx occurs following interaction of the neutrophil with the endothelium following the injection of heterologous antibodies to the glomerular basement membrane. It is an important stage of glomerular injury and it has previously been demonstrated that injury in the heterologous phase of NTN is dependent on neutrophils (Henson 1972). This influx occurs at about 2 hours following NTS, and reaches a maximum at 2-4 hours (Unanue and Dixon 1967). S100A8/A9 is abundantly expressed in neutrophils, and there is an early influx of cells positive for S100A8/A9 which peaks at 4 hours following administration of nephrotoxic serum. This demonstrates that cells positive in S100A8/A9 infiltrate the glomerulus early on in NTN, but then decrease by 48 hours. The non-accelerated heterologous experiment assessed whether mrp14-/- mice had the same amount of early neutrophil influx as WT mice. This experiment demonstrates that S100A8/A9 is not required for neutrophils to interact with the endothelium during NTN and infiltrate the glomerulus. Therefore decreased neutrophil infiltration is not a mechanism by which mrp14-/- mice have decreased disease during NTN. The neutrophils that are deficient in S100A8/A9 may have different functional behaviour with respect to their pro-inflammatory profile, but this was not investigated.

This chapter includes several NTN experiments. The nephrotoxic nephritis animal model can have variable results of disease parameters, therefore when possible; results have been combined to increase the number of animals in each group. Experiment 1 resulted in generally milder disease with none of the mrp14-/- animals affected. Experiment 2 resulted in a shift in disease severity with more WT animals affected and with a minority of mrp14-/- being susceptible to disease. However, when combined the results demonstrate significantly

less disease in the mrp14-/- mice. The results consistently demonstrate a decrease in glomerular macrophage influx in the mrp14-/- mice. This is consistent with the hypothesis that S100A8/A9 has a role in monocyte adhesion, for example by the upregulation of ICAM-1, followed by transmigration through the endothelium to the site of local inflammation. Mice therefore lacking this complex have a decreased macrophage ability to infiltrate the glomerulus. Additionally, once the glomerulus has been infiltrated, as well as a greater number of macrophages being present to participate in inflammation, the complex may then have additional autocrine and paracrine effects to further amplify inflammation. It has been described that it's not just the presence of absence alone of macrophages which contribute to the inflammatory response but also the macrophage function (Kluth, Erwig et al. 2004).

NTN has been considered to be a Th1 model of disease, with T-cells playing a crucial role in disease pathogenesis. This has been illustrated by mice deficient in IFN-γ having decreased renal injury in NTN with a reduction in effectors cells such as CD4 T cells and macrophages (Kitching, Holdsworth et al. 1999). However, it is now increasingly recognised the role of IL17 T-cells in the pathogenesis of autoimmunity, with disease protection in IL-23 p19-/- mice during NTN (Paust, Turner et al. 2009), and protection in IL17-/- mice during NTN (S.Hamour unpublished). In experiment 2, there was significantly less T-cell infiltration in mrp14-/- mice as well as less macrophage infiltration. The decrease in CD4 T cells may then also have contributed to decreased disease in the mrp14-/- mice due to the crucial role T cells are known to play in NTN.

Experiment 1 and 2 had different results following detection of IgG subclasses. Different IgG subclasses are associated with either a Th1 or a Th2 response. IgG2a isotype can fix complement, and a reduction in this subtype has been associated with a reduction in renal injury (Kitching, Holdsworth et al. 1999). The Th-1 cytokine, INF-γ, is able to induce IgG2a production, as well as inhibit IgG1, IgG3 and IgG2b. IgG2a has the ability to also induce macrophage antibody-dependent cellular cytotoxity (Snapper and Paul 1987). During NTN, treatment of mice with the Th2 cytokines (IL-10 or IL-4) has been shown not to result in a change in the overall titres of anti-sheep antibodies, but instead changes the profile of the IgG subclasses. IL-4 resulted in a decrease in the titres of IgG2a, IgG2b and IgG3, with a

decrease in IgG2a and IgG3 following treatment with IL-10. The Th-2 associated IgG1 was shown to be relatively spared in this model. Histologically, the mice treated with the Th-2 cytokines resulted in an attenuation of glomerular injury (Tipping, Kitching et al. 1997). Experiment 1 was characterised by quite mild disease with no differences in renal function between the 2 groups, despite a trend to less thrombosis and proteinuria with significantly less macrophage infiltration. Mrp14-/- mice had significantly less IgG2a, with no significant glomerular injury and no glomerular thrombosis in any of the mice. Although the disease was quite mild in the WT mice, they did have a range of glomerular abnormalities. Experiment 2 was unable to demonstrate a similar result. Generally, experiment 2 differed from experiment 1 with respect to a greater proportion of both animal groups being affected by disease, although the mrp14-/- mice had better preservation of renal function and less macrophage and T cell infiltration than the WT group. Therefore, as disease parameters may have increased in both groups in experiment 2, the difference in IgG2a became less apparent.

Following experiment 2, the T-cell response during NTN was investigated. At rest, when unstimulated, T cells isolated from mrp14-/- mice following NTN had a higher basal rate of proliferation. The role of T-cells in mrp14-/- mice has been further explored in transplantation models. MHC-class II allomismatched cardiac grafts transplanted into WT and mrp14-/- mice resulted in a decreased survival in mrp14-/- mice, with an increase in accumulation of macrophages and T-cells in the mrp14-/- mouse grafts. Additionally, there were higher levels of INF-γ and IL-17 in infiltrating CD4+ T-cells (Shimizu, Libby et al. 2011). Although there are significant differences between this transplantation experiment and NTN, the isolated splenocytes from mrp14-/- in the transplantation study also demonstrated an increase in proliferation rate at rest compared to WT splenocytes, however, there was no difference in either group following stimulation with CD3, consistent with the results that we have obtained. In the transplantation model, the loss of mrp14-/- had a significant effect on expression of co-stimulatory molecules and antigen presentation and T-cell priming. During NTN, consistent with the above results, there is an increase in splenocyte proliferation at rest, with no increase detected following anti-CD3/CD28 stimulation. However, stimulation with sheep IgG resulted in a non-significant trend to less proliferation in the mrp14-/- splenocytes.

I tested the effect of LPS on NTN. Highly purified LPS is a TLR4 ligand. This experiment tested the hypothesis whether direct stimulation of TLR4 by initially low dose then high dose LPS would render the mrp14-/- mice susceptible to renal disease. In the endotoxic shock model, mrp14-/- mice had an increased survival following LPS compared to WT mice (50µg/kg I.P)(Vogl, Tenbrock et al. 2007). The NTN experiment used a lower dose of LPS to ensure that the mice would survive till the end of the experiment 8 days later. It is recognised that batches of nephrotoxic serum contain varying degrees of LPS contamination, with a correlation between the degree of endotoxin contamination and the ability of the nephrotoxic antibody to induce albuminuria in the rat (Karkar and Rees 1997). LPS has previously been demonstrated to cause no glomerular abnormalities when administered alone, however in a rat model of NTN using rabbit globulin the administration of LPS prior to NTS results in an exacerbation of renal injury with increased proteinuria and increased glomerular thrombi. LPS is known to result in increased neutrophil adhesion to the endothelium as well as an increase in neutrophil influx (Tomosugi, Cashman et al. 1989).

In the low dose LPS experiment mrp14-/- mice showed a trend to less thrombosis and significantly improved renal function. In this experiment, there was no difference in the systemic antigen response with a non-significant decrease of the Th-1 associated complement fixing IgG2c. There was no difference in the amount of T-cell infiltration which may have been due to LPS resulting in an early increase in the neutrophil influx in both groups with the resulting T cell infiltration which was equal in both animal groups. However, CD68 macrophage infiltration was significantly less, consistent with the hypothesis that S100A8/A9 has an important role in the adhesion of macrophages to the glomerular endothelium and the resulting transmigration. This group of WT mice also had serum S100A8/A9 levels measured, with very high serum levels in those mice with a severe thrombotic GN. Therefore this links S100A8/A9 expression with disease parameters suggesting that this complex is a biomarker of renal injury in NTN, as well as contributing to disease pathogenesis. Considering that mrp14-/- has disease protection when LPS and NTS are administered during NTN, the following experiment was designed to investigate if disease could therefore be induced when a higher dose of LPS was used after the initiation of disease. Previous studies administering LPS to exacerbate disease in NTN, have given LPS as a pre-treatment prior to the administration of NTS aiming to increase disease primarily

through the increase in the early neutrophil response. In the following experiment, LPS was administered at a higher dose at day 3 after NTS. By day 3, the neutrophil influx has disappeared and monocytes/macrophages are starting to infiltrate the glomerulus and play an important role in disease pathogenesis. Despite similarities in the glomerular mouse and sheep IgG deposition, there were differences in the systemic IgG response to sheep IgG. Mrp14-/- mice had a similar total IgG response but there were differences in the IgG subclasses. From this experiment, we can conclude that direct high-dose TLR4 stimulation with LPS overwhelms the protection resulting from a lack of S100A8/A9, and therefore has the ability to induce disease in mrp14-/- mice of a similar severity to WT mice.

The results of the bone marrow transplant experiment demonstrate that to have protection from renal disease, total deficiency of S100A8/A9 is necessary, as all three animal groups had the same severity of renal disease. This could have been confirmed if we had performed mrp14-/- to mrp14-/- transplants, but these were not possible due to limited animal numbers. This experiment illustrates that circulating haemopoietic cell and intrinsic (radioresistant) cell production of S100A8/A9 are both important mediators of inflammation. This is reminiscent of data from bone marrow chimeras used to investigate the effect of S100A9 deficiency on the development of systemic atherosclerosis (Averill, Barnhart et al. 2011). In that study, absence of haemopoietic S100A9 was not sufficient to suppress systemic inflammation and atherosclerosis, (Croce, Gao et al. 2009). These somewhat surprising results were attributed to S100A9 deficiency in dendritic cells, the presumed main source of S100A8/A9 in atherosclerotic lesions, augmenting inflammation, suggesting that under normal circumstances they may have an anti-inflammatory role in this disease model (Averill, Barnhart et al. 2011)..

Additionally, it is recognised that under inflammatory conditions, non-myeloid cells may also produce S100A8/A9. This is clearly illustrated by the production of S100A8/A9 in the renal collecting ducts, which results in interstitial monocyte recruitment and their differentiation into inflammatory M1-type macrophages causing renal epithelial cell injury and inflammation in a murine ureteric obstruction model (Fujiu, Manabe et al. 2011). However, the question remains unanswered as to which radioresistant cell in the kidney may also be

producing S100A8 and S100A9 and possibly be contributing to glomerulonephritis. Future work should focus on confirming S100A8/A9 expression in the NTN kidney.

The antigen induced arthritis model also supports the role of S100A8/A9 during inflammation. Humoral immunity in WT and mrp14-/- mice was similar between the 2 groups, as was cellular T-cell responses. Similar to NTN, mrp14-/- mice had decreased joint inflammation, with S100A8/A9 stimulation of macrophages having an important role in joint destruction (van Lent, Grevers et al. 2008). Therefore, there is more than one animal model of inflammatory disease demonstrating a role of S1008/A9 in the disease aetiology.

The following chapter therefore investigates the pro-inflammatory mechanism of S100A8/A9 on different cell types known to play an important role in glomerulonephritis.

4.5.1 Summary

- Mrp14-/- mice in NTN have less disease than WT mice, which has not previously been described before.

- Mrp14-/- mice administered LPS and NTS have preserved renal function compared to WT mice.

- Disease can be induced in mrp14-/- mice after the administration of high dose LPS on day 3 of NTN.

- Both myeloid and intrinsic renal production of S100A8/A9 contributes to disease as demonstrated by the bone marrow transplant experiments.

- There is no difference in the early neutrophil influx in WT and mrp14-/- mice.

Chapter 5 Mechanisms of disease protection and the pro-inflammatory effects of S100A8/A9

5.1 Introduction

In the previous chapters, I have demonstrated that S100A8/A9 may have a role in human disease and be a potential biomarker of disease activity. Additionally, the animal work demonstrated that mice deficient in S100A8/A9 are protected from disease demonstrating that the heterodimer may also have a role in disease pathogenesis. Mice deficient in S100A8/A9 are protected in other murine models of autoimmunity, such as the antigen induced arthritis model (van Lent, Grevers et al. 2008). In this model S100A9-/- mice are protected from arthritis, with a significant reduction in osteoclasts within the knee joints after 7 days. This study demonstrated that S100A8, S100A9 and S100A8/A9 had differential effects on osteoclast formation and bone resorption. Both S100A8 and S100A9 are strongly expressed in osteoclasts, although these proteins are not required for the normal development of osteoclast precursors. In-vitro work demonstrated that S100A8 is the active component of the heterodimeric complex, with S100A8 having the ability to upregulate activatory Fc-gamma receptors and MMP more potently than either S100A8/A9 or S100A9. S100A8 homodimers, as well as the heterodimer S100A8/A9, have been found within inflammatory arthritis. This effect of S100A8 on macrophages was abrogated in TLR4-/- deficient cells (van Lent, Grevers et al. 2010). Similarly, stimulation of osteoclasts with S100A8 increased osteoclast numbers and bone resorption unlike stimulation with S100A8/A9 or S100A9 and was dependent on TLR4 but not RAGE (Grevers, de Vries et al. 2011). Pro-inflammatory cytokine secretion by chondrocytes was also stimulated by the individual S100 proteins, with an increase in the mRNA of IL-1β and IL-6 (not TNF-α). Again, similar to previous studies, the effects of S100A8 and S100A9 were mediated through TLR4 with no change in the stimulation assays following blocking of RAGE, in agreement with previous experiment data (Schelbergen, Blom et al. 2012).

In order to investigate the particular role of S100A8/A9 in autoimmune glomerular disease, it is important to consider the cell types which may have a role in mediating disease. Within

the glomerulus; the endothelial cell, the mesangial cell and the infiltrating monocytes/macrophages may all potentially have a role in S100A8/A9-mediated inflammation. TLR4 has already been shown to have a role in crescentic glomerulonephritis with both intrinsic renal cell and infiltrating leukocyte TLR4 expression playing a role in mediating disease (Brown, Lock et al. 2007). Potentially, S100A8/A9 may interact with TLR4 on the endothelium, as well as on novel carboxylated glycans and heparin sulphate proteoglycans, or S100A8/A9 may act in an autocrine manner and once released bind to TLR4 expressed macrophages/monocytes. Mesangial cells, a type of vascular pericyte, provide structural support thus maintaining glomerular integrity, as well as regulating glomerular filtration pressure and are known to express RAGE, through which S100A8/A9 may act, resulting in a proinflammatory effect. TLR4 may also be expressed on mesangial cells, as demonstrated by in-situ hybridisation on kidney tissue and by PCR using primary murine mesangial cell lines (Brown, Lock et al. 2007).

Cytokines, such as IL-8 and MCP-1, have important roles in glomerular inflammation mediating chemotaxis and adhesion of neutrophils and monocytes. MCP-1 is produced by several key cells found within an inflamed glomerulus such as macrophages, mesangial cells, endothelial and smooth muscle cells. TNF-α primed mesangial cells results in an increase in MCP-1 by the mesangial cells, and leads to a dose-dependent increase in monocyte migration (Pai, Ha et al. 1996). Additionally, activated mesangial cells can also produce the pro-inflammatory cytokine IL-12, which has diverse effects on NK cells, B cells and T-cells and has been implicated as a key cytokine in autoimmunity (Bussolati, Mariano et al. 1999). The interaction between mesangial cells and macrophages can be significant and may be mediated by pattern-recognition receptors (PRR). Work done in our laboratory by Dr. Chavele, has demonstrated that mice deficient in the mannose receptor (MR-/-) are protected from crescentic glomerulonephritis using the nephrotoxic nephritis animal model. MR-/- macrophages display a less inflammatory phenotype following their interaction with apoptotic mesangial cells (Chavele, Martinez-Pomares et al. 2010). Further PRRs are the toll-like receptors, which interact with danger associated molecular patterns (DAMPs), such as S100A8/A9. These are generally proteins, released as a consequence of tissue injury, which then promote the inflammatory response and may have a role in autoimmunity. Experiments by Dr. Chavele and by Dr. Sally Hamour in our laboratory (unpublished)

demonstrated that mice deficient in MR and IL-17 respectively, induced with NTN, result in a similar number of glomerular macrophages as WT mice, despite the knockout animals demonstrating significantly less disease, assessed by renal function, proteinuria and glomerular histology. As shown in the previous chapter, the macrophages in both these animal groups are different to the WT with respect to S100A8/A9 positivity, providing further evidence that it is not only the presence or absence of macrophages, but their phenotype which is associated with disease.

Previous work has demonstrated that one mechanism by which mrp14-/- mice were protected in the endotoxic shock model was as a result of a decreased response to LPS. Mrp14-/- bone marrow cells (BMC) had a decrease in TNF-α induction with reduced activation of the transcription factor NF-κB (Vogl, Tenbrock et al. 2007). The secretion of TNF-α was restored following stimulation of bone marrow cells by S100A8 alone, while S100A9 andS100A8/A9 had no effect when given alone, but did promote augmented TNF secretion when co-cultured with LPS.

5.2 Aim

This chapter focuses on the mechanisms which account for the differences in renal disease severity seen in WT and mrp14-/- mice described in the previous chapter. Experiments focus on the differences between WT bone marrow derived macrophages (BMDMs) and BMDMs isolated from mrp14-/- mice, with respect to their interaction with the endothelium, their phagocytic ability and their response to exogenous S100A8/A9. I also explore the interaction of S100A8/A9 on mesangial cells and assess whether TLR4 deficiency results in a limited inflammatory response of mesangial cells following stimulation.

5.3 Experimental design

Mice from both the Hammersmith Hospital, Imperial College London, and from Royal Free Hospital, University College London Central biological service were used for these

experiments. All mouse species were bred on a background of C57BL/6. Kidneys and bone marrow were harvested from WT, TLR4-/- (kind gift from Dr. Nathan Davis, UCL) and mrp14-/- deficient mice. The bone marrow cells were grown and allowed to differentiate into macrophages. The cells lines were grown in appropriate media. BMDMs, endothelial cells and mesangial cells from the different mouse groups were subsequently stimulated with S100A8 and S100A8/A9 (kind gift from Thomas Vogl) overnight. Supernatants were collected and various cytokines were measured by ELISA. The response and cytokine production between the cells groups were compared. Additionally, the phagocytic ability of WT BMDMs and mrp14-/- BMDMs using opsonised beads was compared.

5.4 Results

5.4.1 Characterisation of kidney endothelial cells and mesangial cells

Kidney endothelial and mesangial cells were isolated as previously described. Both cell types were characterised by immunofluorescence staining with antibodies directed against myosin, pancytokeratin and CD31 (for endothelial cells). Both cells groups were distinguished from fibroblasts by being negative for pancytokeratin and positive for myosin. Additionally, endothelial cells were positive for CD31.

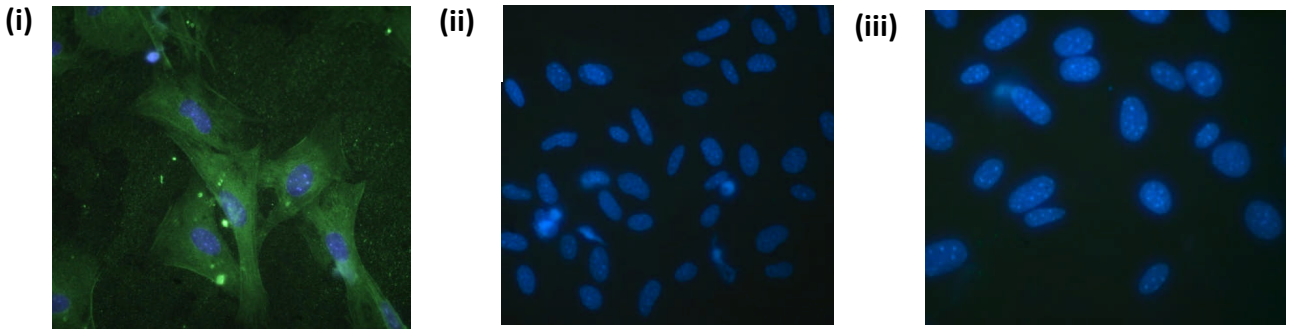

Figure 5-1 Characterisation of the isolated WT mesangial cells.

(i) Demonstrates positive immunofluorescence staining with anti-myosin antibody (green) The cell nuclei are staining using DAPI (4',6' diamino-2-phenylindole)(blue). (ii) The cells are negative for pancytokeratin by immunofluorescence. The cell nuclei are stained with DAPI (blue). (iii) Negative control, anti-myosin antibody omitted, secondary FITC conjugated antibody added and dapi.

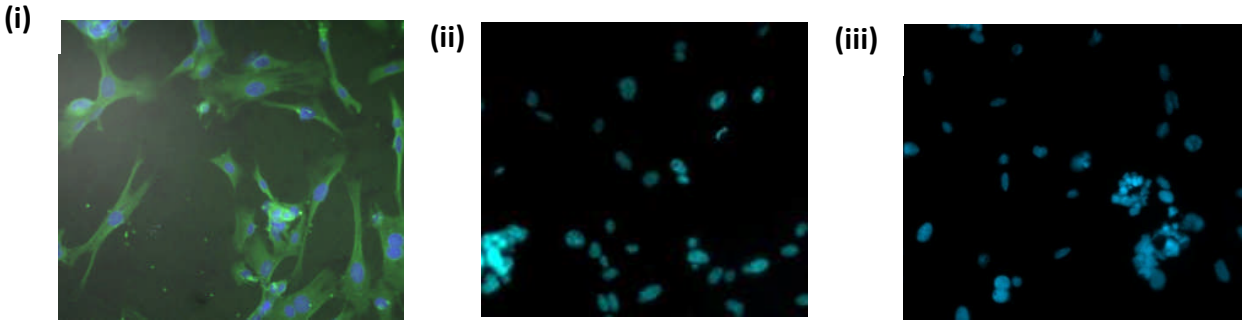

Figure 5-2 Characterisation of the isolated TLR4-/- mesangial cells.

(i) Demonstrates positive staining with anti-myosin antibody by immunofluorescence (green). The cell nuclei are stained using DAPI (4',6' diamino-2-phenylindole). (ii) The cells are negative for pancytokeratin by immunofluorescence. The cell nuclei are again stained with DAPI. (iii) Negative control, anti-myosin antibody omitted, secondary antibody added and dapi.

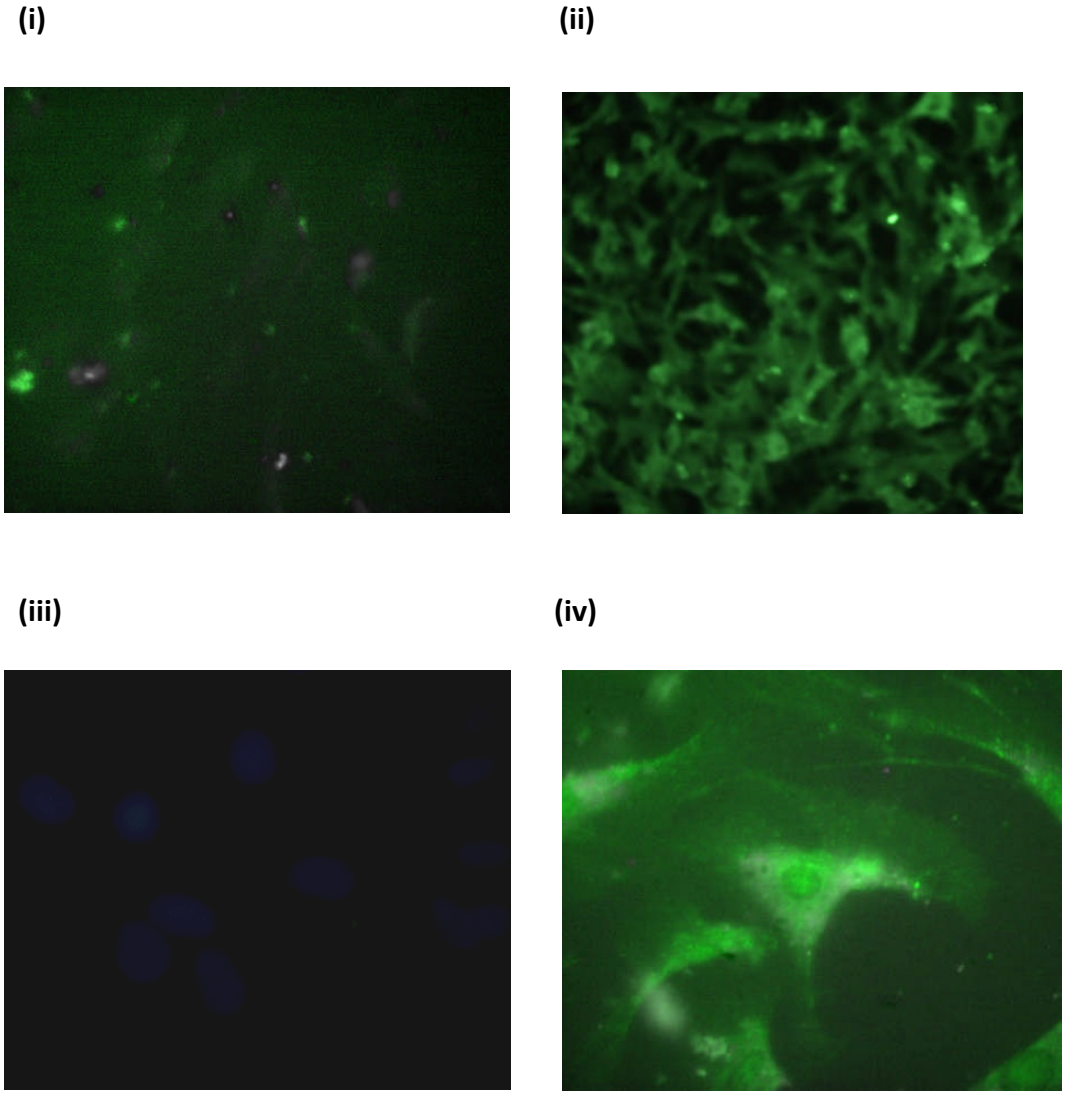

Figure 5-3 Characteristics of the endothelial cells isolated from WT kidney by immunofluorescence.

(i) Negative control, with omission of anti-myosin antibody. The cells have been stained with the secondary FITC conjugated antibody. (ii) The cells express myosin as shown using an anti-myosin antibody (green). (iii) Demonstrates the cells are negative for pancytokeratin. The cell nuclei have stained for DAPI. (iv) The cells are positive for the endothelial marker CD31 (green) as demonstrated with an antibody against CD31.

5.4.2 TLR4 expression is induced in kidney endothelial cells

It has previously been demonstrated that S100A8/A9 is able to have a proinflammatory effect on the endothelium, mediated through binding to heparin sulphate proteoglycans and novel carboxylated glycans or TLR4. I therefore assessed whether the endothelial cell line that I had isolated and cultured was able to express TLR4. The expression of TLR4 was assessed in unstimulated cells or following overnight stimulation with LPS (5μg/mL) or TNF (25ng/mL). After RNA extraction, the RNA was reverse transcribed and DNA amplified. It was possible to detect TLR4 expression by reverse-transcriptase PCR following stimulation of the cells with LPS. No TLR4 was detected in the unstimulated cells or in the cells stimulated with TNF-α

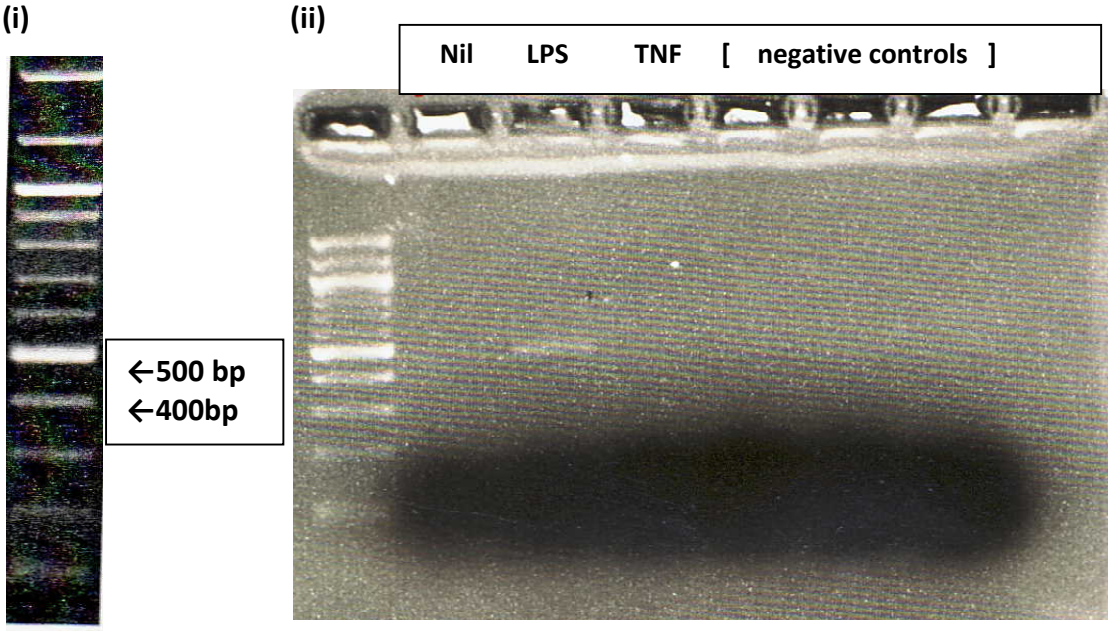

Figure 5-4 TLR4 RNA detected in the cell line by reverse-transcriptase PCR

Gel demonstrating the presence of TLR4 cDNA in the endothelial cell line isolated from wild-type kidneys. The size of the product was 455 base pair corresponded to the size of the PCR product detected on the gel. The last 3 lanes were the negative controls, samples that had not been reverse transcribed before DNA amplification.

5.4.3 S100A8/A9 exerts a pro-inflammatory effect on bone marrow derived macrophages mediated through TLR4

To assess the role of S100A8 and S100A8/A9 on bone marrow derived macrophages (BMDMs), the cytokine profile secretion was assessed by ELISA. Male mice were used in these experiments. BMDMs were isolated as described from WT and TLR4 deficient mice. The media was changed at day 3, and at day 7 the cells were plated out in 6 well plates for stimulation overnight. In this experiment $9x10^5$ BMDMs were used per condition, and performed in triplicate. Following stimulation with S100A8 and S100A8/A9 at 1µg/mL, supernatants were collected and cytokine analysis performed by ELISA. Both S100A8 and S100A/9 had a proinflammatory effect on BMDMs which was abrogated in TLR4-/- BMDMs.

5.4.3.1 Comparing IL-8 secretion between WT and TLR4-/- BMDMs

Wild-type BMDMs produced a significant increase in IL-8 detected following stimulation with TNF/S100A8, and a non-significant increase following stimulation with S100A8 or S100A8/A9 alone. The median values for IL-8 secreted by unstimulated cells was 885pg/ml (range 835.8-894.8pg/ml), following stimulation with S100A8 3929pg/ml [range 3767-8303]) and S100A8/TNF (median 9159pg/ml [range 3467-3760]), while stimulation with S100A8/A9, produced 3667pg/ml (range 3467-3760pg/ml). This is in contrast to the results obtained following the same experimental protocol with BMDMs isolated from male TLR4-/- mice. The median value of IL-8 secreted from unstimulated cells was 714pg/ml, following stimulation with S100A8 and S100A8/A9, there was no difference in IL-8 production, median 760.8pg/ml and 710.6pg/ml respectively. Figure 5.5 demonstrates the IL-8 secretion by WT and TLR4-/- BMDMs under different conditions.

TLR4-/- BMDMs stimulated with LPS, do not produce a detectable increase in secreted cytokines (IL-6 or MCP-1), with values similar to unstimulated TLR4-/- cells. This is in contrast to TLR4-/- BMDMs stimulated with TNF-α, which results in significant cytokine production. The TLR4-/- mice were genotyped by the supplier, confirming the mutant stain (data from Yalda Sharifi).

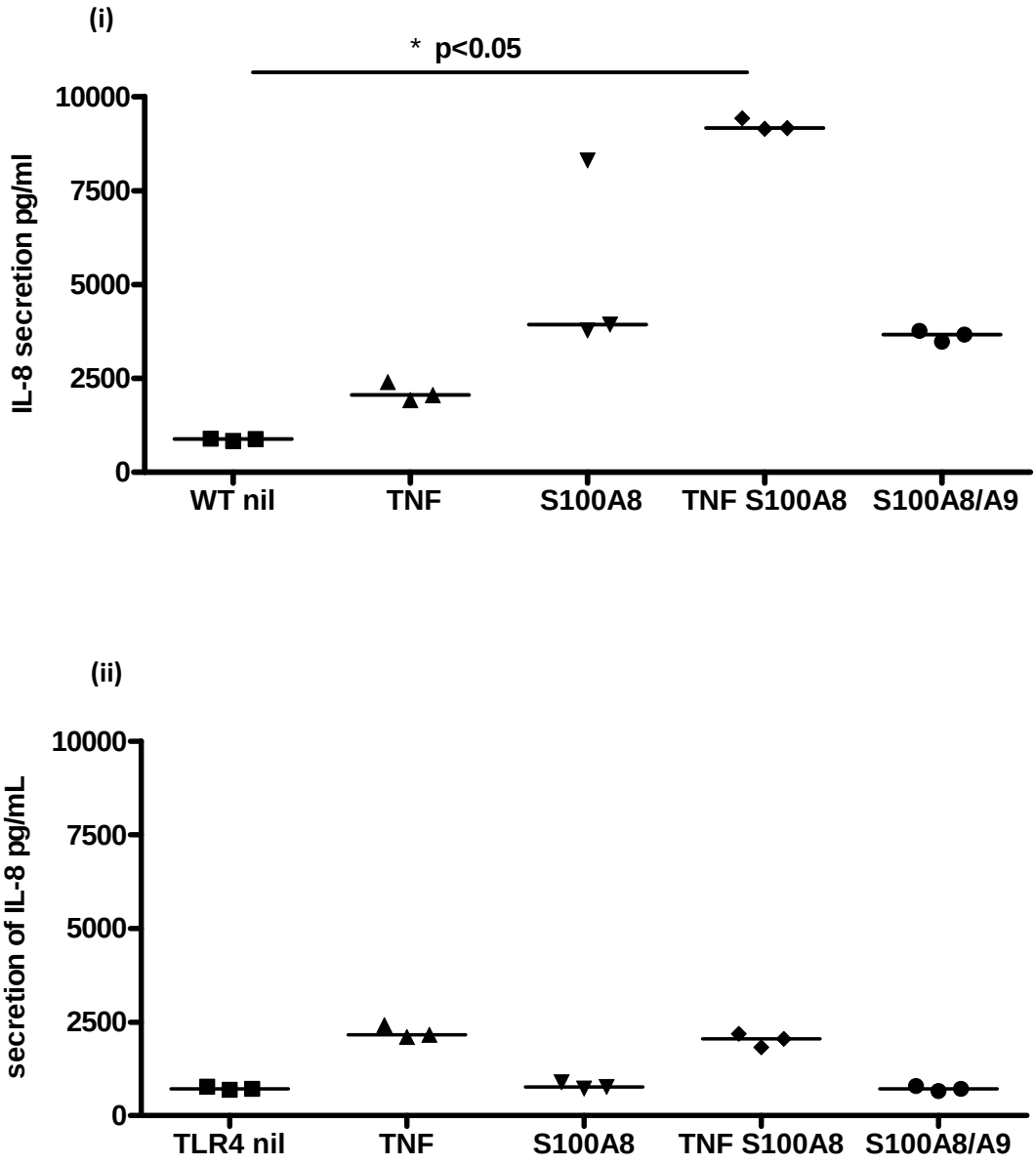

Figure 5-5 S100A8 and S100A8/A9 promote IL-8 secretion from wild-type but not TLR4-/- BMDMs.

Graphs to demonstrate the secretion of IL-8 from BMDM. Each condition was performed in triplicate. (i) The addition of S100A8/TNF resulted in a significant increase in IL-8 (One-way ANOVA). (ii) The increase in IL-8 secretion due to stimulation with S100A8 and S100A8/A9 is abrogated in TLR4-/- BMDM, with no difference in the amount of IL-8 detected in the different conditions. Line represents the median.

5.4.3.2 Comparing TNF-α secretion between WT and TLR4-/- BMDMs

Similar results were obtained when TNF-α secretion was assessed. Unstimulated wild-type BMDMs had no detectable TNF-α. Following stimulation with S100A8 and S100A8/A9 there was a significant increase in the amount of TNF-α detected by ELISA. The median amount of TNF-α increased to 196.8pg/ml (range 194.8-202pg/ml) with S100A8 and to 97.51pg/ml (range 96.54-117.3) with S100A8/A9. TLR4-/- BMDMs had undetectable TNF-α production when unstimulated, and no increase in TNF-α was found following stimulation with S100A8 or S100A8/A9. Figure 5.6 shows the TNF-α production in BMDM.

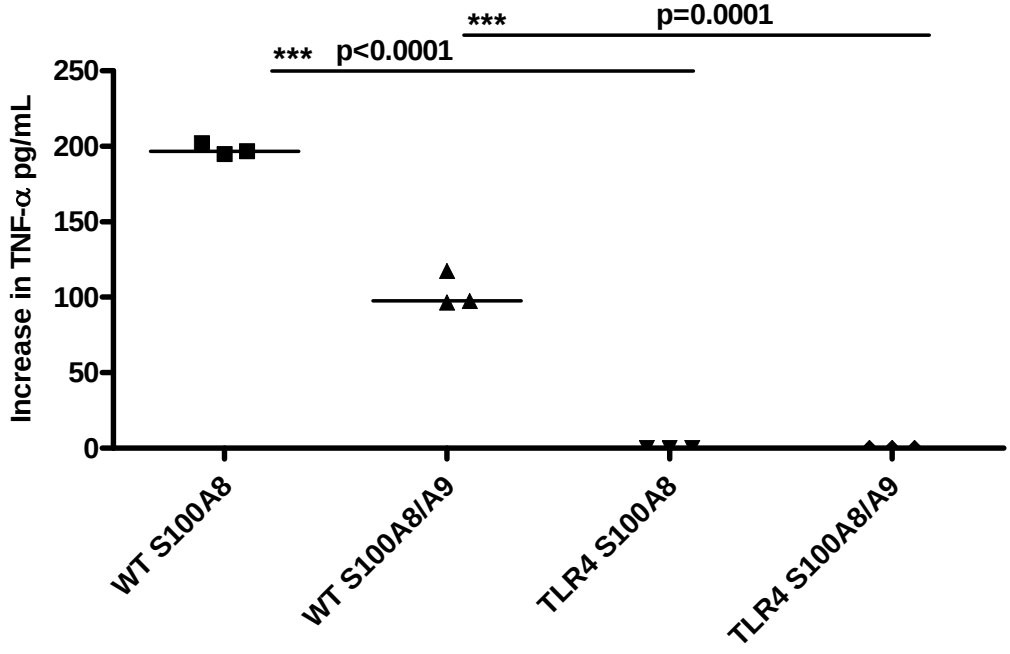

Figure 5-6 TNF-α secretion by S100A8 and S100A8/A9 is mediated through TLR4.

There is significantly more TNF-α secretion following S100A8 or S100A8/A9 stimulation in WT compared to TLR4-/- BMDM, p<0.0001 and p=0.0001 respectively (Unpaired t-test). Each condition performed in triplicate. Line represents the median.

5.4.4 BMDMs from mrp14-/- mice demonstrate a decreased pro-inflammatory response

To assess whether BMDMs from mrp14-/- mice behave differently to wild-type mice, BMDMs were isolated as previously described from male WT and mrp14-/- mice. At day 7, the BMDMs were plated out into 6 well plates and stimulated overnight. In these experiments, a total of 555,555 BMDMs were used per condition. The cells were stimulated with TNF 10ng/ml, S100A8 1µg/ml, S100A8 and TNF, S100A8/A9 1µg/ml and S100A8/A9 and TNF.

5.4.4.1 Mrp14-/- BMDMs produce less IL-8 than WT cells

The quantity of IL-8 produced from WT and mrp14-/- BMDM was compared. At baseline, unstimulated WT cells produced a median of 493pg/ml (range 459.2-601pg/ml) of IL-8. With S100A8 stimulation, this increased to 4787pg/ml (range 3678-5000pg/ml), and after stimulation with S100A8/A9, 4267pg/ml (range 3716-5000pg/ml) both $p<0.001$ (all unpaired t-test).

This increase in IL-8 secretion was conserved when mrp14-/- BMDM were stimulated with S100A8, unstimulated median 977.8pg/ml [range 767.9pg/ml-1033]) increasing to 4278pg/ml [range 3673-4427] ($p<0.0005$). However this increase was diminished but still significant in mrp14-/- cells stimulated with S100A8/A9, median IL-8 secretion 1585pg/ml (range 1135-1718pg/ml) ($p<0.046$)(Unpaired t-test).

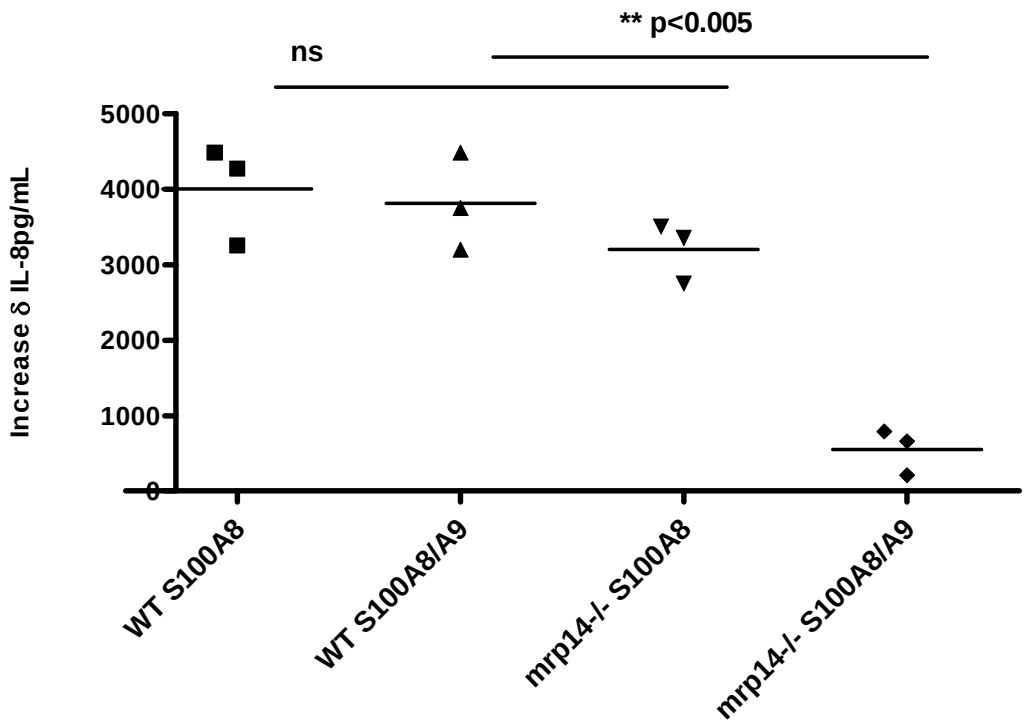

Figure 5-7 WT cells produce significantly more IL-8 than mrp14-/- cells when stimulated with S100A8/A9

The graph demonstrates the relative increase in IL-8 compared to unstimulated cells. The difference in IL-8 secreted following the stimulation of WT and mrp14-/- BMDMs with S100A8 is not significant. However, WT cells produce significantly more IL-8 when stimulated with S100A8/A9 compared to mrp14-/- cells ($p<0.005$)(unpaired t-test). Each condition performed in triplicate.

5.4.4.2 Mrp14-/- BMDMs produce less TNF-α than WT

TNF-α secretion increased in WT cells following stimulation with S100A8 or S100A8/A9; unstimulated WT BMDMs median TNF-α 53.5pg/ml (range 50.2-53.7pg/ml), S100A8 stimulated 321.5pg/ml (range 307.3-366.6pg/ml) and S100A8/A9 stimulated 324.6pg/ml (range 255.1-362.4pg/ml).

Mrp14-/- BMDMs secreted TNF-α at a baseline value of 63.66pg/ml (range 52-73.2pg/ml) increasing to 274.8pg/ml with S100A8 (range 238.3-291pg/ml) and to 96.32pg/ml with S100A8/A9 stimulation (range 92.2-129.7). The increase in TNF-α secreted by WT and mrp14-/- BMDMs following addition of S100A8 and S100A8/A9 was significant, ($p<0.05$ and $p<0.005$ respectively)(unpaired t-test), but stimulated WT cells produced significantly more TNF-α than mrp14-/- cells ($P<0.005$ for S100A8/A9 stimulated WT vs. Mrp14-/-; and $p<0.05$ for S100A8 stimulated WT vs. Mrp14-/-)(unpaired t-test).

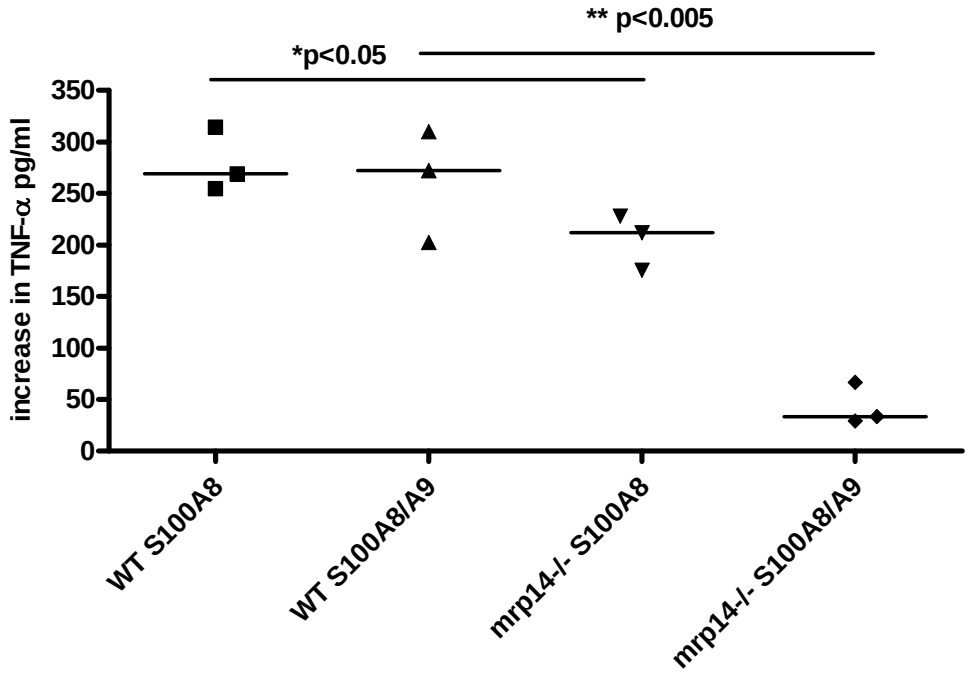

Figure 5-8 WT cells produce significantly more TNF-α than mrp14-/- cells

The graph demonstrates the relative increase in TNF-α secretion compared to unstimulated cells, following stimulation of WT and mrp14-/- cells with S100A8 or S100A8/A9. Conditions performed in triplicate. Mrp14-/- produce significantly less TNF-α following stimulation with both S100A8 and S100A8/A9 compared to WT cells (unpaired t-test). Line represents the median.

5.4.4.3 Mrp14-/- BMDMs produce less IL-6 than WT cells

WT BMDM produced an increase in IL-6 following stimulation with S100A8 and S100A8/A9. There was no detectable IL-6 at baseline in unstimulated cells. Secretion increased to a median of 106pg/ml following addition of S100A8 (range 101.8-113.9pg/ml), and to a median of 96.45pg/ml with the addition of S100A8/A9 (range 58-106.4pg/ml). Unstimulated mrp14-/- cells produced very small quantities of IL-6 at baseline, median 8.7pg/ml (range 0-9.6pg/ml). This increased to 67.8pg/ml (range 61.6-84.6pg/ml) following S100A8 stimulation and 18.23pg/ml following S100A8/A9 stimulation (range 17.6-22.2pg/ml).

Stimulated WT cells secreted significantly more IL-6 than mrp14-/- cells following S100A8 ($p<0.01$) and S100A8/A9 ($p<0.0001$).

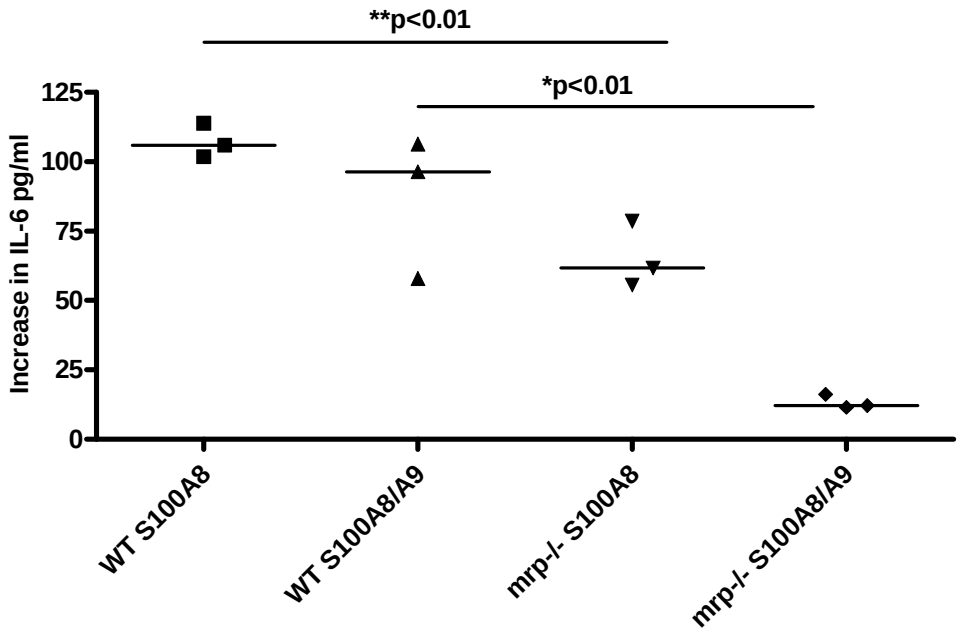

Figure 5-9 WT cells produce significantly more IL-6 than mrp14-/- cells following S100A8 and S100A8/A9 stimulation

Graph to demonstrate the increase in IL-6 secretion following stimulation with S100A8 and S100A8/A9 in WT and mrp14-/- cells. The increase is compared to IL-6 production in unstimulated WT or mrp14-/- cells. There is significantly more IL-6 produced by WT cells after stimulation. Line represents the median.

5.4.5 Th2 cytokines

There was no detectable secretion of either IL-4 or IL-10 by ELISA following the stimulation of WT, TLR4-/- or mrp14-/- BMDMs with S100A8 or S100A8/A9.

5.4.6 BMDMs from mrp14-/- demonstrate decreased phagocytosis

To compare the phagocytic ability of mrp14-/- BMDMs with WT cells, BMDMs were isolated from WT and mrp14-/- mice; plated onto a chamber slide at day 7 at a density of 100,000 cells per well and one day later the phagocytosis assay was performed in triplicate

5.4.6.1 Phagocytosis

The number of phagocytosed beads per 5 macrophages were counted, with 10 replicates per well (a total of 3 wells for each condition was performed) for both WT and mrp14-/- cells. WT BMDMs demonstrated significantly more phagocytosed beads than mrp14-/- BMDMs ($p<0.005$ Mann-Whitney)

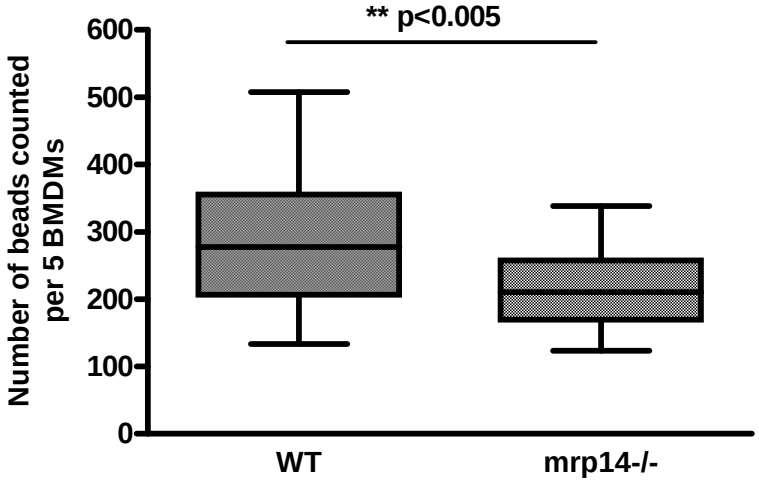

Figure 5-10 Mrp14-/- BMDMs demonstrated significantly less phagocytosis than WT cells

The graph demonstrates the median, interquartile range and range of phagocytosed beads in WT and mrp14-/- BMDMs. A total of 50 BMDMs were counted for each cell type and performed in triplicate.

(i)

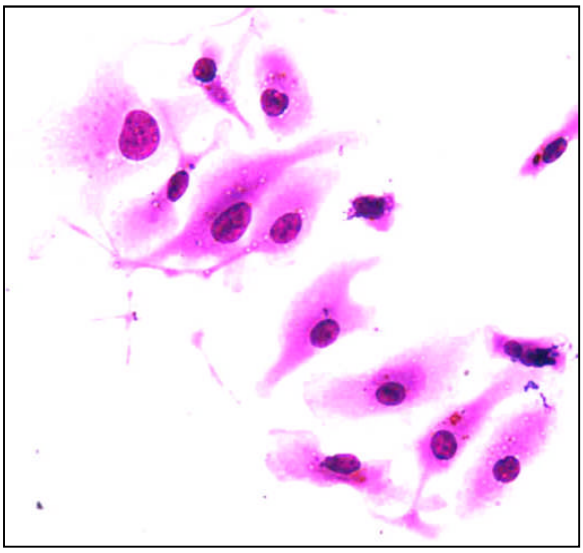

(ii)

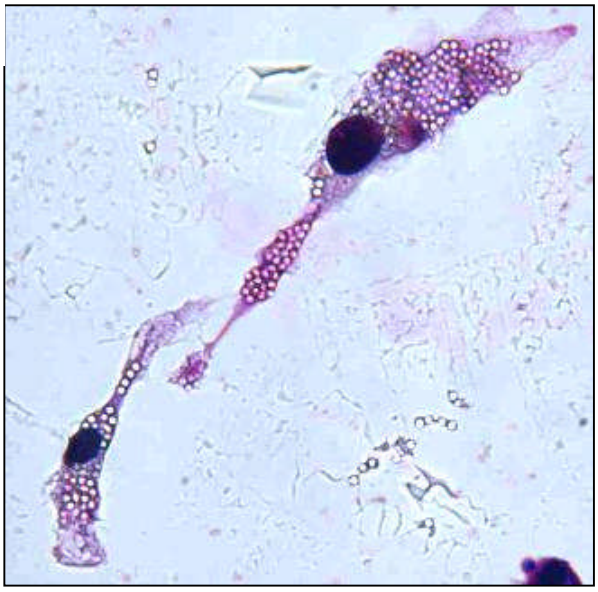

(iii)

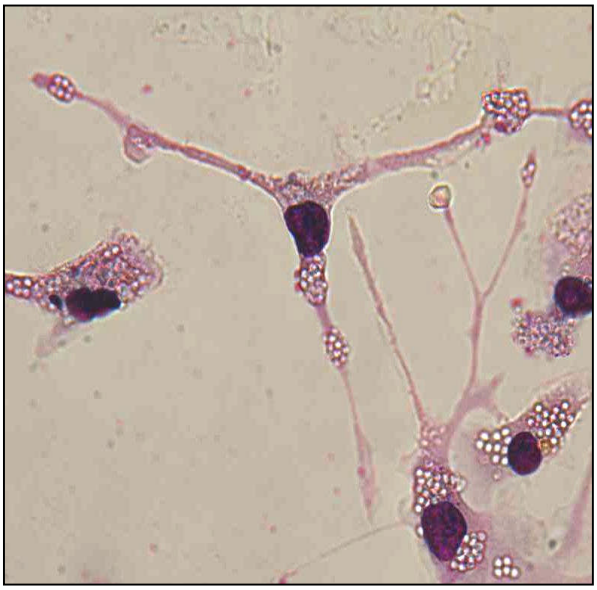

Figure 5-11 Photomicrographs of BMDM during the phagocytosis assay to illustrate the beads ingested by WT or mrp14-/- BMDMs

(i) WT cells (negative control) BMDMs have been incubated with unopsonised beads. (ii) WT BMDMs and (iii) mrp14-/- BMDMs have ingested the opsonised beads. The beads can then be counted once the cells have been fixed and stained.

5.4.6.2 Assessing FcR in WT and mrp14-/- macrophages

To understand why there may be a difference in phagocytosis between WT and mrp14-/- BMDM, unstimulated cells were assessed for expression of Fc receptors using an antibody to CD16/32. This antibody recognises both FcγIII and FcγII expressed on BMDMs. The cells at day 7 were incubated with CD16/32 PE antibody or isotype control antibody followed by cell fixation and analysis by flow cytometry. There were no differences between WT and mrp14-/- BMDMs with regards the percentage of positive gated cells or the mean fluorescent intensity (Mann-Whitney U-test). Each cell type was performed in triplicate.

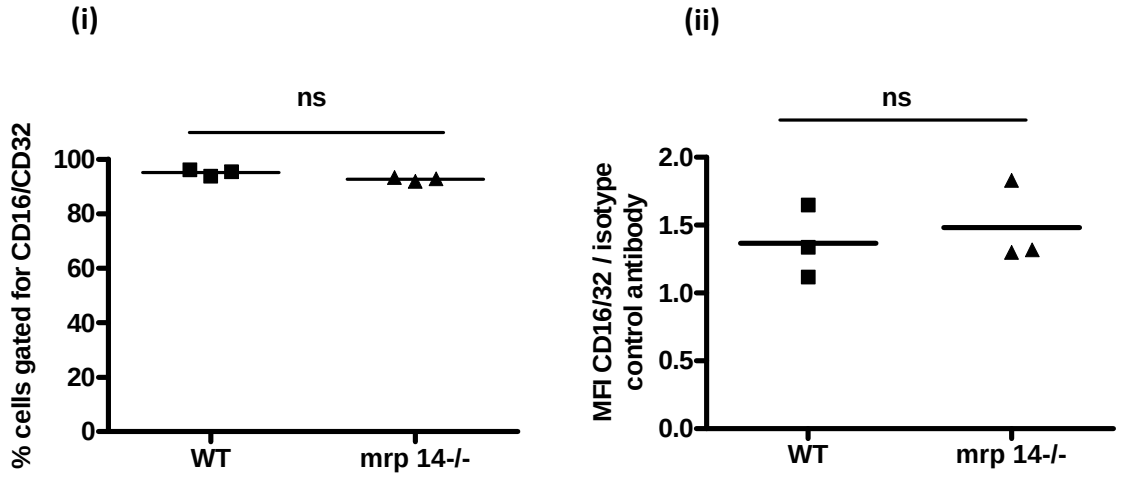

Figure 5-12 WT and mrp14-/- BMDMs demonstrate similar expression of CD16/32

(i) Demonstrates similar percentage of cells gated for CD16/32 in WT and mrp14-/-BMDMs, compared with isotype control PE antibody. (ii) Similar mean fluorescent intensity (MFI) by FACS for CD16/32 in WT and mrp14-/- BMDMs. Non-statistically significant differences between the 2 cell groups (Mann-Whitney U-test). Each experiment performed in triplicate.

5.4.7 Co-culture of endothelial cells with WT but not mrp14-/- BMDMs stimulates inflammatory cytokine production

Co-culture experiments were performed using murine wild-type endothelial cells (EC) and either wild-type or mrp14-/- BMDMs. EC ($3x10^5$) were used in triplicate. The cells were left in complete media for 2 days, followed by serum free media. Day 7 BMDMs were then added to the EC, at a density of $1x10^6$ cells per well. The cells were allowed to co-culture for 24 hours before the supernatants were collected and cytokine analysis performed by ELISA. The following groups were cultured;

- EC alone
- EC+WT BMDMs
- EC+mrp14-/-BMDMs
- WT BMDMs alone
- Mrp14-/- BMDMs alone

5.4.7.1 Endothelial cells co-cultured with mrp14-/- BMDM secrete less MCP-1 than endothelial cells co-cultured with WT BMDMs.

WT BMDMs and mrp14-/- BMDMs produced a small amount of MCP-1 (median values WT 843 pg/ml; mrp14-/- 942 pg/ml) when cultured alone with no significant differences between the WT and mrp14-/- BMDMs. Endothelial cells alone produced an increased amount of MCP-1, median 15340 pg/ml. This increased further with WT BMDMs co-culture median value of 29990pg/ml. Following incubation of endothelial cells with mrp14-/- BMDMs, the median amount of MCP-1 detected decreased to a similar value from endothelial cells alone (median 11849pg/ml). Using a one-way ANOVA to compare all the groups, there was a significant increase in MCP-1 following WT BMDMs co-culture with endothelial cells compared to WT BMDMs alone (One-way ANOVA $p<0.05$).

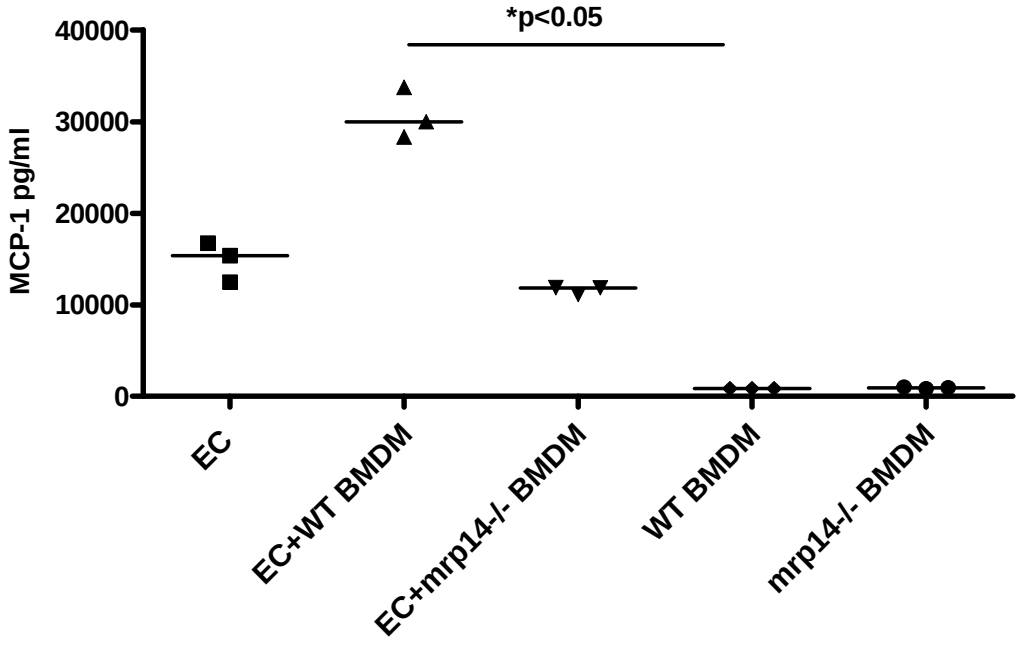

Figure 5-13 EC and WT BMDMs are pro-inflammatory unlike EC and mrp14-/- BMDMs

Graph to demonstrate MCP-1 production in EC-BMDM co-cultures (each condition is performed in triplicate). At baseline, little MCP-1 is produced by BMDMs. Following co-culture, mrp14-/- BMDM stimulate less increase in MCP-1 compared with WT BMDMs, ($p<0.05$)(One-way ANOVA). Line represents the median.

5.4.7.2 EC and mrp14-/- BMDM co-culture produce less IL-8 than EC and WT BMDM

Similar to the previous cytokine analysis, the unstimulated BMDM produced only small quantities of IL-8, as did the EC. There was a significant increase in IL-8 when EC and WT BMDMs were co-cultured (median 1000pg/ml [range 892.3-1000pg/ml) compared to cells alone ($p<0.05$)(One-way ANOVA). However, while co-culture of EC and mrp14-/- BMDM (median 445pg/ml [range 409-535.6]) was greater than the production by EC or mrp14-/- BMDMs alone, it was 50% less than that produced by the co-culture of ECs and WT BMDMs.

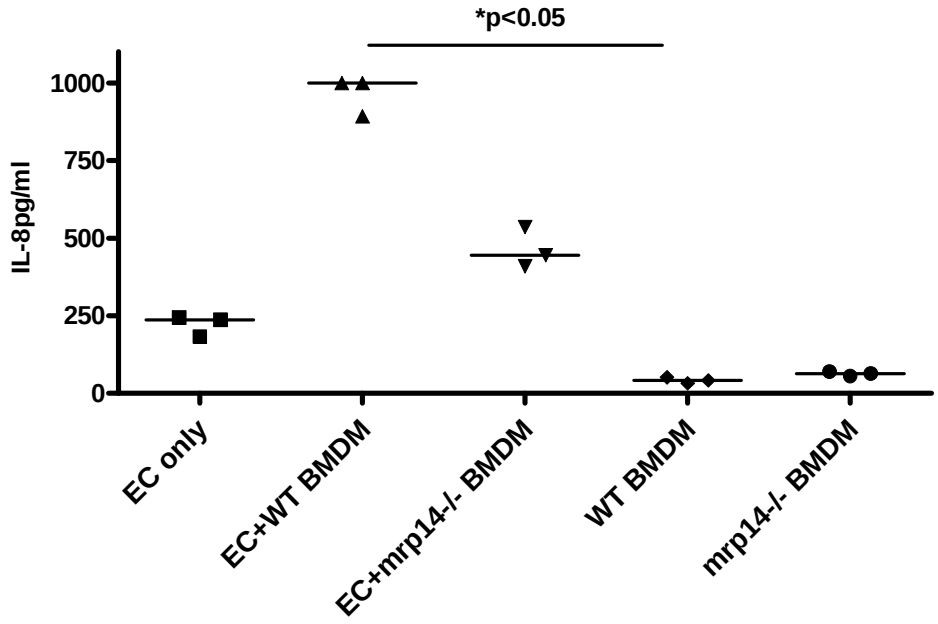

Figure 5-14 EC and WT BMDM co-cultures promote more IL-8 production than EC and mrp14-/- BMDM co-cultures

Graph to demonstrate the IL-8 production in EC-BMDM co-culture. Each condition performed in triplicate. Unstimulated WT and mrp14-/- BMDMs produce a small amount of IL-8. Following co-culture with EC, mrp14-/- BMDM produce some IL-8, however this is also almost half of that produced by WT BMDM-EC co-culture. Line represents the median.

5.4.7.3 EC -mrp14-/- BMDM co-culture produce less IL-6 than EC- WT BMDMs co-culture

The amount of IL-6 detected on ELISA was also investigated. Similar to MCP-1 and IL-8, the greatest increase in IL-6 was following incubation of EC and WT BMDMs (median 870.8pg/ml [range 807.5-980.7]), while EC and mrp14-/- co-culture produced a similar amount of IL-6 (median 181.8pg/ml {range 176.8-202.9pg/ml]) to the culture of mrp14-/- BMDMs alone (113.3pg/ml [range 107-125.6]. A significant increase in IL-6 was observed with incubation of EC and WT BMDMs ($p<0.05$)(1-way ANOVA) compared to endothelial cells alone (median 28.7pg/ml [range 28.3-31.8pg/ml)

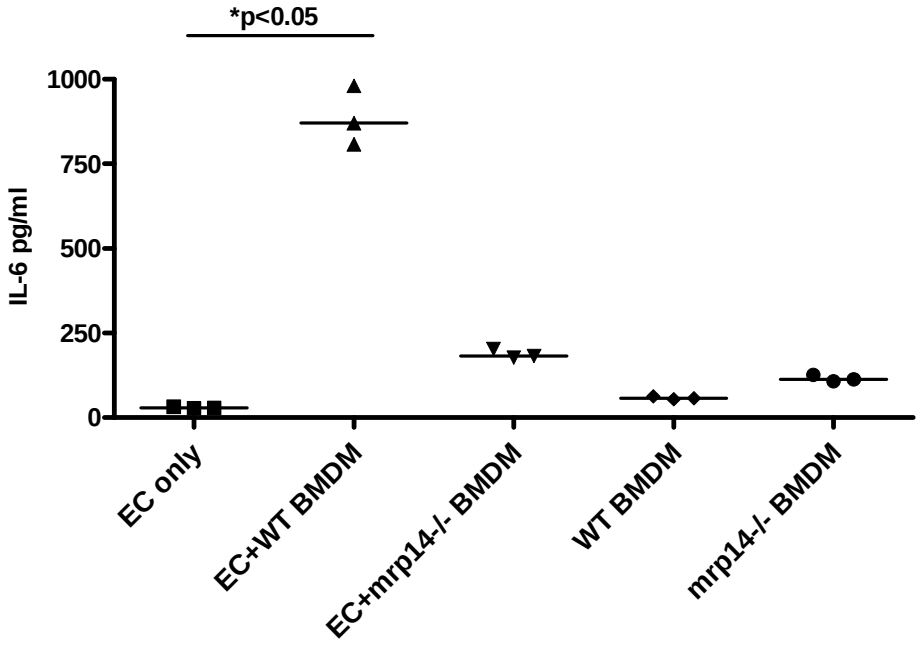

Figure 5-15 EC--WT BMDM co-culture produce increased amount of IL-6 compared to EC-mrp14-/- BMDM co-culture.

Endothelial cells incubated alone produced small quantities of IL-6, with WT and mrp14-/- BMDMs demonstrating a trend to increased IL-6 secretion (ns). There was a significant increase in IL-6 following the co-culture of endothelial cells and WT BMDMs compared with EC-mrp14-/- co-culture ($p<0.05$)(1-way ANOVA). Line represents the median. Each condition performed in triplicate.

5.4.8 S100A8/A9 has a pro-inflammatory effect on mesangial cells which is not mediated through TLR4

Mesangial cells are known to play an important role in nephrotoxic nephritis and are a key source of cytokine secretion. The effect of S100A8 and S100A8/A9 stimulation on mesangial cells was explored using WT, TLR4-deficient and mrp14-deficient mesangial cells to investigate whether TLR4 mediates the effect of S100 protein mediated stimulation. Mesangial cells (MC) were stimulated with S100A8 and S100A8/A9 at a concentration of 1μg/ml. Each condition was performed in triplicate using $7.8x10^5$ cells per condition. Following incubation of the MC with S100A8 or S100A8/A9, the supernatants were collected.

5.4.8.1 S100A8 and S100A8/A9 increase mesangial cell IL-8 secretion

Both S100A8 and S100A8/A9 had a pro-inflammatory effect on mesangial cells, but S100A8 had a greater effect than S100A8/A9. Using WT cells, compared to unstimulated MC, there was an increase in IL-8 secretion following stimulation with S100A8 of 1472pg/ml (range 998-2182). However, in TLR4-/- MC, S100A8 provoked a significantly lesser increase in IL-8 compared to unstimulated cells; median 27.45pg/ml (range 16.57-212.1pg/ml).

By contrast, S100A8/A9 stimulation resulted in similar increases of MC IL-8 in WT and TLR4-/- cells; WT median 376.3pg/ml (range 371.5-402.5pg/ml) and TLR4-/- median 254.3pg/ml (range 169.3-350.3pg/ml), p=ns.

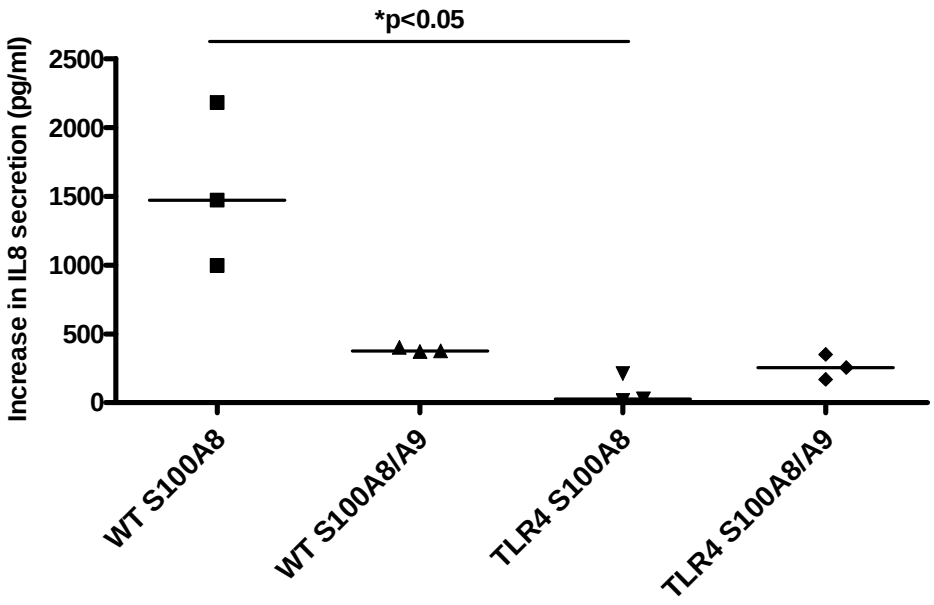

Figure 5-16 TLR4 mediates the pro-inflammatory effect of S100A8 but not S100A8/A9 on MC

(i) The graph demonstrates the increase in IL-8 compared to unstimulated cells (line at the median) when S100A8 is incubated with WT and TLR4-/- mesangial cells. There is a significant difference in IL-8 secretion between unstimulated WT and TLR4 mesangial cells ($p<0.05$)(One-way ANOVA). There is similar IL-8 secretion following stimulation with S100A8/A9, although the effect of S100A8/A9 is not as pro-inflammatory as the effect caused by S100A8. Each condition performed in triplicate.

5.4.8.2 S100A8 increases MCP-1 secretion by MC and is mediated through TLR4

S100A8 had a significant effect on MCP-1 secretion by WT mesangial cells resulting in a median increase (compared to unstimulated cells) of 1958pg/ml (range 1650-2629pg/ml), however, this increase in MCP-1 was significantly attenuated when TLR4-/- MCs were used, median 149pg/ml (range 0-239pg/ml). By contrast, the increase in MCP-1 was similar in WT and TLR4-/- MC after S100A8/A9 stimulation, WT MC median 436.6pg/ml (range 412.8-460pg/ml), and TLR4-/- MC median 400.3pg/ml (range 344.9-494.4pg/ml)(p=ns).

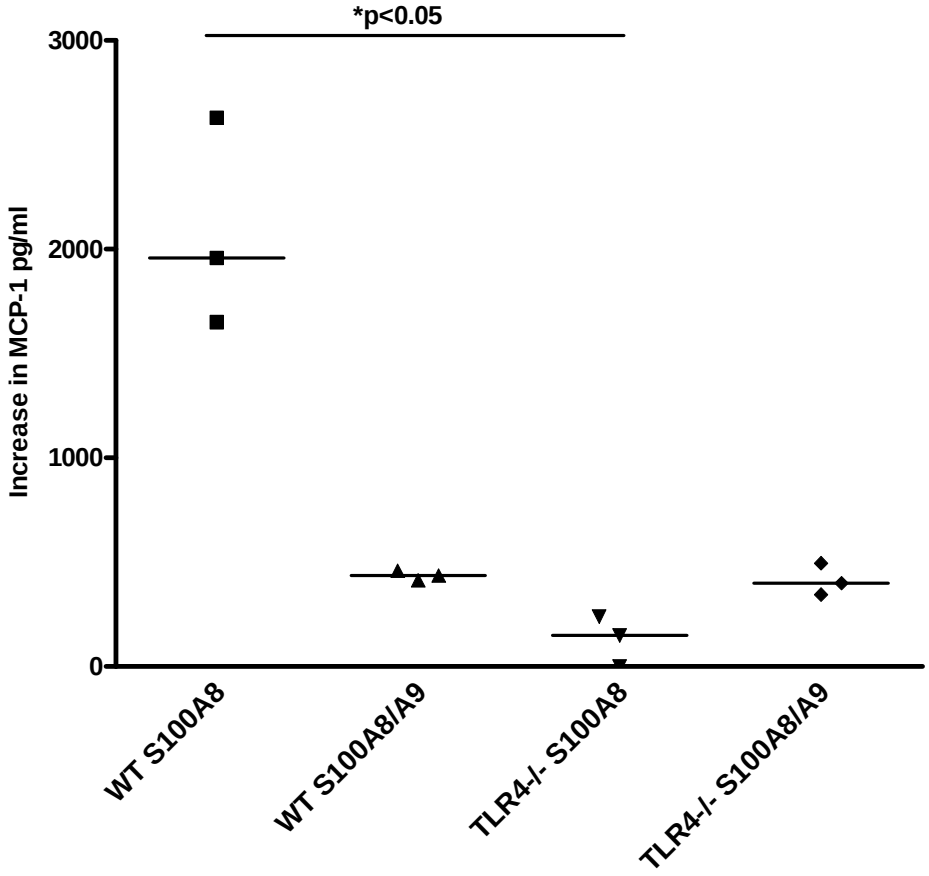

Figure 5-17 S100A8 induced-MCP-1 secretion by mesangial cells is mediated through TLR4.

The proinflammatory effect of S100A8/A9 was less than that of S100A8. S100A8 resulted in significantly more MCP-1 when WT MC were stimulated compared to TLR4-/- (One-way ANOVA $p<0.05$), while no difference was found between WT and TLR4-/- mesangial cells stimulated with S100A8/A9. Line represents the median. Each condition performed in triplicate.

5.4.8.3 S100A8 stimulates IL-6 secretion in MC through TLR4 unlike S100A8/A9

Stimulation of WT MC with S100A8 resulted in a greater IL-6 secretion compared to stimulation with S100A8/A9 (median 13.54pg/ml [range 12.97-14.69pg/ml] vs 6.135pg/ml [range 5.113-7.95pg/ml] respectively). This effect was predominantly mediated through TLR4 as TLR4-/- MCs produced significantly less IL-6 following S100A8 stimulation (0 pg/ml [range 0-7.28pg/ml]), while there was no decrease in IL-6 following S100A8/A9 stimulation of TLR4-/- MC (7.624pg/ml [range 0-9.45pg/ml]). The results show a similar trend to the previous cytokines, although using One-way ANOVA, the results were not significant. However, comparing IL6 secretion by WT and TLR4-/- cells following S100A8 stimulation, the difference is significant ($p<0.05$)(Unpaired t-test).

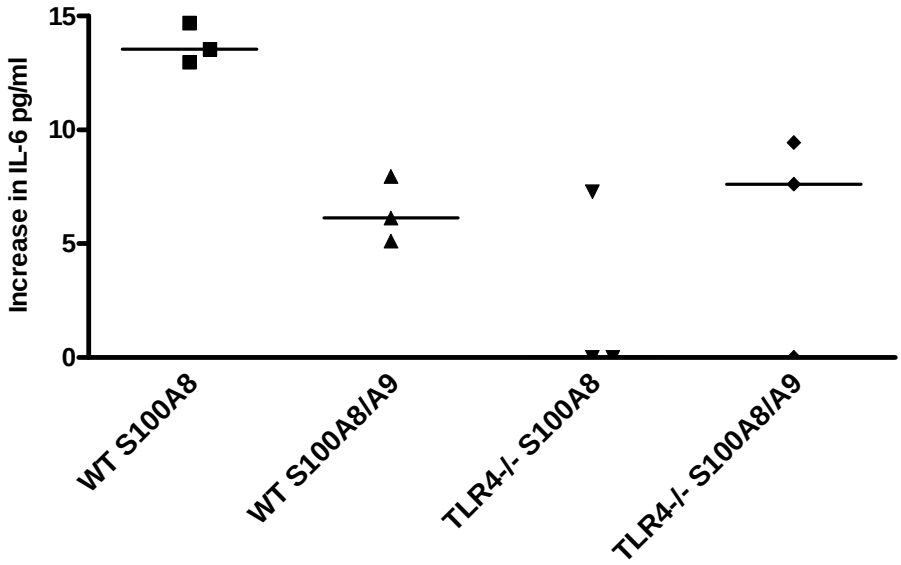

Figure 5-18 WT mesangial cells produce IL-6 when stimulated by S100A8 and S100A8/A9 with the former mediated through TLR4

The graph demonstrates that MC stimulated by S100A8 and S100A8/A9 produce IL-6, which for S100A8 stimulated MC is mediated though TLR4, unlike S100A8/A9. Line represents the median. Each condition performed in triplicate. Differences between the groups were not statistically significant.

5.4.9 The response of mrp14-/- mesangial cells

Since mrp14-/- BMDMs had a significantly reduced pro-inflammatory response to stimulation with S100A8/A9, the response of mrp14-/- mesangial cells was also analysed.

5.4.9.1 WT and mrp14-/- mesangial cells secrete IL-8 after stimulation with S100 proteins

In 2 separate experiments, the response of MC following stimulation was investigated. $3x10^5$ WT mesangial cells per well were used per well in a 6 well plate. Each condition was performed in triplicate. $8x10^5$ mrp14-/- cells were used in separate experiments. Mesangial cells were also stimulated with the pro-inflammatory cytokine, TNFα, which was used to then compare the response to S100A8/A9. To enable a comparison between the WT and mrp14-/- mesangial cells, the results were normalised to cytokine secretion per $1x10^5$.

WT mesangial cells stimulated with TNFα (10ng/ml) produced IL-8 (compared to unstimulated cells/per $1x10^5$cells) with a median increase of 351.5pg/ml (range 325.5-372.9), while following stimulation with S100A8/A9 the median increase was 267.8pg/ml (range 230.5-288.1). Mrp14-/- mesangial cells (normalised to 100,000 cells) had a significantly decreased response to TNF-α and S100A8/A9 stimulation, with a median increase in IL-8 production of 137.6pg/ml (range 125.5-146.5) and 81.28pgml (range 67.62-87.87pg/ml) respectively.

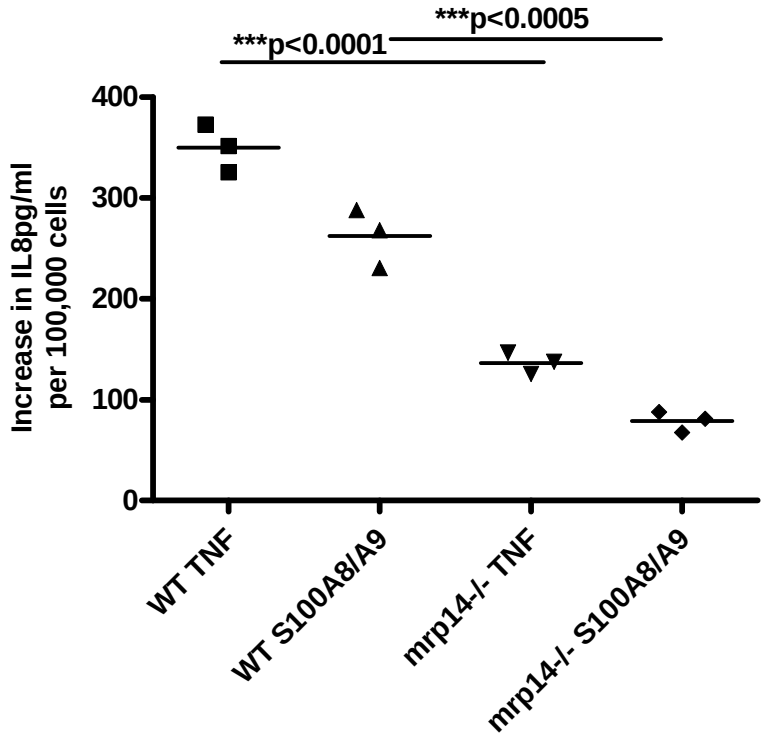

Figure 5-19 Mrp14-/- mesangial cells produce less IL-8 in response to S100A8/A9 and TNF-α than WT mesangial cells

The graph demonstrates the increase in IL-8 secretion by WT and mrp14-/- mesangial cells following stimulation with S100A8/A9 and TNF-α. Each condition was performed in triplicate. There was a significant difference in the amount of IL-8 produced between WT cells stimulated with TNF compared to mrp14-/- cells stimulated with TNF; as well as WT cells stimulated with S100A8/A9 compared to mrp14-/- stimulated with S100A8/A9 (unpaired t-test).

5.4.9.2 Mrp14-/- mesangial cells produce less MCP-1 than WT mesangial cells after S100A8/A9 stimulation

MCP-1 was also measured after stimulation of the mesangial cells with TNF-α and S100A8/A9. Again, the results have been normalised to cytokine production per $1x10^5$cells to allow a comparison between WT and mrp14-/- mesangial cells. The median MCP-1 produced by WT mesangial cells in response to S100A8/A9 was median 403.7pg/ml (range 311.2-491.5pg/ml). Mrp14-/- MC secreted significantly less MCP-1 following stimulation with S100A8/A9, median 103pg.ml (range 99.4-103.9)($p<0.005$)(unpaired t-test).

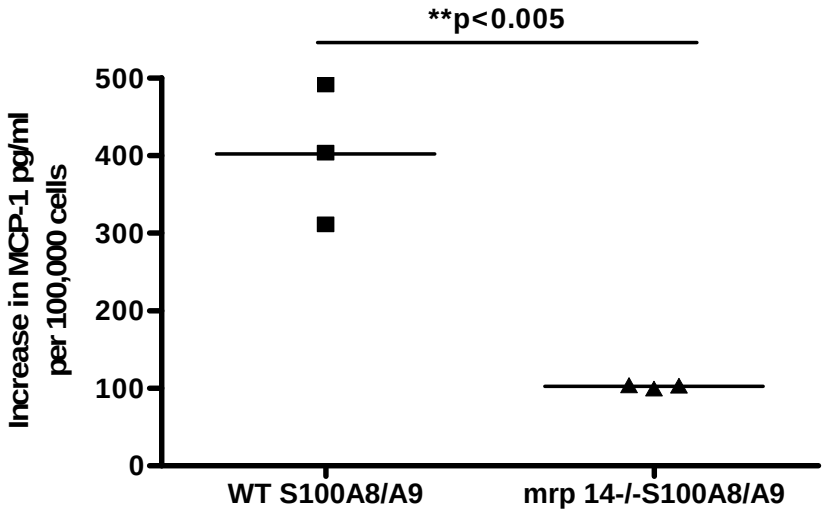

Figure 5-20 Mrp14-/- mesangial cells produce less MCP-1 in response to S100A8/A9 stimulation than WT mesangial cells

The graph above demonstrates the pro-inflammatory effect of S100A8/A9 on mrp14-/- and WT mesangial cells, with significantly less MCP-1 produced by mrp14-/- mesangial cells. Line represents the median. Each condition performed in triplicate.

5.4.9.3 Mrp14-/- mesangial cells secrete more IL-6 than WT mesangial cells

WT and mrp14-/- cells were analysed for the amount of IL-6 produced following stimulation with TNF-α, S100A8/A9 and a combination of TNF-α and S100A8/A9. As different numbers of WT and mrp14-/- mesangial cells were included, the results were again normalised to $1x10^5$. Mrp14-/- mesangial cells, in contrast to mrp14-/- BMDMs, produced a greater amount of IL-6 than WT mesangial cells. In response to TNF-α, WT cells produced a median of 1.12pg/ml (range 0.26-2.1). In response to S100A8/A9, a similar amount of IL-6 was detected, median of 0 (range 0-2.59). This increased following stimulation with TNF-α and S100A8/A9 to a median of 14.78pg/ml (range 11.26-15.34).

Mrp14-/- mesangial cells produced a small amount of IL-6 following stimulation with TNF-α, median 0pg/ml (range 0-1.53). This increased to 6.76pg/ml (range 6.7-14.29pg/ml) following stimulation with S100A8/A9, and increased further to a median of 25.91pg/ml (range 24.26-28.12) following stimulation with TNF-α and S100A8/A9. There was significantly more IL-6 secreted by mrp14-/- than by WT mesangial cells following stimulation with S100A8/A9 ($p<0.05$)(unpaired t-test), and significantly more IL-6 following stimulation of mrp14-/- cells with TNF-α and S100A8/A9 than WT mesangial cells ($p<0.005$)(unpaired t-test).

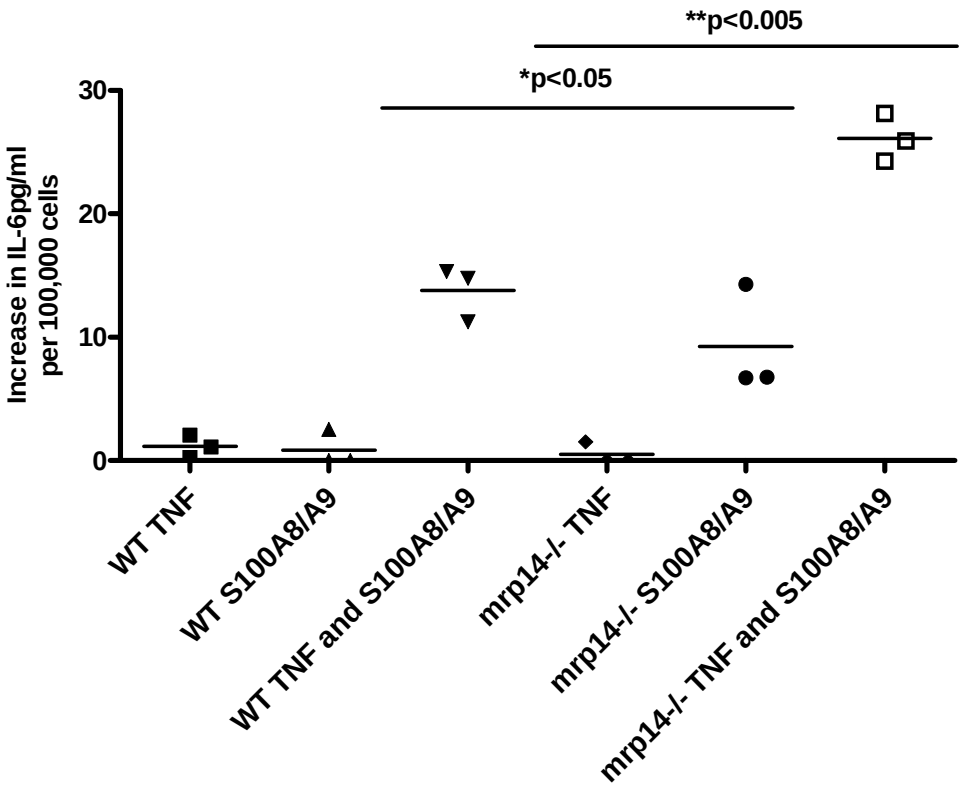

Figure 5-21 WT and mrp14-/- mesangial cells produce maximal IL-6 after stimulation with TNF-α and S100A8/A9.

Demonstrates a small increase in IL-6 secretion following stimulation of WT mesangial cells with TNF-α, with a further increase following stimulation with TNF-α/S100A8/A9. Mrp14-/- mesangial cells produce very little IL-6 in response to TNF. However, mrp14-/- MC produce significantly more IL-6 when stimulated with S100A8/A9 and TNF-α/S100A8A9 than WT mesangial cells ($p<0.05$)($p<0.005$)(unpaired t-test) respectively. Each condition performed in triplicate.

5.5 Discussion

In this chapter, I have investigated the in-vitro effects of S100A8 and S100A8/A9 on different primary renal cell lines and on bone marrow derived macrophages. These cell lines were isolated from murine kidney and murine bone marrow, and are known to play key roles in nephrotoxic nephritis and glomerulonephritis.

In agreement with published work, the interaction between these S100 proteins and TLR4 on BMDMs seems to be critical. Incubation of TNF-α had the expected pro-inflammatory effect on BMDMs, which was similar in WT BMDMs and TLR4-/- BMDMs with respect to IL-8 secretion. However, WT BMDMs had a significant increase in IL-8 secretion following stimulation with S100A8 and S100A8/A9, an effect which was totally abrogated in TLR4-/- BMDMs, demonstrating the critical requirement for this receptor on macrophages for the S100 proteins to exert their autocrine proinflammatory effect. Although S100A8/A9 had a less pronounced proinflammatory effect than S100A8 with regard to IL-8 secretion, there was still a significant difference between the amount of IL-8 secreted when S100A8/A9 was incubated with WT and TLR4-/- bone marrow cells. Analysis of TNF-α secretion by BMDMs also elicited similar results, with no TNF-α being detectable following stimulation of TLR4-/- bone marrow cells, and a significant increase when WT BMDMs were stimulated with S100A8 and S100A8/A9. The experiments described above would be consistent with the hypothesis that the S100 proteins, once bound to TLR4, induces activation of a signal transduction cascade which results in the transcription of several important pro-inflammatory cytokines including IL-8 and TNF-α.

Following the comparison between WT and TLR4-/- BMDMs, WT and mrp14-/- BMDMs were subsequently compared. Mrp14-/- phagocytes have a slight abnormality of calcium signalling compared to WT cells, but otherwise the myelopoietic potential of mrp14-/- bone marrow is normal {McNeill, 2007 #5654}(Manitz, Horst et al. 2003). Previous studies have shown crucial differences between mrp14-/- and WT BMDMs with respect to their inflammatory response. Unstimulated, WT and mrp14-/- demonstrate no major differences in global gene expression as assessed by an Affymetrix gene chip microarray. However, following the administration of LPS, the expression of many genes involved in macrophage activation was reduced in mrp14-/- bone marrow cells (BMCs) compared to WT BMCs (Vogl,

Tenbrock et al. 2007). Extracellular S100A8/A9 added to mrp14-/- LPS-stimulated BMCs resulted in a dose dependent increase in TNF-α, demonstrating that the addition of S100A8/A9 was able to compensate for the blunted LPS response of mrp14-/- cells. This study also demonstrated that the S100A8/A9 complex was active only with LPS, whereas S100A8 was active alone on BMCs, and has the ability to induce the production of TNF-α without the addition of LPS. These data suggest that the differences in S100A8 and the heterodimer may be due to the binding of S100A8 to S100A9 preventing S100A8-dependent stimulation of TLR4. Additionally, the S100A8/A9 complex appears to require a secondary stimulus (such as LPS) to have a pro-inflammatory effect on BMCs (Vogl, Tenbrock et al. 2007). Some of the results in this chapter differ somewhat from these published findings. In keeping with the published results S100A8 alone was able to have a pro-inflammatory effect on BMDMs from WT mice. However, in this chapter, the administration of S100A8/A9 to WT BMDMs was able to have a similar, although less pronounced effect compared to that of S100A8, with respect to the secretion of TNF-α, IL-8 and IL-6. Additionally, I found that there is a blunted pro-inflammatory response of mrp14-/- BMDM upon the addition of the S100A8/A9 heterodimeric complex, while previous work demonstrated that addition of S100A8/A9 to mrp14-/- BMCs was able to reverse the non-inflammatory phenotype. There are a few differences in the methods used however between my work and the published data. The paper by Vogl et al, used bone marrow cells which had been isolated from murine femurs and tibias and following red cell lysis were cultured in media. By contrast, my experiments used cells isolated following bone marrow cell extraction and grown in L929 (macrophage) conditioned media to allow the proliferation and differentiation of the myeloid progenitor cells into macrophages. Also, TNF-α secretion following WT BMC stimulation with LPS or S100A8 or S100A8/A9 was analysed following just 4 hours of incubation by Vogl et al. The addition of extracellular S100A8/A9 on mrp14-/- cells was followed by TNF-α analysis after 9 hours. In the experiments in this chapter, supernatants were harvested following an overnight incubation period. It is possible that this could account for some differences in the inflammatory response of the mrp14-/- or WT BMCs. Importantly, the source of recombinant S100A8 and S100A8/A9 was similar, a kind gift from T. Vogl, so this is also unlikely to be responsible for any differences in the response of cells to the effects of these molecules.

The BMDM experiments suggest that S100A8/A9 serves to amplify the inflammatory response, as a lack of endogenous S100A8/A9 resulted in a decreased pro-inflammatory response in macrophages, cells that usually secrete S100A8/A9 in response to pro-inflammatory signals. This is supported by in-vivo murine experiments. Using an endotoxic shock model, mrp14-/- mice have a significantly longer survival than WT mice, with significantly less TNF-α and IL-6 production. After administration of S100A8/A9 this protection was lost, with the resultant decrease in survival that was comparable to that of WT mice (Vogl, Tenbrock et al. 2007).

Previous studies have investigated the pro-inflammatory effect of extracellular S100A8/A9 on the endothelium. Since endothelial cell-leukocyte interactions are crucial in both human and experimental glomerulonephritis, the interaction between endothelial cells and WT and mrp14-/- BMDMs was investigated. These experiments consistently demonstrated that unstimulated BMDMs alone had little pro-inflammatory activity. Endothelial cells isolated from the kidney secreted some cytokines at rest, however, the co-culture of WT BMDMs and endothelial cells consistently resulted in significant cytokine production. The culture of mrp14-/- BMDMs with endothelial cells also consistently resulted in less cytokine production than WT BMDMs and ECs. This difference is consistent with the idea that S100A8/A9 acts to amplify the inflammatory responses. Once macrophages have been activated, the complex is released and is able to act in an autocrine manner on macrophages and in a paracrine manner on endothelial cells resulting in a positive inflammatory loop with the production and secretion of cytokines. Macrophages which lack S100A8/A9 are therefore unable to contribute to this amplification loop and have less cytokine production in co-culture experiments. This amplification loop could be further amplified in vivo within the kidney by production of S100A8 and S100A9 by various other cell types including fibroblasts and renal epithelial cells. A similar amplification loop to the one described above, has been suggested to play a role in the pathogenesis of rheumatoid arthritis. S100A8 and S100A9 released during synovial inflammation may then influence the function of osteoclasts resulting in bony erosions and remodelling seen in inflammatory arthritis. This hypothesis is further supported by the effect of a monoclonal antibody to S100A9 resulting in decreased joint injury in the murine arthritis model as well as a decrease in local and systemic cytokine release (Cesaro, Anceriz et al. 2012). As well as macrophage-derived

S100A8/A9 having a role in mediating inflammation and joint destruction in the antigen induced arthritis model, chondrocytes have been shown to express these proteins. Pro-inflammatory cytokine stimulation of a murine chondrocyte cell line resulted in detectable S100A8 and S100A9 mRNA as well as protein, therefore establishing a positive feedback mechanism by which S100A8 proceeded to stimulate the secretion of pro-inflammatory cytokines, such as IL-6, from the same chondrocyte cell line as well as the activation of the transcription factor NF-κB. These pro-inflammatory effects were demonstrated to occur despite low expression of the known S100A8/A9 receptor TLR4, and in the presence of an anti-RAGE antibody, implicating another unknown receptor in mediating the pro-inflammatory effects of S100A8 (van Lent, Grevers et al. 2008).

Mesangial cells stimulated with S100A8 and S100A8/A9 resulted in the production of pro-inflammatory cytokines. As described above, chondrocytes had detectable expression of IL-6 mRNA by RT-PCR when stimulated with S100A8, without detection of other pro-inflammatory cytokines such as TNF-α and IL-1 (van Lent, Grevers et al. 2008). The mesangial cells when stimulated with S100A8 and S100A8/A9 had a more pronounced pro-inflammatory effect than that described for chondrocytes. IL-6 secretion was modest in the mesangial cells, but greater amounts of MCP-1 and IL-8 were secreted. These cytokines are involved in further macrophage and neutrophil recruitment to the glomerulus. S100A8 mediated its effects on mesangial cells through TLR4, supported by data demonstrating that pro-inflammatory cytokine secretion was significantly attenuated in TLR4-/- mesangial cells. S100A8/A9 had a more modest pro-inflammatory effect, but was still able to generate cytokines in the absence of a secondary stimulus, with similar cytokine levels in WT and TLR4-/- mesangial cells, suggesting that other receptors are involved in mediating this effect. Possible candidates include RAGE, as well as other receptors containing carboxylated glycans.

Macrophages containing S100A8/A9 are present in both human and experimental glomerulonephritis, and these data suggest that once secreted, the heterodimer can exert a stimulatory, proinflammatory effect on mesangial and endothelial cells while also having an autocrine effect on macrophages.

Similar to mrp14-/- BMDMs, mrp14-/- mesangial cells demonstrated significantly less pro-inflammatory response to stimulation with S100A8 or S100A8/A9. Stimulation with S100A8 generally resulted in a profound inflammatory response, with the results often higher than the highest standard of the ELISA standard curve, despite several attempts to optimise the dilution (therefore results not included). A direct comparison between the responses of WT and mrp14-/- mesangial cells was permitted by correcting the results to cytokine secretion per $1x10^5$ cells. The behaviour of mrp14-/- mesangial cells has not previously been described. These results demonstrate that mrp14-/- MCs have the capacity to react to pro-inflammatory stimuli such as S100A8/A9 and to produce pro-inflammatory cytokines, but to a lesser amount than the WT mesangial cells- with the exception of IL-6. S100A8/A9 has a role in glomerular inflammation as mesangial cells respond and secrete cytokines. These results suggest S100A8/A9 stimulates mesangial cells through TLR4 dependent and independent mechanisms.

Summary:

- S100A8 and S100A8/A9 induces the production and secretion of pro-inflammatory cytokines by BMDMs which is mediated through TLR4.
- Mrp14-/- BMDMs produce significantly less pro-inflammatory cytokines than WT BMDMs suggesting that endogenous S100A8/A9 production is necessary to amplify the pro-inflammatory response.
- Mrp14-/- demonstrate less phagocytosis that WT BMDMs despite a similar expression of activatory Fc-receptors.
- Endothelial cells co-cultured with WT BMDMs results in significantly higher levels of pro-inflammatory cytokines than EC co-cultured with mrp14-/- demonstrating the autocrine and paracrine effect of S100A8/A9 secreted by BMDMs.
- S100A8/A9 stimulates the production of pro-inflammatory cytokines by mesangial cells in a TLR4 independent effect, unlike stimulation by S100A8, with mrp14-/- mesangial cells secreting less cytokines in response to stimulation than WT mesangial cells, except IL-6 secretion.

Chapter 6 Discussion

6.1. Summary of results

Chapter 3 explored the role of S100A8/A9 in human glomerulonephritis. I demonstrated the presence of S100A8/A9 expressing cells in the renal biopsies of patients with ANCA associated glomerulonephritis, and that the presence of these cells correlates with acute, inflammatory lesions while they are absent in the sclerotic predominant GN. Additionally, there was a dense infiltrate of S100A8/A9 positive cells around inflamed blood vessels within the kidney. Patients with active AAV had elevated serum levels of calprotectin, and although levels decreased during disease remission, they did not normalise. Those patients with non-renal involvement, from the NORAM trial, had lower levels than those with renal involvement. The patients in this cohort who subsequently relapsed demonstrated significantly higher levels during the early time-points after the initiation of immunosuppressive therapy, suggesting that serum calprotectin may be a useful biomarker for disease relapse in this cohort of patients with limited disease. Similar to the serum calprotectin levels, patients with both active and inactive disease had detectable expression of calprotectin on the cell surface of monocytes and neutrophils, which although was less during disease remission, did not reach the same level as healthy controls. Human IgG, isolated from healthy controls, as well as from patients with high titres of PR3-ANCA and MPO-ANCA IgG, were able to upregulate monocyte expression of calprotectin, but this was clearly not ANCA specific.

Chapter 4 investigated the role of S100A8/A9 during nephrotoxic nephritis. Mrp14-/- mice demonstrated significantly less renal injury and less leukocyte infiltration than WT mice, an effect which was reversed by the addition of high dose LPS during disease progression. These effects occurred despite similar sheep and mouse IgG glomerular deposition and a similar antigen-specific total IgG response. The non-accelerated model demonstrated that WT and mrp14-/- mice have a similar early response in terms of glomerular neutrophil infiltration, suggesting that differences in disease relate more to macrophage recruitment and activation at later time points. The bone marrow transplant experiment illustrates that

total deficiency of S100A8/A9 is necessary for protection from glomerulonephritis, although I have not conclusively demonstrated which intrinsic (radioresistant) cell is required to produce S100A8/A9 and maintain disease susceptibility. A control cohort of mrp14-/- to mrp14-/- transplant mice would have been useful to compare the other three groups to and confirm disease protection.

Chapter 5 explored the in-vitro pro-inflammatory effects of S100A8/A9 and S100A8 on BMDMs and mesangial cells. The pro-inflammatory effect on BMDMs was mediated through TLR4, however on mesangial cells the effect of S100A8/A9 was TLR4 independent, as opposed to the effect of S100A8 which was predominantly mediated through TLR4. Mrp14-/- BMDMs had a blunted response to the proinflammatory effects of S100A8/A9, with significantly less secretion of cytokines known to play a role in renal inflammation. The co-culture of WT endothelial cells and WT BMDMs resulted in the detection of significant production of cytokines as opposed to that of WT endothelial cells and mrp14-/- BMDMs, which was a significantly less inflammatory combination. Mrp14-/- macrophages also demonstrate less phagocytic ability despite similar expression of Fc-γ receptors. Lastly, stimulation of mrp14-/- mesangial cells resulted in the production of less cytokines than WT mesangial cells, similar to the response of mrp14-/- BMDMs. S100A8/A9 had a pro-inflammatory effect on WT mesangial cells, although this effect was not mediated exclusively thought TLR4. This suggests that intrinsic production of S100A8/A9 may have a role in the generation of a mesangial cell inflammatory response.

6.2. Thesis limitations

6.2.1. Limitation of using mrp14-/- mice

Mice which either have a gene deleted, or over-expressed, have proven to be a very valuable tool in the investigation of disease. The deletion of S100A8 (mrp 8) results in embryonic death, a not uncommon occurrence in the generation of transgenic mice. Therefore, using this approach it is not possible to investigate the role of S100A8 in nephrotoxic nephritis independent to that of S100A9. However, deletion of mrp14-/-

(S100A9) does result in complete absence of both proteins due to degradation of S100A8 in the absence of its binding partner, S100A9. The mice were a kind gift from Professor Ivars, who has provided the mice for many of the published work on S100A8/A9.

However, the deletion of genes may have some undesired effects. Mrp14-/- mice don't have an obvious phenotype, with normal growth and development occurring. However, the result of gene deletion may have subtle developmental affects on the mouse and may affect their response in NTN, independent of the gene deleted. Additionally, undefined salvage pathways may exist which subsequently impact on disease susceptibility.

Mrp14-/- mice were generated using the embryonic stem cell line derived from 129/Ola mice which were subsequently injected into the blastocysts of C57BL/6 mice (Manitz, Horst et al. 2003). However, the 129/Ola is a different strain of mouse to the C57BL/6, and despite backcrossing for several generations, the knock-out mice may not be completely genetically similar to the wild-type control C57BL/6 mice used for experiments. Additionally, by deleting the gene of interest, there may be an effect on genes that are nearby in the genome. The strain of the mouse also has several effects, with NTN in the C57BL/6 being a Th1 driven disease. It would have been more accurate to have used littermate mice that are the offspring of mice heterozygous for the mrp14-/- deletion, therefore eliminating minor genetic differences between totally unrelated C57BL/6 wild-type controls. This was not done in this thesis due to difficulties obtaining mice homozygous for the mutation, as well as generating wild-type mice from heterozygous parents with respect to the experiments including mice of a similar age and sex.

6.2.2. Limitations of the animal model used

The model used in this thesis is the nephrotoxic nephritis animal model. This is not a vasculitis model, but instead a model of immune-mediated glomerulonephritis characterised by macrophage and T cell infiltration and glomerular thrombosis. There were not many glomerular crescents in our experimental mice; instead the histology was dominated by glomerular thrombosis, which is in contrast to human disease of AAV. Additionally, NTN is characterised by variation within the animal groups. Relatively large numbers of animals are needed to see an overall effect. This variation can partly be

explained by several different steps required to induce disease which may have some inter-mouse variability, for example the pre-immunisation and the injection of NTS may differ in the amount administered by more than 1 operator. However, the mice were all housed under the same conditions, and injected with the same batch of sheep IgG, CFA and NTS- which was prepared at the same time, by the same single operator. Despite attempts to be as accurate as possible, there still remains a difference in disease susceptibility within the same experimental group. Therefore, when possible, the groups were combined to investigate if there was an overall significant effect. This combination of animals and the resultant increase in animal numbers, allowed analysis of various disease parameters, which had previously been a trend when analysing smaller groups, to then became statistically significant. However, this model is less labour-intensive than some of the vasculitis animal models and is commonly used to investigate the pathogenesis of glomerulonephritis.

6.3. Hypothesis of the role of S100A8/A9 in human and experimental glomerulonephritis

The data is this thesis suggests that S100A8/A9 has a role in both human and experimental GN. I initially demonstrated that patients with focal and crescentic GN had an infiltrate of S100A8/A9 positive cells within the glomeruli with active lesions and in the blood vessels. The positive cells represent monocytes and infiltrating macrophages recruited from the circulation. Previous work has demonstrated that the heterodimer is down-regulated and absent from more chronic lesions, therefore it is not surprising that patients with a sclerotic predominant GN have an absence of cells expressing S100A8/A9. This work has illustrated that different phenotypes of macrophages exist, with S100A8/A9 representing the pro-inflammatory infiltrating macrophage, the presence of which correlates with the response to immunosuppressive therapy.

Patients with AAV had very high levels of serum S100A8/A9, with detectable surface expression on a significant proportion of neutrophils and monocytes. The source of the serum levels has presumed to be from monocytes and especially neutrophils due to the abundant constitutive expression of S100A8/A9 in the myeloid cell. I was unable to

demonstrate that human endothelial cells can be stimulated to produce the heterodimer. In the environment of high levels of IgG, for example MPO-ANCA IgG or PR3-ANCA IgG, S100A8/A9 intracellular expression can be increased. This effect is not specific to ANCA IgG, as IgG isolated from the serum of healthy controls had a similar effect. However, increased serum IgG may then contribute to inflammation by increasing the intracellular expression of S100A8/A9 in monocytes. The human work demonstrated the presence of S100A8/A9 during disease, but it's the animal work which has provided evidence for S100A8/A9 having a role in the inflammatory response rather than just being a disease biomarker.

The nephrotoxic nephritis experiments demonstrated that mrp14-/- mice are protected from severe renal disease. This work provided evidence that S100A8/A9 has an active role in the pathogenesis of GN. This protection was overcome by the administration of high dose LPS.

The pathological role of S100A8/A9 can be divided into the autocrine and paracrine actions of this complex as well as the cells involved. The murine in-vitro work demonstrated that BMDMs respond to S100A8/A9 through TLR4, resulting in the production and secretion of TNF-α, IL-6 and IL-8. Additionally, the combination of macrophages and endothelial cells is very pro-inflammatory in contrast to mrp14-/- BMDMs and endothelial cells, demonstrating that S100A8/A9 secreted from BMDMs has an inflammatory effect on both cell types. S100A8/A9 can then amplify the inflammatory response- this is supported by the resistance of mrp14-/- BMDMs to the pro-inflammatory effects of S100A8/A9, which resulted in very little cytokine secretion. A further protective effect of mrp14-/- could be due to the decreased phagocytosis ability of mrp14-/- macrophages. Mesangial cells are also responsive to the pro-inflammatory effects of S100A8/A9. The pro-inflammatory effects of S100A8 are mediated through TLR4 on mesangial cells however; S100A8/A9 has a TLR4 independent effect on mesangial cells, resulting in the production of MCP-1, IL-8 and IL-6. Within the inflammed glomerulus, S100A8/A9 may be secreted by macrophages, which then stimulate the production of inflammatory cytokines by mesangial cells, endothelial cells and also by macrophages, therefore demonstrating that both bone marrow derived cells and intrinsic renal cells play a role in the amplification of S100A8/A9 secreted within an inflammed glomerulus.

The cytokines secreted following S100A8/A9 stimulation of intrinsic renal cells and infiltrating leucocytes have several pathophysiological effects which are implicated in the pathogenesis of AAV and glomerulonephritis. IL-6 is a cytokine with multiple effects. Soluble IL-6R has the ability to stimulate mononuclear cell recruitment and to influence T-cell differentiation towards pro-inflammatory T-cells. IL-6 can also induce B-cell differentiation into B cells producing immunoglobulin. In combination with TGF-β, IL-6 is necessary for the differentiation of CD4+ T cells into IL-17-secreting T-cells (Th17 cells). Additionally, IL-6 has the ability to inhibit the formation of Tregs and to induce the production of cytotoxic T cells by CD8+ cells. A monoclonal antibody against IL-6R has been used in the treatment of many inflammatory diseases such as rheumatoid arthritis (Tanaka, Narazaki et al. 2012). Additionally, there is a case report of the use of an IL-6R antibody in the treatment of MPO-ANCA vasculitis (Sumida, Ubara et al. 2011).

IL-8 production by TNF-α stimulated endothelial cells has a significant role in neutrophil migration, and recruitment of leukocytes to the site of inflammation (Smart and Casale 1994). Additionally, IL-8 acts with TNF-α to result in neutrophil degranulation, and the resultant expression of PR3 on the neutrophil membrane, therefore demonstrating the crucial role this cytokine has in the pathogenesis of AAV (Csernok, Ernst et al. 1994). PR3 also has the ability to enhance production of IL-8 by endothelial cells (Berger, Seelen et al. 1996). IL-8 mRNA has been demonstrated to be present in AAV glomerulonephritis within both the inflammed glomerular and interstitial compartments. As well as IL-8 production by endothelial cells; mesangial cells and proximal tubular cells can also produce this cytokine. ANCA can also stimulate production of IL-8, therefore supporting the pathogenic role of IL-8 in AAV (Cockwell, Brooks et al. 1999).

MCP-1 is a monocyte and macrophage attractant. Patients with AAV GN have been demonstrated to have elevated urinary levels of MCP-1, with increased glomerular and interstitial expression. Both intrinsic renal cells, such as endothelial cells and mesangial cells, and infiltrating macrophages can produce this cytokine, with elevated urinary levels correlating with disease activity (Tam, Sanders et al. 2004).

TNF-α is a cytokine with numerous effects. TNF-α is not expressed in the kidney under normal physiological conditions. Following stimulation, renal cells such as mesangial cells,

tubular cells, endothelial cells and podocytes can produce this cytokine as can haemopoetic cells which are the major source of TNF-α production. This cytokine has many effects, such as localised endothelial cell activation and increased permeability with the upregulation and expression of adhesion receptors on the endothelial cell, vasodilatation mediated through nitric oxide release as well as the release of cytokines and the up-regulation of MHC class I and class II molecules. TNF-α is also responsible for the priming of neutrophils and monocytes, inducing the expression of PR3 and MPO on the cell surface which is a critical step in the cross-binding of ANCAs (Ernandez and Mayadas 2009). Despite the numerous roles of TNF-α in the pathogenesis of AAV, blockade of TNF-α by Etanercept (Wegener's Granulomatosis Etanercept Trial [WGET]) was characterised by a low response rate and a high rate of complications, illustrating the complex role of cytokine blockade in autoimmunity (2005).

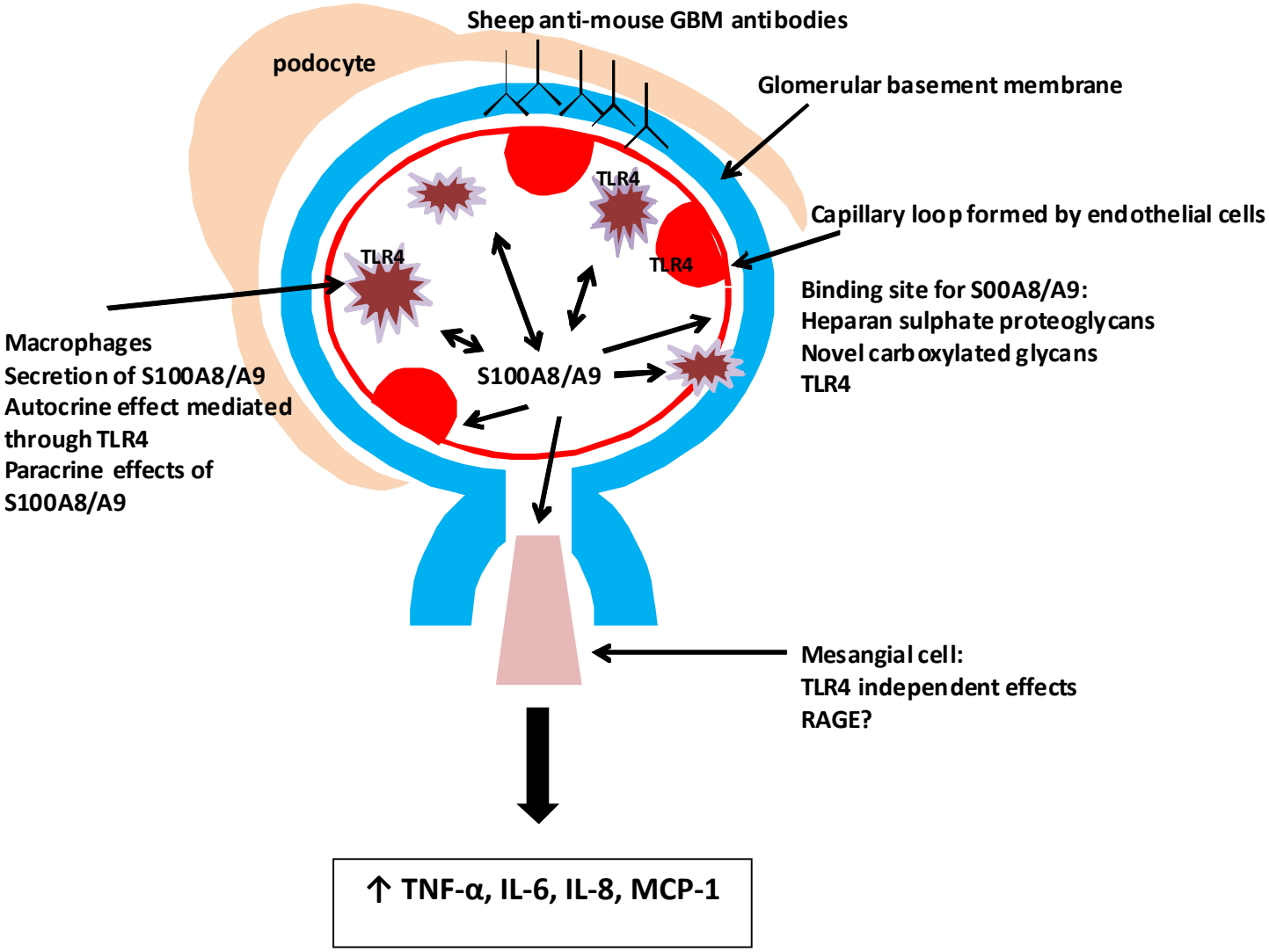

Figure 6-1 Role of S100A8/A9 in nephrotoxic nephritis

The diagram demonstrates the possible mechanisms of glomerular injury caused by S100A8/A9 in nephrotoxic nephritis. Monocyte/macrophage infiltration occurs day 3-4 following injection of NTS. Macrophages secrete S100A8/A9 in response to glomerular endothelial cell injury. S100A8/A9 is able to bind to macrophages via TLR4 and cause secretion of pro-inflammatory cytokines. Additionally, S100A8/A9 positive macrophages are pro-inflammatory and activate the endothelium further. Secreted S100A8/A9 can bind to the endothelium to amplify inflammation. The mesangial cell also contributes through TLR4 independent effects.

6.4. Unanswered questions relating to this work

Following the experimental work included in this thesis, a number of unanswered questions remain.

S100A8/A9 neutrophil function

The non-accelerated NTN experiments demonstrate at 2 hours following injection of nephrotoxic serum, WT and mrp14-/- mice had the same number of infiltrating neutrophils. However, this thesis does not include any functional data comparing WT and mrp14-/- neutrophils. Although there was the same number of neutrophils, it is unknown if both groups of neutrophils have the same response in the inflammed glomerulus. The question remains unanswered as to whether mrp14-/- neutrophils have a less pro-inflammatory effect in response to the planted antigen of sheep anti-mouse GBM antibodies compared to WT neutrophils. Neutrophils have a major role in human and experimental vasculitis. To investigate the role of S00A8/A9 and neutrophils, I would initially investigate the in-vitro secretion of S100A8/A9 following neutrophil degranulation in the presence of TNF-α and ANCAs, as this would confirm that neutrophils are a major source of the high serum levels of S100A8/A9 seen in patients with AAV. I would then repeat the experiments that I performed with BMDMs, using murine granulocytes instead. These experiments would compare the responses of mrp14-/- and WT granulocytes to stimulation with S100A8/A9 and S100A8 (with and without TNF-α) with respect to ROS production, nitric oxide synthesis and the production of inflammatory cytokines. The use of TLR4-/- granulocytes would confirm the importance of this receptor in mediating the pro-inflammatory effects.

Renal production of S100A8/A9

The BMDM experimental data in this thesis suggests that S100A8/A9 has a pro-inflammatory amplification effect as demonstrated by the decreased inflammatory response of mrp14-/- macrophages. Mrp14-/- mesangial cells had a similar response to WT mesangial cells. Renal collecting duct epithelial cells have been shown to play a crucial role in regulating inflammation and fibrosis, characterised by S100A8 and S100A9 production (Fujiu, Manabe et al. 2011). Although immunohistochemistry demonstrated the presence of

S100A8/A9 positive macrophages in human and experimental glomerulonephritis, it is possible that other cells in the kidney also produced these proteins. The antibodies used in immunohistochemistry recognise an epitope present on the heterodimer. The individual components of the heterodimer were not investigated, therefore it is possible that S100A8 and S100A9 were produced and secreted by other cell types within the kidney, for example mesangial cells and podocytes, and may contribute to the inflammatory response. This is supported by the bone marrow transplant data, which demonstrated that myeloid absence of S100A8/A9 is not sufficient to protect against renal injury in NTN.

Vasculitis animal models and S100A8/A9

The in vivo experiments in this thesis utilise the nephrotoxic nephritis animal model, which is a model of immune complex glomerulonephritis and is not a model of vasculitis. The next logical step would be to repeat the work included in this thesis in a vasculitis model. The murine model of MPO-ANCA disease (Xiao, Heeringa et al. 2002) has provided a reproducible model of vasculitis and has improved understanding of the pathogenesis of disease. To elucidate the role of mrp14-/- in experimental vasculitis, I would initially use this animal model with mrp14-/- knock-out mice. Additionally, the rat model of MPO-ANCA vasculitis could be utilised to demonstrate the efficacy of a molecule targeting S100A9 (Bjork, Bjork et al. 2009).

Receptor for advanced glycation end products (RAGE)

RAGE has been described to be present on cultured endothelial cells, mononuclear phagocytes and mesangial cells, with AGE-RAGE interactions having a role in the progression of diabetic nephropathy (Matsui, Yamagishi et al. 2009). S100A8/A9 was demonstrated in this thesis to have a pro-inflammatory effect on mesangial cells, independent of TLR4. However, the exact receptor to which S100A8/A9 binds to on mesangial cells remains unanswered. Similarly, the critical receptor on endothelial cells to which S100A8/A9 binds to remains uncertain. Heparan sulphate proteoglycans and novel carboxylated glycans have been shown to bind to S100A8/A9 on endothelial cells. RAGE and TLR4 may also bind S100A8/A9 on endothelial cells. In an investigation into the pathogenesis of atherosclerosis, human umbilical vein endothelial cells pre-incubated with AGE-albumin resulted in

upregulation of RAGE, and binding of S100A8/A9. This resulted in the increased secretion of IL-6, MCP-1, ICAM-1 and VCAM-1 (Ehlermann, Eggers et al. 2006). Therefore, S100A8/A9 may also bind to glomerular endothelial cells through this mechanism resulting in the upregulation of cytokines which have a role in glomerulonephritis and vasculitis.

S100A8/A9 as a therapeutic target

S100A9 has been described as the target of quinoline-3-carboxamides, which prevent the binding of S100A9 to RAGE and TLR4, instead resulting in the binding of this compound to S100A9 (Bjork, Bjork et al. 2009). A quinoline-3-carboxamide derivative has been used in the MRL-lpr/lpr lupus-prone mouse model. These mice spontaneously develop severe disease including an immune complex GN. The drug was added to murine drinking water and was effective in preventing the development of disease, as well as being an effective treatment (Bengtsson, Sturfelt et al. 2012). Survival in mice has been shown to be prolonged after the initiation of the drug, even when the disease was clinically overt (Carlsten, Jonsson et al. 2004). This supports the immunomodulatory role of these compounds without significant immunosuppressive activity.

However, more work needs to be done in this area to ensure that blockade of S100A8/A9 won't significantly affect the host response to infections. This is illustrated by the heterodimer having a key role in defence against Klebsiella pneumonia, whereby mrp14-/- mice demonstrated increased bacterial dissemination, decreased macrophage ability to phagocytose Klebsiella and reduced survival (Achouiti, Vogl et al. 2012).

The role of interstitial macrophages

The work in this thesis has concentrated on glomerular macrophages during NTN. However, as previous work has demonstrated, the accumulation of interstitial macrophages plays a crucial role in the development of chronic renal failure. The differences in interstitial macrophages in the WT and mrp14-/- mice were not compared, and it is unknown whether the macrophages in this compartment differed in the 2 animal groups.

6.5. Concluding remarks

The work in this thesis suggests that S100A8/A9 may have a novel role in AAV and glomerulonephritis. The human work describes S100A8/A9 as a potential biomarker in early systemic AAV, and the presence of S100A8/A9 positive cells in the renal biopsy, link S100A8/A9 with renal outcome. The animal work demonstrates a role for S100A8/A9 in the pathogenesis of GN, with the in-vitro work illustrating the effect of S100A8/A9 and S100A8 on different cell types known to play a crucial role in renal inflammation.

S100A8/A9 has been described as an important factor in the pathogenesis of diseases such as arthritis; therefore the work described in this thesis may therefore be relevant in the study of other auto-immune diseases. The work described may also increase our understanding of the inflammatory response as well as a possible link between infections, LPS, TLR4 and the innate immune response.

This thesis is all original work. Where others have contributed it has been acknowledged.

(2005). "Etanercept plus standard therapy for Wegener's granulomatosis." N Engl J Med **352**(4): 351-361.
Abbate, M., R. Kalluri, et al. (1998). "Experimental Goodpasture's syndrome in Wistar-Kyoto rats immunized with alpha3 chain of type IV collagen." Kidney Int **54**(5): 1550-1561.
Abdulahad, W. H., Y. M. van der Geld, et al. (2006). "Persistent expansion of CD4+ effector memory T cells in Wegener's granulomatosis." Kidney Int **70**(5): 938-947.
Achouiti, A., T. Vogl, et al. (2012). "Myeloid-related protein-14 contributes to protective immunity in gram-negative pneumonia derived sepsis." PLoS Pathog **8**(10): e1002987.
Aitman, T. J., R. Dong, et al. (2006). "Copy number polymorphism in Fcgr3 predisposes to glomerulonephritis in rats and humans." Nature **439**(7078): 851-855.
Anders, H. J. and D. Schlondorff (2007). "Toll-like receptors: emerging concepts in kidney disease." Curr Opin Nephrol Hypertens **16**(3): 177-183.
Andres Cerezo, L., H. Mann, et al. (2011). "Decreases in serum levels of S100A8/9 (calprotectin) correlate with improvements in total swollen joint count in patients with recent-onset rheumatoid arthritis." Arthritis Res Ther **13**(4): R122.
Arbuckle, M. R., M. T. McClain, et al. (2003). "Development of autoantibodies before the clinical onset of systemic lupus erythematosus." N Engl J Med **349**(16): 1526-1533.
Arda Goceroglu, C. R., Robert A. De Lind van Wijngaarden, Annelies Evaline Berden, Kerstin W. Westman, Oliver Flossmann, Herbert Hauer, David R.W. Jayne, Niels Rasmussen, Laure-Helene Noel, Franco Ferrario, Ruediger Waldherr, Charles D. Pusey, Ron Wolterbeek, Ernst C. Hagen, Jan A. Bruijn, Ingeborg . Bajema. (2012). The New Histopathologic Classification for ANCA-Associated Glomerulonephritis Predicts Renal Relapse Reanl Week, ASN.
Atallah, M., A. Krispin, et al. (2012). "Constitutive neutrophil apoptosis: regulation by cell concentration via S100 A8/9 and the MEK-ERK pathway." PLoS One **7**(2): e29333.
Averill, M. M., S. Barnhart, et al. (2011). "S100A9 differentially modifies phenotypic states of neutrophils, macrophages, and dendritic cells: implications for atherosclerosis and adipose tissue inflammation." Circulation **123**(11): 1216-1226.
Banas, B., B. Luckow, et al. (1999). "Chemokine and chemokine receptor expression in a novel human mesangial cell line." J Am Soc Nephrol **10**(11): 2314-2322.
Banchereau, J. and R. M. Steinman (1998). "Dendritic cells and the control of immunity." Nature **392**(6673): 245-252.
Beck, L. H., Jr., R. G. Bonegio, et al. (2009). "M-type phospholipase A2 receptor as target antigen in idiopathic membranous nephropathy." N Engl J Med **361**(1): 11-21.
Behmoaras, J., J. Smith, et al. (2010). "Genetic loci modulate macrophage activity and glomerular damage in experimental glomerulonephritis." J Am Soc Nephrol **21**(7): 1136-1144.
Bengtsson, A. A., G. Sturfelt, et al. (2012). "Pharmacokinetics, tolerability, and preliminary efficacy of paquinimod (ABR-215757), a new quinoline-3-carboxamide derivative: studies in lupus-prone mice and a multicenter, randomized, double-blind, placebo-controlled, repeat-dose, dose-ranging study in patients with systemic lupus erythematosus." Arthritis Rheum **64**(5): 1579-1588.
Berden, A. E., F. Ferrario, et al. (2010). "Histopathologic classification of ANCA-associated glomerulonephritis." J Am Soc Nephrol **21**(10): 1628-1636.

Berger, S. P., M. A. Seelen, et al. (1996). "Proteinase 3, the major autoantigen of Wegener's granulomatosis, enhances IL-8 production by endothelial cells in vitro." J Am Soc Nephrol **7**(5): 694-701.

Bhardwaj, R. S., C. Zotz, et al. (1992). "The calcium-binding proteins MRP8 and MRP14 form a membrane-associated heterodimer in a subset of monocytes/macrophages present in acute but absent in chronic inflammatory lesions." Eur J Immunol **22**(7): 1891-1897.

Bjork, P., A. Bjork, et al. (2009). "Identification of human S100A9 as a novel target for treatment of autoimmune disease via binding to quinoline-3-carboxamides." PLoS Biol **7**(4): e97.

Blantz, R. C., F. B. Gabbai, et al. (1993). "Role of mesangial cell in glomerular response to volume and angiotensin II." Am J Physiol **264**(1 Pt 2): F158-165.

Booth, A. D., M. K. Almond, et al. (2003). "Outcome of ANCA-associated renal vasculitis: a 5-year retrospective study." Am J Kidney Dis **41**(4): 776-784.

Boyd, J. H., B. Kan, et al. (2008). "S100A8 and S100A9 mediate endotoxin-induced cardiomyocyte dysfunction via the receptor for advanced glycation end products." Circ Res **102**(10): 1239-1246.

Brinkmann, V., U. Reichard, et al. (2004). "Neutrophil extracellular traps kill bacteria." Science **303**(5663): 1532-1535.

Brown, H. J., H. R. Lock, et al. (2007). "Toll-like receptor 4 ligation on intrinsic renal cells contributes to the induction of antibody-mediated glomerulonephritis via CXCL1 and CXCL2." J Am Soc Nephrol **18**(6): 1732-1739.

Brown, H. J., S. H. Sacks, et al. (2006). "Toll-like receptor 2 agonists exacerbate accelerated nephrotoxic nephritis." J Am Soc Nephrol **17**(7): 1931-1939.

Burkhardt, K., M. Radespiel-Troger, et al. (2001). "An increase in myeloid-related protein serum levels precedes acute renal allograft rejection." J Am Soc Nephrol **12**(9): 1947-1957.

Burkhardt, K., S. Schwarz, et al. (2009). "Myeloid-related protein 8/14 complex describes microcirculatory alterations in patients with type 2 diabetes and nephropathy." Cardiovasc Diabetol **8**: 10.

Bussolati, B., F. Mariano, et al. (1999). "Interleukin-12 is synthesized by mesangial cells and stimulates platelet-activating factor synthesis, cytoskeletal reorganization, and cell shape change." Am J Pathol **154**(2): 623-632.

Cao, Q., Y. Wang, et al. (2010). "IL-10/TGF-beta-modified macrophages induce regulatory T cells and protect against adriamycin nephrosis." J Am Soc Nephrol **21**(6): 933-942.

Carla L. Ellis, R. M., Lorraine C. Racusen, Duvuru Geetha (2012). New Histopathologic Classification of Anti-Neutrophil Cytoplasmic Antibody Associated Pauci-Immune Glomerulonephritis: Correlation with Renal Outcome Renal Week, ASN.

Carlsten, H., C. Jonsson, et al. (2004). "The impact of a new immunomodulator oxo-quinoline-3-carboxamide on the progression of experimental lupus." Int Immunopharmacol **4**(12): 1515-1523.

Carr, E. J., M. R. Clatworthy, et al. (2009). "Contrasting genetic association of IL2RA with SLE and ANCA-associated vasculitis." BMC Med Genet **10**: 22.

Carr, E. J., H. A. Niederer, et al. (2009). "Confirmation of the genetic association of CTLA4 and PTPN22 with ANCA-associated vasculitis." BMC Med Genet **10**: 121.

Caughey, G. H. (1991). "The structure and airway biology of mast cell proteinases." Am J Respir Cell Mol Biol **4**(5): 387-394.

Cesaro, A., N. Anceriz, et al. (2012). "An Inflammation Loop Orchestrated by S100A9 and Calprotectin Is Critical for Development of Arthritis." PLoS One **7**(9): e45478.
Chang, D. Y., L. H. Wu, et al. (2012). "Re-evaluation of the histopathologic classification of ANCA-associated glomerulonephritis: a study of 121 patients in a single center." Nephrol Dial Transplant **27**(6): 2343-2349.
Chavele, K. M., L. Martinez-Pomares, et al. (2010). "Mannose receptor interacts with Fc receptors and is critical for the development of crescentic glomerulonephritis in mice." J Clin Invest **120**(5): 1469-1478.
Chavele, K. M., D. Shukla, et al. (2010). "Regulation of myeloperoxidase-specific T cell responses during disease remission in antineutrophil cytoplasmic antibody-associated vasculitis: the role of Treg cells and tryptophan degradation." Arthritis Rheum **62**(5): 1539-1548.
Cochrane, C. G., E. R. Unanue, et al. (1965). "A Role of Polymorphonuclear Leukocytes and Complement in Nephrotoxic Nephritis." J Exp Med **122**: 99-116.
Cockwell, P., C. J. Brooks, et al. (1999). "Interleukin-8: A pathogenetic role in antineutrophil cytoplasmic autoantibody-associated glomerulonephritis." Kidney Int **55**(3): 852-863.
Cook, H. T., S. J. Singh, et al. (1999). "Interleukin-4 ameliorates crescentic glomerulonephritis in Wistar Kyoto rats." Kidney Int **55**(4): 1319-1326.
Couser, W. G. (2012). "Basic and translational concepts of immune-mediated glomerular diseases." J Am Soc Nephrol **23**(3): 381-399.
Couzi, L., P. Merville, et al. (2007). "Predominance of CD8+ T lymphocytes among periglomerular infiltrating cells and link to the prognosis of class III and class IV lupus nephritis." Arthritis Rheum **56**(7): 2362-2370.
Cove-Smith, A. and B. M. Hendry (2008). "The regulation of mesangial cell proliferation." Nephron Exp Nephrol **108**(4): e74-79.
Croce, K., H. Gao, et al. (2009). "Myeloid-related protein-8/14 is critical for the biological response to vascular injury." Circulation **120**(5): 427-436.
Csernok, E., M. Ai, et al. (2006). "Wegener autoantigen induces maturation of dendritic cells and licenses them for Th1 priming via the protease-activated receptor-2 pathway." Blood **107**(11): 4440-4448.
Csernok, E., M. Ernst, et al. (1994). "Activated neutrophils express proteinase 3 on their plasma membrane in vitro and in vivo." Clin Exp Immunol **95**(2): 244-250.
Cunningham, M. A., X. R. Huang, et al. (1999). "Prominence of cell-mediated immunity effectors in "pauci-immune" glomerulonephritis." J Am Soc Nephrol **10**(3): 499-506.
Dass, S., E. M. Vital, et al. (2007). "Development of psoriasis after B cell depletion with rituximab." Arthritis Rheum **56**(8): 2715-2718.
De Groot, K., N. Rasmussen, et al. (2005). "Randomized trial of cyclophosphamide versus methotrexate for induction of remission in early systemic antineutrophil cytoplasmic antibody-associated vasculitis." Arthritis Rheum **52**(8): 2461-2469.
De Rycke, L., D. Baeten, et al. (2005). "Differential expression and response to anti-TNFalpha treatment of infiltrating versus resident tissue macrophage subsets in autoimmune arthritis." J Pathol **206**(1): 17-27.
Donaghy, M. and A. J. Rees (1983). "Cigarette smoking and lung haemorrhage in glomerulonephritis caused by autoantibodies to glomerular basement membrane." Lancet **2**(8364): 1390-1393.
Du, C. Q., L. Yang, et al. (2012). "The elevated serum S100A8/A9 during acute myocardial infarction is not of cardiac myocyte origin." Inflammation **35**(3): 787-796.

Duffield, J. S., L. P. Erwig, et al. (2000). "Activated macrophages direct apoptosis and suppress mitosis of mesangial cells." J Immunol **164**(4): 2110-2119.
Duffield, J. S., P. G. Tipping, et al. (2005). "Conditional ablation of macrophages halts progression of crescentic glomerulonephritis." Am J Pathol **167**(5): 1207-1219.
Ehlermann, P., K. Eggers, et al. (2006). "Increased proinflammatory endothelial response to S100A8/A9 after preactivation through advanced glycation end products." Cardiovasc Diabetol **5**: 6.
Eikmans, M., M. C. Roos-van Groningen, et al. (2005). "Expression of surfactant protein-C, S100A8, S100A9, and B cell markers in renal allografts: investigation of the prognostic value." J Am Soc Nephrol **16**(12): 3771-3786.
El Fassi, D., C. H. Nielsen, et al. (2008). "Ulcerative colitis following B lymphocyte depletion with rituximab in a patient with Graves' disease." Gut **57**(5): 714-715.
Eller, K., D. Wolf, et al. (2011). "IL-9 production by regulatory T cells recruits mast cells that are essential for regulatory T cell-induced immune suppression." J Immunol **186**(1): 83-91.
Eriksson, P., C. Sandell, et al. (2010). "B cell abnormalities in Wegener's granulomatosis and microscopic polyangiitis: role of CD25+-expressing B cells." J Rheumatol **37**(10): 2086-2095.
Ernandez, T. and T. N. Mayadas (2009). "Immunoregulatory role of TNFalpha in inflammatory kidney diseases." Kidney Int **76**(3): 262-276.
Erwig, L. P., D. C. Kluth, et al. (1998). "Initial cytokine exposure determines function of macrophages and renders them unresponsive to other cytokines." J Immunol **161**(4): 1983-1988.
Erwig, L. P., K. Stewart, et al. (2000). "Macrophages from inflamed but not normal glomeruli are unresponsive to anti-inflammatory cytokines." Am J Pathol **156**(1): 295-301.
Eue, I., B. Pietz, et al. (2000). "Transendothelial migration of 27E10+ human monocytes." Int Immunol **12**(11): 1593-1604.
Falk, R. J., R. S. Terrell, et al. (1990). "Anti-neutrophil cytoplasmic autoantibodies induce neutrophils to degranulate and produce oxygen radicals in vitro." Proc Natl Acad Sci U S A **87**(11): 4115-4119.
Fanciulli, M., P. J. Norsworthy, et al. (2007). "FCGR3B copy number variation is associated with susceptibility to systemic, but not organ-specific, autoimmunity." Nat Genet **39**(6): 721-723.
Ferenbach, D. A., T. A. Sheldrake, et al. (2012). "Macrophage/monocyte depletion by clodronate, but not diphtheria toxin, improves renal ischemia/reperfusion injury in mice." Kidney Int **82**(8): 928-933.
Fisher, M., C. D. Pusey, et al. (1997). "Susceptibility to anti-glomerular basement membrane disease is strongly associated with HLA-DRB1 genes." Kidney Int **51**(1): 222-229.
Foell, D., N. Wulffraat, et al. (2010). "Methotrexate withdrawal at 6 vs 12 months in juvenile idiopathic arthritis in remission: a randomized clinical trial." JAMA **303**(13): 1266-1273.
Frosch, M., M. Ahlmann, et al. (2009). "The myeloid-related proteins 8 and 14 complex, a novel ligand of toll-like receptor 4, and interleukin-1beta form a positive feedback mechanism in systemic-onset juvenile idiopathic arthritis." Arthritis Rheum **60**(3): 883-891.
Frosch, M., A. Strey, et al. (2000). "Myeloid-related proteins 8 and 14 are specifically secreted during interaction of phagocytes and activated endothelium and are useful

markers for monitoring disease activity in pauciarticular-onset juvenile rheumatoid arthritis." Arthritis Rheum **43**(3): 628-637.
Frosch, M., T. Vogl, et al. (2004). "Expression of MRP8 and MRP14 by macrophages is a marker for severe forms of glomerulonephritis." J Leukoc Biol **75**(2): 198-206.
Fujiu, K., I. Manabe, et al. (2011). "Renal collecting duct epithelial cells regulate inflammation in tubulointerstitial damage in mice." J Clin Invest **121**(9): 3425-3441.
Gan, P. Y., O. M. Steinmetz, et al. (2010). "Th17 cells promote autoimmune anti-myeloperoxidase glomerulonephritis." J Am Soc Nephrol **21**(6): 925-931.
Gan, P. Y., S. A. Summers, et al. (2012). "Mast cells contribute to peripheral tolerance and attenuate autoimmune vasculitis." J Am Soc Nephrol **23**(12): 1955-1966.
Germuth, F. G., Jr. (1953). "A comparative histologic and immunologic study in rabbits of induced hypersensitivity of the serum sickness type." J Exp Med **97**(2): 257-282.
Gilg, J., C. Castledine, et al. (2012). "Chapter 1 UK RRT Incidence in 2010: National and Centre-Speci fi c Analyses." Nephron Clin Pract **120 Suppl 1**: c1-c27.
Giorgini, A., H. J. Brown, et al. (2010). "Toll-like receptor 4 stimulation triggers crescentic glomerulonephritis by multiple mechanisms including a direct effect on renal cells." Am J Pathol **177**(2): 644-653.
Goebeler, M., J. Roth, et al. (1994). "Expression and complex formation of S100-like proteins MRP8 and MRP14 by macrophages during renal allograft rejection." Transplantation **58**(3): 355-361.
Goebeler, M., J. Roth, et al. (1993). "Expression and complex assembly of calcium-binding proteins MRP8 and MRP14 during differentiation of murine myelomonocytic cells." J Leukoc Biol **53**(1): 11-18.
Goebeler, M., J. Roth, et al. (1995). "Increase of calcium levels in epithelial cells induces translocation of calcium-binding proteins migration inhibitory factor-related protein 8 (MRP8) and MRP14 to keratin intermediate filaments." Biochem J **309 (Pt 2)**: 419-424.
Gou, S. J., J. Yuan, et al. (2012). "Circulating complement activation in patients with anti-neutrophil cytoplasmic antibody-associated vasculitis." Kidney Int.
Grevers, L. C., T. J. de Vries, et al. (2011). "S100A8 enhances osteoclastic bone resorption in vitro through activation of Toll-like receptor 4: implications for bone destruction in murine antigen-induced arthritis." Arthritis Rheum **63**(5): 1365-1375.
Haga, H. J., J. G. Brun, et al. (1993). "Calprotectin in patients with systemic lupus erythematosus: relation to clinical and laboratory parameters of disease activity." Lupus **2**(1): 47-50.
Hammer, H. B., M. K. Fagerhol, et al. (2011). "The soluble biomarker calprotectin (a S100 protein) is associated to ultrasonographic synovitis scores and is sensitive to change in patients with rheumatoid arthritis treated with adalimumab." Arthritis Res Ther **13**(5): R178.
Harper, L., P. Cockwell, et al. (2001). "Neutrophil priming and apoptosis in anti-neutrophil cytoplasmic autoantibody-associated vasculitis." Kidney Int **59**(5): 1729-1738.
Heller, F., S. Frischmann, et al. (2011). "Urinary calprotectin and the distinction between prerenal and intrinsic acute kidney injury." Clin J Am Soc Nephrol **6**(10): 2347-2355.
Henson, P. M. (1972). "Pathologic mechanisms in neutrophil-mediated injury." Am J Pathol **68**(3): 593-612.

Hermani, A., B. De Servi, et al. (2006). "S100A8 and S100A9 activate MAP kinase and NF-kappaB signaling pathways and trigger translocation of RAGE in human prostate cancer cells." Exp Cell Res **312**(2): 184-197.
Hessian, P. A., J. Edgeworth, et al. (1993). "MRP-8 and MRP-14, two abundant Ca(2+)-binding proteins of neutrophils and monocytes." J Leukoc Biol **53**(2): 197-204.
Hill, G. S., M. Delahousse, et al. (2001). "Predictive power of the second renal biopsy in lupus nephritis: significance of macrophages." Kidney Int **59**(1): 304-316.
Hirono, K., D. Foell, et al. (2006). "Expression of myeloid-related protein-8 and -14 in patients with acute Kawasaki disease." J Am Coll Cardiol **48**(6): 1257-1264.
Hobbs, J. A., R. May, et al. (2003). "Myeloid cell function in MRP-14 (S100A9) null mice." Mol Cell Biol **23**(7): 2564-2576.
Hochegger, K., F. Siebenhaar, et al. (2005). "Role of mast cells in experimental anti-glomerular basement membrane glomerulonephritis." Eur J Immunol **35**(10): 3074-3082.
Hochheiser, K., D. R. Engel, et al. (2011). "Kidney Dendritic Cells Become Pathogenic during Crescentic Glomerulonephritis with Proteinuria." J Am Soc Nephrol **22**(2): 306-316.
Hogg, N., C. Allen, et al. (1989). "Monoclonal antibody 5.5 reacts with p8,14, a myeloid molecule associated with some vascular endothelium." Eur J Immunol **19**(6): 1053-1061.
Holdsworth, S. R., T. J. Neale, et al. (1981). "Abrogation of macrophage-dependent injury in experimental glomerulonephritis in the rabbit. Use of an antimacrophage serum." J Clin Invest **68**(3): 686-698.
Holzinger, D., M. Frosch, et al. (2012). "The Toll-like receptor 4 agonist MRP8/14 protein complex is a sensitive indicator for disease activity and predicts relapses in systemic-onset juvenile idiopathic arthritis." Ann Rheum Dis **71**(6): 974-980.
Hong, Y., D. Eleftheriou, et al. (2012). "Anti-neutrophil cytoplasmic antibodies stimulate release of neutrophil microparticles." J Am Soc Nephrol **23**(1): 49-62.
Hopfer, H., R. Maron, et al. (2003). "The importance of cell-mediated immunity in the course and severity of autoimmune anti-glomerular basement membrane disease in mice." FASEB J **17**(8): 860-868.
Hora, K., J. A. Satriano, et al. (1992). "Receptors for IgG complexes activate synthesis of monocyte chemoattractant peptide 1 and colony-stimulating factor 1." Proc Natl Acad Sci U S A **89**(5): 1745-1749.
Hruby, Z. and K. F. Beck (1997). "Cytotoxic effect of autocrine and macrophage-derived nitric oxide on cultured rat mesangial cells." Clin Exp Immunol **107**(1): 76-82.
Hruskova, Z., Z. Rihova, et al. (2009). "Intracellular cytokine production in ANCA-associated vasculitis: low levels of interleukin-10 in remission are associated with a higher relapse rate in the long-term follow-up." Arch Med Res **40**(4): 276-284.
Hsu, K., R. J. Passey, et al. (2005). "Regulation of S100A8 by glucocorticoids." J Immunol **174**(4): 2318-2326.
Hu, S. P., C. Harrison, et al. (1996). "Induction of the chemotactic S100 protein, CP-10, in monocyte/macrophages by lipopolysaccharide." Blood **87**(9): 3919-3928.
Huang, X. R., P. G. Tipping, et al. (1997). "Mechanisms of T cell-induced glomerular injury in anti-glomerular basement membrane (GBM) glomerulonephritis in rats." Clin Exp Immunol **109**(1): 134-142.

Huang, X. R., P. G. Tipping, et al. (1997). "Th1 responsiveness to nephritogenic antigens determines susceptibility to crescentic glomerulonephritis in mice." Kidney Int **51**(1): 94-103.
Huugen, D., A. van Esch, et al. (2007). "Inhibition of complement factor C5 protects against anti-myeloperoxidase antibody-mediated glomerulonephritis in mice." Kidney Int **71**(7): 646-654.
Ivanov, II, B. S. McKenzie, et al. (2006). "The orphan nuclear receptor RORgammat directs the differentiation program of proinflammatory IL-17+ T helper cells." Cell **126**(6): 1121-1133.
Iwata, Y., T. Matsushita, et al. (2011). "Characterization of a rare IL-10-competent B-cell subset in humans that parallels mouse regulatory B10 cells." Blood **117**(2): 530-541.
Jennette, J. C., R. J. Falk, et al. (1994). "Nomenclature of systemic vasculitides. Proposal of an international consensus conference." Arthritis Rheum **37**(2): 187-192.
Jones, R. B., J. W. Tervaert, et al. (2010). "Rituximab versus cyclophosphamide in ANCA-associated renal vasculitis." N Engl J Med **363**(3): 211-220.
Jung, M., A. Sola, et al. (2012). "Infusion of IL-10-expressing cells protects against renal ischemia through induction of lipocalin-2." Kidney Int **81**(10): 969-982.
Kain, R., M. Exner, et al. (2008). "Molecular mimicry in pauci-immune focal necrotizing glomerulonephritis." Nat Med **14**(10): 1088-1096.
Kambham, N. (2012). "Crescentic Glomerulonephritis: an update on Pauci-immune and Anti-GBM diseases." Adv Anat Pathol **19**(2): 111-124.
Karkar, A. M. and A. J. Rees (1997). "Influence of endotoxin contamination on anti-GBM antibody induced glomerular injury in rats." Kidney Int **52**(6): 1579-1583.
Kay, C. F. (1940). "The Mechanism by Which Experimental Nephritis Is Produced in Rabbits Injected with Nephrotoxic Duck Serum." J Exp Med **72**(5): 559-572.
Kelley, J. M., P. A. Monach, et al. (2011). "IgA and IgG antineutrophil cytoplasmic antibody engagement of Fc receptor genetic variants influences granulomatosis with polyangiitis." Proc Natl Acad Sci U S A **108**(51): 20736-20741.
Kerkhoff, C., W. Nacken, et al. (2005). "The arachidonic acid-binding protein S100A8/A9 promotes NADPH oxidase activation by interaction with p67phox and Rac-2." FASEB J **19**(3): 467-469.
Kessenbrock, K., M. Krumbholz, et al. (2009). "Netting neutrophils in autoimmune small-vessel vasculitis." Nat Med **15**(6): 623-625.
Kettritz, R., J. C. Jennette, et al. (1997). "Crosslinking of ANCA-antigens stimulates superoxide release by human neutrophils." J Am Soc Nephrol **8**(3): 386-394.
Kido, J., N. Hayashi, et al. (2005). "Calprotectin expression in human monocytes: induction by porphyromonas gingivalis lipopolysaccharide, tumor necrosis factor-alpha, and interleukin-1beta." J Periodontol **76**(3): 437-442.
Kitching, A. R., S. R. Holdsworth, et al. (1999). "IFN-gamma mediates crescent formation and cell-mediated immune injury in murine glomerulonephritis." J Am Soc Nephrol **10**(4): 752-759.
Kitching, A. R., P. G. Tipping, et al. (1998). "Interleukin-4 deficiency enhances Th1 responses and crescentic glomerulonephritis in mice." Kidney Int **53**(1): 112-118.
Kluth, D. C., L. P. Erwig, et al. (2004). "Multiple facets of macrophages in renal injury." Kidney Int **66**(2): 542-557.
Knight, A., S. Sandin, et al. (2008). "Risks and relative risks of Wegener's granulomatosis among close relatives of patients with the disease." Arthritis Rheum **58**(1): 302-307.

Knight, A., S. Sandin, et al. (2010). "Increased risk of autoimmune disease in families with Wegener's granulomatosis." J Rheumatol **37**(12): 2553-2558.
Korn, T., E. Bettelli, et al. (2009). "IL-17 and Th17 Cells." Annu Rev Immunol **27**: 485-517.
Kumar, A., A. Steinkasserer, et al. (2003). "Interleukin-10 influences the expression of MRP8 and MRP14 in human dendritic cells." Int Arch Allergy Immunol **132**(1): 40-47.
Kuwabara, T., K. Mori, et al. (2012). "Exacerbation of diabetic nephropathy by hyperlipidaemia is mediated by Toll-like receptor 4 in mice." Diabetologia **55**(8): 2256-2266.
Lackmann, M., C. J. Cornish, et al. (1992). "Purification and structural analysis of a murine chemotactic cytokine (CP-10) with sequence homology to S100 proteins." J Biol Chem **267**(11): 7499-7504.
Lagasse, E. and R. G. Clerc (1988). "Cloning and expression of two human genes encoding calcium-binding proteins that are regulated during myeloid differentiation." Mol Cell Biol **8**(6): 2402-2410.
Lagasse, E. and I. L. Weissman (1992). "Mouse MRP8 and MRP14, two intracellular calcium-binding proteins associated with the development of the myeloid lineage." Blood **79**(8): 1907-1915.
Langrish, C. L., Y. Chen, et al. (2005). "IL-23 drives a pathogenic T cell population that induces autoimmune inflammation." J Exp Med **201**(2): 233-240.
Lee, S., S. Huen, et al. (2011). "Distinct macrophage phenotypes contribute to kidney injury and repair." J Am Soc Nephrol **22**(2): 317-326.
Lee, Y. H., S. J. Choi, et al. (2012). "CTLA-4 and TNF-alpha promoter-308 A/G polymorphisms and ANCA-associated vasculitis susceptibility: a meta-analysis." Mol Biol Rep **39**(1): 319-326.
Li, S., S. R. Holdsworth, et al. (1997). "Antibody independent crescentic glomerulonephritis in mu chain deficient mice." Kidney Int **51**(3): 672-678.
Li, S., C. Kurts, et al. (1998). "Major histocompatibility complex class II expression by intrinsic renal cells is required for crescentic glomerulonephritis." J Exp Med **188**(3): 597-602.
Lim, S. Y., M. Raftery, et al. (2008). "S-nitrosylated S100A8: novel anti-inflammatory properties." J Immunol **181**(8): 5627-5636.
Lim, S. Y., M. J. Raftery, et al. (2011). "Oxidative modifications of DAMPs suppress inflammation: the case for S100A8 and S100A9." Antioxid Redox Signal **15**(8): 2235-2248.
Lionaki, S., E. R. Blyth, et al. (2012). "Classification of antineutrophil cytoplasmic autoantibody vasculitides: The role of antineutrophil cytoplasmic autoantibody specificity for myeloperoxidase or proteinase 3 in disease recognition and prognosis." Arthritis Rheum **64**(10): 3452-3462.
Little, M. A., B. Al-Ani, et al. (2012). "Anti-proteinase 3 anti-neutrophil cytoplasm autoantibodies recapitulate systemic vasculitis in mice with a humanized immune system." PLoS One **7**(1): e28626.
Little, M. A., P. Nightingale, et al. (2010). "Early mortality in systemic vasculitis: relative contribution of adverse events and active vasculitis." Ann Rheum Dis **69**(6): 1036-1043.
Little, M. A., C. L. Smyth, et al. (2005). "Antineutrophil cytoplasm antibodies directed against myeloperoxidase augment leukocyte-microvascular interactions in vivo." Blood **106**(6): 2050-2058.

Little, M. A., L. Smyth, et al. (2009). "Experimental autoimmune vasculitis: an animal model of anti-neutrophil cytoplasmic autoantibody-associated systemic vasculitis." Am J Pathol **174**(4): 1212-1220.
Lood, C., M. Stenstrom, et al. (2011). "Protein synthesis of the pro-inflammatory S100A8/A9 complex in plasmacytoid dendritic cells and cell surface S100A8/A9 on leukocyte subpopulations in systemic lupus erythematosus." Arthritis Res Ther **13**(2): R60.
Loser, K., T. Vogl, et al. (2010). "The Toll-like receptor 4 ligands Mrp8 and Mrp14 are crucial in the development of autoreactive CD8+ T cells." Nat Med **16**(6): 713-717.
Lugering, N., T. Kucharzik, et al. (1997). "Importance of combined treatment with IL-10 and IL-4, but not IL-13, for inhibition of monocyte release of the Ca(2+)-binding protein MRP8/14." Immunology **91**(1): 130-134.
Lyons, P. A., T. F. Rayner, et al. (2012). "Genetically distinct subsets within ANCA-associated vasculitis." N Engl J Med **367**(3): 214-223.
Mahr, A., S. Katsahian, et al. (2012). "Revisiting the classification of clinical phenotypes of anti-neutrophil cytoplasmic antibody-associated vasculitis: a cluster analysis." Ann Rheum Dis.
Manitz, M. P., B. Horst, et al. (2003). "Loss of S100A9 (MRP14) results in reduced interleukin-8-induced CD11b surface expression, a polarized microfilament system, and diminished responsiveness to chemoattractants in vitro." Mol Cell Biol **23**(3): 1034-1043.
Manolakis, A. C., A. N. Kapsoritakis, et al. (2011). "Calprotectin, calgranulin C, and other members of the s100 protein family in inflammatory bowel disease." Dig Dis Sci **56**(6): 1601-1611.
Marinaki, S., I. Neumann, et al. (2005). "Abnormalities of CD4 T cell subpopulations in ANCA-associated vasculitis." Clin Exp Immunol **140**(1): 181-191.
Martin, M., R. Schwinzer, et al. (1989). "Glomerular mesangial cells in local inflammation. Induction of the expression of MHC class II antigens by IFN-gamma." J Immunol **142**(6): 1887-1894.
Matsui, T., S. Yamagishi, et al. (2009). "Nifedipine, a calcium channel blocker, inhibits advanced glycation end product (AGE)-elicited mesangial cell damage by suppressing AGE receptor (RAGE) expression via peroxisome proliferator-activated receptor-gamma activation." Biochem Biophys Res Commun **385**(2): 269-272.
McKinney, E. F., P. A. Lyons, et al. (2010). "A CD8+ T cell transcription signature predicts prognosis in autoimmune disease." Nat Med **16**(5): 586-591, 581p following 591.
Monach, P. A., G. Tomasson, et al. (2011). "Circulating markers of vascular injury and angiogenesis in antineutrophil cytoplasmic antibody-associated vasculitis." Arthritis Rheum **63**(12): 3988-3997.
Moore, B. W. (1965). "A soluble protein characteristic of the nervous system." Biochem Biophys Res Commun **19**(6): 739-744.
Morgan, M. D., C. J. Day, et al. (2010). "Patients with Wegener's granulomatosis demonstrate a relative deficiency and functional impairment of T-regulatory cells." Immunology **130**(1): 64-73.
Morris, H., M. D. Morgan, et al. (2011). "ANCA-associated vasculitis is linked to carriage of the Z allele of alpha(1) antitrypsin and its polymers." Ann Rheum Dis **70**(10): 1851-1856.
Morrow, D. A., Y. Wang, et al. (2008). "Myeloid-related protein 8/14 and the risk of cardiovascular death or myocardial infarction after an acute coronary syndrome in

the Pravastatin or Atorvastatin Evaluation and Infection Therapy: Thrombolysis in Myocardial Infarction (PROVE IT-TIMI 22) trial." Am Heart J **155**(1): 49-55.
Mortensen, E. S. and O. P. Rekvig (2009). "Nephritogenic potential of anti-DNA antibodies against necrotic nucleosomes." J Am Soc Nephrol **20**(4): 696-704.
Mosser, D. M. and J. P. Edwards (2008). "Exploring the full spectrum of macrophage activation." Nat Rev Immunol **8**(12): 958-969.
Nacken, W., C. Sopalla, et al. (2000). "Biochemical characterization of the murine S100A9 (MRP14) protein suggests that it is functionally equivalent to its human counterpart despite its low degree of sequence homology." Eur J Biochem **267**(2): 560-565.
Naish, P. F., N. M. Thomson, et al. (1975). "The role of polymorphonuclear leucocytes in the autologous phase of nephrotoxic nephritis." Clin Exp Immunol **22**(1): 102-111.
Nangaku, M. and W. G. Couser (2005). "Mechanisms of immune-deposit formation and the mediation of immune renal injury." Clin Exp Nephrol **9**(3): 183-191.
Newton, R. A. and N. Hogg (1998). "The human S100 protein MRP-14 is a novel activator of the beta 2 integrin Mac-1 on neutrophils." J Immunol **160**(3): 1427-1435.
Nogueira, E., S. Hamour, et al. (2010). "Serum IL-17 and IL-23 levels and autoantigen-specific Th17 cells are elevated in patients with ANCA-associated vasculitis." Nephrol Dial Transplant **25**(7): 2209-2217.
Nolan, S. L., N. Kalia, et al. (2008). "Mechanisms of ANCA-mediated leukocyte-endothelial cell interactions in vivo." J Am Soc Nephrol **19**(5): 973-984.
Ntatsaki, E., R. A. Watts, et al. (2010). "Epidemiology of ANCA-associated vasculitis." Rheum Dis Clin North Am **36**(3): 447-461.
Odink, K., N. Cerletti, et al. (1987). "Two calcium-binding proteins in infiltrate macrophages of rheumatoid arthritis." Nature **330**(6143): 80-82.
Odobasic, D., P. Y. Gan, et al. (2011). "Interleukin-17A promotes early but attenuates established disease in crescentic glomerulonephritis in mice." Am J Pathol **179**(3): 1188-1198.
Pai, R., H. Ha, et al. (1996). "Role of tumor necrosis factor-alpha on mesangial cell MCP-1 expression and monocyte migration: mechanisms mediated by signal transduction." J Am Soc Nephrol **7**(6): 914-923.
Park, S. Y., S. Ueda, et al. (1998). "Resistance of Fc receptor- deficient mice to fatal glomerulonephritis." J Clin Invest **102**(6): 1229-1238.
Passey, R. J., E. Williams, et al. (1999). "A null mutation in the inflammation-associated S100 protein S100A8 causes early resorption of the mouse embryo." J Immunol **163**(4): 2209-2216.
Paust, H. J., J. E. Turner, et al. (2009). "The IL-23/Th17 axis contributes to renal injury in experimental glomerulonephritis." J Am Soc Nephrol **20**(5): 969-979.
Pavon, E. J., S. Garcia-Rodriguez, et al. (2012). "Increased expression and phosphorylation of the two S100A9 isoforms in mononuclear cells from patients with systemic lupus erythematosus: a proteomic signature for circulating low-density granulocytes." J Proteomics **75**(6): 1778-1791.
Pedchenko, V., O. Bondar, et al. (2010). "Molecular architecture of the Goodpasture autoantigen in anti-GBM nephritis." N Engl J Med **363**(4): 343-354.
Peng, W. H., W. X. Jian, et al. (2011). "Increased serum myeloid-related protein 8/14 level is associated with atherosclerosis in type 2 diabetic patients." Cardiovasc Diabetol **10**: 41.

Peng, Y., C. A. Sigua, et al. (2008). "Deletion of toll-like receptor-4 downregulates protein kinase C-zeta and attenuates liver injury in experimental pancreatitis." Surgery **143**(5): 679-685.
Pinching, A. J., A. J. Rees, et al. (1980). "Relapses in Wegener's granulomatosis: the role of infection." Br Med J **281**(6244): 836-838.
Popa, E. R., C. F. Franssen, et al. (2002). "In vitro cytokine production and proliferation of T cells from patients with anti-proteinase 3- and antimyeloperoxidase-associated vasculitis, in response to proteinase 3 and myeloperoxidase." Arthritis Rheum **46**(7): 1894-1904.
Pusey, C. D., M. J. Holland, et al. (1991). "Experimental autoimmune glomerulonephritis induced by homologous and isologous glomerular basement membrane in Brown-Norway rats." Nephrol Dial Transplant **6**(7): 457-465.
Rahimi, F., K. Hsu, et al. (2005). "FGF-2, IL-1beta and TGF-beta regulate fibroblast expression of S100A8." FEBS J **272**(11): 2811-2827.
Rammes, A., J. Roth, et al. (1997). "Myeloid-related protein (MRP) 8 and MRP14, calcium-binding proteins of the S100 family, are secreted by activated monocytes via a novel, tubulin-dependent pathway." J Biol Chem **272**(14): 9496-9502.
Rastaldi, M. P., F. Ferrario, et al. (2000). "Glomerular monocyte-macrophage features in ANCA-positive renal vasculitis and cryoglobulinemic nephritis." J Am Soc Nephrol **11**(11): 2036-2043.
Rees, A. J. (2010). "Monocyte and macrophage biology: an overview." Semin Nephrol **30**(3): 216-233.
Reynolds, J., P. R. Cook, et al. (2012). "Genetic susceptibility to experimental autoimmune glomerulonephritis in the Wistar Kyoto rat." Am J Pathol **180**(5): 1843-1851.
Reynolds, J., V. A. Norgan, et al. (2002). "Anti-CD8 monoclonal antibody therapy is effective in the prevention and treatment of experimental autoimmune glomerulonephritis." J Am Soc Nephrol **13**(2): 359-369.
Reynolds, J. and C. D. Pusey (1994). "In vivo treatment with a monoclonal antibody to T helper cells in experimental autoimmune glomerulonephritis in the BN rat." Clin Exp Immunol **95**(1): 122-127.
Ricanek, P., S. Brackmann, et al. (2011). "Evaluation of disease activity in IBD at the time of diagnosis by the use of clinical, biochemical, and fecal markers." Scand J Gastroenterol **46**(9): 1081-1091.
Rimbert, M., M. Hamidou, et al. (2011). "Decreased numbers of blood dendritic cells and defective function of regulatory T cells in antineutrophil cytoplasmic antibody-associated vasculitis." PLoS One **6**(4): e18734.
Riser, B. L., P. Cortes, et al. (1996). "Cyclic stretching force selectively up-regulates transforming growth factor-beta isoforms in cultured rat mesangial cells." Am J Pathol **148**(6): 1915-1923.
Riva, M., E. Kallberg, et al. (2012). "Induction of nuclear factor-kappaB responses by the S100A9 protein is Toll-like receptor-4-dependent." Immunology **137**(2): 172-182.
Robinson, M. J., P. Tessier, et al. (2002). "The S100 family heterodimer, MRP-8/14, binds with high affinity to heparin and heparan sulfate glycosaminoglycans on endothelial cells." J Biol Chem **277**(5): 3658-3665.
Robson, M. G. (2009). "Toll-like receptors and renal disease." Nephron Exp Nephrol **113**(1): e1-7.

Roth, J., F. Burwinkel, et al. (1993). "MRP8 and MRP14, S-100-like proteins associated with myeloid differentiation, are translocated to plasma membrane and intermediate filaments in a calcium-dependent manner." Blood **82**(6): 1875-1883.
Roth, J., M. Goebeler, et al. (2001). "S100A8 and S100A9 in inflammatory diseases." Lancet **357**(9261): 1041.
Roth, J., S. Teigelkamp, et al. (1992). "Complex pattern of the myelo-monocytic differentiation antigens MRP8 and MRP14 during chronic airway inflammation." Immunobiology **186**(3-4): 304-314.
Ruth, A. J., A. R. Kitching, et al. (2006). "Anti-neutrophil cytoplasmic antibodies and effector CD4+ cells play nonredundant roles in anti-myeloperoxidase crescentic glomerulonephritis." J Am Soc Nephrol **17**(7): 1940-1949.
Ruth, A. J., A. R. Kitching, et al. (2003). "Intrinsic renal cell expression of CD40 directs Th1 effectors inducing experimental crescentic glomerulonephritis." J Am Soc Nephrol **14**(11): 2813-2822.
Ryan, J. J., P. J. Mason, et al. (1998). "Recombinant alpha-chains of type IV collagen demonstrate that the amino terminal of the Goodpasture autoantigen is crucial for antibody recognition." Clin Exp Immunol **113**(1): 17-27.
Ryckman, C., C. Gilbert, et al. (2004). "Monosodium urate monohydrate crystals induce the release of the proinflammatory protein S100A8/A9 from neutrophils." J Leukoc Biol **76**(2): 433-440.
Ryckman, C., K. Vandal, et al. (2003). "Proinflammatory activities of S100: proteins S100A8, S100A9, and S100A8/A9 induce neutrophil chemotaxis and adhesion." J Immunol **170**(6): 3233-3242.
Sado, Y., I. Naito, et al. (1986). "Strain specific responses of inbred rats on the severity of experimental autoimmune glomerulonephritis." J Clin Lab Immunol **19**(4): 193-199.
Salama, A. D., A. N. Chaudhry, et al. (2003). "Regulation by CD25+ lymphocytes of autoantigen-specific T-cell responses in Goodpasture's (anti-GBM) disease." Kidney Int **64**(5): 1685-1694.
Salama, A. D., A. N. Chaudhry, et al. (2001). "In Goodpasture's disease, CD4(+) T cells escape thymic deletion and are reactive with the autoantigen alpha3(IV)NC1." J Am Soc Nephrol **12**(9): 1908-1915.
Sangaletti, S., C. Tripodo, et al. (2012). "Neutrophil extracellular traps mediate transfer of cytoplasmic neutrophil antigens to myeloid dendritic cells toward ANCA induction and associated autoimmunity." Blood **120**(15): 3007-3018.
Santiago, A., J. Satriano, et al. (1989). "A specific Fc gamma receptor on cultured rat mesangial cells." J Immunol **143**(8): 2575-2582.
Satriano, J. A., B. Banas, et al. (1997). "Regulation of RANTES and ICAM-1 expression in murine mesangial cells." J Am Soc Nephrol **8**(4): 596-603.
Saus, J., J. Wieslander, et al. (1988). "Identification of the Goodpasture antigen as the alpha 3(IV) chain of collagen IV." J Biol Chem **263**(26): 13374-13380.
Scandiuzzi, L., W. Beghdadi, et al. (2010). "Mouse mast cell protease-4 deteriorates renal function by contributing to inflammation and fibrosis in immune complex-mediated glomerulonephritis." J Immunol **185**(1): 624-633.
Schaub, N., T. Reichlin, et al. (2012). "Markers of plaque instability in the early diagnosis and risk stratification of acute myocardial infarction." Clin Chem **58**(1): 246-256.

Schelbergen, R. F., A. B. Blom, et al. (2012). "Alarmins S100A8 and S100A9 elicit a catabolic effect in human osteoarthritic chondrocytes that is dependent on Toll-like receptor 4." Arthritis Rheum **64**(5): 1477-1487.
Schlieben, D. J., S. M. Korbet, et al. (2005). "Pulmonary-renal syndrome in a newborn with placental transmission of ANCAs." Am J Kidney Dis **45**(4): 758-761.
Schlondorff, D. and B. Banas (2009). "The mesangial cell revisited: no cell is an island." J Am Soc Nephrol **20**(6): 1179-1187.
Scholz, J., V. Lukacs-Kornek, et al. (2008). "Renal dendritic cells stimulate IL-10 production and attenuate nephrotoxic nephritis." J Am Soc Nephrol **19**(3): 527-537.
Schreiber, A., H. Xiao, et al. (2006). "Bone marrow-derived cells are sufficient and necessary targets to mediate glomerulonephritis and vasculitis induced by anti-myeloperoxidase antibodies." J Am Soc Nephrol **17**(12): 3355-3364.
Schreiber, A., H. Xiao, et al. (2009). "C5a receptor mediates neutrophil activation and ANCA-induced glomerulonephritis." J Am Soc Nephrol **20**(2): 289-298.
Segelmark, M., R. Butkowski, et al. (1990). "Antigen restriction and IgG subclasses among anti-GBM autoantibodies." Nephrol Dial Transplant **5**(12): 991-996.
Sfikakis, P. P., V. L. Souliotis, et al. (2007). "Increased expression of the FoxP3 functional marker of regulatory T cells following B cell depletion with rituximab in patients with lupus nephritis." Clin Immunol **123**(1): 66-73.
Sharon Lee Ford, K. P., Anthony Longano, Stephen R. Holdsworth, A. Richard Kitching, Shaun A. Summers. (2012). Renal Function and Sclerotic Glomerular Injury Predicts Poor Prognosis in Patients Presenting with Anti-Neutrophil Cytoplasmic Antibody Associated Vasculitis Renal Week, ASN.
Sharp, P. E., J. Martin-Ramirez, et al. (2012). "Increased incidence of anti-GBM disease in Fcgamma receptor 2b deficient mice, but not mice with conditional deletion of Fcgr2b on either B cells or myeloid cells alone." Mol Immunol **50**(1-2): 49-56.
Shimizu, K., P. Libby, et al. (2011). "Loss of myeloid related protein-8/14 exacerbates cardiac allograft rejection." Circulation **124**(25): 2920-2932.
Silva, F., U. Specks, et al. (2009). "Successful pregnancy and delivery of a healthy newborn despite transplacental transfer of antimyeloperoxidase antibodies from a mother with microscopic polyangiitis." Am J Kidney Dis **54**(3): 542-545.
Simard, J. C., D. Girard, et al. (2010). "Induction of neutrophil degranulation by S100A9 via a MAPK-dependent mechanism." J Leukoc Biol **87**(5): 905-914.
Simard, J. C., M. M. Simon, et al. (2011). "Damage-associated molecular pattern S100A9 increases bactericidal activity of human neutrophils by enhancing phagocytosis." J Immunol **186**(6): 3622-3631.
Smart, S. J. and T. B. Casale (1994). "TNF-alpha-induced transendothelial neutrophil migration is IL-8 dependent." Am J Physiol **266**(3 Pt 1): L238-245.
Smith, J., P. C. Lai, et al. (2007). "Genes expressed by both mesangial cells and bone marrow-derived cells underlie genetic susceptibility to crescentic glomerulonephritis in the rat." J Am Soc Nephrol **18**(6): 1816-1823.
Smith, L. A. and D. R. Gaya (2012). "Utility of faecal calprotectin analysis in adult inflammatory bowel disease." World J Gastroenterol **18**(46): 6782-6789.
Snapper, C. M. and W. E. Paul (1987). "Interferon-gamma and B cell stimulatory factor-1 reciprocally regulate Ig isotype production." Science **236**(4804): 944-947.

Sohnle, P. G., M. J. Hunter, et al. (2000). "Zinc-reversible antimicrobial activity of recombinant calprotectin (migration inhibitory factor-related proteins 8 and 14)." J Infect Dis **182**(4): 1272-1275.

Soyfoo, M. S., J. Roth, et al. (2009). "Phagocyte-specific S100A8/A9 protein levels during disease exacerbations and infections in systemic lupus erythematosus." J Rheumatol **36**(10): 2190-2194.

Srikrishna, G., K. Panneerselvam, et al. (2001). "Two proteins modulating transendothelial migration of leukocytes recognize novel carboxylated glycans on endothelial cells." J Immunol **166**(7): 4678-4688.

Steblay, R. W. (1962). "Glomerulonephritis induced in sheep by injections of heterologous glomerular basement membrane and Freund's complete adjuvant." J Exp Med **116**: 253-272.

Stegeman, C. A., J. W. Tervaert, et al. (1996). "Trimethoprim-sulfamethoxazole (co-trimoxazole) for the prevention of relapses of Wegener's granulomatosis. Dutch Co-Trimoxazole Wegener Study Group." N Engl J Med **335**(1): 16-20.

Stevenson, A., M. Yaqoob, et al. (1995). "Biochemical markers of basement membrane disturbances and occupational exposure to hydrocarbons and mixed solvents." QJM **88**(1): 23-28.

Stone, J. H., P. A. Merkel, et al. (2010). "Rituximab versus cyclophosphamide for ANCA-associated vasculitis." N Engl J Med **363**(3): 221-232.

Stout, R. D., C. Jiang, et al. (2005). "Macrophages sequentially change their functional phenotype in response to changes in microenvironmental influences." J Immunol **175**(1): 342-349.

Sumida, K., Y. Ubara, et al. (2011). "Complete remission of myeloperoxidase-anti-neutrophil cytoplasmic antibody-associated crescentic glomerulonephritis complicated with rheumatoid arthritis using a humanized anti-interleukin 6 receptor antibody." Rheumatology (Oxford) **50**(10): 1928-1930.

Summers, S. A., O. M. Steinmetz, et al. (2011). "Toll-like receptor 2 induces Th17 myeloperoxidase autoimmunity while Toll-like receptor 9 drives Th1 autoimmunity in murine vasculitis." Arthritis Rheum **63**(4): 1124-1135.

Summers, S. A., B. S. van der Veen, et al. (2010). "Intrinsic renal cell and leukocyte-derived TLR4 aggravate experimental anti-MPO glomerulonephritis." Kidney Int **78**(12): 1263-1274.

Sunahori, K., M. Yamamura, et al. (2006). "The S100A8/A9 heterodimer amplifies proinflammatory cytokine production by macrophages via activation of nuclear factor kappa B and p38 mitogen-activated protein kinase in rheumatoid arthritis." Arthritis Res Ther **8**(3): R69.

Tadema, H., W. H. Abdulahad, et al. (2011). "Increased expression of Toll-like receptors by monocytes and natural killer cells in ANCA-associated vasculitis." PLoS One **6**(9): e24315.

Tam, F. W., J. S. Sanders, et al. (2004). "Urinary monocyte chemoattractant protein-1 (MCP-1) is a marker of active renal vasculitis." Nephrol Dial Transplant **19**(11): 2761-2768.

Tanaka, T., M. Narazaki, et al. (2012). "Therapeutic targeting of the interleukin-6 receptor." Annu Rev Pharmacol Toxicol **52**: 199-219.

Tarzi, R. M., H. T. Cook, et al. (2011). "Crescentic glomerulonephritis: new aspects of pathogenesis." Semin Nephrol **31**(4): 361-368.

Tarzi, R. M., K. A. Davies, et al. (2003). "Both Fcgamma receptor I and Fcgamma receptor III mediate disease in accelerated nephrotoxic nephritis." Am J Pathol **162**(5): 1677-1683.

Tarzi, R. M., K. A. Davies, et al. (2002). "Nephrotoxic nephritis is mediated by Fcgamma receptors on circulating leukocytes and not intrinsic renal cells." Kidney Int **62**(6): 2087-2096.

Thorey, I. S., J. Roth, et al. (2001). "The Ca2+-binding proteins S100A8 and S100A9 are encoded by novel injury-regulated genes." J Biol Chem **276**(38): 35818-35825.

Timoshanko, J. R., A. R. Kitching, et al. (2001). "Interleukin-12 from intrinsic cells is an effector of renal injury in crescentic glomerulonephritis." J Am Soc Nephrol **12**(3): 464-471.

Timoshanko, J. R., A. R. Kitching, et al. (2004). "Leukocyte-derived interleukin-1beta interacts with renal interleukin-1 receptor I to promote renal tumor necrosis factor and glomerular injury in murine crescentic glomerulonephritis." Am J Pathol **164**(6): 1967-1977.

Timoshanko, J. R., A. R. Kitching, et al. (2006). "A pathogenetic role for mast cells in experimental crescentic glomerulonephritis." J Am Soc Nephrol **17**(1): 150-159.

Tipping, P. G. and S. R. Holdsworth (2006). "T cells in crescentic glomerulonephritis." J Am Soc Nephrol **17**(5): 1253-1263.

Tipping, P. G., X. R. Huang, et al. (1998). "Crescentic glomerulonephritis in CD4- and CD8-deficient mice. Requirement for CD4 but not CD8 cells." Am J Pathol **152**(6): 1541-1548.

Tipping, P. G., A. R. Kitching, et al. (1997). "Immune modulation with interleukin-4 and interleukin-10 prevents crescent formation and glomerular injury in experimental glomerulonephritis." Eur J Immunol **27**(2): 530-537.

Tomasson, G., P. C. Grayson, et al. (2011). "Value of ANCA measurements during remission to predict a relapse of ANCA-associated vasculitis--a meta-analysis." Rheumatology (Oxford).

Tomasson, G., P. C. Grayson, et al. (2012). "Value of ANCA measurements during remission to predict a relapse of ANCA-associated vasculitis--a meta-analysis." Rheumatology (Oxford) **51**(1): 100-109.

Tomosugi, N. I., S. J. Cashman, et al. (1989). "Modulation of antibody-mediated glomerular injury in vivo by bacterial lipopolysaccharide, tumor necrosis factor, and IL-1." J Immunol **142**(9): 3083-3090.

Toth, T., R. Toth-Jakatics, et al. (1999). "Mast cells in rapidly progressive glomerulonephritis." J Am Soc Nephrol **10**(7): 1498-1505.

Turner, J. E., C. Krebs, et al. (2012). "IL-17A Production by Renal gammadelta T Cells Promotes Kidney Injury in Crescentic GN." J Am Soc Nephrol **23**(9): 1486-1495.

Unanue, E. R. and F. J. Dixon (1967). "Experimental glomerulonephritis: immunological events and pathogenetic mechanisms." Adv Immunol **6**: 1-90.

Urban, C. F., D. Ermert, et al. (2009). "Neutrophil extracellular traps contain calprotectin, a cytosolic protein complex involved in host defense against Candida albicans." PLoS Pathog **5**(10): e1000639.

van der Vlag, J. and J. H. Berden (2011). "Lupus nephritis: role of antinucleosome autoantibodies." Semin Nephrol **31**(4): 376-389.

van der Woude, F. J., N. Rasmussen, et al. (1985). "Autoantibodies against neutrophils and monocytes: tool for diagnosis and marker of disease activity in Wegener's granulomatosis." Lancet **1**(8426): 425-429.
van Lent, P., A. Blom, et al. (2011). "Active involvement of "alarmins" S100A8 and S100A9 in regulation of synovial activation and joint destruction during mouse and human osteoarthritis." Arthritis Rheum.
van Lent, P. L., A. B. Blom, et al. (2012). "Active involvement of alarmins S100A8 and S100A9 in the regulation of synovial activation and joint destruction during mouse and human osteoarthritis." Arthritis Rheum **64**(5): 1466-1476.
van Lent, P. L., L. Grevers, et al. (2008). "Myeloid-related proteins S100A8/S100A9 regulate joint inflammation and cartilage destruction during antigen-induced arthritis." Ann Rheum Dis **67**(12): 1750-1758.
van Lent, P. L., L. C. Grevers, et al. (2008). "Stimulation of chondrocyte-mediated cartilage destruction by S100A8 in experimental murine arthritis." Arthritis Rheum **58**(12): 3776-3787.
van Lent, P. L., L. C. Grevers, et al. (2010). "S100A8 causes a shift toward expression of activatory Fcgamma receptors on macrophages via toll-like receptor 4 and regulates Fcgamma receptor expression in synovium during chronic experimental arthritis." Arthritis Rheum **62**(11): 3353-3364.
van Zoelen, M. A., T. Vogl, et al. (2009). "Expression and role of myeloid-related protein-14 in clinical and experimental sepsis." Am J Respir Crit Care Med **180**(11): 1098-1106.
Velden, J., H. J. Paust, et al. (2012). "Renal IL-17 expression in human ANCA-associated glomerulonephritis." Am J Physiol Renal Physiol **302**(12): F1663-1673.
Viemann, D., K. Barczyk, et al. (2007). "MRP8/MRP14 impairs endothelial integrity and induces a caspase-dependent and -independent cell death program." Blood **109**(6): 2453-2460.
Viemann, D., A. Strey, et al. (2005). "Myeloid-related proteins 8 and 14 induce a specific inflammatory response in human microvascular endothelial cells." Blood **105**(7): 2955-2962.
Vogl, T., S. Ludwig, et al. (2004). "MRP8 and MRP14 control microtubule reorganization during transendothelial migration of phagocytes." Blood **104**(13): 4260-4268.
Vogl, T., J. Roth, et al. (1999). "Calcium-induced noncovalently linked tetramers of MRP8 and MRP14 detected by ultraviolet matrix-assisted laser desorption/ionization mass spectrometry." J Am Soc Mass Spectrom **10**(11): 1124-1130.
Vogl, T., K. Tenbrock, et al. (2007). "Mrp8 and Mrp14 are endogenous activators of Toll-like receptor 4, promoting lethal, endotoxin-induced shock." Nat Med **13**(9): 1042-1049.
Voll, R. E., M. Herrmann, et al. (1997). "Immunosuppressive effects of apoptotic cells." Nature **390**(6658): 350-351.
Volz, H. C., D. Laohachewin, et al. (2012). "S100A8/A9 aggravates post-ischemic heart failure through activation of RAGE-dependent NF-kappaB signaling." Basic Res Cardiol **107**(2): 250.
Vora, A. N., M. P. Bonaca, et al. (2012). "Diagnostic evaluation of the MRP-8/14 for the emergency assessment of chest pain." J Thromb Thrombolysis **34**(2): 229-234.
Wang, Y., Q. Cao, et al. (2008). "By homing to the kidney, activated macrophages potently exacerbate renal injury." Am J Pathol **172**(6): 1491-1499.
Wang, Y., Y. P. Wang, et al. (2007). "Ex vivo programmed macrophages ameliorate experimental chronic inflammatory renal disease." Kidney Int **72**(3): 290-299.

Watts, R. A., S. E. Lane, et al. (2000). "Epidemiology of systemic vasculitis: a ten-year study in the United Kingdom." Arthritis Rheum **43**(2): 414-419.
Watts, R. A., S. E. Lane, et al. (2001). "Epidemiology of vasculitis in Europe." Ann Rheum Dis **60**(12): 1156-1157.
Watts, R. A., J. Mooney, et al. (2012). "The contrasting epidemiology of granulomatosis with polyangiitis (Wegener's) and microscopic polyangiitis." Rheumatology (Oxford) **51**(5): 926-931.
Watts, R. A., D. G. Scott, et al. (2008). "Renal vasculitis in Japan and the UK--are there differences in epidemiology and clinical phenotype?" Nephrol Dial Transplant **23**(12): 3928-3931.
Wilde, B., P. van Paassen, et al. (2009). "Dendritic cells in renal biopsies of patients with ANCA-associated vasculitis." Nephrol Dial Transplant **24**(7): 2151-2156.
Wittkowski, H., J. B. Kuemmerle-Deschner, et al. (2011). "MRP8 and MRP14, phagocyte-specific danger signals, are sensitive biomarkers of disease activity in cryopyrin-associated periodic syndromes." Ann Rheum Dis **70**(12): 2075-2081.
Wolf, D., K. Hochegger, et al. (2005). "CD4+CD25+ regulatory T cells inhibit experimental anti-glomerular basement membrane glomerulonephritis in mice." J Am Soc Nephrol **16**(5): 1360-1370.
Wong, D., R. G. Phelps, et al. (2001). "The Goodpasture antigen is expressed in the human thymus." Kidney Int **60**(5): 1777-1783.
Xiao, H., P. Heeringa, et al. (2002). "Antineutrophil cytoplasmic autoantibodies specific for myeloperoxidase cause glomerulonephritis and vasculitis in mice." J Clin Invest **110**(7): 955-963.
Xiao, H., P. Heeringa, et al. (2005). "The role of neutrophils in the induction of glomerulonephritis by anti-myeloperoxidase antibodies." Am J Pathol **167**(1): 39-45.
Xiao, H., A. Schreiber, et al. (2007). "Alternative complement pathway in the pathogenesis of disease mediated by anti-neutrophil cytoplasmic autoantibodies." Am J Pathol **170**(1): 52-64.
Xiao, S., C. R. Brooks, et al. (2012). "Defect in regulatory B-cell function and development of systemic autoimmunity in T-cell Ig mucin 1 (Tim-1) mucin domain-mutant mice." Proc Natl Acad Sci U S A **109**(30): 12105-12110.
Xu, K. and C. L. Geczy (2000). "IFN-gamma and TNF regulate macrophage expression of the chemotactic S100 protein S100A8." J Immunol **164**(9): 4916-4923.
Xu, K., T. Yen, et al. (2001). "Il-10 up-regulates macrophage expression of the S100 protein S100A8." J Immunol **166**(10): 6358-6366.
Yan, S. F., R. Ramasamy, et al. (2003). "Glycation, inflammation, and RAGE: a scaffold for the macrovascular complications of diabetes and beyond." Circ Res **93**(12): 1159-1169.
Yang, J. J., R. Kettritz, et al. (1996). "Apoptosis of endothelial cells induced by the neutrophil serine proteases proteinase 3 and elastase." Am J Pathol **149**(5): 1617-1626.
Yao, Z., M. K. Spriggs, et al. (1997). "Molecular characterization of the human interleukin (IL)-17 receptor." Cytokine **9**(11): 794-800.
Yap, K. L., J. B. Ames, et al. (1999). "Diversity of conformational states and changes within the EF-hand protein superfamily." Proteins **37**(3): 499-507.
Yen, T., C. A. Harrison, et al. (1997). "Induction of the S100 chemotactic protein, CP-10, in murine microvascular endothelial cells by proinflammatory stimuli." Blood **90**(12): 4812-4821.

Yui, S., M. Mikami, et al. (1997). "Growth-inhibitory and apoptosis-inducing activities of calprotectin derived from inflammatory exudate cells on normal fibroblasts: regulation by metal ions." J Leukoc Biol **61**(1): 50-57.
Zreiqat, H., C. R. Howlett, et al. (2007). "S100A8/S100A9 and their association with cartilage and bone." J Mol Histol **38**(5): 381-391.
Zwadlo, G., R. Schlegel, et al. (1986). "A monoclonal antibody to a subset of human monocytes found only in the peripheral blood and inflammatory tissues." J Immunol **137**(2): 512-518.